Epidemiology and Physiological Impact of Aerial *Phytophthora pluvialis* in New Zealand and Oregon Forest Systems

Mireia Gómez Gallego

Primary Supervisor: Dr. Martin Bader

Secondary Supervisor: Dr. Nari Williams

A thesis submitted to Auckland University of Technology in fulfilment of the requirements for the degree of Doctor of Philosophy (PhD)

December, 2018

Table of contents

List of figures

List of tables

List of abbreviations

SI: Susceptible-infectious model

SIPQ: Susceptible-Infectious-Infected extended model.

RNC: Red needle cast

SNC: Swiss needle cast

qPCR: Real-time PCR

T: Temperature

RH: Relative humidity

C: Carbon

N: Nitrogen

h: Height

d: Diameter

NSC: Non-structural carbohydrates.

Attestation of authorship

I hereby declare that this submission is my own work and that, to the best of my knowledge and belief, it contains no material previously published or written by another person, except where explicitly defined, nor material which to a substantial extent has been submitted for the award of any degree or diploma of a university or other institution of higher learning.

_____

Mireia Gómez Gallego

Co-authored papers

Chapter 2 Gómez-Gallego, M., Gommers, R., Bader, M. K. F., Williams, N. M. Modelling the key drivers of forest disease epidemics from the laboratory to the field. (Submitted to PLoS ONE)	Gómez-Gallego, M 80% Gommers, R 15% Bader, M 2.5% Williams, N 2.5%
Contribution: MG, designed, executed and analysed the data of the on-plant inoculation, contributed to the extension of the model and the model fitting of the on-plant inoculation data, contributed to the execution of the detached-needle assay and wrote the manuscript (80%); RG, led to the development and extension of the model, executed the computations of model fittings (15%); MB and NW designed the detached-needle assay and contributed to the extension of the model (2.5% each); all the authors reviewed and approved the final version.	
Chapter 3 Gómez-Gallego, M., Bader, M. K. F., Scott, P. M., Leuzinger, S., Williams, N. M. 2017. *Phytophthora pluvialis* studies on Douglas-fir require Swiss needle cast suppression. Plant Disease 101: 1259-1262.	Gómez-Gallego, M 85% Bader, M 5% Scott, P 2.5% Leuzinger, S 2.5% Williams, N 5%
Contribution: MG, designed, executed, analysed the data of the two assays and wrote the manuscript (85%); MB, contributed to the experimental design and the data analyses (5%); PS and SL, contributed to the experimental design (2.5% each); NW, contributed to the experimental design and the discussion of the results (5%); all the authors reviewed and approved the final version.	
Chapter 4 Gómez-Gallego, M., LeBoldus, J., Bader, M. K. F., Hansen, E., Donaldson, L., Williams, N. M. Pathogen loads of *Phytophthora pluvialis* and *Nothophaeocryptopus gaeumannii* populations co-existing within exotic plantations of New Zealand in contrast to Douglas-fir's endemic range in the US Pacific Northwest. (Submitted to Phytopathology)	Gómez-Gallego, M 80% LeBoldus, J 6% Bader, M 4% Hansen, E 2% Donaldson, L 2% Williams, N 6%
Contribution: MG, designed, executed (from field to laboratory), analysed the data and wrote the manuscript (80%); JL, designed and partly executed the study (6%); MB, contributed to the design and the data analyses (4%); EH, contributed to the experimental design (2%); LD, executed the microscopy imaging (2%); NW, contributed to the experimental design and the discussion of the results (6%); all the authors reviewed and approved the final version.	

Chapter 5 Gómez-Gallego, M., Williams, N. M., Leuzinger, S., Scott, P., Bader, M. K. F. A two-year defoliation experiment in *Pinus radiata* grafts: does the lower canopy matter? (Submitted to Tree Physiology)	Gómez-Gallego, M 85% Williams, N 2% Leuzinger, S 2% Scott, P 2% Bader, M 8%
Contribution: MG, designed, executed, analysed the data and wrote the manuscript (85%); NW, PS and SL contributed to the experimental design and discussion of the results (2% each); MB, contributed to the experimental design, data analyses and the discussion of the results (5%); all the authors reviewed and approved the final version.	
Appendix 1 Wakelin, S.A., Gómez-Gallego, M., Jones, E., Smaill, S., Lear, G., Lambie, S. 2018. Climate change induced drought impacts on plant diseases in New Zealand. Australasian Plant Pathology 47(1): 101-114.	Wakelin, S 40% Gómez-Gallego, M 30% Jones, E 10% Smaill, S 10% Lear, G 5% Lambie, S 5%
Contribution: SW, lead the project and wrote the main body of the manuscript (40%); MG, contributed to the main body of the manuscript and wrote the case study of *P. pluvialis* (30%); EJ, SS, GL and SL, contributed to Table 1 (Table 6.1 in the present thesis) (10%, EJ and SS; and 5%, GL and SL); all the authors reviewed and approved the final version.	

_____	_____	_____	_____
Nari Williams	Martin Bader	Sebastian Leuzinger	Peter Scott
_____	_____	_____	_____
Ralf Gommers	Jared LeBoldus	Everett Hansen	Lloyd Donaldson
_____	_____	_____	_____
Steve Wakelin	Eirian Jones	Simeon Smaill	Gavin Lear
_____			
Suzanne Lambie			

Acknowledgements

Caminante, son tus huellas
el camino y nada más;
caminante, no hay camino,
se hace camino al andar.

Wanderer, your footsteps are
the road and nothing more;
wanderer, there is no road,
the road is made by walking.

Antonio Machado

I am very grateful for many things in my life, especially for the great people who is part of it. I want to dedicate this work to my family and my life-long friends, without whom I wouldn't have taken this opportunity in the other side of the world. Their support (video-calls, messages, jokes, visits) before and during my PhD journey has been crucial. I want to warmly thank my family for your unconditional support: my parents, Emi and Manuel, my sister Laura and my brother-in-law, Javi, and the best niece and nephews on Earth: Sol, Martí and Marcel. And my bigger non-blood family: Mireia, Txus, Pedro, Laura, Alberto, Luisma, Susana, Puri, Anna, Cristina, Maite, Tere, Pruden, Núria, Fede, Eva, Mònica, Custi, Rosa, Raquel, Rosamari, Pim, Jordi and many others. It's priceless to have them in my life.

It's been fantastic to know new great people in New Zealand. My friends here have been an essential part of this journey too. They have become part of my life and have made my PhD and my time in New Zealand even more enjoyable and exciting.

I am truly thankful to my supervisory (dream) team. To Dr Nari Williams, for her contagious courage, for her endless support, for her generosity, for her sincere friendship. She is a role model in how to share knowledge and opportunities, and how to collaborate in science. This is an attitude that can be hard to find within the research community, but it is what truly defines an outstanding scientist. I have also been really amazed at how Nari had always time for me, despite her busy schedule.

To Dr Martin Bader, for his firm support. He has been like a quiet shore in moments of anchorless drift. I've learnt a lot from his solid and organized way of doing science, from the research questions to the final publications. I have improved an awful lot my statistics skills thanks to him. And I have very much enjoyed his beautiful corrections to my writing. Martin and Nari have always believed in me, and given me enough independence for the development of my own research questions and experiments. This has enormously helped me develop my skills.

Dr Sebastian Leuzinger and Dr Peter Scott have been nicely supporting me in the background. Thanks to Sebastian for his valuable input in the physiological experiments, for his availability, for his guidance in my being part of the AUT, and for being always the first in answering key emails. Thanks to Peter for his encouraging words and his contagious love for Phytophthoras. I've learnt from him that creativity is the engine of science, and free thinking is needed to deal with some challenging unanswered scientific questions.

The Forest Protection team at Scion has surely been one of the pillars of this PhD. Most of the work presented here wouldn't have been possible without the assistance of my colleagues in the laboratory and field work. The nice environment within the team has encouraged and inspired me.

The three-month stay in the Oregon State University was a great opportunity for me to expand my research in *Phytophthora pluvialis* epidemiology in Douglas-fir. I am very thankful to Dr Jared LeBoldus, for the trips together to the field and the exchange of research ideas, and to Prof Everett Hansen for sharing his expertise in *Phytophthora* and the Swiss needle cast disease. Being part of both teams during three months has enriched my knowledge and this thesis. I very much thank the Swiss needle cast cooperative for the help in the field work and welcoming and valuing my research.

Doing my PhD in New Zealand and Oregon has meant getting to know different ways of managing forest resources. As a Forest Engineer, I have enjoyed this. Ecosystems are under huge pressure from climate change, and many contradictions arise from the way we manage forest systems to achieve both productivity and resilience. I'm thankful for those contradictions, which keep me on the track of thinking, in a humble attitude. The "Ph" of the PhD has given me the space to think ahead, to see myself capable to tackle challenges instead of accepting the *status quo*. New challenges require deep and daring thinking, even though that may mean being out of one's comfort zone.

Finally, I want to thank nature. Working with living organisms teaches me patience. Nature brings about a different pace, challenges any narrow-minded ideas, and places us back where we should be: maybe not in the centre, but alongside.

Abstract

Forest health is threatened by invasive plant-infecting fungi and fungal-like organisms, whose frequency has increased with international trade in recent decades. While planted forests are particularly vulnerable to invasive pathogens, the area under production is increasing due to the growing world population and the subsequent growing demand of fibre. *Phytophthora* species are a remarkable group of pathogens in agricultural and forest systems. Over the past few decades, numerous members of this genus have been reported to affect conifer plantations as foliar pathogens. *Phytophthora pluvialis* is the causal agent of red needle cast disease (RNC) affecting *Pinus radiata* plantations in New Zealand (NZ) since 2008. The pathogen was described as a new species following its recovery from baited stream and soils from mixed tanoak and Douglas-fir (*Pseudotsuga menziesii*) forests in southwestern Oregon (US). More recently, *P. pluvialis* has been associated with early defoliation in Douglas-fir in both countries. This thesis had two main objectives: (1) to gain knowledge on the epidemiology of *P. pluvialis* in the two hosts in NZ and Oregon forests systems, and (2) to analyse the physiological impact of *P. pluvialis* infection on the host.

Detached-needle assays and on-plant inoculations were performed on radiata pine to analyse the key drivers of the RNC disease. The data was fitted into an epidemiological model extended to account for the dynamics of the pathogen on the infected needles. Primary infection presented a peak 4 days after inoculation, from which polycyclic infections developed reaching a peak 22 days after inoculation. Susceptible and resistant genotypes differed in the pathogen death rate (2.5 times lower in susceptible genotypes), and higher presence of external proliferation of mycelium and sporangia (90% vs 25% of the infected needles). Real-time PCR (qPCR) effectively detected *P. pluvialis* earlier after inoculation, but it was less efficient at later stages of the epidemic, than isolations. Isolations were not influenced by the presence of lesions, while 19% of lesioned needle maximized qPCR detection.

In Douglas-fir, detached-needle and -twig assays showed the co-infection of needles by both *P. pluvialis* and the ascomycete fungus *Nothophaeocryptopus gaeumannii*, which is the cause of the Swiss needle cast disease globally. The coexistence of both pathogens was confirmed in NZ and the US Pacific Northwest (PNW) at different spatial scales ranging from the needles to the region. Both pathogens were more abundant in the host's exotic environment, NZ, in contrast to its endemic range of the PNW. Their relative abundance was negatively correlated in the PNW, where both pathogens are presumed to have coexisted for longer. Higher winter relative humidity values led to larger *P. pluvialis* abundance in Douglas-fir.

The physiological impact of needle loss associated with RNC was studied in an artificial inoculation experiment simulating the defoliation pattern of the disease. Two RNC-susceptible genotypes were treated. Growth and carbon (C) allocation in the genotype with initial higher specific leaf area were unaffected by defoliation. In contrast, the other genotype suffered C shortage. Diameter of radiata pine at 3 cm up from the graft union was 23% and 32% lower in defoliated plants one and two growing seasons after defoliation, respectively. Height and total

aboveground biomass reductions of 36% and 55%, respectively, were only noted after the second growing season following defoliation. A decrease in sugar storage in roots during canopy development, followed by a recovery in root sugar reserves were also observed after the second growing season following defoliation.

Trees affected by RNC seem to recover after canopy development, but the reduction in growth and transient reductions in C reserves may make them more vulnerable to other biotic or abiotic stressors. RNC impact on host's productivity and resilience should be analysed through an integrative approach. Compartmental models offer a great opportunity to integrate within a common framework several disciplines needed to implement smarter disease management strategies: plant pathology, ecophysiology, chemistry and forest economy.

Chapter 1. Introduction

Rationale and thesis aims

Forests play a key role in the well-being and survival of humankind. In the mid-term, forests ensure food security and help combat poverty, providing food, fibres and green growth opportunities. In addition, forests deliver vital long-term ecosystem services, such as clean air, watershed protection, conservation of biodiversity and mitigation of climate change (FAO 2015). Natural and planted forests accomplish different roles, but can also share similar functions. For example, both have a role in climate regulation, and in the protection of soil and water. However, planted forests are usually established to obtain goods and services, such as fuel and timber supply or carbon sequestration, and to reduce the pressure on natural forests (Jandl et al. 2013, FAO 2015). With an increasing world population, predicted to reach 9.6-9.7 billion in 2050, the demand on food and fibre will become more pressing (Gerland et al. 2014, UNDESA 2015). The proportion of planted forests has accordingly been rapidly increasing in the last decades, and currently planted forests account for 7% of the world's forest area (FAO 2015).

The health of forests is increasingly threatened by global change-related disturbances. One of the most rapidly changing biological threats is the emergence of new diseases and pests (Wingfield et al. 2015). Disease alerts for invasive fungal and fungal-like plant pathogens have reached unprecedented records, mainly due to introductions through international trade (Anderson et al. 2004, Fisher et al. 2012, Santini et al. 2013, Roy et al. 2014, Wingfield et al. 2015, Hurley et al. 2017). Planted forests are particularly vulnerable to invasive pathogens. This raises the challenge of how to design and manage plantation forestry to minimize losses. Plantations are most commonly composed of a majority of a single non-native species, especially in the tropics and the Southern hemisphere (Wingfield et al. 2015), while in Europe the recommendations include the increase of diversification of species composition and planting of indigenous species (COM, 2005). The lack of tree species diversity increases the susceptibility of forests to pathogens at both the stand and regional levels (Pautasso et al. 2005, Haas et al. 2011). Even though non-native species have been separated from their natural enemies, plantation trees can be reunited with their coevolved pathogens (Dickie et al. 2017). This interaction can be favourable for the pathogen in the new environmental conditions leading to notable damage. Non-native tree species can also encounter native pathogens, to which they have no resistance, or novel introduced pathogens (Wingfield et al. 2015). Not only can monoculture plantations be infected and suffer remarkable loss, but those interactions can enhance pathogen spillover onto native plants (Dickie et al. 2017), such as *Phytophthora ramorum* infecting Japanese larch in Ireland and the further infection of chestnut trees (O'Hanlon et al. 2015). Therefore, introduced pathogens in plantation forestry present a double challenge: the need to reduce the disease impact in planted forests and the need to limit the potential impact of new pathogens on native forest.

Phytophthora species are effective pathogens with an unusual genetic architecture that may favour rapid evolution of pathogenicity (Hayden et al. 2013, Mcgowan and Fitzpatrick 2017). Many *Phytophthora* species are benign in plant communities they coevolved with (Vettraino et al. 2011). But, given the opportunity of introduction to new hosts in new environments, they have the potential to cause dramatic epidemics in exotic plantations and natural forests around the world (Hansen 2008). *Phytophthora* diseases infecting foliage of conifers are relatively new and a growing concern in economically important planted species such as radiata pine (*Pinus radiata* [D. Don]). Namely, *Phytophthora pinifolia* was first detected in 2004 in radiata pine plantations in Chile causing the so-called 'Daño foliar del pino' (Durán et al. 2008). An epidemic of *Phytophthora ramorum* has been seen to infect larch tree plantations (*Larix*) in the UK and Ireland, resulting in sudden larch death, in 2009 (Brasier and Webber 2010, Harris and Webber 2016, Harris et al. 2018).

Phytophthora pluvialis Reeser, Sutton and Hansen was noted as the cause of the red needle cast (RNC) disease in radiata pine plantations in New Zealand, in 2008 (Dick et al. 2014). More recently, early defoliation episodes in *Pseudotsuga menziesii* (Mirb.) Franco (Douglas-fir) have been attributed to *P. pluvialis* in Oregon (US) and New Zealand (Hansen et al. 2015). The symptoms of infection by *P. pluvialis* in radiata pine include browning needles which confers a reddish appearance to the affected portion of the crown. Infection typically starts in late autumn from the lower canopy and extends upwards to the top of the canopy (Dick et al. 2014). The symptomatic needles eventually cast during late spring-summer. Highly severe episodes have been observed to take place every 2-3 years (Ganley et al. 2014). Less is known about *P. pluvialis* infection in Douglas-fir. Defoliation of infected Douglas-fir needles typically occurs when symptoms are barely noticeable. Both asymptomatic and pale-olive coloured infected needles readily detach from the stem (Dick et al. 2014).

Radiata pine and Douglas-fir are both highly productive tree species, and are grown as non-native plantations in many parts of the world. In Oregon, Douglas-fir is native and is the most important conifer due to its ecological and economic significance (Ritokova et al. 2016). In New Zealand, radiata pine represents 90% of the 1.7 million hectares of the non-native plantation estate, followed by the non-native Douglas fir, planted on approximately 110 thousand hectares (New Zealand Forest Owners Association 2014). The economic importance of these tree species and the possible loss of productivity make it crucial to improve our knowledge of *P. pluvialis* impacts in these forest systems. Further, not only productivity but also net primary production, i.e. the amount of carbon and energy that enters a given ecosystem, is known to be affected by pathogenic infection (Pinkard, Battaglia, et al. 2011).

The overarching aim of the thesis was to better understand the epidemiology and physiological impact of *P. pluvialis* on radiata pine and Douglas-fir forest systems in New Zealand and the US Pacific Northwest. To achieve this objective, the thesis followed these specific aims:

1. To identify the key drivers of *P. pluvialis* epidemiology in *Pinus radiata* and *Pseudotsuga menziesii*.
2. To analyse the environmental conditions supporting *P. pluvialis* infection.

3. To identify the possible interactions of *P. pluvialis* infection and other foliar pathogens in Douglas-fir.
4. To analyse the physiological impact of the defoliation pattern caused by RNC on host carbon (C) assimilation and C allocation to growth and storage.
5. To review the possible impact of climate change on the RNC disease, through the impact of extreme climate events, such as predicted drought, on the disease.

Thesis structure

The thesis consists of two primary sections: (1) epidemiology and (2) physiological impact (Fig 1.1). The first part includes the research related to *P. pluvialis* epidemiology, and comprises three chapters. Chapters 2 focuses on the epidemiology of *P. pluvialis* on radiata pine, while chapters 3 and 4 center around Douglas-fir infection by *P. pluvialis* and its interaction with *Nothophaeocryptopus gaeumannii*, causal agent of the Swiss needle cast disease (Temel et al. 2004).

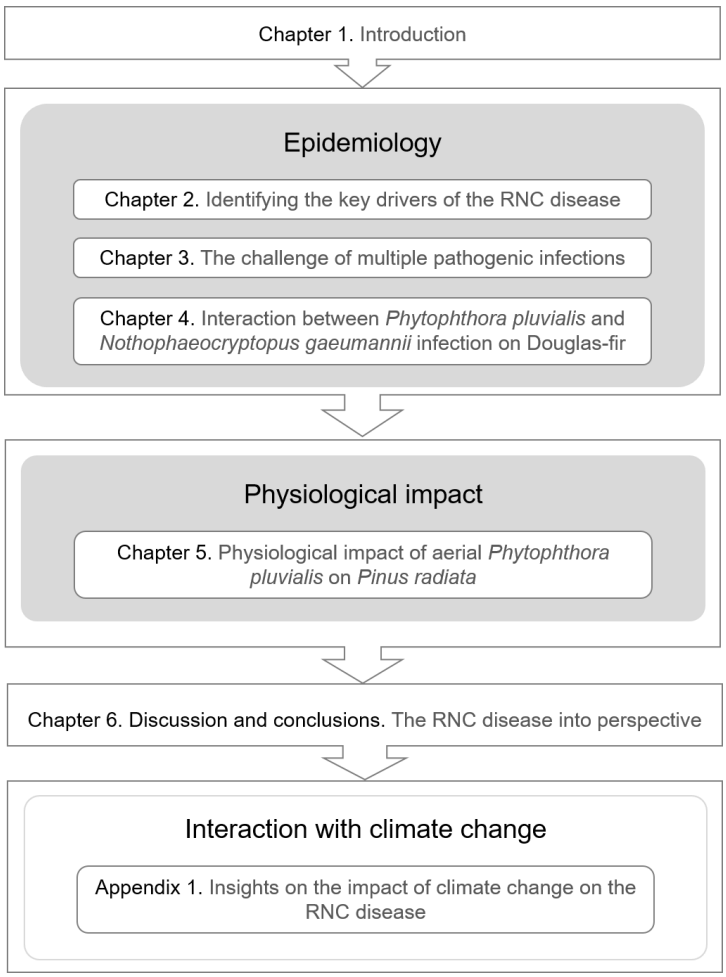

Figure 1.1. Structure of the thesis by chapters.

No common literature review is included as a chapter. It is part of the 'Introduction' section in each chapter, with further reference to the literature in the respective chapter discussion. Chapter 2

presents an SI (Susceptible-Infectious) epidemiological model fitted with empirical data from inoculation experiments on detached needle and whole radiata pine grafts. This chapter analyses the main drivers of *P. pluvialis* epidemiology on radiata pine. Infection of Douglas-fir trees by *P. pluvialis* is investigated in chapters 3 and 4. Detached needle and twig assays are presented in chapter 3. Those experiments showed the ability of *P. pluvialis* to co-infect needles where *N. gaeumannii* is already growing. The importance of taking *N. gaeumannii* into account when analyzing *P. pluvialis* infection on Douglas-fir is demonstrated along with a methodology to perform *P. pluvialis* inoculation on *N. gaeumannii*-free needles. Chapter 4 presents the first ever study on the extent of *P. pluvialis* and *N. gaeumannii* co-existence in Oregon and New Zealand Douglas-fir forests. This chapter also describes the weather and climate conditions that modulate *P. pluvialis* and *N. gaeumannii* infection on Douglas-fi in both regions.

The second part of the thesis addresses the physiological impact of *P. pluvialis* on radiata pine C assimilation and allocation. This part is presented in chapter 5. This research was approached by means of a two-year greenhouse experiment, where RNC-induced defoliation was mimicked across two consecutive seasons. The compensatory responses and impact of the defoliation on photosynthesis, growth and carbon storage on radiata pine grafts were monitored.

The findings of both epidemiology and physiological impacts of *P. pluvialis* infection are given in a comprehensive summary, in chapter 6, where conclusions of the thesis are stated and discussed.

Appendix 1 consists of a review on the RNC disease interaction with climate change, particularly extreme events, such as drought episodes.

Chapter 2. Understanding *P. pluvialis* infection dynamics: from needles to plants

This chapter comprises a co-authored manuscript submitted to PLoS ONE.

Gómez-Gallego, M., Gommers, R., Bader, M. K. F., Williams, N. M. 2018. Modelling the key drivers of an aerial *Phytophthora* foliar disease epidemic, from the needles to the whole plant.

Prelude

The use of compartmental models in epidemiology has shed some light on infection dynamics and the identification of the main drivers of plant disease. In this chapter, I present the extension of an SI (Susceptible-Infectious) epidemiological model for red needle cast (RNC) (Wake et al. 2018) to fitted with empirical data with which the behaviour of *P. pluvialis* infection can be further articulated. The data from two inoculation experiments are used to quantify key parameters in RNC epidemiology. Namely, primary and secondary infection rates, pathogen reproduction and death rates, and peaks of infection. Detached-needle and whole-plant inoculation experiments were performed in different radiata pine genotypes. In the detached-needle assay, four resistant and four susceptible genotypes were compared to elucidate which parameters determine the differences between resistance and susceptibility to RNC. In the on-plant inoculation trial, four susceptible genotypes were studied to analyse both primary and secondary infections at the plant level. Two main diagnostic methods were also compared: *P. pluvialis* isolation in culture media and qPCR detection.

This study sets the basis for further exploration of RNC epidemiology by providing data on the timing of the exponential phase of the epidemics. The following experiments were designed within these timeframes. This study also provides a comprehensive comparison among *P. pluvialis* detection methods, comparing presence of symptoms to isolation rates and qPCR detection.

Abstract

Understanding the epidemiology of infectious diseases in a host population is a major challenge in forestry. Radiata pine plantations in New Zealand are impacted by a foliar disease, red needle cast (RNC), caused by *Phytophthora pluvialis*. This pathogen is dispersed by water splash with polycyclic infection affecting the lower part of the tree canopy. In this study, we extended an SI (Susceptible-Infectious) model presented for RNC to analyse the key epidemiological drivers. We conducted two experiments to empirically fit the extended model: a detached-needle assay and an *in vivo* inoculation. We used the detached-needle assay data to compare resistant and susceptible genotypes, and the *in vivo* inoculation data was used to inform sustained infection of the whole plant. We also compared isolations and real-time quantitative PCR (qPCR) to assess *P. pluvialis* infection. The primary infection rate and the incubation time were similar for susceptible and resistant genotypes. The pathogen death rate was 2.5 times higher for resistant than susceptible genotypes. Further, external proliferation of mycelium and sporangia were only observed on 28% of the resistant ramets compared to 90% of the susceptible ones. Detection methods were the single most important factor influencing parameter estimates of the model, giving qualitatively different epidemic outputs. In the early stages of infection, qPCR proved to be more efficient than isolations but the reverse was true at later points in time. Isolations were not influenced by the presence of lesions in the needles, while 19% of lesioned needle maximized qPCR detection. A primary infection peak identified via qPCR occurred at 4 days after inoculation (dai) with a secondary peak observed 22 dai. Our results have important implications to the management of RNC, by highlighting the main differences in the response of susceptible and resistant genotypes, and comparing the most common assessment methods to detect RNC epidemics.

Introduction

Research on the epidemiology of plant pathogens and the development of sustainable strategies for disease control might have never been so pressing. The frequency of the emergence of invasive plant-infecting fungi and fungal-like organisms has increased enormously with international trade in recent decades (Fisher et al. 2012). Forestry plantations have been threatened by such invasive diseases with new associations between pathogenic species and non-native hosts being increasingly noted globally (Wingfield 2003, Wingfield et al. 2015, Hurley et al. 2017). The efficacy of sustainable disease management in plantation forests is underpinned by the fundamental dynamics of disease epidemiology, interactions with susceptible hosts, the biological limitations and potential of the pathogen, and the respective physiologies within a mutual environment. Understanding this dynamic interaction presents an opportunity to develop smarter disease management strategies and reduce the impact of disease in the field.

Phytophthora species are a relatively newly recognized cause of foliar diseases in *Pinus radiata D. Don*, the key plantation forest species in New Zealand (NZ), Chile and Australia (Forest Owners Association New Zealand 2016, Salas et al. 2016, Australian Bureau of Agricultural and Resource Economics and Sciences 2018). New reports of 'Daño Foliar de Pino' in Chile in 2008, and observations of the red needle cast (RNC) disease in New Zealand soon thereafter, highlighted the potential significance of foliar *Phytophthora* impacts on *P. radiata* plantation forestry (Durán et al. 2008, Dick et al. 2014). RNC was first reported in *P. radiata* stands on the east coast of New Zealand in late April 2008 (Dick et al. 2014). Symptoms of RNC emerge in late autumn and continue to develop through until mid to late spring. Infection is characterised by an olive discoloration of affected needles, frequently accompanied by resinous dark bands on the needles (Dick et al. 2014). Affected foliage quickly turns orange to brown, lending a reddish hue to the affected crown. Infected needle fascicles are cast with new needles emerging in late spring often unaffected by disease. Initial studies have shown that severe defoliation events associated with RNC can reduce tree growth by up to 38% in the year following infection (Beets et al. 2013). Isolations from symptomatic needles onto *Phytophthora* selective media yielded the newly described *Phytophthora pluvialis* Reeser, Sutton and Hansen. The same pathogen was subsequently identified as a contributing pathogen of early defoliation in Douglas-fir in NZ and the US Pacific Northwest (Dick et al. 2014, Hansen et al. 2015).

Early work on the RNC disease focused on confirming the cause, disease expression, timing and risks for trade. However, limited work has been done to date to progress a deeper understanding of the epidemiology of the disease. Some knowledge gaps still remain on the drivers of sustained RNC infection, characterized by the polycyclic nature of the splash-dispersed *P. pluvialis*, on the timing and peaks of primary and secondary infections, and on host susceptibility and resistance to RNC. Further, several diagnostic methods have been used to date, i.e. isolations in culture media and real-time quantitative PCR (qPCR) (Gomez-Gallego et al. 2017, O'Neill et al. 2018), but no comprehensive analysis on their efficiency and potential shortcomings have been performed.

Epidemiological models have been previously applied to give insight into key aspects of disease management. For example, compartmental models have explored disease prediction through the characterization of latent infectious periods and transmission rates (Otten et al. 2003, Vergu et al. 2010, Cunniffe et al. 2012, Leclerc et al. 2014), while others have focused on the efficacy of control methods, such as cultural practices (Mammeri et al. 2014), or induced resistance (Abdul Latif et al. 2014). In this paper, we further explore a generic mathematical SI (susceptible-infectious) model for RNC that articulates the RNC disease dynamic introduced by Wake et al (2018). Our contributions are twofold. First, we extend the SI model to account for the dynamics of pathogen-host interaction. Then, we apply the extended model to two experiments: a detached-needle assay and an *in vivo* inoculation. The empirical data from those two experiments allowed us to (1) determine incubation times, infection rates, and pathogen mortality rates for susceptible and resistant genotypes. Moreover, we (2) quantified differences between the main RNC diagnostic methods (isolation and qPCR), and (3) analysed primary and secondary infection peaks in a sustained RNC infection episode. For our first aim, we performed a detached-needle assay to use empirical data to fit the model. This assay also provided data on the latent infectious periods, and the peak of primary infection. For our second and third aims, an *in vivo* inoculation experiment was carried out in a controlled temperature fog room. This data was further analysed to evaluate the correlations between presence of lesions and the two main diagnostic methods, isolations and qPCR detection. This paper provides the first investigation into the epidemiology of the RNC disease.

Materials and Methods

We performed two different inoculation experiments in order to parameterise an extended version of an established model for red needle cast (Wake et al. 2018). To characterize the primary infection of the pathogen, i.e. the infection initiated from incoming inoculum (Gilligan and Kleczkowski 1997), we designed a detached-needle assay, where only individual detached pine needles were inoculated and monitored for 11 days. This period has been previously demonstrated to cover the period of primary infection up to peak infection and to needle senescence (Graham et al. 2018). To study the secondary infection by the pathogen, i.e. the infection originated by spread from infected to susceptible needles (Gilligan and Kleczkowski 1997), we performed an *in vivo* inoculation experiment. Whole plants were inoculated with the pathogen and monitored for a longer period, up to 28 days, within which secondary infection could be observed. Whole plants provide sufficient needle mass to host secondary infection events.

Inoculum preparation

Zoospore inoculum was prepared as described previously by Rolando et al. (Rolando et al. 2014) with modification to produce sufficient inoculum for the scale of the trials. *P. pluvialis* isolates used for inoculum preparation for the detached-needle assay were NZFS3901, 3902, 4014, 4015, 4016 and 4017, and NZFS4019, 4234, 4267, 4268, 4317, 4325, for the *in vivo* inoculation. Different isolates were used as the pathogenicity phenotype of *P. pluvialis* has been found to attenuate

over time with laboratory culturing. All isolates were routinely passed through radiata pine needles prior to each experiment to confirm their ability to infect. A mix of isolates was used to enable selection for the most virulent one (Young et al. 2018) and favour infection, as commonly performed in epidemiological studies (Matthiesen et al. 2016, Cara et al. 2018). All isolates used as source of inoculum were identified using morphological and molecular techniques. Isolates have typically remained active for up to 12 months, but were routinely removed from the screening programme as soon as they failed to re-infect *P. radiata* and replaced with fresh isolates sourced from the field. The isolates were cultured on carrot agar (10% carrot broth, 15 g/L agar, 200 mg/L ampicillin, 0.05 g/L nystatin, 0.01 g/L rifampicin, 0.4 ml/L pimaricin) at 17 ºC for three days. Plugs of agar and mycelium were taken from the leading edge of the colonies, flooded with 55 ml of clarified carrot broth (Erwin and Ribeiro 1996) in vented 175 cm^2 flat bottomed flasks (Nunc EasYFlasks, Thermo Scientific) and incubated for three days in the dark at 17 ºC. The resulting mycelial mats were rinsed thoroughly in a steady stream of deionized water, drained, and then reflooded with 55 ml of sterile pond water. The pond water was collected from a local pond and autoclaved before being used to induce sporangia production and sporulation of *P. pluvialis* cultures. The flasks were re-incubated in the dark for further three days. Zoospore release was induced by cold-shocking the cultures at 4 ºC in the dark for 45 min, followed by exposure at room temperature (21 ºC), and by placing cultures on a light box if required (Rolando et al. 2014). Upon release, the zoospore inoculum of all six isolates was combined to form a single mixed inoculum. Zoospore concentrations were determined using a haemocytometer, reaching a minimum of 1 x 10^4 zoospores/ml, for the detached-needle assay, and 3 x 10^3 zoospores/ml, for the whole-plant assay. Zoospore solutions were applied within two hours of preparation.

Detached-needle assay

Plant material and inoculation treatment

Pinus radiata genotypes were preselected from the Radiata Pine Breeding Company's Elite Clones series as published previously (Graham et al. 2018). Four genotypes were selected for higher susceptibility and four genotypes for higher resistance to RNC, respectively. Plants were clonally propagated from stool beds as bare-rooted cuttings, planted in Scion's nursery in Rotorua, New Zealand. Thirty-five healthy fascicles were collected from each of the six ramets (clonal plants) from each of the eight genotypes. The fascicles were assigned to treatments following a split-split plot design with two independent blocks, water control and *P. pluvialis* inoculation (whole plots), seven sampling time points (0, 1, 3, 5, 7, 9, 11 days after inoculation) separated in single incubation trays (split plot), and eight genotypes (split-split plot). Five fascicles from each ramet and each genotype were place in each tray, after their exposure to dip inoculation in 15-mL flat bottom plastic tubes containing 4.5 mL of either water or *P. pluvialis* zoospore suspension. The experimental design is shown in S2.1 Fig, only for control treatment, which is identical to *P. pluvialis* inoculation treatment.

Each tube accommodated five fascicles and was inoculated with 4.5 ml of either the *P. pluvialis* zoospore suspension (see 'Inoculum preparation') or sterile pond water (control) and incubated at room temperature overnight (18 hours). Fascicles were placed on trays moistened with wet paper towels, covered in plastic film and incubated in a controlled environment (17 ºC, 65-70% relative humidity, 14 h photoperiod) for 10 days. The allocation of individual samples within trays was randomized at the block level and the position of incubation of each tray within the growth room randomized to account for variation within the incubation room. Tubes were randomized prior to inoculation with the layout carried through for needle incubation.

Assessment of P. pluvialis *infection*

Pathogen presence and growth was assessed by measuring lesion length, pathogen isolation in culture media, and by fluorescence microscopy observations. At each harvest point, the needles within each fascicle were separated, and the lesions counted and measured to the nearest mm. The five fascicles within each replicate were allocated at random for parallel analysis by isolation, immersed in FAA fixative (50% ethanol, 5% (v/v) acetic acid, 3.7% (v/v) formaldehyde), snap frozen and stored at -80 ºC for further analyses.

Total needle length and lesion length, characteristic of early symptoms of RNC (olive-coloured discoloration and black bands, (Dick et al. 2014)) were recorded for each needle, the percentage of lesioned needle length calculated, and averaged for each fascicle. For isolations, the proximal 3 cm of each needle that had been exposed to inoculum/water was surface sterilised for 30 seconds in 70% ethanol, rinsed in sterile deionised water and patted dry with paper towels. Each needle was sectioned into three pieces and plated onto *Phytophthora* selective CRN media (10% carrot broth, 15 g/L agar, 200 mg/L ampicillin, 0.05 g/L nystatin, 0.01 g/L rifampicin, 0.4 ml/L pimaricin). Plates were incubated at 17 ºC in the dark for up to 14 days and the proportion of isolations recorded for each fascicle. *Phytophthora pluvialis* colonies were morphologically identified (Reeser et al. 2013) by subculturing and inducing sporangia production in pond water (Erwin and Ribeiro 1996).

Microscopic observations were made of the production of *P. pluvialis* spore and mycelial structures on the surface of pine needles fixed at harvest and stored in FAA fixative. Whole fascicles were removed from the FAA solution, patted dry, the proximal 3 cm dissected and placed in a 0.01% solution of calcofluor white dissolved in ultra-pure water (Sigma Aldrich) for 30 seconds. Excess calcofluor was removed by carefully rinsing in sterile deionized water and the sections dried on a tissue before placing on a microscope slide without a cover slip. Needles were observed using an Olympus BX61 fluorescence microscope under UV excitation with the presence of *P. pluvialis* mycelium and sporangia noted for each needle within fascicle.

In vivo inoculation

Plant material and inoculation treatment

The experiment was conducted on 3-year-old *P. radiata* grafts (Proseed, Scion nursery) of four RNC-susceptible genotypes. Ninety grafts were assigned to treatments following a split-plot design with two independent blocks, water control and *P. pluvialis* inoculation (whole plots), and four genotypes (split plot). The experimental design is shown in S2.2 Fig.

The experiment was performed in two fog rooms, to avoid cross infection of control plants in the same room, with an overhead misting system under identical conditions: 10 h photoperiod, 95-100% relative humidity, 10 ºC at night/ 17 ºC during the day. Mist was applied for 1 min continuously, every 10 min. At the beginning of the experiment, needles and branches of the grafts already placed in the fog room, as per *P. pluvialis* inoculation treatment, were thoroughly sprayed with zoospore suspensions (see 'Inoculum preparation') using a low-pressure spray (1 MPa) until inoculum run off. Control grafts were placed on the control fog room without any inoculation treatment, and kept under the same conditions.

Assessment of P. pluvialis *infection*

P. pluvialis infection was monitored by performing isolations and qPCR. Two fascicles (two to four needles per fascicle) per plant were harvested three times a week from four days after inoculation (dai) for one month totalling 12 sampling dates. Fascicles were kept in dampened paper towels and processed within 4 hours of collection. Total needle length and lesion length were recorded, and the percentage of lesioned needle area calculated. One random fascicle was surface sterilized in 70% ethanol for 30 s, rinsed in sterile deionized water, blotted dry on filter paper, and plated onto *Phytophthora* selective CRN media (see above). *Phytophthora pluvialis* colonies were identified morphologically (Reeser et al. 2013) by subculturing in 10% carrot agar and inducing sporangia production in sterilized pond water (Erwin and Ribeiro 1996). *P. pluvialis* isolation was recorded for each fascicle.

The second fascicle was immediately frozen with liquid nitrogen in 5 ml tubes. Genomic DNA extractions and qPCR were performed by a commercial service provider (Slipstream Automation, Palmerston North, New Zealand) using a CTAB/Chloroform-based procedure in an automated robotic workflow. qPCR reactions targeting *P. radiata* and *P. pluvialis* were performed separately (uniplex reactions) in 10-µl aliquots with 1X TaqMan Universal Master Mix, 0.2 µM BHQ-labelled probe, 0.4 µM forward and reverse primers, 1 µl DNA template. Probe and primer sets used for each organism are listed in Table 2.1 (Chettri et al. 2012). The following qPCR conditions were used for *P. radiata*: initial incubation of 10 min at 95 °C followed by incubation of 40 cycles of 10 s at 95 °C and 20 s at 58 °C. For *P. pluvialis*, reaction conditions were: initial incubation of 10 min at 95 °C followed by incubation of 40 cycles of 15 s at 96 °C and 1 min at 60 °C.

Table 2.1. TaqMan probe, primer sets and target genes for relative quantification of *Pinus radiata* and *Phytophthora pluvialis* in DNA extracts of *P. radiata* needles.

Species	Target gene	Probe/ primer	Sequence (5' → 3')	Product size
P. radiata	*CAD*[a]	Probe945[1]	5' /CAL Fluor Orange 560/TGT GAA CCA TGA CGG CAC CC/BHQ1/ 3'	101 bp
		CAD918F[2]	CAG CAA GAG GAT TTG GAC CTA	
		CAD1019R[3]	TTC AAT ACC CAC ATC TGA TCA AC	
P. pluvialis	*Ypt1*[b]	Ypap[1]	5' /FAM/TCC TCC TTG GTA ACG CTA A/BHQ1/ 3'	227 bp
		Ypap2F[2]	AAC TTG GTG CGG TAT TCA CG	
		Ypap2R[3]	ATC AGT TAG CTC CTT TCC	

[a] Chettri et al. 2012, [b] McDougal et al. in prep

[1] TaqMan probes: *P. radiata* probe is labelled with the reporter CAL Fluor Orange 560 (Amidite, emission 556 nm) on the 5' end, the reporter dye for *P. pluvialis* is FAM (6-carboxy-fluorescein; emission 518 nm), all probes are labelled with BHQ1 on the 3' as a quencher; [2] Forward primer; [3] Reverse primer.

Standard curves were constructed amplifying DNA from the two target species: *P. radiata* and *P. pluvialis*. Total DNA was serially diluted 10-fold with sterile PCR-grade water. Linear regressions were performed between log-transformed DNA concentration and Cq using the software R version 3.5.1 (R Core Team 2017). Coefficients of determination (R^2) obtained from linear regression for both species were 1. Standard curves were used to approximate the concentration in ng/µL for each species and sample. The ratio of *P. pluvialis* DNA to *P. radiata* DNA was used as a measure of pathogen abundance.

Assessment of quantification methods and symptom expression

To assess the correlation between re-isolation and qPCR methods with symptom expression, statistical analyses was performed using the software R version 3.5.1 (R Core Team 2017). Both *P. pluvialis* isolation and qPCR detection success (binary dependent variables) were modelled using generalized additive mixed models (GAMMs) with binomial error distribution (function gamm4, package gamm4, Wood and Scheipl 2017). *P. pluvialis* DNA abundance (dependent variable) was likewise modelled using a tweedie error distribution (p = 1.44). In the three models, 'plant identity' nested within 'genotype' were incorporated as random effects to account for repeated measures. 'Dai' and 'lesioned needle length' (proportion) were included in the smoother term separately. Their interaction was tested using bivariate smoothers (t2 argument), followed by a model comparison based on the Akaike Information Criterion (AIC). Backward model selection using AIC test was further used to determine the optimal smoother terms.

Model development

Wake et al (2018) formulated an SI model for the RNC disease, with an additional state variable (P), to account for the pathogen spore density, i.e. the amount of pathogen units that can generate infection (Fig 2.1a). We extended this model to account for the pathogen-host dynamics once infection had started (Fig 2.1b-c). Particularly, we added a new state variable (Q) which corresponds to the fraction of needles that are infected with live pathogen on them (Fig 2.1b-c).

Therefore, the total fraction of infected needles (I) can host either live (Q) or dead pathogen ($I - Q$). This extension helps differentiate between needle death and pathogen death, and allows the empirical contrast of the model fit using data from the detached-needle assay and on-plant inoculation. The extended model presented here is referred to as SIPQ. formulated an SI model for the RNC disease (hereafter referred to as original model, Fig 1a). The original model presents two compartmented state variables for pine needles: susceptible, but not yet infected, i.e. healthy (*S*), and infected (*I*). Infected needles cannot return to the *S* compartment as they die and cast after infection at a rate *x* (Fig 1a). The additional state variable (P) accounts for the pathogen spore density, i.e. the amount of pathogen units that can generate infection (Fig 1a). The pathogen inoculum (*P*) is increased by the spores produced on the infected needles (*g*), and tempered by the mortality rate of spores (*m*). We extended this model (Fig 1b, hereafter referred to as extended model or SIPQ) to account for the pathogen-host dynamics once needles become infected. To do this, we divided the *I* compartment into two new compartments: needles that are infected with live pathogen on them (Q, Fig 1b), and needles that are infected with non-viable pathogen on them, i.e. terminal needles (*T*). Therefore, the total proportion of infected needles (I) can host either infectious (Q) or non-viable pathogen (T), with $I = Q + T$. This division helps clarify the pathogen-host dynamic, with implications in the epidemiology of the disease. On the one hand, infected needles with live pathogen (*Q*) are the only infectious ones, i.e. capable of supporting reproduction of the pathogen and inoculum build-up. On the other hand, terminal needles (*T*) are not infectious anymore. Hence, they do not contribute to the inoculum build-up, but they can have an impact on the tree physiology as they are still attached to the tree. Those needles are presumably carbon sinks, due to the impairment of the photosynthetic apparatus usually associated to foliar infection (Manter, Bond, et al. 2003). This may have an impact on different other processes with feedbacks to the disease epidemic, such as the amount of available carbon and its allocation to defense, or to crown expansion (development of new born needles). Pathogen death has also epidemiological significance in terms the pathogen change to non-wild type colony which is less fit (Kasuga et al. 2016). Thus, the extended model allows for future incorporation of these feedbacks.

The reproduction of spores takes place in the Q compartment and feeds the *P* compartment, as per the original model. This extension helps differentiate between needle death and pathogen death, and allows the empirical contrast of the model fit using data from the detached-needle assay and *in vivo* inoculation. For the purpose of the present study, we omitted the emergence of new born needles input to the *S* compartment, since the conditions of the experiments performed here do not allow new needles to develop and enter the system. The detached-needle assay develops on a fixed amount of needles, and the *in vivo* inoculation experiment lasts 28 days, during which no new needles were formed, due to the winter conditions. However, it is important to note that, for multi-season experiments, new born needles would be developed, and other would naturally die. In this case, *b* (in the original model) will be different from 0, and a new flow should be added from the *S* compartment which would correspond to the needles dying for reasons other than the RNC disease.

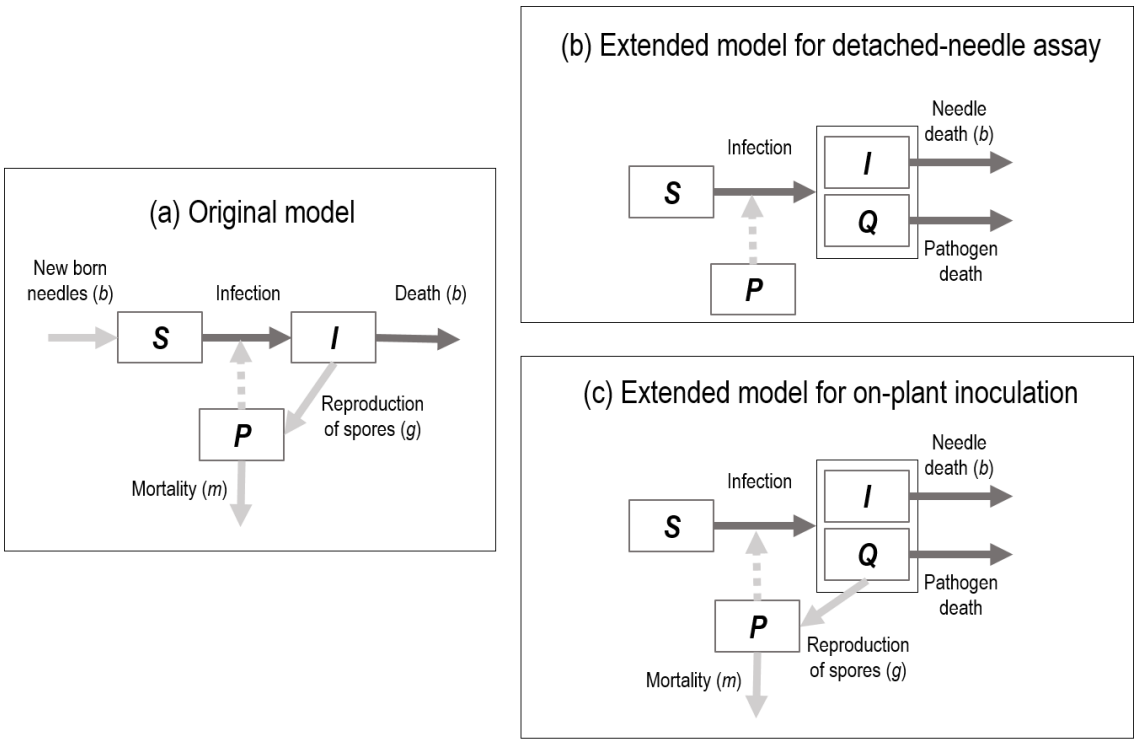

Figure 2.1. Modifications of the SI original model (a) by Wake et al. (2018) to obtain the SIPQ model (b) to use the empirical data provided by the detached-needle assay and *in vivo* inoculation.

For the SIPQ model, the five differential equations for proportion of healthy needles (*S*, Eq 2.1), spore density (*P*, Eq 2.2), proportion of needles with infectious pathogen (*Q*, Eq 2.3), and proportion of needles with non-viable pathogen (*T*, Eq 2.4) are:

$$\frac{dS}{dt} = -kSP \tag{2.1}$$

$$\frac{dP}{dt} = gI\left(1 - \frac{min(P, P_{max})}{P_{max}}\right) - mP \tag{2.2}$$

$$\frac{dQ}{dt} = kSP - nQ \tag{2.3}$$

$$\frac{dT}{dt} = nQ - xT \tag{2.4}$$

As the model acts on a proportional interpretation, the total proportion of infected needles (*I*) is given by $I = 1 - S$. Table 2.2 gives a description of all model parameters in Eqs 2.1-2.4. Fig 2.2 illustrates model behaviour with two different assumptions: *P* saturated and constant (first-column plots, see section 'Applying the model to the detached-needle assay'), and *P* varying along the infection period (second-column plots, see section 'Applying the model to the *in vivo* inoculation'). The effect of changes in the two most important model parameters – *k,* infection rate, and *n*, pathogen death rate – is also shown.

Table 2.2. Description of variables and parameters used in the SIPQ model for RNC infection with *Phytophthora pluvialis*.

Parameter	Description
S	state variable for the proportion of needles that is healthy
I	state variable for the proportion of needles that has been infected
P	state variable for spore density on the needle surface
Q	state variable for the proportion of needles with infectious pathogen in them
T	state variable for the proportion of needles with non-viable pathogen in them
x	death rate of infected needles
k	infection rate
g	spore birth rate
m	death rate of spores
n	death rate of pathogen in host material

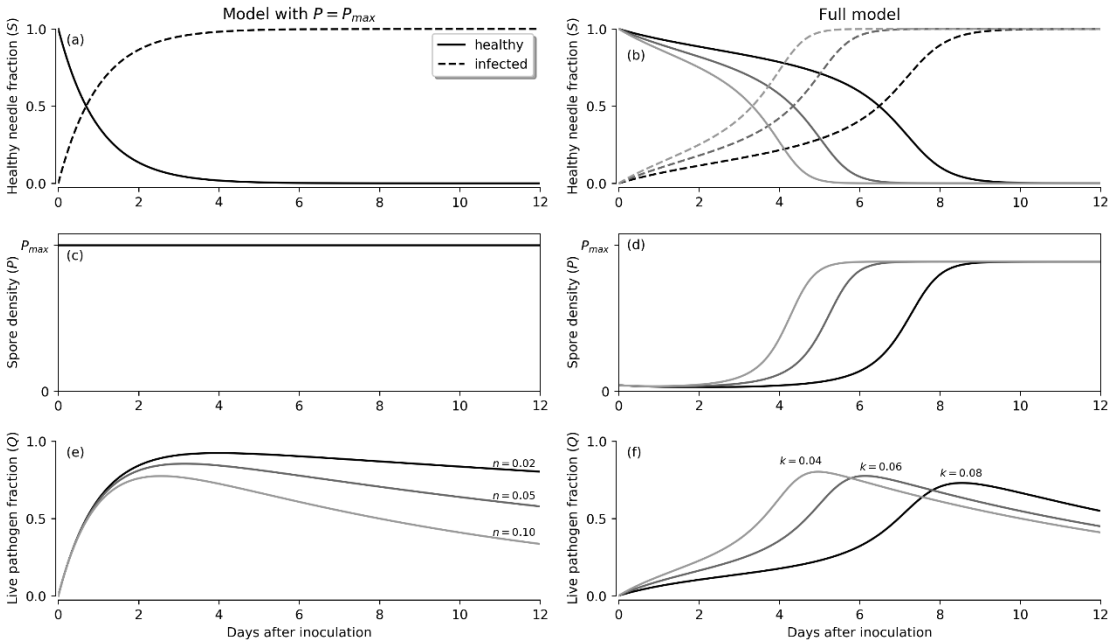

Figure 2.2. Illustration of the time-dependent behaviour of the model ODE (ordinary differential equations) of Eqs 2.1-2.2 and 2.4 under various conditions. First column plots correspond to the model extended for the detached-needle assay, and second column plots, to the extension for the *in vivo* inoculation. Fraction of healthy needles, *S* (a-b), spore density, *P* (c-d), and fraction of needles with live pathogen, *Q* (e-f) are shown. n: pathogen death rate; k: infection rate.

Applying the epidemiological model

Applying the model to the detached-needle assay

In the detached-needle assay, individual fascicles were dip inoculated with a zoospore suspension. In this process, the zoospores primarily infect at the surface of the inoculum due to negative gravitaxis and oxygen chemotaxis (Allen and Newhook 1973, Häder 1999), at which point they encyst on the plant surface, and germinate penetrating through to the intercellular space (Fawke et al. 2015). Following a period of intercellular growth, mycelium emerges through stomatal openings and sporangia are produced. We designate incubation time (τ_m) to the time delay from inoculation to the re-emergence of mycelium growth and sporangia production on the needle surface. From the detached-needle assay, we obtained three measured variables (observables): isolation rate (R_{isol}, Eq 2.5), which is obtained by isolation of pathogen from needle fragments into culture media; presence of mycelium on the needle surface (R_{myc}, Eq 2.6) and presence of sporangia (R_{spor}, Eq 2.7), observed using fluorescence microscope. Those observables relate to the live pathogen on the needle, Q.

$$R_{isol} = c_i Q \tag{2.5}$$

$$R_{myc} = c_m Q(t - \tau_m) \tag{2.6}$$

$$R_{spor} = c_s Q(t - \tau_s) \tag{2.7}$$

where $c_{i,m,s}$ are the detection responses for the observables, i.e. the experimental test sensitivities, and τ_m and τ_s are the time delays between infection and the growth of mycelium and sporangia(i.e. incubation time), respectively. In the detached-needle assay, we assumed that the time delay between growth of mycelium on the needle surface and sporangia production can be neglected as their emergence could not be differentiated in this instance. We assumed that this time delay was shorter than the time between our individual observations (sampling period of two days). Therefore, we assumed that $\tau_m = \tau_s$ in the detached-needle assay. The incubation periods have typically taken the form of Weibull, Frechet or gamma distributions, i.e. long-tailed distributions with an asymmetric peak and support on the positive domain (Cairns 1990). We modelled the incubation time probability density $p(\tau_m)$ by a Frechet distribution with a shape parameter of 2 (Eq 8) because it yields approximately the right shape (see Fig 3), and the scale and location parameters provide enough degrees of freedom to fit the experimental observations.

$$p(\tau_m) = \frac{2}{\sigma}\left(\frac{t-\mu}{\sigma}\right)^{-3} \exp^{-\left(\frac{t-\mu}{\sigma}\right)^{-2}} \tag{2.8}$$

We report the mode of this distribution as the fit parameter τ_m.

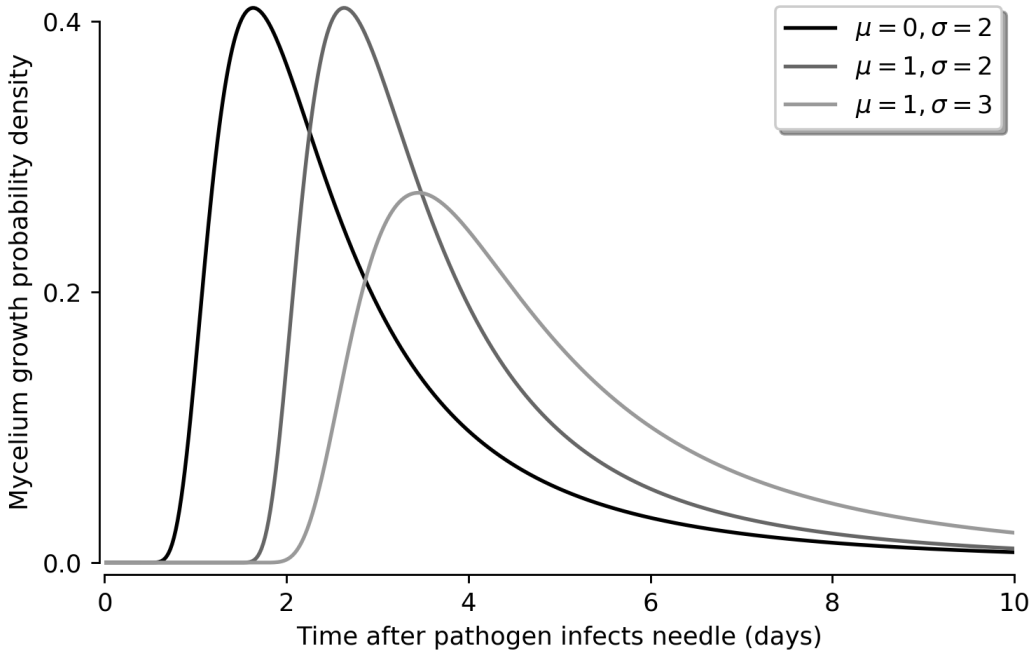

Figure 2.3. Shape of distribution for modelling incubation time (τ_m) for different values of the location (μ) and shape (α) parameters of that distribution.

The empirical conditions of the detached-needle assay imposed two additional assumptions. As the inoculation took place in a fixed number of needles, the needle birth rate was assumed to be zero ($b = 0$). Furthermore, the dip inoculation procedure implied that needles were saturated with spores, i.e. at the maximum carrying capacity of the needles. Hence, we used $P = P_{max}$ along the whole experimental period of 11 days. From that assumption, we resolved that infection dynamics was only due to primary infection. Finally, we also assumed that all the infected needles can produce isolates.

Fitting the detached-needle assay experimental data

The initial conditions to solve the model were $S_0 = 1$ and $Q_0 = 0$. The ordinary differential equations for *S* and *Q* (Eqs 2.1 and 2.3) can be solved analytically (see Supplementary material).

We used a Bayesian approach to estimate parameter values and their uncertainties (VanderPlas 2014). The likelihood function given our model $\hat{y}$ with modelled Gaussian errors with standard deviation σ added is given in Eq 2.9.

$$\mathcal{L}(\{t_i\}, \{y_i\} | k, n, c_m, \tau_m) \propto (2\pi\sigma^2)^{-\frac{N}{2}} \prod_{i=1}^{N} \exp\left[\frac{-(y_i - \hat{y}(t_i|k,n,c_m,\tau_m))^2}{2\sigma^2}\right], \quad (2.9)$$

where *N* is the number of data points, and y_i represents and observable. The parameters k, n and τ_m need to be positive and, to make the fit process converge, it is helpful that they are bounded. The parameter c_m is a detection response and must range 0-1 by definition. Hence, based on our biological understanding from previous work and inspection of our raw experimental data, we used bounds that are at least 4 times larger than values we can realistically expect, the prior distribution contains the following bounds on parameter values: k and n in (0, 0.3), c_m in (0,

1), τ_m in (0, 6) and $\sigma > 0$. Within those bounds, we used a flat prior. We used an Affine Invariant Markov chain Monte Carlo (MCMC) sampler (Goodman and Weare 2010), provided in the emcee package (Foreman-Mackey et al. 2013), to sample the posterior distribution. We used 100 sampling chains, initialized by adding 20% random noise around the maximum likelihood estimate of parameter values, with 15000 steps of which the first 1000 were burn-in samples. At each step, we solved $\hat{y}$ by numerical integration over $p(\tau_m)$.

To verify that MCMC sample was well-behaved, we calculated the parameter autocorrelation lengths. The autocorrelation lengths were 760 samples, i.e. chain length was 18 independent samples, for parameter k; and in the range of 50-230 samples, i.e. > 60 independent samples, for all the other parameters. Jump acceptance fractions were in the range of 0.28-0.32 for all the chains. For more details and plots of all parameter covariances, see the Supplementary material.

Applying the model to the on-plant inoculation

The experimental observables for the *in vivo* inoculation are the isolation rate, which in this experiment is the proportion of pathogen detected by isolation (R_{isol}, Eq 2.10) and by qPCR (R_{qpcr}, Eq 2.11), as well as the pathogen-to-host DNA ratio from qPCR and sporangia (R_{dna}, Eq 2.12).

$$R_{isol} = c_i\, Q \tag{2.10}$$

$$R_{qpcr} = c_q Q \tag{2.11}$$

$$R_{dna} = c_d Q \tag{2.12}$$

The assumptions made for the detached-needle assay are valid for the *in vivo* inoculation, with one exception. The spore density is not constant in the *in vivo* inoculation, hence *P* is variable (Fig 2.1c, Fig 2.3d). In this experiment, we thoroughly sprayed the plants with a suspension of zoospores. The amount of spores reaching the needles that were subsequently sampled is not defined. It cannot be assumed that spore density was at the maximum carrying capacity of the needles at the time of inoculation. Further, across the assay, spore density changes due to secondary infection, which in turn may decline with time (Otten et al. 2003).

In the *in vivo* inoculation, we cannot model τ_m because we did not perform microscopic observations of mycelium and sporangia (R_{myc}, R_{spor}). Instead, we used the parameter (g) in Eq 2 to determine the spore birth rate. Like in the detached-needle assay, we assumed that the needle birth rate (b) was zero for the 28-day period the experiment spanned. Indeed, we did not observe development of new shoots and needles, as the fog-room conditions of temperature, photoperiod and humidity were chosen such that they resemble as closely as possible a New Zealand winter season.

Fitting the in vivo *inoculation experimental data*

The initial conditions to solve the model were $S_0 = 1$ and $Q_0 = 0$. The state variable P_o was unknown, as the inoculum was sprayed on the plant. Therefore, P_o was a fitted parameter. We observed that our measurements exhibit heterocedasticity. We modelled this with additive and

multiplicative Gaussian terms, to account for both constant errors and contributions that are proportional to the pathogen concentration (Eq 2.13).

$$\Delta y_i = \left(0.4 + \frac{y_i}{max(y)}\right)\sigma \quad (2.13)$$

The number of time series data points and the amount of noise did not allow the determination of m. Simulations showed that a minimum of 20 data points would be required to determine m (see Supplementary material). Thus, we fixed m to a constant value of 0.15, which is biologically reasonable and lays in the middle of the range of values for m, for which good model fits can be obtained.

Taking into account all previous considerations, the model followed Eqs 2.1, 2.3, 2.4, 2.14 (replacing Eq 2.2) and 2.15 (replacing Eq 2.9).

$$\frac{dP}{dt} = gI\left(1 - \frac{min(P, P_{max})}{P_{max}}\right) - 0.15P \quad (2.14)$$

$$\mathcal{L}(\{t_i\}, \{y_i\}|k, n, g, P_0, c_{i,q,d}, \sigma) \propto (2\pi\sigma^2)^{-\frac{N}{2}} \prod_{i=1}^{N} \exp\left[\frac{-(y_i - \hat{y}(t_i|k,n,g,P_0,c_{i,q,d},\sigma))^2}{2(\Delta y_i)^2}\right], \quad (2.15)$$

Similarly to the detached needle assay, we used a flat prior, with the following bounds: k in (0, 0.05), n in (0, 1), g in (0, 50), P_0 in (0, P_{max}), $c_{i,q,d}$ in (0, 1), and $\sigma > 0$. The MCMC sampler did not converge well due to the limited amount of data. The parameter autocorrelation lengths were on the order of the chain length. However, jump acceptance fractions were acceptable, in the range of 0.25-0.42 for all the chains. We verified that the parameter estimates agreed with the maximum likelihood estimate and with brute force optimization. Thus, estimates and confidence intervals should be reliable. For more details, see Supplementary material.

Results

Detached-needle assay: comparing susceptible and resistant genotypes

The model fit for the detached-needle data is shown in Fig 2.4. The infection rates and the incubation times were similar for both resistant and susceptible genotypes (Table 2.3). Pathogen death rate was 2.5 times higher for resistant than susceptible genotypes (Fig 2.4a-b, Table 2.3). Further, only 28% of the resistant ramets produced mycelium and sporangia, whereas 90% of the susceptible ramets did (Table 2.3).

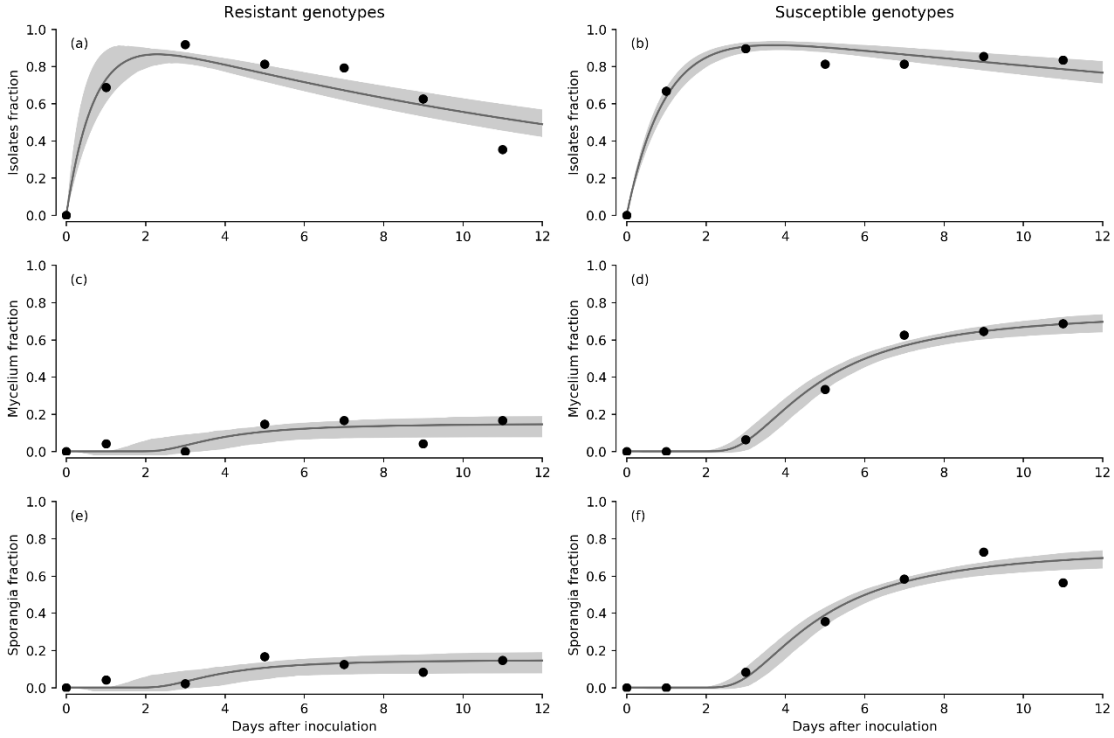

Figure 2.4. Time series data for the isolates (a-b), mycelium (c-d) and sporangia (e-f) fractions from the detached-needle assay for resistant (a, c, e) and susceptible (b, d, f) genotypes, with the SIPQ model fits to the data. Shaded areas are the 95% credible regions of the fit.

Table 2.3. Model parameter estimates (median) for the detached-needle assay with 95% credible regions.

Parameter	Resistant genotypes	Susceptible genotypes
k	$0.014^{+0.017}_{-0.004}$	$0.010^{+0.002}_{-0.002}$
n	$0.063^{+0.014}_{-0.012}$	$0.024^{+0.008}_{-0.007}$
c_m	$0.28^{+0.35}_{-0.12}$	$0.90^{+0.09}_{-0.17}$
τ_m	$3.2^{+1.5}_{-1.6}$	$3.7^{+0.4}_{-0.4}$

The distribution of lesions lengths also differed between resistant and susceptible genotypes (Fig 2.5). In resistant genotypes, small lesions and no lesions appeared to be most frequent, while in susceptible genotypes, lesion lengths spread from 0 to 100 mm (Fig 2.5). Susceptible genotypes presented higher sporangia production (Fig 2.6a), which aligned with higher lesion lengths, except for genotype g7 which showed low sporangia production despite the highest lesion length magnitude within susceptible genotypes (Fig 2.6b). Sporangia production was also related to proportion of needles with lesions, showing susceptible and resistant genotypes grouped apart, except for susceptible g7 (Fig 2.6c).

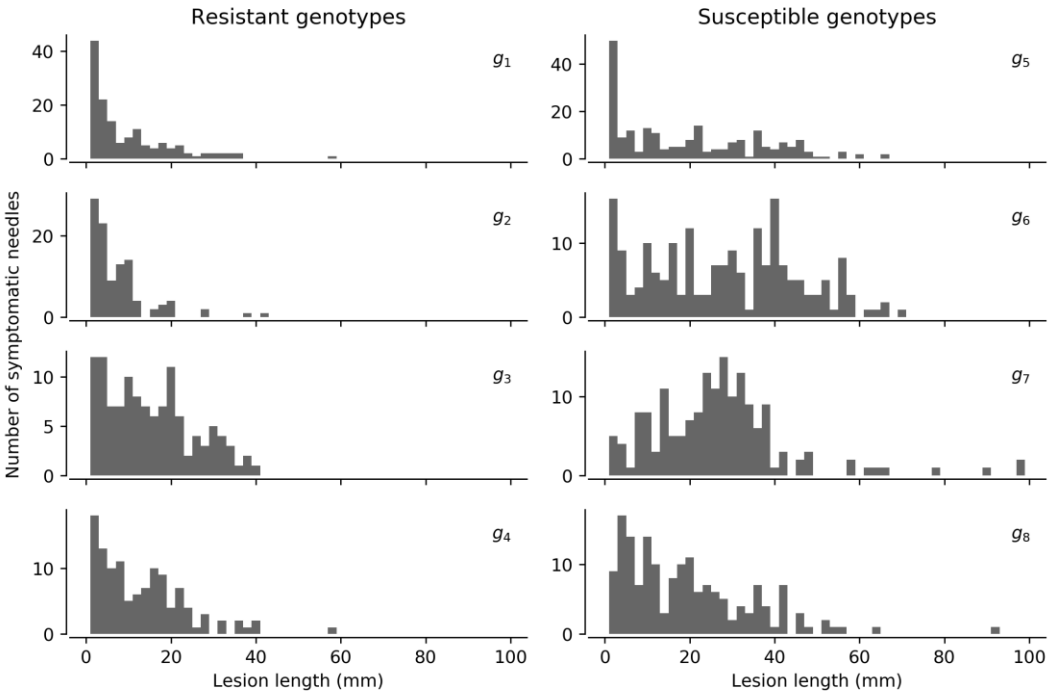

Figure 2.5. Histograms of lesion lengths per genotype for four resistant (g1, g2, g3, g4) and four susceptible (g5, g6, g7, g8) genotypes in the detached-needle assay.

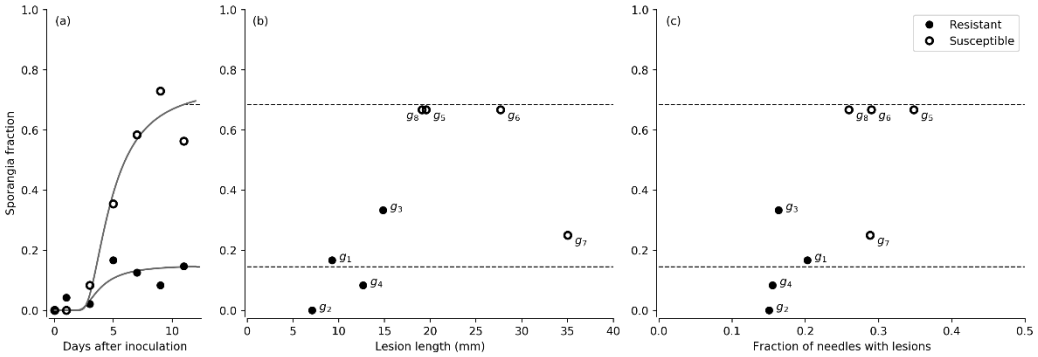

Figure 2.6. Connecting the model fit for sporangia fraction (a) to the lesion lengths (b) and the fraction of needles with lesions (c), both at the last time point in the time series (11 days). This is the only point at which the lesions were measured.

In vivo inoculation

The proportion of needles with live pathogen (detected by isolations and qPCR) and with lesions and the proportion of lesioned needle length presented all a first peak at four days after inoculation (Fig 2.7a-b, d). Detection by qPCR and pathogen-to-host DNA ratio were maximum at 20 days after inoculation, and then decreased (Fig 2.7a). In contrast, the peak of detection was reached at 22 and 26 days after inoculation by isolation (Fig 2.7a). Detection by qPCR was more effective and showed an earlier and higher peak than isolations (Figs 2.7a and 2.8a-b). Pathogen-to-host DNA ratio peaked at a similar time to the proportion of needles with live pathogen (Figs 2.7a, c

and 2.8b, c). The estimation of *n* is mainly determined by the negative slope of *Q* after the maximum live pathogen proportion has been reached (as illustrated in Fig 2.8c). As data of detection by isolation has only two time points after that peak, the fit for detection by isolation is the least well behaved, in particular for *n* (see Supplementary material).

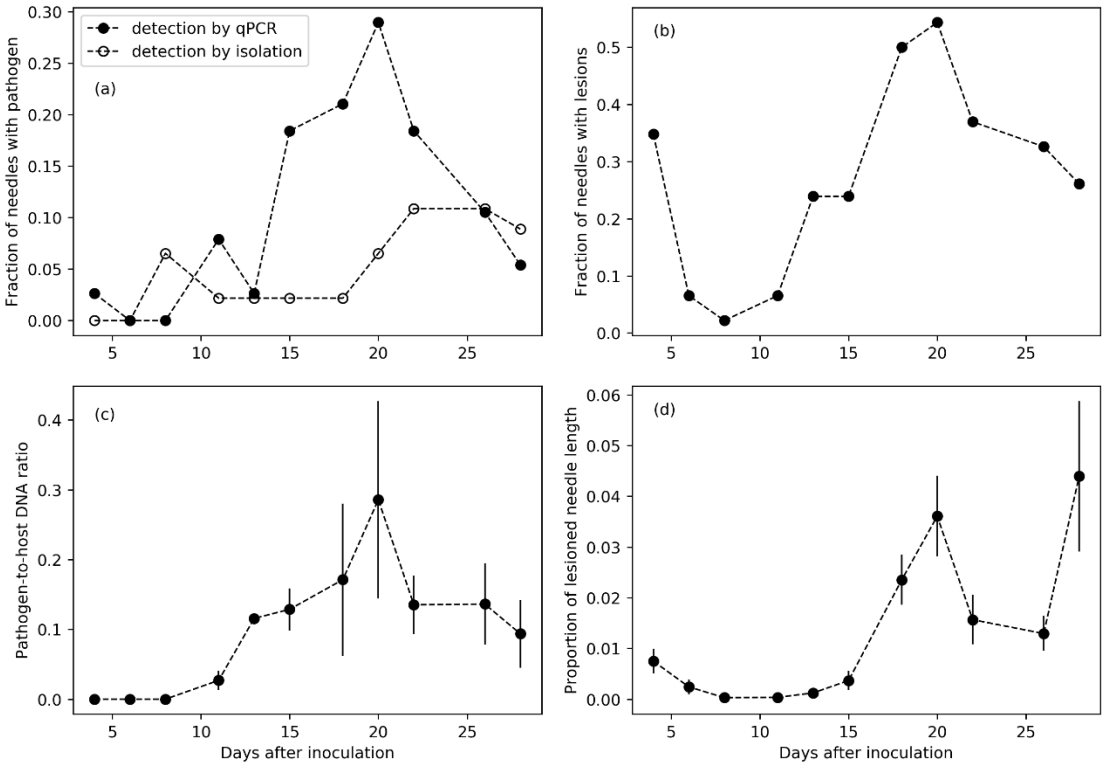

Figure 2.7. Time series data for the fraction of needles with live pathogen (a) detected by qPCR and isolations, fraction of needles with lesions (b), pathogen-to-host DNA ratios (c) and proportion of lesioned needle length (d) averaged per time point in the on-plant inoculation. Symbol and bars represent means ± standard error.

The infection rate (*k*), the spore birth rate (*g*) and the proportion of needles with live pathogen (detection response, $c_{i,q,d}$) were predicted to be higher when qPCR methods were used to assess infection, compared to isolation (Table 2.4). Further, the pathogen death rate (*n*) and the carrying capacity of spores at inoculation were predicted to be higher when isolation was used to assess infection. However, the 95% credible regions were wide with overlap between the three methods compared. This is due to the limited number of data points in the time series data, and the relatively large amount of noise per point (see standard errors bars in Fig 2.7c, d).

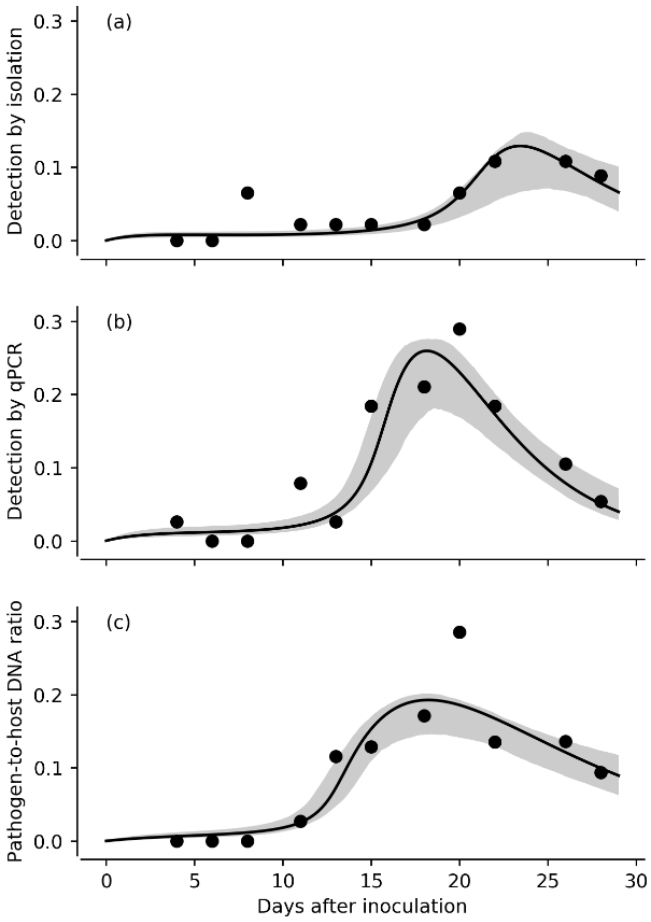

Figure 2.8. SIPQ model fits for the fraction of needles with live pathogen detected by isolations (a), qPCR (b), and the pathogen-to-host ratio (c) for the on-plant inoculation. Shaded areas are the 95% credible regions of the fit.

Table 2.4. Model parameter estimates for the on-plant inoculation with 95% credible regions for infection rate (*k*), pathogen death rate (*n*), spore birth rate (*g*), carrying capacity of spores for each needle at inoculation time (P_0) and the detection response for the observables ($c_{i,q,d}$).

Parameter	Isolation	qPCR	DNA ratio
k	$0.0041^{+0.0086}_{-0.0029}$	$0.0056^{+0.018}_{-0.003}$	$0.0036^{+0.016}_{-0.0022}$
n	$0.54^{+0.41}_{-0.47}$	$0.36^{+0.38}_{-0.23}$	$0.16^{+0.48}_{-0.13}$
g	$4.5^{+7.3}_{-2.8}$	$7.4^{+10}_{-5.1}$	$12^{+20}_{-9.4}$
P_0	$1.9^{+3}_{-1.2}$	$1.2^{+1.7}_{-0.81}$	$1.4^{+2.1}_{-0.94}$
$c_{i,q,d}$	$0.82^{+0.88}_{-0.64}$	$0.94^{+0.92}_{-0.6}$	$0.53^{+1.2}_{-0.34}$

Assessment of quantification methods and symptom expression

For the *in vivo* inoculation, we complemented the model fits with GAMM models to analyse the link between quantification methods (isolation and qPCR) and lesion length. The GAMM models showed an increase of the isolation rate across time and no effect of lesion length on isolation

success (Table 2.5). In contrast, detection of *P. pluvialis* through qPCR did correlate with the proportion of lesioned needle length, with a maximum of qPCR detection rate of 19% symptomatic tissue (total needle length) at 18 days after inoculation, according to the predictions of the GAMM model (Table 2.5, Fig 2.9a). *P. pluvialis* abundance on the needles measured as pathogen-to-host DNA ratio decreased with both days after inoculation and the proportion of lesioned needle length (Table 2.5, Fig 2.9b).

Table 2.5. Results from the best-fitted generalized additive mixed models for the isolation rate, qPCR detection rate, and *P. pluvialis* abundance measured as pathogen-to-host DNA ratio. Dai: Days after inoculation; lesion: proportion of lesioned needle length; edf: estimated degrees of freedom; t2: bivariate smooth term.

	Isolation rate			**qPCR detection rate**			***P. pluvialis* abundance**		
	Family: binomial Link: log			Family: binomial. Link: logit			Family: tweedie (1.44). Link: log		
Parametric coefficients	**Estimate (SE)**	**z**	**P**	**Estimate (SE)**	**z**	**P**	**Estimate (SE)**	**z**	**P**
Intercept	-4.96 (0.71)	-6.98	<0.001	-3.04 (0.31)	-9.78	<0.001	-4.83 (0.26)	-18.71	<0.001
Dai	0.10 (0.03)	3.02	0.003						
Bivariate smooth terms	**edf**	**Chi.sq**	**P**	**edf**	**Chi.sq**	**P**	**edf**	**F**	**P**
t2(Dai, lesion)				6.79	23.73	0.003	3	23.88	<0.001

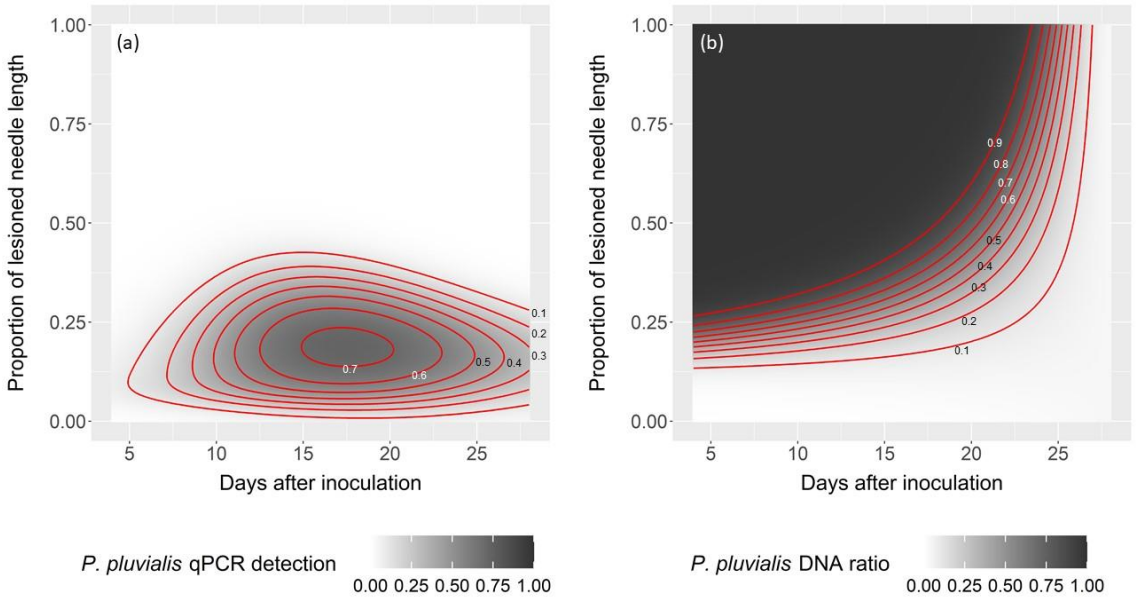

Figure 2.9. Predicted fraction of needles with live pathogen, i.e. *P. pluvialis* qPCR detection rate (a), and *P. pluvialis* DNA ratio (pathogen-to-host DNA ration, b) as a function of days after inoculation and the proportion of lesioned needle length. Predictions were derived from generalized additive mixed effects models applied to the on-plant inoculation data. Both predictors (x and y axes) are statistically significant at $\alpha = 0.05$.

Discussion

In this study, we developed an extended RNC epidemiological model, which was tested against experimental data for susceptible and resistant genotypes to parameterize the infection drivers in both detached-needle and *in vivo* inoculations. Moreover, we scaled up our epidemiological model to analyze the infection dynamics for susceptible genotypes at the whole-plant level. With this *in vivo* inoculation data, we also contrasted the methods of detection used in assessing infection in relation to symptom expression. The extended model introduced the state variable *Q* which allowed us to account for the dynamics of the pathogen on the needle. That is particularly important for the polycyclic RNC disease. This model fits presented here provided insights into the drivers of the RNC epidemic. Whole-plant infection dynamics identified the challenge of high noise in the sampling points, but indicated that the detection method applied to assess disease was the single most important factor influencing parameter estimates.

Comparing susceptible and resistant genotypes

The detached-needle assay was carried out under laboratory conditions, which favoured infection and pathogen development through maximum pathogen load and minimizing defence ability to fight disease by needles detached from stems. Thus, the susceptible plant material in this experiment provided optimal conditions for the pathogen and the maximum likely values for k (infection rate) and minimum values of τ_m (incubation time).

While infection rates (*k*) and incubation times (τ_m) were similar between susceptible and resistant genotypes, the pathogen death rate (*n*) was 2.5 times higher for resistant genotypes (Table 2). Mycelium and sporangia were produced extensively in susceptible, but not in resistant genotypes (Table 2.2). Therefore, in resistant genotypes, the pathogen was observed to infect, but seldom produced reproductive structures. Fewer and smaller lesions were produced by the pathogen in the resistant genotypes (Figs 2.5 and 2.6), suggesting that the survival of the pathogen is limited within the necrotrophic phase in the resistant genotypes. Lesion development appeared to align with sporulation, with low levels of both in resistant genotypes (Fig 2.6). This indicates that the necrotrophic phase of *P. pluvialis* may be linked to the sporulation of the pathogen. The incubation time was surprisingly not linked to disease resistance, and was either constant across host individuals, or dependent on other unknown factors. The differences detected through the SIPQ model between resistant and susceptible genotypes suggested a stronger defence strategy or pathway in resistant genotypes, which may be informative for disease resistance screening and applied management of the disease. Other Phytophthora hosts have been reported to present intraspecific variability in susceptibility (*Phytophthora ramorum*, O'Hanlon et al. 2016). A better understanding of the defence response in resistant genotypes should be given attention in further research.

The detached-needle assay model fit reflected the primary infection rate of the pathogen, as the experimental design did not allow for secondary inoculum production and infection of newly emergent needles. The peak of the infection took place 3 days after inoculation (Fig 2.4a-b) and

was similar in both susceptible and resistant genotypes. This peak was in conditions optimal for pathogen development, and may well occur later in the field.

Scaling up to whole-plant infection dynamics

In our *in vivo* inoculation, we aimed to describe the sustained infection dynamics of whole plants to account for variable amounts of inoculum across primary and secondary infection and their respective transmission rates being closer to what occurs naturally in the field. We commenced disease monitoring 4 days after inoculation. Pathogen isolation, qPCR detection rate and lesion development each presented dual peaks. For qPCR detection and lesions, the first peak occurred at the first sampling point (4 dai), while for isolations the primary peak was observed at the second sampling point (6 dai) (Fig 2.7a-b, d). A distinguishable peak for primary infection has been previously reported in other epidemiological studies (Otten et al. 2003, Mammeri et al. 2014). Having distinguished this primary infection cycle, we were able to quantify the polycyclic infection by *P. pluvialis*. Based on the *in vivo* experiment, re-infection cycles will occur within 4-6 days. The peak at 6 days after inoculation detected by isolations in the *in vivo* inoculation was delayed by three days compared to the detached-needle assay (same detection method). This lag in the *in vivo* inoculation trial is most likely attributable to more vigorous defences afforded by the intact physiological connection between needles and the remaining plant body in contrast to detached needles.

Following secondary infection and the resultant second peak of the epidemic, the infection rate detected by qPCR decreased more quickly compared to isolations. Secondary infection has been recognized to slow down due to several factors. First, there is a decrease in availability of uninfected susceptible plant material (Otten et al. 2003) so that the probability of the spores reaching healthy needles decreases. This is particularly true for this study in which the experimental conditions simulated the winter season. In these conditions, over the course of the experiment, no new flush was observed and hence no new needles were available for infection. Secondly, the susceptibility of plants decreases due to the systemic acquired resistance. This process confers a stronger defence response upon secondary infection to leaves distal to the primary focus of infection (Ryals et al. 1996, Jung et al. 2009). Finally, needle age may also have a role in modulating the transmission rate of infection. RNC disease has been recognised to preferentially infect fully mature needles (Dick et al. 2014). In our experiment, we observed this preference, however, current-year needles also became infected under high infection pressure. We presume that current-year needles may be better defended than older needles, in agreement with the optimal defence theory (Zangerl and Bazzaz 1979), slowing down pathogen development. Our experimental design did not allow us to distinguish between primary and secondary infection at the needle scale. However, the pattern of infection is consistent with polycyclic infection observed for *Phytophthora* pathogens and *P. pluvialis* epidemiology observed to date (Ganley et al. 2014). We can therefore infer that the first peak was due to primary infection, i.e. zoospore solution being the source of the inoculum, matching the detached-needle assay (approx. 3 days after inoculation), and the second peak was due to secondary infections from sporulating needles.

Comparing *P. pluvialis* assessment procedures

Diagnostic methods seem to play a crucial role in defining the dynamics of *P. pluvialis* infection and associated development of RNC. In our method comparison (Table 2.4, Fig 2.8), the 95% credible regions overlap due to high noise in the sampling points. However, it is clear that the isolation and qPCR approaches lead to qualitatively different epidemic outputs and, moreover, the detection method also had the greatest influence on the parameter estimates in our models.

Regardless of the detection method, the infection level decreases after an early peak, whereas the proportion of lesioned needle length peaks at the end of the experiment. We observed that secondary infections due to other pathogens (*Dothistroma* sp., *Cyclaneusma* sp., *Pestalotiopsis* sp.) took place with lesions that occupied space on the needles. Even though the grafts were sanitized before the experiment, residual spores from other pathogens are likely to have remained on and within the well-established grafts and contributed to the proportion of necrotic tissue not available for infection by *P. pluvialis*. Detection by qPCR predicted an earlier second peak and a sharper decrease in the epidemic compared to isolations (Fig 2.8a-b). These differences can be explained by two factors. On the one hand, the latent detection by isolations may reflect a lack of intercellular invasion by *P. pluvialis* in the early stages of infection whereby surface sterilization may actually kill the mycelium established peripherally within the stomata. On the other hand, the low detection rates by qPCR at the later stages of the epidemic suggests that qPCR is more sensitive to the presence of secondary pathogens and/or dead cells than isolations. Indeed, proportion of lesioned needle length did not explain the variability in isolation rates, which was only explained by the days after inoculation (Table 2.4). In contrast, both *P. pluvialis* qPCR detection rate and DNA ratio were significantly influenced by both days after inoculation and lesion length (Table 2.4, Fig 2.9a). Detection by qPCR was optimal when 19% of the needle was lesioned with longer lesions associated with decreased qPCR detection, probably due to the presence of inhibitors (Fig 2.9a) (Hughes et al. 2006, Schena et al. 2006, Vettraino et al. 2010). While isolations measure the viability (outgrowth) of the pathogen, qPCR measures the presence of *P. pluvialis* DNA, being the pathogen either viable or dead. We argue that the timeframe of the experiment is short enough for the DNA to degrade. Hence, qPCR detection may include non-viable *P. pluvialis* inoculum. The proportions given by isolations and qPCR detection are proportions of infected needles, in contrast to *P. pluvialis* DNA ratio, which measured the average amount of DNA of *P. pluvialis* on the needles with respect to *P. radiata* DNA. This ratio was predicted to decrease with the days after inoculation, but was higher with larger lesion lengths (Fig 2.9b). Thus, in needles with lesions larger than the 25% of the needle length, detection rates are low (false negative), but, when positive, qPCR accurately detects high amounts of DNA, as expected (Fig 2.9a-b). This indicates a threshold-dependent accuracy for qPCR-based determination of *P. pluvialis* DNA. That can be due to the fact that a larger presence of necrotic tissue may contain higher levels of inhibitors which can adversely affect qPCR (Hughes et al. 2006, Schena et al. 2006).

The extension of the SI to the SIPQ epidemiological model provided substantial information about the drivers of RNC disease. In a polycyclic infection, it is important to include the proportion of infected needles with live pathogen on them, as well as the rates of pathogen birth and death. Thus, we were able to estimate the primary peak of the infection at the plant level to occur after 4 to 6 days (depending on the detection method), reflecting the period needed for *P. pluvialis* to establish re-infection. Our analyses showed that the choice of *Phytophthora* assessment method is key for epidemic prediction. qPCR was more sensitive than isolations earlier in the infection process, making it the best option for quantifying the early stages of disease epidemics. However, a combined detection method may yield the most realistic scenario. With the characterization of the disease epidemic at the tree level presented here, a spatial characterization at the forest level can be explored. The SIPQ model shows promise for expanding its use to infer prediction models for the RNC disease. Silvicultural settings, edaphic and (seasonal) climatic conditions associated with *P. radiata* plantations can readily be incorporated into the SIPQ model allowing the identification and quantification of further disease-conducive factors. That would provide a wider modelling framework to successfully establish integrated disease management programmes for the RNC deisease.

Supplementary material

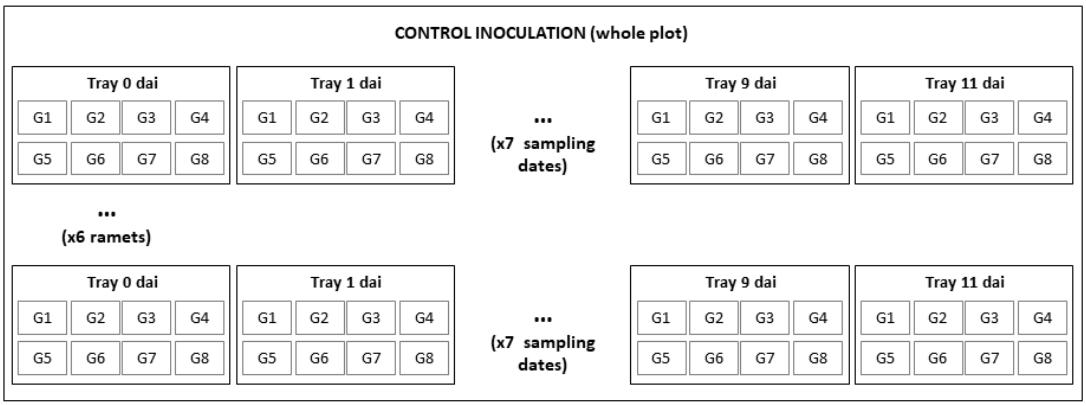

Figure S2.1. Experimental design for the detached-needle assay, only shown for control treatment. Each tray has five fascicles from one ramet from each genotype and is harvested at a certain date. There are six trays sampled at a certain date. The *P. pluvialis* inoculation treatment has the same implementation. The trays are randomly distributed in the space.

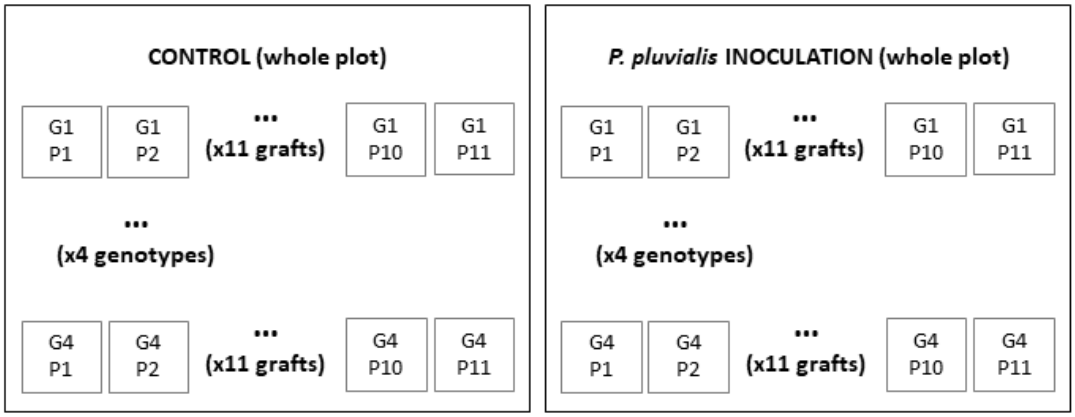

Figure S2.2. Experimental design for the *in vivo* inoculation experiment. All the plants are randomly distribute in each room. All the plants are sampled in each sampling date.

Analytical solution for the detached-needle assay model fit

Given the needle assay experimental details, which imply no new needle birth ($b = 0$) and spore density saturation ($P = P_{max}$), the model follows Eqs 2.15 and 2.16.

$$\frac{dS}{dt} = -kSP \tag{2.15}$$

$$\frac{dQ}{dt} = -\frac{dS}{dt} - nQ \tag{2.16}$$

The solution for *S* is a simple exponential decay, $S(t) = e^{-kPt}$. The solution for Q follows Eq 2.17.

$$Q(t) = \begin{cases} -kPte^{-kPt} & \text{for } n = kP \\ \frac{kP}{n-kP}(e^{-kPt} - e^{-nt}) & \text{otherwise} \end{cases} \tag{2.17}$$

Detached-needle assay model fit details

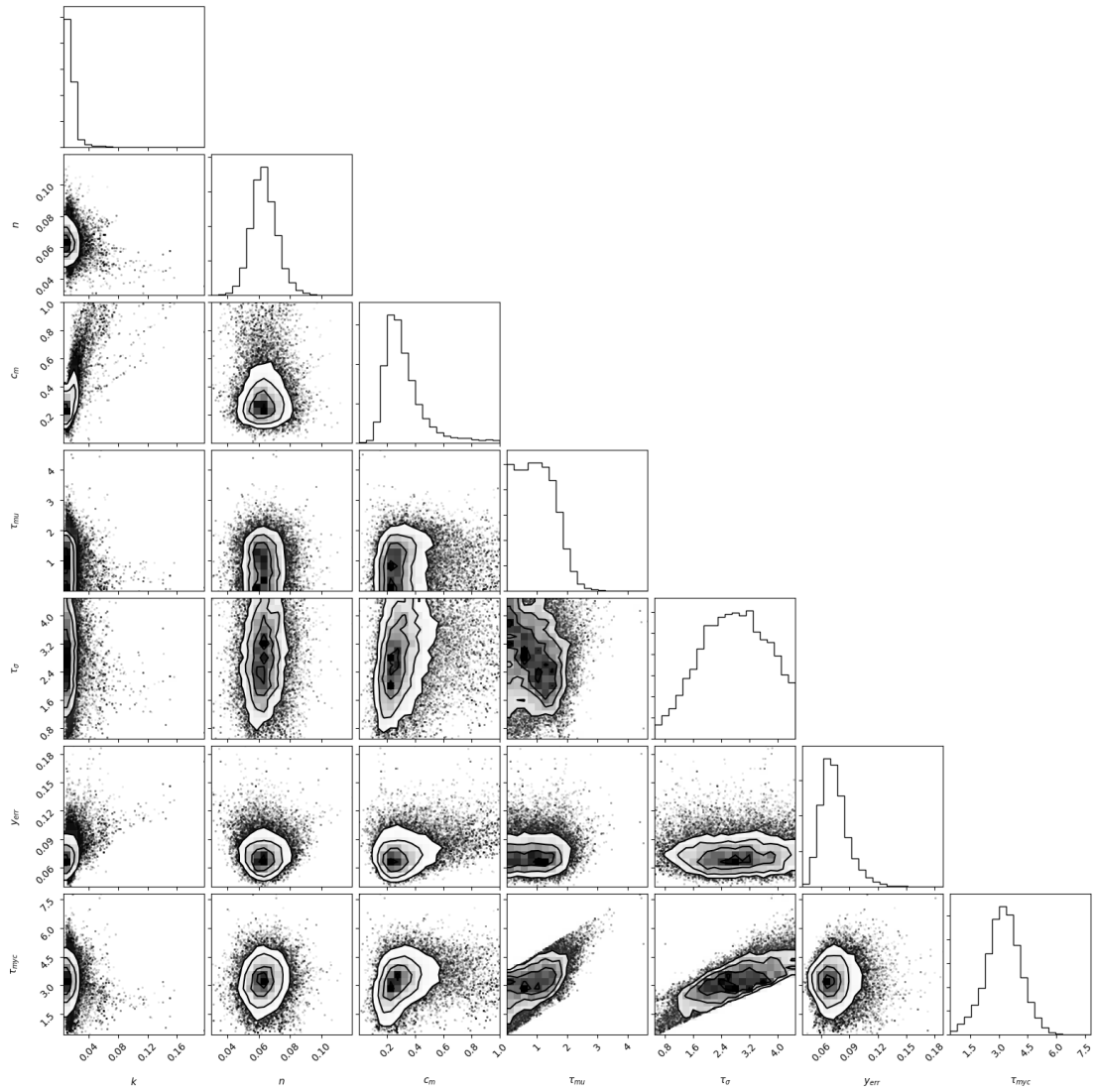

Figure S2.3. Posterior probability distributions of model parameters for the fit of the model with ($\boldsymbol{P = P_{max}}$) to the detached-needle assay data for resistant genotypes.

Simulations to verify stability of *in vivo* inoculation model fit

To investigate the sensitivity of parameter estimates on the number of data points in the in vivo time series data, we generated noisy data with a varying number of data points. We used the following 'true' parameter values to see how accurately we could recover those: $k = 0.01$, $n = 0.1$, $m = 0.15$, g= 5, $P_0 = 1$, $c = 0.5$ and $\sigma = 0.012$. We started with a data point every day for 30 days. That gave the results as in Fig S2.4 for parameter estimates and an indication of the credible region, and in Fig S2.5 for the covariances between all parameters. This fit reproduced the true parameter values quite well. Fig S2.6 and Fig S2.7 showed the same figures for generated data with the same time points as in the experiment (12 points in total). It is clearly visible that the model fit is shifted to earlier times from what it should be. The covariances between *m* and several

other parameters were starting to look very stretched. This effect got worse with fewer time points and increasing noise.

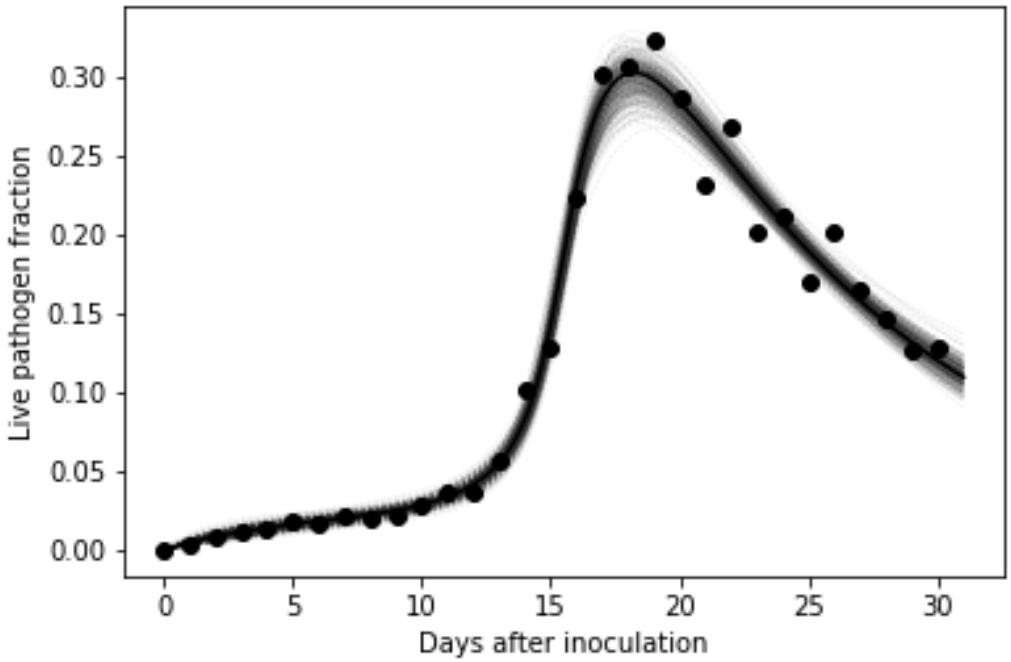

Figure S2.4. Fit of generated data with 30 time points. Solid black line is the model result for the parameter estimates. Thin lines are 400 randomly sampled lines from the full MCMC sampler chain.

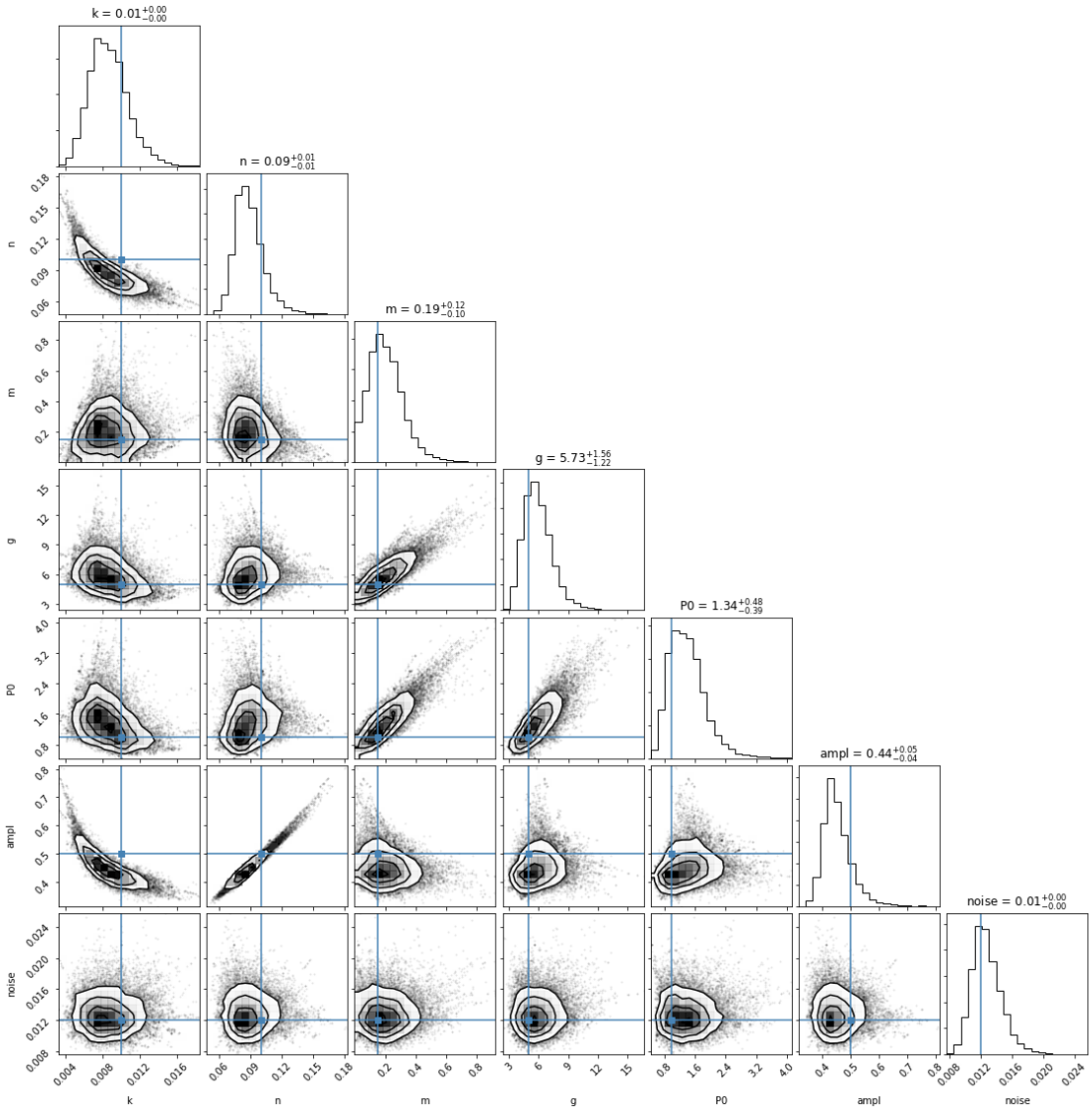

Figure S2.5. Posterior probability distributions of model parameters, for the fit of the model to the generated data with 30 time points. The histograms along the diagonal show the single parameter distributions, the off-diagonal plots show the covariances between parameters.

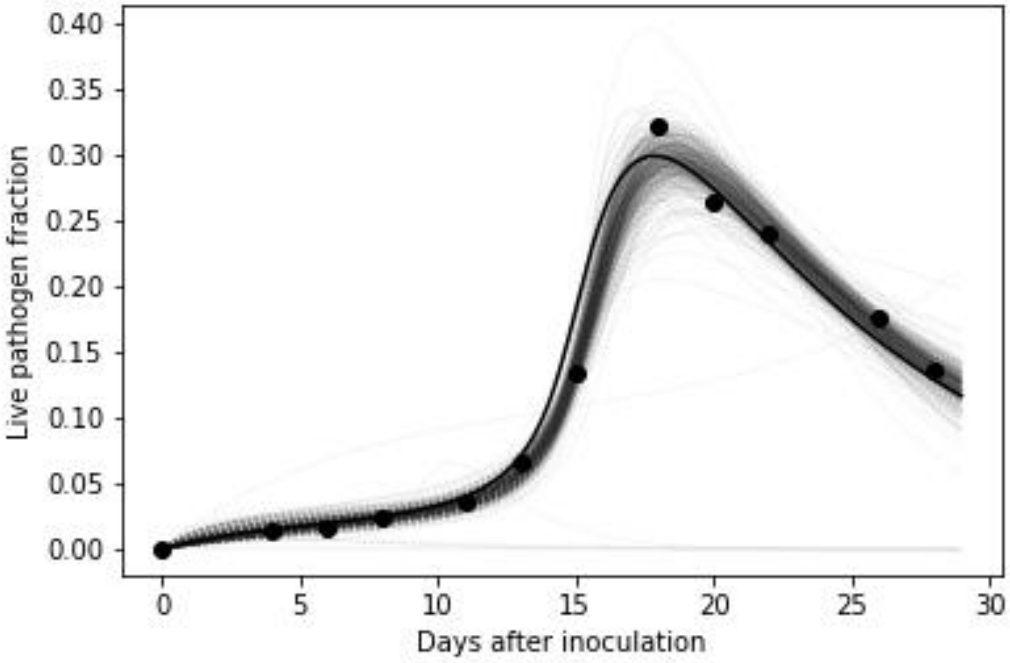

Figure S2.6. Fit of generated data with the same time points as in the *in vivo* inoculation. Solid black line is the model result for the parameter estimates. Thin lines are 400 randomly sampled lines from the full MCMC sampler chain.

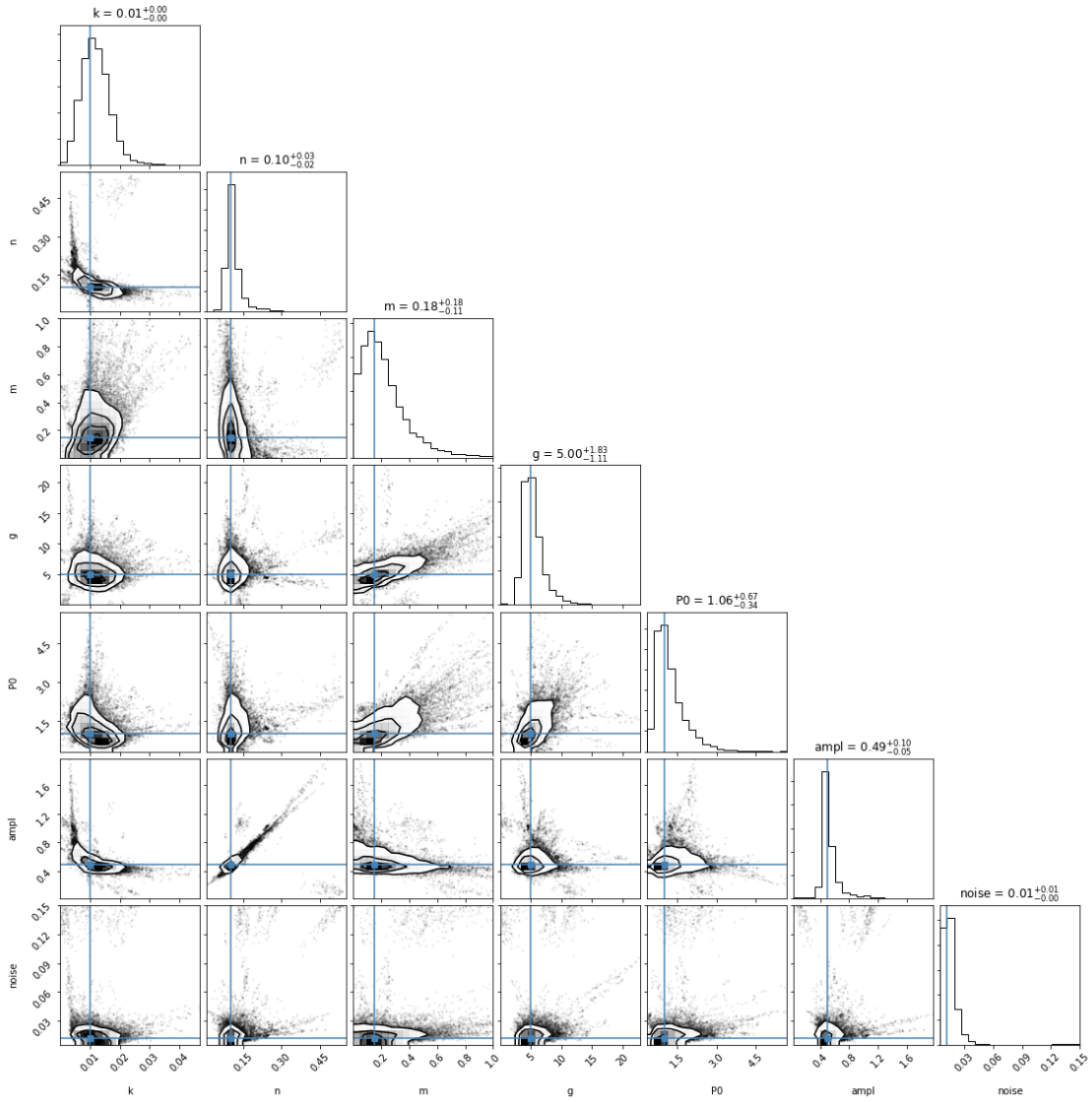

Figure S2.7. Posterior probability distributions of model parameters, for the fit of the model to the generated data with the same time points as in the *in vivo* inoculation.

In vivo inoculation model fit details

Figs S2.8-S2.10 show the parameter covariances for the *in vivo* inoculation model fits.

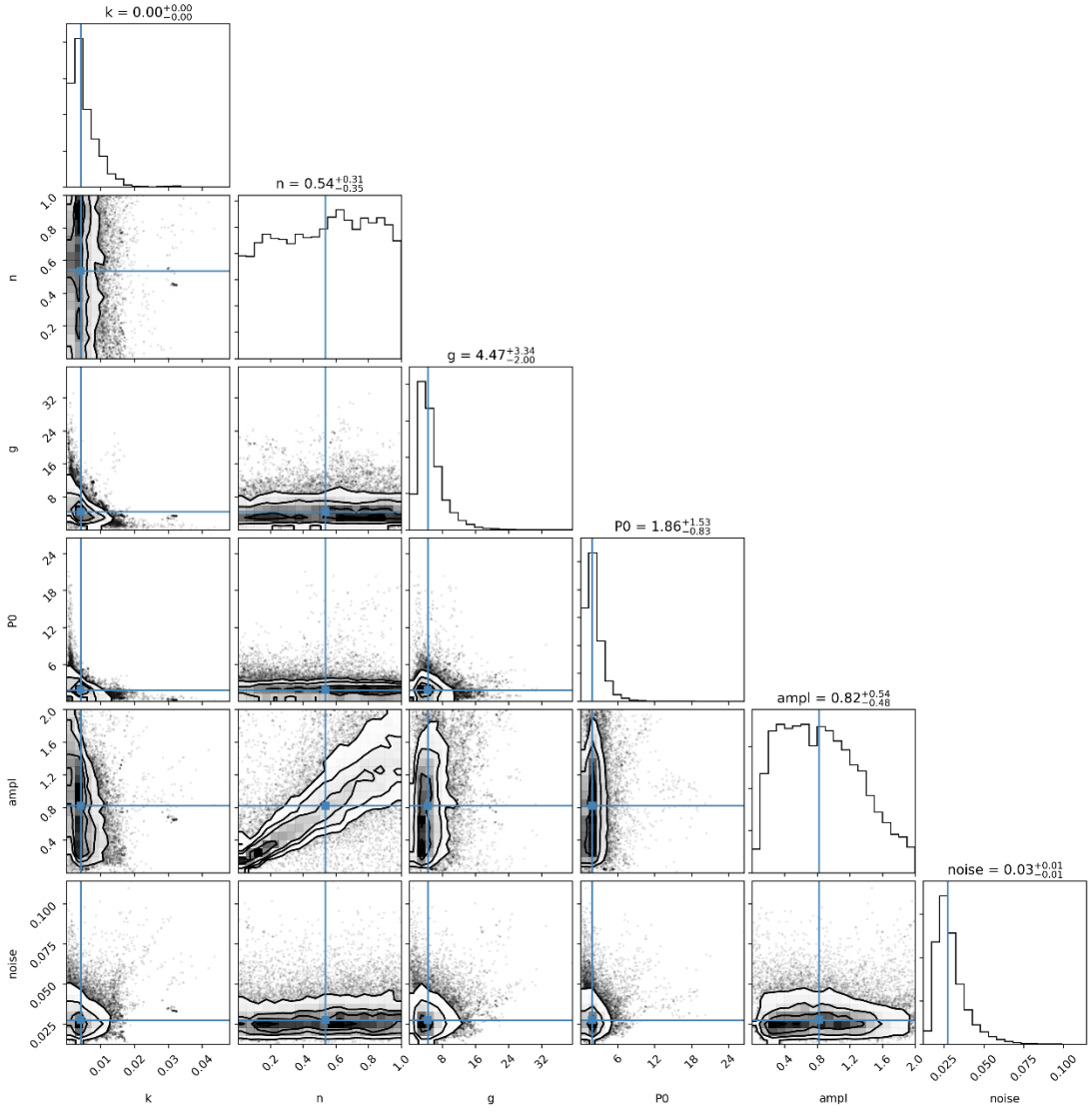

Figure S2.8. Posterior probability distributions of model parameters for the model fit to the *detection by isolation* data of the *in vivo* inoculation.

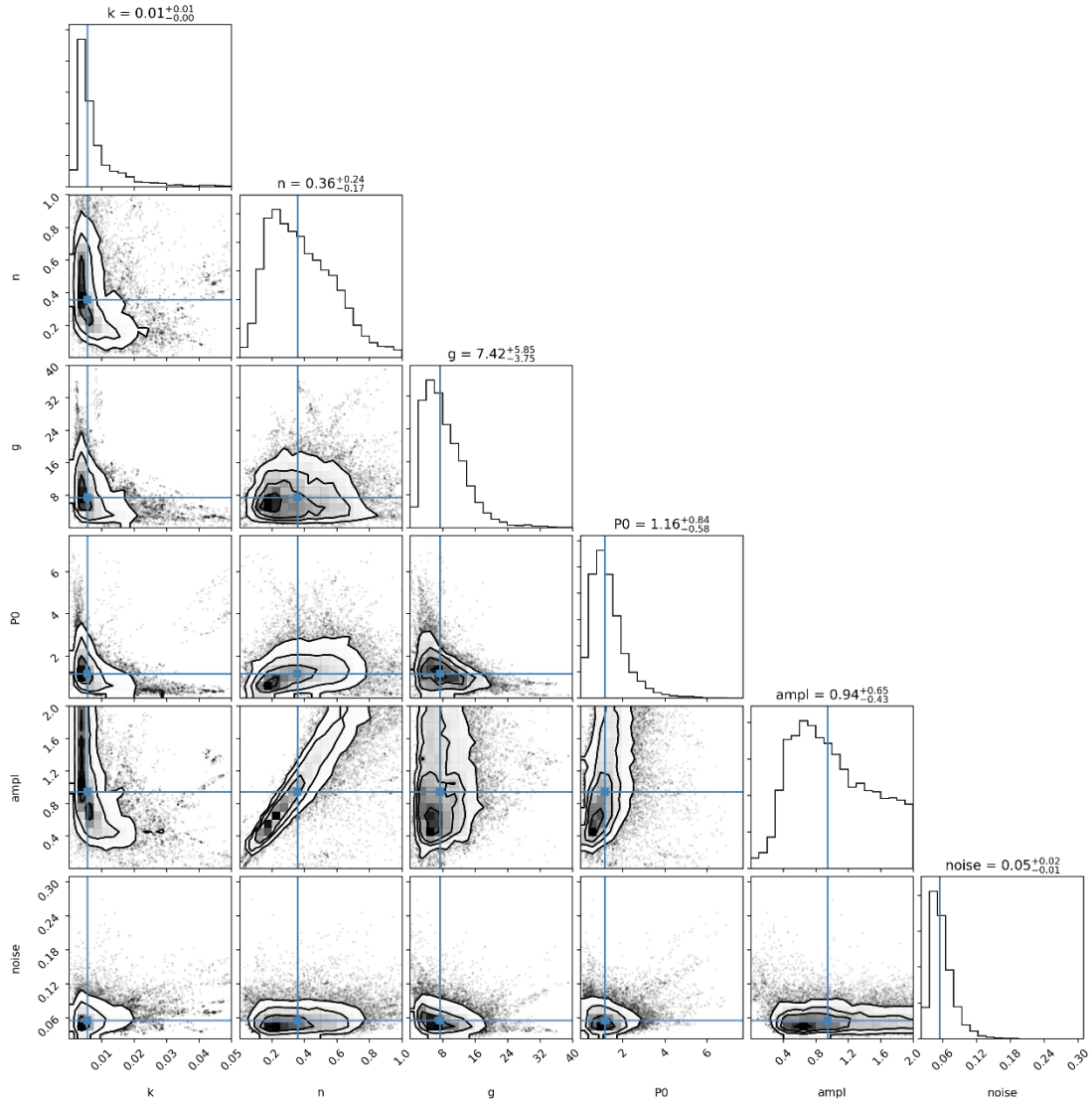

Figure S2.9. Posterior probability distributions of model parameters for the model fit to the *detection by qPCR* data of the *in vivo* inoculation.

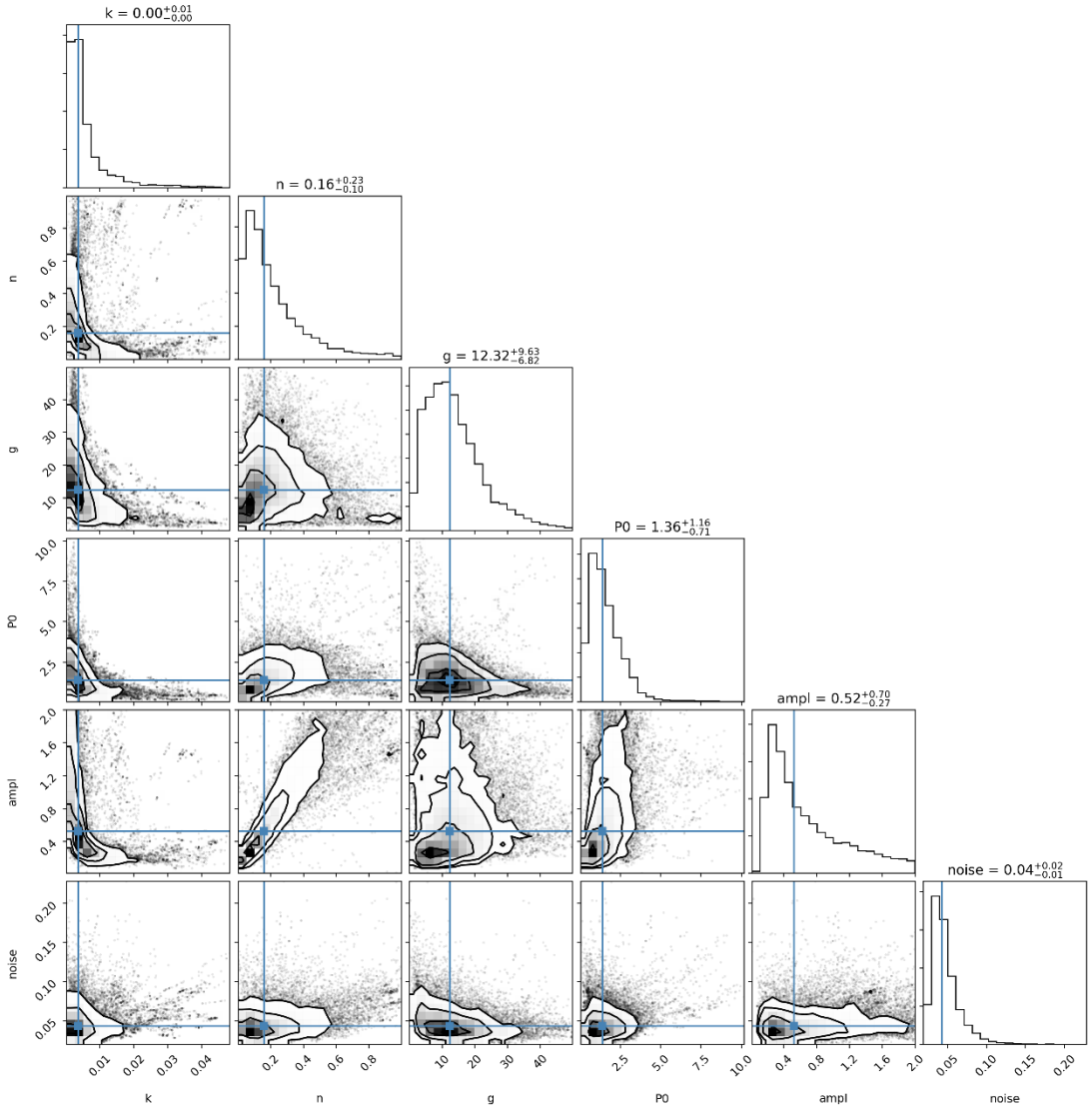

Figure S2.10. Posterior probability distributions of model parameters for the model fit to the *pathogen-to-host DNA ratio* data of the *in vivo* inoculation.

Chapter 3. The challenge of multiple pathogenic infections

This chapter comprises the following co-authored paper published in Plant Disease:

Gómez-Gallego, M., Bader, M. K.-F., Scott, P. M., Leuzinger, S., Williams, N. M. 2017. *Phytophthora pluvialis* studies on Douglas-fir require Swiss needle cast suppression. Plant Disease 101: 1259-1262.

Prelude

Douglas-fir was recognized as a host of *P. pluvialis*, following the description of the RNC disease in *P. radiata* plantations in New Zealand. Most of our knowledge on the *P. pluvialis* life cycle and epidemiology had then been based on its infection of *P. radiata* in New Zealand, as per chapter 2. I started the study of *P. pluvialis* infection of Douglas-fir with a series of detached needle and twig assays to describe the timing of infection and symptomatology on Douglas-fir needles, and determined whether twig infection occurs. However, I encountered the challenge of the widespread presence of *Nothophaeocryptopus gaeumannii* infection.

Dip inoculation procedures routinely used in radiata pine inoculation appeared to be ill-suited for Douglas-fir. Both *P. pluvialis* and water control dip inoculation in Douglas-fir detached needles and twigs produced similar lesions, due to the unexpected development of *N. gaeumannii*, triggered by immersion in water. In the following paper, I present the results of the inoculation assays in Douglas-fir together with methodological recommendations to avoid *N. gaeumannii* development when performing *P. pluvialis*-only research.

It should be noted that in the published manuscript, *Nothophaeocryptopus gaeumannii* is referred to as *Phaeocryptopus gaeumannii*, with the taxonomic classification changed after the publication of this paper. The nomenclature has been updated it in the text presented here.

Abstract

Phytophthora pluvialis is associated with early defoliation and shoot dieback in Douglas fir in Oregon and New Zealand. In 2013, *P. pluvialis* was described from mixed tanoak-Douglas-fir forests in the Pacific Northwest and concurrently recognized as the main causal agent of red needle cast (RNC) in New Zealand radiata pine plantations. Little is known about its infection cycle and impact on host physiology. *Phytophthora pluvialis* studies in Douglas fir are challenging due to the ubiquitous presence of the endophyte *Nothophaeocryptopus gaeumannii,* which produces similar symptoms and premature defoliation with persistent needle wetness, known as Swiss needle cast (SNC). Nonetheless, our study showed *P. pluvialis* infection in the presence of SNC. Exclusive expression of *P. pluvialis* is difficult to achieve as both diseases are promoted by high humidity. Here we established a 'dry leaf' strategy to suppress SNC when inoculating Douglas fir needles for RNC studies. Sheltering plants along with drip irrigation to avoid needle wetness during the *N. gaeumannii* sporulation period suppressed its development in the new season flush. Current-year needles from sheltered saplings presented less than 3% of their stomata blocked by pseudothecia, whereas those from unsheltered saplings had around 42% of their stomata occluded by pseudothecia The diminished endophyte inoculum enabled bias-reduced studies of *P. pluvialis* impacts on Douglas fir without the confounding effects of stomatal blockage and premature defoliation caused by *N. gaeumannii*.

Introduction

Phytophthora pluvialis Reeser, Sutton, and Hansen has been shown to be the main causal agent of red needle cast (RNC) in radiata pine (*Pinus radiata* (D. Don)) plantations in New Zealand noted since 2008 (Dick et al. 2014). This oomycete was first isolated from baited streams, soil and canopy drip in mixed tanoak-Douglas fir forests in Oregon where it is believed to be endemic with multiple hosts (Reeser et al. 2013). More recently, *P. pluvialis* has been reported to cause needle loss and shoot dieback in Douglas fir (*Pseudotsuga menziesii* (Mirb.) Franco) plantations and has been isolated from Douglas fir needles from trees with symptoms of premature defoliation akin to Swiss needle cast (SNC) in Oregon and New Zealand (Hansen et al. 2015).

In both radiata pine and Douglas fir, *P. pluvialis* infection is characterized by the production of olive-coloured lesions and black resinous bands on needles followed by accelerated senescence and casting. Based on studies on radiata pine, infection requires damp and cool weather conditions and typically occurs from autumn to early spring (Dick et al. 2014). During this time, different degrees of defoliation can be observed in the field, normally starting at the bottom of the canopy. Little is known about the *P. pluvialis* infection cycle in Douglas fir, and its impact on tree growth and survival.

Douglas fir is considered one of the most important tree species in the timber trade worldwide. It is a dominant tree species in the U.S. Pacific Northwest, with remarkable ecological and economic significance. It is the most abundant exotic tree species cultivated in Central Europe (Schmid et al. 2014), and the second most important exotic plantation species in New Zealand, with 110 thousand planted hectares (New Zealand Forest Owners Association 2014). During the last decades, the productivity of Douglas fir has been reduced by SNC, caused by the widespread fungus *Nothophaeocryptopus gaeumannii* (Rohde) Petrak. Swiss needle cast occurs where Douglas fir is grown as an exotic species (Boyce 1940; Castaño et al. 2014; Hood 1999; Lanier 1966; Merrill and Longenecker 1973; Morton and Patton 1970; Osorio 2007; Temel et al. 2003), and throughout the species' natural range of the Pacific Northwest (Hansen et al. 2000; Hood 1982).

In contrast to RNC on Douglas fir, the impacts of SNC have been thoroughly described (Hansen et al. 2000; Kimberley et al. 2011; Maguire et al. 2002; Manter et al. 2003a; Manter et al. 2000; Temel et al. 2004). Swiss needle cast causes defoliation and consequent growth reduction with an estimated mean volume growth loss of 23% in Oregon plantations in 1996 and in severe cases as high as 52% (Maguire et al. 2002). Defoliation has been shown to be proportional to the number of stomata occluded by pseudothecia of the fungus (Hansen et al. 2000; Manter et al. 2003b). The abscission of the foliage occurs shortly after becoming a carbon sink, which is reached when 25% of stomata are occluded by pseudothecia (Manter et al. 2003b).

Nothophaeocryptopus gaeumannii ascospore dispersal and new infections are facilitated by high humidity and needle wetness (Manter et al. 2005a), similar to the conditions in which *P. pluvialis* thrives. *Nothophaeocryptopus gaeumannii* sporulation takes place in spring, spanning the period of flush and expansion of new Douglas fir foliage (Hood 1999, Stone et al. 2008). Moreover, there

is no asexual stage and only one infection cycle occurs each year (Stone, Capitano, et al. 2008). As both SNC and RNC are promoted by high humidity levels in the foliage environment, we encountered difficulties in achieving exclusive *P. pluvialis* infection on Douglas fir. A detached needle assay applying a dip inoculation with *P. pluvialis* resulted in dual expression of RNC and SNC demonstrating the unsuitability of this routine inoculation method (Dick et al. 2014).

In previous experiments involving *N. gaeumannii*, protectant fungicides (i.e. chlorothalonil; Manter et al. 2003a; Manter et al. 2003b) have been used to create control plants. However, this fungicide has been used previously to control other *Phytophthora* diseases (Hamm and Clough 1999, Ratajkiewicz et al 2016, Sujkowski et al. 1995, Vawdrey et al. 2015). Hence, the study of *P. pluvialis* epidemiology can be biased by chlorothalonil application, and an alternative strategy should be designed. The aim of this study was to devise a procedure to minimize *N. gaeumannii* inoculum in order to reduce the dual disease expression bias currently involved in RNC studies with Douglas fir. We hypothesized that keeping Douglas fir plants sheltered from rain, fog and overhead irrigation during the flushing period and providing drip irrigation instead would reduce leaf wetness to condensation events and hence minimize *N. gaeumannii* spore formation and colonization of new foliage. This procedure would yield new foliage with low *N. gaeumannii* abundance for bias-reduced studies of *P. pluvialis* on Douglas fir.

Material and methods

Phytophthora pluvialis detached needle assay

Zoospore production

Zoospore production was performed as described by Dick et al (2014). Plugs of agar and mycelium taken from the leading edge of the colonies were flooded with 75 ml of clarified carrot broth (Erwin and Ribeiro 1996) in 500 ml vented flat bottomed flasks (Medi'Ray, New Zealand) and incubated in the dark at 17 °C for 4 days. The resulting mycelial mats were rinsed thoroughly in a steady stream of deionized water, drained, then re-flooded with 75 ml of sterile pond water, and incubated for 3 more days. Zoospore release was induced by cold-shocking the cultures at 4 °C in the dark for 45 minutes, followed by exposure at room temperature (21 °C), and by placing cultures on a light box if required. Zoospore concentrations were determined using a haemocytometer, reaching a minimum of 3×10^3 zoospores per mL. Zoospore suspensions were used within two hours of preparation. The isolates used as source of inoculum had been identified using morphological and molecular techniques. The origin of the isolates is given in Table 3.1.

Needle inoculation

Current-year needles (around 3 months old) were collected from 12 six-year-old open-pollinated Douglas fir saplings grown in the open in 25 L growth bags at the Scion nursery (Rotorua, New Zealand) in February 2016 (mid-summer). Fifty needles were removed from each of the 12

saplings. Twenty-five needles were treated with *P. pluvialis* zoospore suspensions and the remaining 25 were treated with sterile pond water. In both treatments, five needles were placed vertically, basal end down, in each of five 2 mL microcentrifuge tubes containing 250 µL of either zoospore suspension or sterile pond water for a period of 24 hours. Afterwards, the needles were placed on moistened paper towels in sealed trays and incubated at 17 ^{o}C with a 12 hour photoperiod for 11 days.

Table 3.1. Origin of *Phytophthora pluvialis* isolates used for Douglas fir inoculations from the Scion culture collection.

Isolate no.	Date collected	Location
NZFS 4171	16/07/2015	Kaingaroa Forest 1899724, 5713610
NZFS 4172	17/07/2015	Kaingaroa Forest 1889140, 5706150
NZFS 4175	12/08/2015	Reporoa, 1904572, 5743513
NZFS 4234	12/08/2015	Golden Downs 1589477, 5398855
NZFS 4267	22/09/2015	Kinleith, 1851803, 5781881
NZFS 4285	04/10/2015	Kinleith 1860169, 5771033
NZFS 4286	04/10/2015	Kinleith 1860169, 5771033

After 11 days, total needle length and lesion length, characteristic of the early symptoms of RNC (olive-coloured discolouration and black bands, Dick et al. 2014) were recorded, and the percentage of lesioned needle length calculated. All needles were surface sterilised by washing them in 70% ethanol for 30 seconds, rinsed in sterile deionised water and dabbed on filter paper, and subsequently placed onto PARP (pimaricin, ampicillin, rifampicin, pentachloronitrobenzene PCNB) agar as described by Jeffers and Martin (1986). *Phytophthora* colonies were morphologically identified to species (Reeser et al. 2013) by both subculturing in 10% carrot agar selective media and inducing sporangia production in pond water (Erwin and Ribeiro 1996).

Nothophaeocryptopus gaeumannii suppression assays

Five of the six-year-old Douglas fir saplings grown in the open and hence naturally containing *P. gaeumannii* were transferred to sheltered conditions and watered with drip irrigation throughout the sporulation season from November 2015 to February 2016. Another five saplings kept outdoors under natural environmental conditions served as controls.

Nothophaeocryptopus gaeumannii pseudothecia density was assessed in ten current-year (around 5 months old) and ten one-year-old needles collected from each sapling on the 27th of April 2016 following the methods of Manter et al (2001) with a few modifications. In brief, the number of pseudothecia emerging from 80 to 100 consecutive stomata at the bottom, mid and upper third of the needle were determined by visually counting (at 135.3x total magnification,

optical microscope Reichert, Austria) pseudothecia-occluded and pseudothecia-free stomata in one randomly chosen row of stomata. The pseudothecia density in the adjacent one-year-old needles was taken as the baseline presence of *N. gaeumannii* in each tree. The pseudothecia density in current-year needles served as a control for the water and zoospore suspension dip inoculations.

A *P. pluvialis* detached needle was performed in the same way as described above to test the suppression of *N. gaeumannii* (inoculation started on the 28th April 2016). Additionally, a detached twig assay was performed. Ten branch tips including needles were sampled from each of the ten saplings and inoculated in 50 mL plastic centrifuge tubes containing either 10 mL of zoospore suspension or sterile pond water. At the end of the experiment, all needles and twigs (stem and needles) from both experiments were assessed for the presence or absence of typical RNC lesions, surface sterilized and cultured for *Phytophthora* re-isolation and identification, as stated above. One needle per tube from the detached needle assay (10 needles per sapling) was randomly chosen to assess the density of *N. gaeumannii* pseudothecia. Moreover, the presence or absence of typical RNC lesions four and eight days after inoculation was monitored to assess the timing of lesion development in needles from both experiments, and stems from the twig experiment.

Data analysis

Linear mixed effects models were used to test the effects of *P. pluvialis* inoculation in the detached needle assay. The two measured response variables were percentage of lesioned needle length and percentage of *P. pluvialis* isolates of the five needles per tube. Both response variables were logit transformed (R-package car) prior to analysis. 'Tube' was nested within 'sapling' as a random term.

In the *N. gaeumannii* suppression assay, a generalized linear model with a binomial error distribution was used to test the effects of zoospore suspension, water dip and no treatment control, on average pseudothecia density per sapling as a response variable. The baseline pseudothecia density in one-year-old needles was included in the model as an offset term.

All analyses were carried out with R Statistical Software version 3.3.0 (R Development Core Team 2016) using the lme (R-package *nlme*, Pinheiro et al. 2016) and glm functions.

Results

Phytophthora pluvialis detached needle assay

In the absence of SNC suppression, both the water control and the needles inoculated with *P. pluvialis* produced a similar percentage of lesioned needle length eleven days after inoculation. On average, both treatments yielded around 7% of lesioned needle length (Fig 3.1a). Lesions in the water control and *P. pluvialis* treated needles were similar, presenting as pale olive discoloration and occasionally black marks. Eleven days after inoculation, *P. pluvialis* was recovered from 35% of the pathogen-treated needles while no isolates were derived from the uninoculated control plants (Fig 3.1b). *Nothophaeocryptopus gaeumannii* pseudothecia were observed in both water control and *P. pluvialis* infected needles (data not shown).

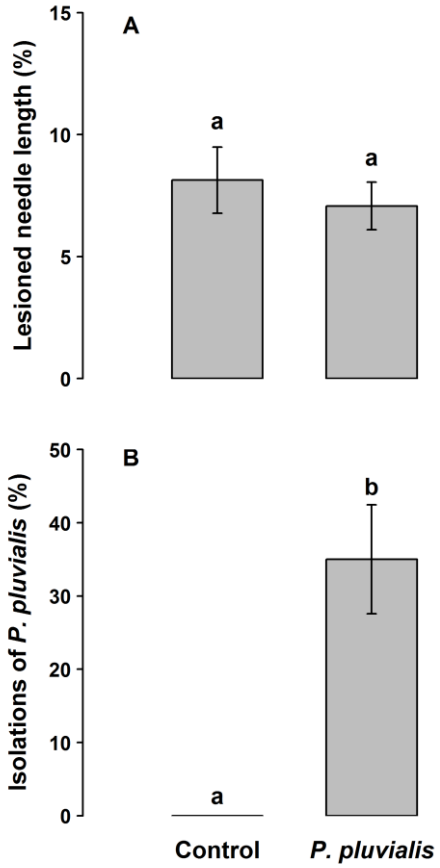

Figure 3.1. (a) Lesioned needle length (percentage of the total needle length showing symptoms of infection) in detached Douglas fir needles dipped into water (control) or dip inoculated with *P. pluvialis* zoospore solution (*P. pluvialis*); and (b) percentage of isolation attempts yielding *P. pluvialis* in the two treatments. Different lower case letters indicate statistically significant differences within groups at α = 0.05 (post-hoc comparison using Tukey contrasts). Means ± SE, n = 12.

Nothophaeocryptopus gaeumannii suppression assays

Saplings grown under sheltered conditions using drip irrigation to minimize needle wetness showed significantly less SNC infection compared to unsheltered plants. This effect varied with the inoculation treatment (dry control, water control or *P. pluvialis* inoculation) resulting in a significant interaction (L = 51.07, DF = 2, $P < 0.0001$). Current-year needles from sheltered saplings presented less than 3% of their stomata blocked by pseudothecia, whereas those from unsheltered saplings had around 42% of their stomata occluded by pseudothecia (Fig 3.2).

Dry controls yielded significantly less pseudothecia than those receiving dip inoculations (water, *P. pluvialis*), irrespective of whether they were growing under sheltered or unsheltered conditions (Fig 3.2). Further, there was no difference in the development of SNC between the saplings inoculated with water or zoospore solution (Fig 3.2).

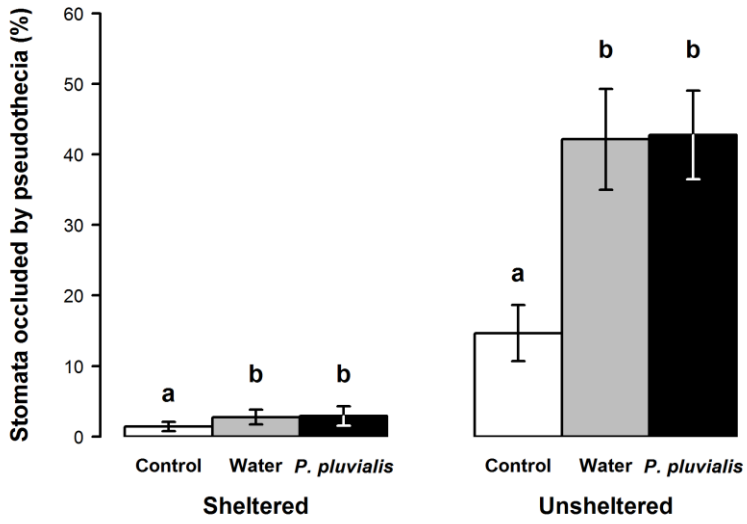

Figure 3.2. *Nothophaeocryptopus gaeumannii* pseudothecia density (percentage of stomata occluded by pseudothecia) in needles of Douglas fir sheltered and unsheltered plants, under different inoculation treatments: no inoculation (control), dip inoculation with water (water) and dip inoculation with *Phytophthora pluvialis* zoospore solution. Different lower case letters indicate statistically significant differences within groups at α = 0.05 (post-hoc comparison using Tukey contrasts). Means ± SE, n = 10.

Both the detached needle and detached twig assays yielded visible needle lesions, but *P. pluvialis* isolates were only obtained from inoculated needles and twigs. Although no stem lesions were observed at all, surface-sterilized stems from sheltered and unsheltered plants yielded *P. pluvialis* isolates, confirming the presence of the pathogen (Table 3.2).

Visible needle lesions developed more rapidly in the detached needle assay compared to twig inoculation. In the detached needle assay, about 85% of those needles that had produced lesions at the end of the experiment were symptomatic within four days after inoculation. By contrast, in the detached twig assay, only 0.2% of the lesioned needles recorded at the end of the experiment were symptomatic four days after inoculation, increasing to 95% on day eight.

Table 3.2. Presence (+) / absence (-) of lesions and *P. pluvialis* isolations in the detached needle and detached twig assays for sheltered and unsheltered plants.

	Detached needles		Detached twigs	
	Sheltered	**Unsheltered**	**Sheltered**	**Unsheltered**
Presence of needle lesions	+	+	+	+
Presence of stem lesions			-	-
P. pluvialis isolates from needles	+	+	+	+
P. pluvialis isolates from stem			+	+

Discussion

The study of the complex plant-pathogen interaction between *P. pluvialis* and Douglas fir presents great challenges to researchers. The key difficulties lie in the dual disease expression of RNC and SNC in areas where both pathogens co-occur and the inefficacy of visual symptoms alone for disease differentiation. Here, we tested whether avoidance of leaf wetness throughout the *N. gaeumannii* sporulation period would suppress SNC expression and enable inoculation with *P. pluvialis* without the confounding effects of *N. gaeumannii*.

Our study showed that diagnosis solely based on visual symptoms is not able to distinguish SNC from RNC (Fig 3.1a). Pseudothecia density has been previously well correlated to chlorosis and needle retention (Winton et al. 2003). Moreover, the blockage of stomata by *N. gaeumannii* is likely to physically impede *P. pluvialis* infection. Microscope-aided counting of these fruiting bodies provided a simple and direct means of *N. gaeumannii* quantification. In contrast, the lack of such easily discernible structures makes the quantification of *P. pluvialis* infection in Douglas fir much more difficult.

The earlier onset of symptoms in detached needles compared to the needles in the twig assay suggests greater rate of infection in more rapidly senescing tissues. This increased susceptibility may result from accelerated biochemical changes and tissue dehydration in detached needles. In contrast, physiological deterioration is likely to proceed more slowly in needles still connected to stems resulting in prolonged defence to infection as suggested by the delayed emergence of symptoms in the twig assay. Therefore, the use of detached twigs in inoculation studies more realistically represents the infection process and the physiological changes taking place in planta.

Irrespective of *P. pluvialis* inoculation, our detached needle experiment demonstrated that not accounting for the presence of *N. gaeumannii* will result in SNC expression. Here this caused 42% stomatal occlusion exceeding the 25% threshold of needle cast (Manter et al. 2003b).

Our findings highlight the importance of minimizing *N. gaeumannii* sporulation through the prevention of needle surface wetting by sheltering and drip watering plants from spring to summer to allow bias-reduced epidemiological studies of *P. pluvialis* in Douglas fir. While chlorothalonil

fungicide has been used to create SNC-free control plants in previous studies (Manter et al. 2003a; Manter et al. 2003b), such an approach may also impact *Phytophthora* development, as it has been used before to control other *Phytophthora* diseases (Hamm and Clough 1999, Ratajkiewicz et al 2016, Sujkowski et al. 1995, Vawdrey et al. 2015). With the 'dry leaf' approach presented here, the effects of *P. pluvialis* on the physiology of current-year needles can be investigated without confounding effects of *N. gaeumannii*. Extrapolation to the whole-plant level requires a more refined approach because of the presence of *N. gaeumannii* in previous-year needles. Based on our approach it might be assumed that a reduction in abundance of this pre-existing fungal inoculum would occur only gradually over several years of growth under sheltered conditions. For multi-year trials assessing infection and physiological impacts across multiple needle age classes, plants should be sourced free of *N. gaeumannii* and grown under sheltered conditions in the absence of inoculum.

While the interaction between the two pathogens is an issue in laboratory inoculation studies, we speculate that, under field conditions, infection of the new season's growth by *P. pluvialis and N. gaeumannii* may be separated temporally. This would imply that defoliation events caused by RNC may have previously been reported as SNC contributing to unseasonal and extended periods of needle casting. The implications for forest pathology research, monitoring and disease management are significant given the pronounced differences in pathogen taxonomy, epidemiology and potential management. Differentiating the impact of RNC will require a better understanding of the interplay between both pathogens and calls for targeted diagnosis and monitoring throughout the year. At this stage, informative diagnosis requires a combination of microscopy and molecular tools to address infection by *P. pluvialis* and *N. gaeumannii*. Future studies may benefit from incorporating quantitative PCR measurements to directly quantify both pathogens in parallel. Such assays along with RNA sequence analyses could help disentangle the temporal impacts of both pathogens and their interaction, respectively. Whether *P. pluvialis* triggers needle cast in Douglas fir at similar levels to SNC or those reported for RNC in radiata pine remains to be shown by extended epidemiological studies using the 'dry leaf' approach put forward here.

Chapter 4. Interaction between *P. pluvialis* and *Nothophaeocryptopus gaeumannii* infection on Douglas-fir

This chapter comprises the following co-authored paper submitted to Phytopathology:

Gómez-Gallego, M., LeBoldus, J., Bader, M. K. F., Hansen, E., Donaldson, L., Williams, N. M. Pathogen loads of *Phytophthora pluvialis* and *Nothophaeocryptopus gaeumannii* populations co-existing within exotic plantations of New Zealand in contrast to Douglas-fir's endemic range in the US Pacific Northwest.

Prelude

In chapter 3, I introduced the challenge of multiple pathogenic infection by *P. pluvialis* and *N. gaeumannii* of Douglas-fir needles. While this study demonstrated the potential for co-infection by both pathogens in the laboratory, it was unknown whether that would take place in the field and under what environmental conditions. Therefore, I designed a field sampling study to ascertain the levels of infection by each pathogen in Douglas-fir in the regions where they have both been reported. The Swiss needle cast (SNC) disease, caused by *N. gaeumannii*, is well-established wherever Douglas-fir is grown. *P. pluvialis* had been reported both in Oregon (US Pacific Northwest), where SNC and Douglas fir are native, and New Zealand, where both the host and the SNC disease are introduced.

The manuscript presented in this chapter includes the study of the co-existence of *P. pluvialis* and *N. gaeumannii* in Oregon and New Zealand. Accurate data on the distribution of both pathogens is reported. Further, the effect of weather and climatic variables on the distribution of both pathogens is also analysed. This study opens a new chapter in the research on aerial *Phytophthora* pathogens and their interaction with foliar fungal diseases in forest systems.

Abstract

The emergence of *Phytophthora pluvialis* as a foliar pathogen of Douglas-fir in New Zealand (NZ) and the US Pacific Northwest (PNW) has raised questions about its interaction with the widespread Swiss needle cast (SNC) disease. During spring 2017, we repeatedly sampled 30 trees along an environmental gradient in NZ and in the PNW to assess the seasonality of *P. pluvialis* and *Nothophaeocryptopus gaeumannii*, causal agent of SNC. Additionally, we sampled 292 trees in NZ and the PNW to analyse *P. pluvialis* epidemic and its association to *N. gaeumannii*. Both pathogens were consistently more abundant in the host's exotic environment, NZ. In both regions, the two pathogens coexist at different spatial scales ranging from region to needles. Their relative abundance was negatively correlated in the PNW, where both pathogens have presumably coexisted for longer. Our findings confirm the interaction of *P. pluvialis* and *N. gaeumannii* as foliar pathogens of Douglas-fir and suggest a within-site spatial variation in the PNW.

Introduction

Oomycetes in the genus *Phytophthora* are an aggressive group of pathogens in agricultural and forest ecosystems. In forests, they had been traditionally recognized as belowground pathogens, soil-borne, and causing root rot in trees (Day 1938, Newhook and Podger 1972, Brasier et al. 1993, Vettraino et al. 2005). However, increasing disease reports revealed greater diversity in biology and life styles within the *Phytophthora* genus. In forest ecosystems, infections have been described from the roots to the leaves (Hansen et al. 2003, Brasier et al. 2005, Hansen 2015, Kozanitas et al. 2017). Over the last decade, *Phytophthora* diseases infecting the foliage of conifers have emerged and are a growing concern for economically important plantation species (Durán et al. 2008, Brasier and Webber 2010, Dick et al. 2014).

Phytophthora pluvialis Reeser, Sutton, and Hansen belongs to this group and is the causal agent of the red needle cast (RNC) disease in radiata pine (*Pinus radiata* [D. Don]) (Dick et al. 2014). Recently, it has also been reported to cause early defoliation and shoot dieback on Douglas-fir (*Pseudotsuga menziesii* [Mirb.] Franco) in Oregon (US) and New Zealand (NZ) (Hansen et al. 2015). *P. pluvialis* typically infects the lower canopy of both radiata pine and Douglas-fir trees (Dick et al. 2014, Hansen et al. 2015). Infection can progress upwards to the top of the live crown under prolonged periods of weather conducive for pathogen development. In New Zealand, epidemic episodes of polycyclic infections start in autumn with a peak in late winter and early spring. While symptomatic needles in radiata pine turn red prior to being cast, in Douglas-fir, needles usually fall from trees before symptoms are clearly visible.

The casting observed from Douglas-fir has raised the question whether *P. pluvialis* plays a role in defoliation events previously associated with the Swiss needle cast (SNC) disease caused by the ascomycete *Nothophaeocryptopus gaeumannii* (T. Rohde) Videira, C. Nakash., U. Braun and Crous. In its native range, the US Pacific Northwest (PNW), this fungus was considered unimportant (Boyce 1940), until the first significant outbreaks took place in the late 1980s and 1990s (Hansen et al. 2000). The disease has since spread from 53,050 ha in 1996 to 238,705 ha in 2015 in the Oregon Coast Range (Ritokova et al. 2016). In New Zealand, it was first detected in 1959 in the North Island (NI) and gradually progressed to the southern tip of the South Island (SI) by the late-1980s (Hood and Kershaw 1975, Hood et al. 1990).

The potential for co-infection of Douglas-fir needles by *P. pluvialis* and *N. gaeumannii* has recently been demonstrated in a detached needle assay (Gomez-Gallego et al. 2017). The primary mechanism of pathogenicity of *N. gaeumannii* is through pseudothecia developing within stomata, impeding their function leading to impaired photosynthesis (Manter et al. 2000). The resulting negative needle carbon budgets cause defoliation and growth reduction (Manter et al. 2003). *P. pluvialis* partially caducous sporangia can either germinate directly, or release zoospores which would reach needle surfaces by water splash. Following release, the zoospores would encyst and colonize the intercellular space. Sporangia clusters emerge from stomatal openings, and the cycle starts again. Stomata are an important component of both pathogens' etiology, but the seasonality and epidemiology of both diseases seem to be different. *P. pluvialis* is polycyclic, in contrast to

the monocyclic nature of *N. gaeumannii*, with only one infection cycle per year occurring during the late spring following ascospore release (Hood et al. 1990).

The establishment of new pathogens in an ecosystem is a result of their obligatory interaction with susceptible hosts in a conducive environment. Although less explored, a pathogen's interactions with other microorganisms is extremely important in shaping the development of disease outbreaks (Dickie et al. 2017). In general, co-infection is considered to select for increased within-host growth rates due to competition (Nowak and May 1994, van Baalen and Sabelis 1995, Alizon et al. 2009, Laine 2011). However, pathogens cannot coexist in the same host in the long term in competition for the same resources (Alizon and van Baalen 2008). This competition will lead to an evolutionary equilibrium, whose outcome will depend on several factors such as priority effects, availability of nutrients, climate and genotype (Simpson et al. 2004, Al-Naimi et al. 2005, Laine 2011, Abdullah et al. 2017, Kozanitas et al. 2017).

Tree leaves are nutritionally defined niches, where pathogens with similar requirements naturally compete. There are several hypothesized outcomes of these interactions. For example, following an initial increase in growth, depletion of resources can lead to a growth reduction over time, impacting both microorganisms (Rankin et al. 2007, Jonkers et al. 2012). Conversely, competition for resources could result in the selection of species which present the most efficient resource exploitation strategies to outgrow its competitors (Abdullah et al. 2017). *N. gaeumannii* creates appressoria to access intracellular space and extract nutrients (Stone, Capitano, et al. 2008). Although this infection structure is common in *Phytophthora* species (Hayden et al. 2013, Fawke et al. 2015), they have not been observed on *P. pluvialis* infected needles to date.

Other pathogen-pathogen interactions, which would lead to the selection of one species over the other, are competitive exclusion via chemical or mechanical interference, and indirect (or apparent) competition through targeted defense responses (Mideo 2009, Abdullah et al. 2017). Neutral interactions, where both pathogens can co-exist, can also occur when pathogens undergo niche specialization either in space or in time (Al-Naimi et al. 2005, Fitt et al. 2006, Abdullah et al. 2017, Desprez-Loustau et al. 2018). *P. pluvialis* was first detected in 2002 in baited streams, soil, and canopy drip in mixed tanoak-Douglas-fir forest in southwest Oregon (Reeser et al. 2013). It has been suggested that *P. pluvialis* is endemic to Oregon (Reeser et al. 2013, Brar et al. 2018). Regardless of its centre of origin, it is clear that *P. pluvialis* has been present in the PNW for longer than in NZ (Brar et al. 2018). Thus, the PNW and NZ offer an opportunity to investigate differences in epidemiology and begin to characterize the interaction between *P. pluvialis* and *N. gaeumannii*.

In the present study, we aimed to (1) explore the extent of *P. pluvialis* epidemics in both the PNW and NZ, through a one-time regional sampling in an extended area in each country to quantify the presence and abundance of *P. pluvialis*. Furthermore, we intended to (2) compare the relative abundance of the two pathogens to investigate the interaction of *P. pluvialis* and *N. gaeumannii* in two environments: the PNW, native for *N. gaeumannii* and Douglas-fir; and NZ, exotic for *N. gaeumannii* and Douglas-fir and where *P. pluvialis* has been more recently introduced. We hypothesized that in the PNW, the levels of *P. pluvialis* and *N. gaeumannii* would be lower than in the NZ population due to a longer period of co-existence, having past initial increased growth

rates. We also speculated that the NZ environment would support greater pathogen abundance due to the non-native nature of both pathogens and their host in this country and because of the mono-specific plantation setting. Finally, we aimed to (3) determine the climatic drivers shaping the abundance of the two pathogens, by analysing the correlation between different climatic variables and the abundance of each pathogen.

Material and methods

Study sites and field sampling

The study area included two different regions (hereafter referred to as countries): NZ and the PNW. Both countries have a temperate climate of the oceanic subtype, i.e. 4 to 7 months with a monthly mean air temperatures over 10 ºC and the coldest month greater than 0 ºC (Belda et al. 2014). Two studies were carried out in both countries: a study of the interaction of *P. pluvialis* and *N. gaeumannii* across an environmental gradient with a fortnightly sampling design, and an extensive regional sampling to compare detection rates of both pathogens at a regional level.

Fortnightly sampling

Six study sites were selected across an environmental gradient of temperature and precipitation in both countries. In NZ, the sites were located in the central plateau of the NI. In the PNW (referred to as 'Oregon' for the fortnightly sampling), the six sites were situated in the state of Oregon, and followed a longitudinal gradient from the central Oregon coast to the Cascade mountain range (Supplementary Table S4.1, Fig S4.1a). Sites were selected from Douglas-fir plantations that were 11-14 years old (Supplementary Table S4.1, Fig S4.1a). Five trees, at least 5 m apart, were selected along the edge of each plantation, where *P. pluvialis* infection is more notable. Accessible branches were shaken by hand, and the cast needles were collected on a tarp spread under the tree, placed in a labelled bag, transferred to the lab at 4 ºC and processed within 24 h.

To monitor the seasonal pathogen infection dynamics along the environmental gradient, the same trees were sampled every two weeks. The sampling period corresponded to the meteorological spring in both countries. In the PNW the sampling began on the 2nd of March and ended the 2nd of June 2017. In NZ, the sampling began the 23rd of August and ended the 21st of November 2017. To capture the microclimate at each site, hourly values of temperature (T), relative humidity (RH) and dew point T were recorded during the sampling period using a HOBO data logger with external T and RH sensors (MX2300 Ext Temp/RH, Onset Computer Corporation, MA, USA). HOBO's were placed on an accessible branch of the middle tree at each site.

To examine the interaction of both pathogens growing on the needle surface, subsamples of harvested needles from the fortnightly NZ sampling were screened to analyse the growth patterns of both pathogens in the field. Needles were selected from two sites in the NI of NZ the first sampling date on the 31/08/2017 (sites MAM, -38.21667, 176.07955, and TAR, -38.13933,

176.59114, further details in Supplementary Table S4.1). Needle segments were fixed in 4% glutaraldehyde for 1 h at room temperature, washed in water, dehydrated in an ethanol series, and air dried. Dried segments were mounted on aluminium stubs with conductive carbon tape and coated with chromium before examination with a field emission scanning electron microscope (JEOL 6700, Tokyo, Japan).

Regional sampling

To estimate the distribution of the pathogens in both countries, a one-time sampling survey was conducted along a latitudinal transect in both countries. The survey was carried out at the same time of the year (season) in each country, immediately before Douglas-fir flush. In the PNW, 39 sites (134 trees, 3 - 6 trees/site) were sampled along the coastal fog belt from southern Washington state to northern California, in addition to the central Oregon Cascades range. In NZ, a total of 36 sites (158 trees, 2-5 trees/site) were sampled on both islands.

Climate data

Climate data from weather stations were collected with two aims: (i) to calculate previous-year climate parameters which could explain infection by both or either pathogen; and (ii) extrapolate data to gaps present in the onsite weather data time series. Climate data were obtained for all sites involved with both the fortnightly and regional sampling.

For the PNW, climate data were interpolated from gridMet 4x4 km (http://www.climatologylab.org/gridmet.html). Climate variables were daily minima and maxima for both air temperature (T) and relative humidity (RH), and precipitation (P). Mean daily RH and T were approximated by averaging minimum and maximum values. For NZ sites, the same climatic variables were obtained from NIWA (National Institute of Water and Atmospheric Research, Ltd New Zealand). However, only a single daily value of RH was available, measured at 9 am. This value was considered as the mean RH for the NZ data set.

All primary climate data series, both from weather stations and onsite weather data loggers, were detrended applying the Gaussian smoothing function (smth.gaussian, package smoother in R; Hamilton, 2015) with a window width of three days. Other climate parameters were derived to test a range of biologically meaningful variables which could explain infection by either pathogen. Binary variables were calculated, where 1 corresponded to previous-day T higher than 5, 6, 7, 8, 9 or 10ºC, and 0, lower than those T values. In another set of variables, 1 corresponded to previous-day RH higher than 90, 95, 97, 98%; and similarly a combination of those levels of both T and RH, where 1 corresponded to previous-day T higher than 5 ºC and RH higher than 90% and so on. The number of days previous to sampling dates with combinations of those conditions was also calculated: T > 5, 7, 8, 9, 10, 12ºC and RH > 90, 95, 96 and 97%.

Dew point temperature was approximated by the following formula: $T_{dew} = T - \frac{100 - RH}{5}$, where T is the average daily temperature, and RH is the average daily relative humidity.

Growing degree days (GDD) were calculated using the GDD function from package chillR in R (Luedeling, 2018). Different base T values were used: 4, 5, 7, 8, 9 and 10 ºC.

From the weather station data, average winter, spring and summer T and RH were calculated, as well as seasonal and annual rainfall. In the PNW, months considered for each season were: December to February for winter, March to May and April to June for spring (two different periods were considered), and June to August for summer. In NZ, June to August were accounted for as winter, September to November and October to December as spring, and December to February as summer.

In order to extrapolate data gaps in onsite weather data series, two strategies were followed. In the PNW, weather data was lacking for the two first sampling dates, since the data loggers only became available prior to the third sampling date. In this case, data resulting from the bilinear interpolation using gridMed were used to perform correlations with the existing onsite weather data for all the parameters: mean, minimum and maximum daily T and RH. Correlations for the maximum RH for all the sites, mean RH for sites CAS and N04 and minimum RH for site N04 gave adjusted R^2 values lower than 0.40 and were not used to predict values correspondent to the first two sampling dates. In NZ, complete weather data was available for four out of the six sites and this data was used to interpolate a 4-week gap at KIN, and to extrapolate the initial 6-week gap at MAM, with adjusted R^2 values higher than 0.52.

Isolation and identification of *Phytophthora pluvialis*

All PNW samples were processed in the laboratory facilities of the Department of Botany and Plant Pathology (Oregon State University, Corvallis) and the NZ samples were processed in the Scion laboratories (New Zealand Forest Research Institute, Rotorua). Ten needles showing typical pale-olive lesions (Gomez-Gallego et al. 2017) were selected to perform isolations targeting *P. pluvialis*. Needles with an active lesion margin presenting both symptomatic and asymptomatic tissue were targeted to favour those with active pathogen growth. When these conditions were not met, either asymptomatic or completely symptomatic needles were selected. Five out of the 10 needles were surface sterilized for 10 sec in 5% sodium hypochlorite, rinsed with sterilized distilled water, and plated onto selective corn-based agar media (10 mg/L pimaricin, 200 mg/L ampicillin, 10 mg/L rifampicin), while the other five needles were plated without sterilizing to avoid possible pathogen loss with the sterilization step. Another set of needles up to ca. 125 mg (wet weight) were placed into individual tubes and frozen at -20ºC until DNA extraction was performed.

Plates were kept at 17 ºC for up to 15 days, growth was evaluated on a daily basis. Mycelium was collected from the growing colony margin and subcultured onto either carrot- or corn-based agar without antibiotics. Subcultures were identified morphologically after 4 days (Reeser et al. 2013). In the absence of reproductive structures in culture, the isolates were placed into pond water to encourage sporulation (Erwin and Ribeiro 1996).

DNA extractions and real time qPCR

Genomic DNA was extracted from frozen needle samples using the Nucleospin Plant II kit (Macherey-Nagel) in a 96-well plate format. DNA was extracted as per method N96 (Telfer et al. 2013) with a slight modification in the volume of lysis buffer PL2, which was increased further [975 µL PL2 and 25 µL RNase A (total 1000 µL)]. In Oregon, the final steps – DNA binding to the silica membrane and washing – were performed by centrifuging the plates instead of using the vacuum manifold. DNA extracts were quantified by spectrophotometry using NanoDrop (DeNovix DS-11 FX+, in NZ, and ND-1000 UV-Vis Spectrophotometer, in Oregon) determining the absorbance of each sample at 230, 260 and 280 nm wavelengths. The ratios A260/A230 and A260/A280 were used to assess DNA quality and to detect organic compound and protein contamination, respectively. The 96-well plates containing the DNA extracts were diluted to 1:10 to perform relative quantitative PCR (qPCR) for Douglas-fir and *N. gaeumannii*, and to 1:2 for *P. pluvialis*. The dilution rate was determined by performing qPCR reactions on a subsample of DNA extracts.

The multiplex approach was ruled out due to variable reaction optima, the potential for PCR bias and appreciably lower abundance of *P. pluvialis* detected in preliminary trials with respect to both *N. gaeumannii* and *Pseudotsuga menziesii* (Bustin et al. 2009). Therefore, we approached the relative quantification of each pathogen by running the assays singly. Probe and primer pairs used and the target single copy gene for each organism are listed in Table 4.1 (Winton *et al.*, 2002, for Douglas-fir and *N. gaeumannii*; and McDougal et al., in prep, for *P. pluvialis*). All qPCR reactions were performed in a total volume of 20 µL containing 5 µL of template DNA, 10 µL of PerfeCTa qPCR Tough Mix (Quantabio), 150 nM of probe and 400 nM of each primer. In Oregon, qPCR reactions were performed by the CFX96 Touch Real-Time PCR Detection Systems (Bio-Rad). In NZ, the QuantStudio 6 Flex Real-Time PCR System (Thermo Fisher Scientific) was used. Both systems processed 96-well plates. Reaction conditions for Douglas-fir and *N. gaeumannii* were: 10 min at 50 ˚C, 5 min at 95 ˚C and 40 cycles of 95 ˚C for 15 s and 60 ˚C for 1 min (Winton et al. 2002). For *P. pluvialis*, reaction conditions were: 10 min at 95 ˚C and 45 cycles of 96 ˚C for 15 s and 60 ˚C for 1 min (McDougal et al, in prep). The cycle threshold (Cq) values for each reaction were calculated automatically using the associated software (CFX manager software v3.1.1517.0823 and QuantStudio Real-Time PCR software v1.3).

Standard curves were constructed amplifying DNA from the three target species: Douglas-fir, *N. gaeumannii* and *P. pluvialis*. Total DNA was serially 10-fold diluted with sterile PCR-grade water. In different plates, two standard curves were performed for each target species. Three technical replicates were run per dilution level. Linear regressions were performed between log-transformed DNA concentration and Cq using the software R version 3.5.1 (R Core Team 2017). Coefficients of determination (R^2) obtained from linear regression for *N. gaeumanni*, *P. pluvialis* and Douglas-fir standard curves were, respectively, 0.99, 0.99 and 0.96, in Oregon, and 0.94, 0.97 and 0.97, in NZ. In every qPCR assay, we included two technical replicates of the DNA

positive controls used for standard curves (1:10 dilution) and water replaced template DNA for negative controls (two replicates). The maximum Cq value obtained in the average standard curve was considered the limit of detection for the corresponding target species. Cq values exceeding these thresholds were considered false positives.

Table 4.1. TaqMan probe, primer sets and target genes for relative quantification of *Nothophaeocryptopus gaeumannii* and *Phytophthora pluvialis* in DNA extracts of Douglas-fir (*Pseudotsuga menziesii*) needles. Size: product size.

Species	Target gene	Probe/ primer	Sequence (5' → 3')	Size
P. menziessi	*Leafy/ Floricaula*[a]	LFY1015P[c]	5' /5HEX/TAA CCG GCG CCT GAA TGC TTC/3BHQ1/ 3'	114 bp
		LFY989F[d]	GGTCACAAACCAAGTATTTCGACA	
		LFY1102R[e]	TGTTCAACATCCAGGCAATGA	
N. geaumannii	*β-tubuline*[a]	PG336BTUBP[c]	5' /56-FAM/CGA GCG CAT GAA CGT CTA CTT CAA CG/3BHQ1/ 3'	122 bp
		PGBT308F[d]	GGTACAATGGCACGTCTGATCTC	
		PGBT429R[e]	GGACGCCTATATCGCAAGTCA	
P. pluvialis	*Ypt1*[b]	Ypap[c]	5' /FAM/TCC TCC TTG GTA ACG CTA A/BHQ1/ 3'	227 bp
		Ypap2F[d]	AACTTGGTGCGGTATTCACG	
		Ypap2R[e]	ATCAGTTAGCTCCTTTCC	

[a] Winton et al. (2002); [b] McDougal et al., in prep; [c] TaqMan probes: Douglas-fir probe is labelled with the reporter HEX (Hexachlorofluorescein, emission 555 nm) on the 5' end, the reporter dye for N. gaeumannii and P. pluvialis is FAM (6-carboxy-fluorescein; emission 518 nm), all probes are labelled with BHQ_1 on the 3' as a quencher; [d] Forward primer; [e] Reverse prime

Pathogen-to-host DNA ratios were used to analyse the relative abundance of each pathogen. *N. gaeumannii* has often been assessed by pseudothecia density present on needles, which provides a direct link to the physiological impact on the plant (Hansen et al. 2000, Manter et al. 2000, Manter, Bond, et al. 2003). However, quantification by qPCR has been shown to be highly correlated to pseudothecia density and levels of disease severity in the field (Winton et al. 2003). Further, qPCR allows direct comparison with *P. pluvialis*, for which no alternative quantification methods based on fruiting structures have previously been implemented. To allow unbiased comparison, ratios of *P. pluvialis* and *N. gaeumannii* DNA concentration to Douglas-fir DNA concentration were calculated (hereafter referred to as '*P. pluvialis* abundance' and '*N. gaeumannii* abundance', respectively). To obtain these ratios, standard curves were used to approximate the concentration in ng/µL for each species and sample. The proportion of *P. pluvialis* and *N. gaeumannii* positive qPCR analyses per site was also calculated ('Proportion of infected trees').

Data analysis

All statistical analysis were conducted using the software R version 3.5.1 (R Core Team 2017). For the fortnight data, we used generalised additive mixed models (GAMMs), utilising a flexible

semi-parametric method to characterize non-linear relationships and one or more explanatory variables. Pathogen-to-host DNA ratios were averaged for each site and modelled using GAMM, with a tweedie error distribution family (function gamm, package mgcv; Wood, 2017) (Eq 4.1 and 4.2).

Equation 4.1. Best-fitted model for *P. pluvialis* DNA ratio as a response variable for the fortnightly sampling data.

$$Ppratio_i = \beta_0 + \beta_1 country_i + \beta_2 GDD_i + \beta_3 GDD_i * country_i + \beta_4 Ngratio_i + u \cdot sampling_i * country_i + \epsilon_i \ ,$$

where, *P. pluvialis* abundance of tree i ($Ppratio_i$) is modelled as a linear function of the country, growing degree days at the moment of sampling (GDD_i) and its interaction with country ($GDD_i * country_i$), and *N. gaeumannii* abundance ($Ngratio_i$). In this and subsequent models, 'sampling' nested within 'country' was incorporated as random effect ($sampling_i * country_i$) to account for repeated measures. ϵ_i corresponds to the residual error.

Equation 4.2. Best-fitted model for *N. gaeumannii* DNA ratio as a response variable for the fortnightly sampling data.

$$Ngratio_i = \beta_0 + s(RH_{spring,i}) + \beta_1 country_i + \beta_2 T_{winter,i} + \beta_3 Ppratio_i + u \cdot sampling_i * country_i + \epsilon_i \ ,$$

where, *N. gaeumannii* abundance of tree i ($Ngratio_i$) is modelled as a smooth function (s) of the mean previous-spring relative humidity ($RH_{spring,i}$), country, mean previous-winter temperature ($T_{winter,i}$) and *P. pluvialis* abundance ($Ppratio_i$).

The proportion of *P. pluvialis* infected trees was modelled in a similar fashion using a binomial error distribution, following Eq 4.3.

Equation 4.3. Best-fitted model for the proportion of *P. pluvialis* infected trees as a response variable for the fortnightly sampling data.

$$Ppinfected_i = \beta_0 + \beta_1 country_i + \beta_2 GDD_i + \beta_3 GDD_i * country_i + u \cdot sampling_i * country_i + \epsilon_i \ ,$$

where $Ppinfected_i$ is the proportion of infected trees per site.

For the regional data, we used the same family distributions, but since there were no repeated measures involved, we ran the generalised additive models (GAM) without a random term (function gam, R package mgcv, Wood 2011). Model formulations for the same response variables used in the fortnightly sampling (Eqs 4.1, 4.2, 4.3) are in Eqs 4.4, 4.5, and 4.6 for the regional sampling.

Equation 4.4. Best-fitted model for *P. pluvialis* DNA ratio as a response variable for the regional sampling data.

$$Ppratio_i = \beta_0 + \beta_1 country_i + \beta_{42} Ngratio_i + \beta_3 RH_{winter,i} + \epsilon_i \ ,$$

where, $RH_{winter,i}$ is the mean previous-winter RH.

Equation 4.5. Best-fitted model for *N. gaeumannii* DNA ratio as a response variable for the regional sampling data.

$$Ngratio_i = \beta_0 + \beta_1 country_i + \beta_2 T_{winter,i} + \beta_3 T_{winter,i} * country_i + \beta_4 Ppratio_i + \beta_5 Ppratio_i * country_i + \epsilon_i$$

Equation 4.6. Best-fitted model for the proportion of *P. pluvialis* infected trees as a response variable for the fortnightly sampling data.

$$Ppinfected_i = \beta_0 + s(RH_{winter,i}) + \beta_1 country_i + \beta_2 GDD_i + \epsilon_i ,$$

Backwards model selection was used to determine the optimal smoothers and parametric terms of the GAMs using the Akaike Information Criterion (AIC). In order to reduce the large number of explanatory variables, the microclimatic site variables were grouped in three groups depending on the variable they were derived from (T, RH, and GDD). Seasonal climatic variables were grouped by T, RH and P and by winter or spring (two spring periods considered and summer). The saturated model was run with one variable from each group, and comparison between AIC was considered to choose the best explanatory variable of each group. Climatic variables on a continuous scale were included in the smoother term of the GAMs, while the binary variables were included in the parametric term. '*P. pluvialis* abundance' was included in the smoother term of the model for '*N. gaeumannii* abundance' as a response variable, and vice versa. 'Country' was included in the parametric term, and its interaction with the climatic variables was also tested (i.e. whether separate smoothers for each country were warranted). Significant variables showing a linear pattern were included in the parametric term. Concurvity was analysed to detect possible co-linearity among predictors, and no co-linearity was detected among predictors of the best-fitted models. Graphical model validation tools (residual plots for variance homogeneity and quantile–quantile plots for normality) were used to assess the underlying model assumptions, and suitability of chosen error distributions.

Results

Fortnightly sampling

Both *P. pluvialis* and *N. gaeumannii* were consistently more abundant NZ than in the PNW (Figs 4.1 and 4.2a-b). In NZ, more trees tested positive for *P. pluvialis* (69%) from the cultured needle samples (10 needles/sample) across all dates. In contrast, only 7% of needle samples plated from Oregon were positive. The results paralleled detection rates by qPCR with 85% and 15% for NZ and Oregon, respectively. The abundance of both pathogens (pathogen-to-host DNA ratio) was greater in NZ with a mean *P. pluvialis* abundance of 0.008 than in Oregon with a mean of 0.36 in NZ (Fig 4.1c-d). Similarly, *N. gaeumannii* abundance was greater in NZ with a mean of 0.97, compared to a mean of 0.37 in Oregon (Fig 4.1c-d). Regardless of the country, *N. gaeumannii* was significantly more abundant than *P. pluvialis*. Even though the amount of *N. gaeumannii* DNA present in the needles was different between the countries, the proportion of *N. gaeumannii*-

infected trees was similar (average values of 0.99 vs 0.95, for NZ and Oregon, respectively). With very few exceptions, SNC was detected in all trees in the fortnightly sampling.

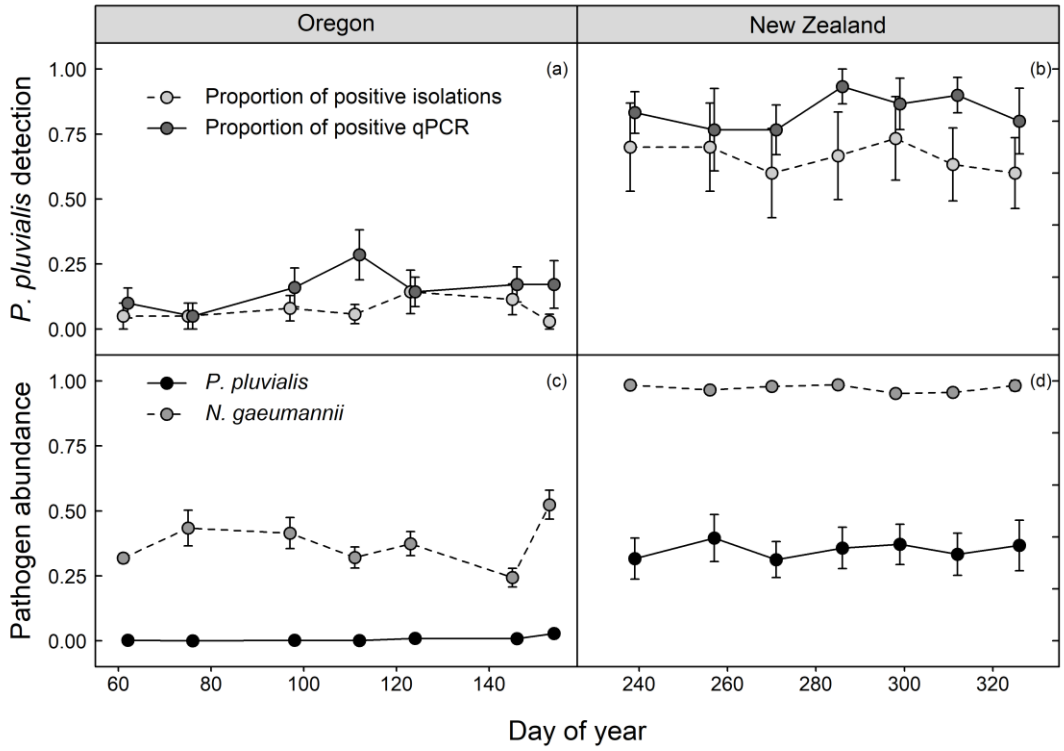

Figure 4.1. *Phytophthora pluvialis* detection rates by means of isolation in culture media and qPCR in Oregon (a) and New Zealand (b), and pathogen abundance, measured as pathogen-to-host DNA ratio, for *P. pluvialis* and *Nothophaeocryptopus gaeumannii* in Oregon (c) and New Zealand (d) across time obtained in the 3-month spring fortnightly sampling.

P. pluvialis detection by qPCR exceeded or equalled isolation rates, and was considered more effective to assess *P. pluvialis* infection. Isolation results corroborated the validity of qPCR in both labs (Fig 4.1a-b). In NZ, there was no apparent seasonality to *N. gaeumannii* infection (Fig 4.1d). In the PNW, both pathogens' infection varied across the 3-month sampling period, with *P. pluvialis* peaking in mid-spring (second fortnight of April) while *N. gaeumannii* reached the maximum abundance at the beginning of summer (Fig 4.1c).

The GAMMs accounted for at least 86% of the total variation in both *N. gaeumannii* and *P. pluvialis* abundance, and the proportion *P. pluvialis* infected trees. One site in the NI of NZ (site KER, -38.33564, 176.38888, Supplementary Table S4.1) was excluded from *P. pluvialis* analyses due to the absence of RNC at the site and surrounding area. The seasonality in *P. pluvialis* models was captured by the growing degree days (GDD). GDD was only significant in the PNW in the model with *P. pluvialis* abundance as response variable (Table 4.2). The model suggests that *P. pluvialis* abundance decreases with increasing GDD (Fig 4.3). *N. gaeumannii* abundance was positively correlated with *P. pluvialis* abundance in both countries (Table 4.2). GDD had a statistically significant effect on the proportion of *P. pluvialis* infected trees, regardless of the country, indicating an increase in *P. pluvialis* infected trees with increasing GDD (Table 4.2). *N. gaeumannii* abundance appeared to have no effect on the proportion of *P. pluvialis* infected trees,

but the mean daily relative humidity was significant and had a significant interaction with country (Table 4.2). In the PNW, an increase in the daily RH resulted in an increase in the proportion of *P. pluvialis* infected trees, while the opposite effect was observed in NZ. *N. gaeumannii* abundance was explained by mean winter T and spring RH (April to June, PNW), which were significant only for the PNW (Table 4.2). In NZ, the amount of *N. gaeumannii* was fairly constant across the season and with an average DNA ratio of 0.97 (± 0.01) (Fig 4.1d).

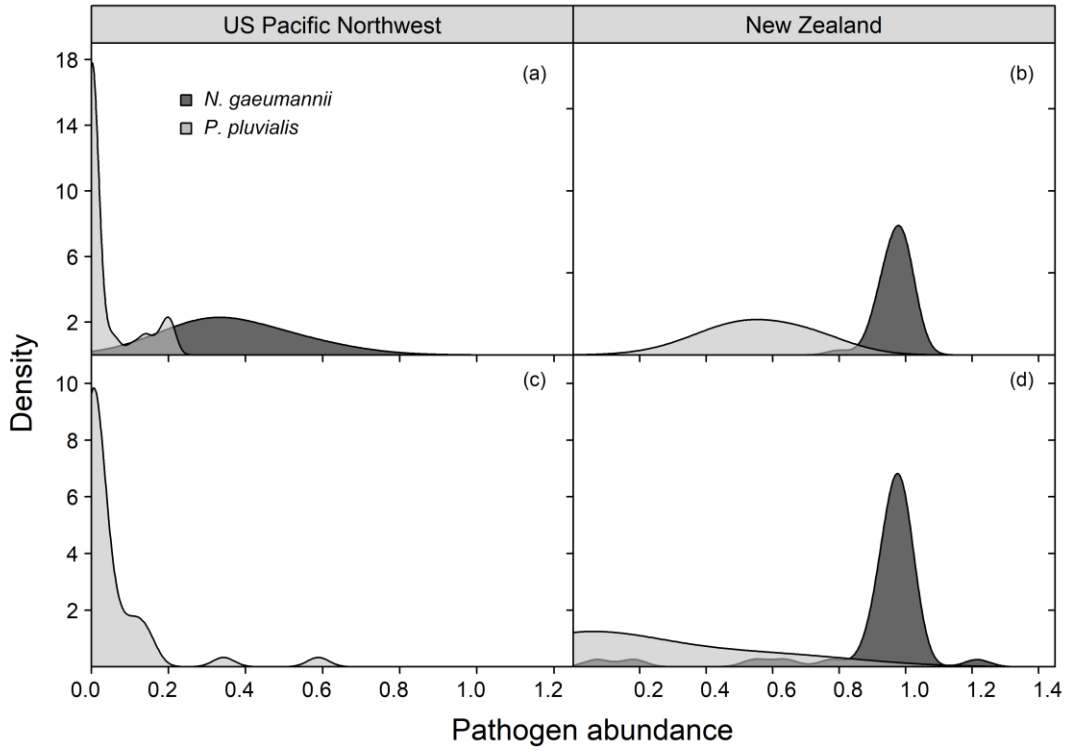

Figure 4.2. Kernel density estimates for pathogen abundance measured as pathogen-to-host DNA ratios for *Nothophaeocryptopus gaeumannii* and *Phytophthora pluvialis* for the spring fortnightly sampling (a, b) and the regional sampling (c, d) in the US Pacific Northwest (a, c) and New Zealand (b, d).

The examination of Douglas-fir needles using SEM microscopy showed the growth of both *N. gaeumannii* and *P. pluvialis* on the needle surface (Fig 4.4). Both clusters of *P. pluvialis* sporangia and *N. gaeumanni* pseudothecia were found on the screened needles occupying neighbouring stomata (Fig 4.4a-c). The samples were collected on the 31st August 2017 (last day of southern hemisphere winter) on the NI (sites MAM and TAR, Supplementary Table S4.1). Early release of *N. gaeumannii* ascospores and mature pseudothecia were observed on some of the needles (Fig 4.4e-f).

Table 4.2. Results from the best-fitted generalized additive mixed models for the pathogen-to-host DNA ratio and the proportion of positive qPCR per site for the fortnight sampling. Country, Oregon (reference) vs. New Zealand; GDD, growing degree days with 5 ºC base temperature; Ng, *N. gaeumannii* abundance; DailyRH, mean daily relative humidity; WinterT, mean winter temperature. edf: estimated degrees of freedom; s: smoother term.

	***P. pluvialis* abundance** Family: tweedie (1.45). Link: log R^2 adj: 0.86			**Proportion of *P. pluvialis* infected trees** Family: binomial. Link: logit R^2 adj: 0.90			***N. gaeumannii* abundance** Family: tweedie (1.01). Link: log R^2 adj: 0.93		
Parametric coefficients	**Estimate (SE)**	**t**	**P**	**Estimate (SE)**	**t**	**P**	**Estimate (SE)**	**t**	**P**
Intercept	-3.18 (0.50)	-6.34	<0.001	-8.68 (3.49)	-2.49	0.02	-3.74 (0.60)	-6.23	<0.001
Country	-0.43 (0.79)	0.54	0.59	18.15 (5.19)	3.50	<0.001	3.74 (0.61)	-6.11	<0.001
GDD	-0.01 (0.01)	-2.32	0.02	0.01 (0.01)	2.38	0.02			
GDD * Country	0.02 (0.01)	2.62	0.01						
Ng abundance	2.06 (1.14)	1.81	0.075						
DailyRH				0.07 (0.04)	1.70	0.09			
DailyRH* Country				-0.16 (0.06)	-2.72	0.01			
WinterT							0.66 (0.14)	4.71	<0.001
WinterT * Country							-0.67 (0.14)	-4.73	<0.001
Smooth terms	**edf**	**F**	**P**	**edf**	**Chi.sq**	**P**	**edf**	**F**	**P**
s(Spring RH): OR							3.71	18.6	<0.001
s(Spring RH): NZ							1	0.20	0.66

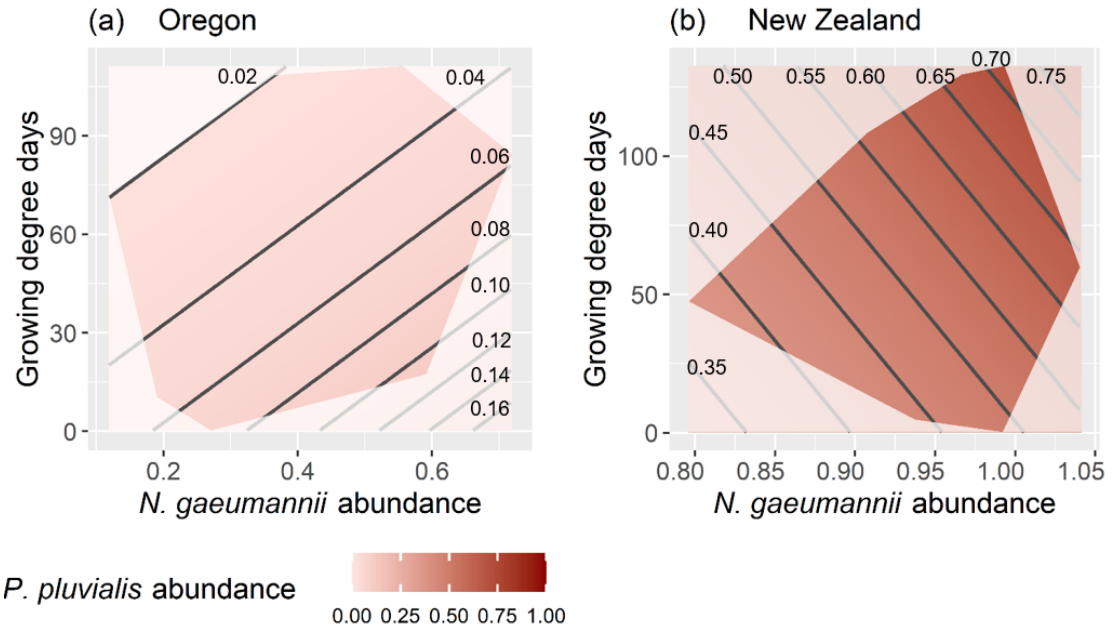

Figure 4.3. Predicted *Phytophthora pluvialis* abundance (*P. pluvialis*-to-host DNA ratios) as a function of growing degree days and *Nothophaeocryptopus gaeumannii* abundance (*N. gaeumannii*-to-host DNA ratios). Predictions were derived from generalized additive mixed effects models applied to the fortnightly sampling data from the US Pacific Northwest (Oregon) (a) and New Zealand (b). Highlighted polygons

indicate the range of the raw data and predictions outside this range should not be considered. Both axis variables are statistically significant except for y-axis (growing degree days) in panel (b).

Regional sampling

Aggregated results from all sites in the regional sampling led to similar results than the fortnightly sampling. *P. pluvialis* and *N. gaeumannii* were more abundant in NZ than in the PNW, with average values of 0.20 and 0.91 vs 0.05 and 0.36, respectively (Fig 4.2c-d). While *N. gaeumannii* was detected by qPCR in all the sampled trees in both NZ and the PNW, *P. pluvialis* was present in 47% and 20% of the trees, respectively. The regional distribution of values for normalized *N. gaeumannii* and *P. pluvialis* abundance is shown in Fig 4.5.

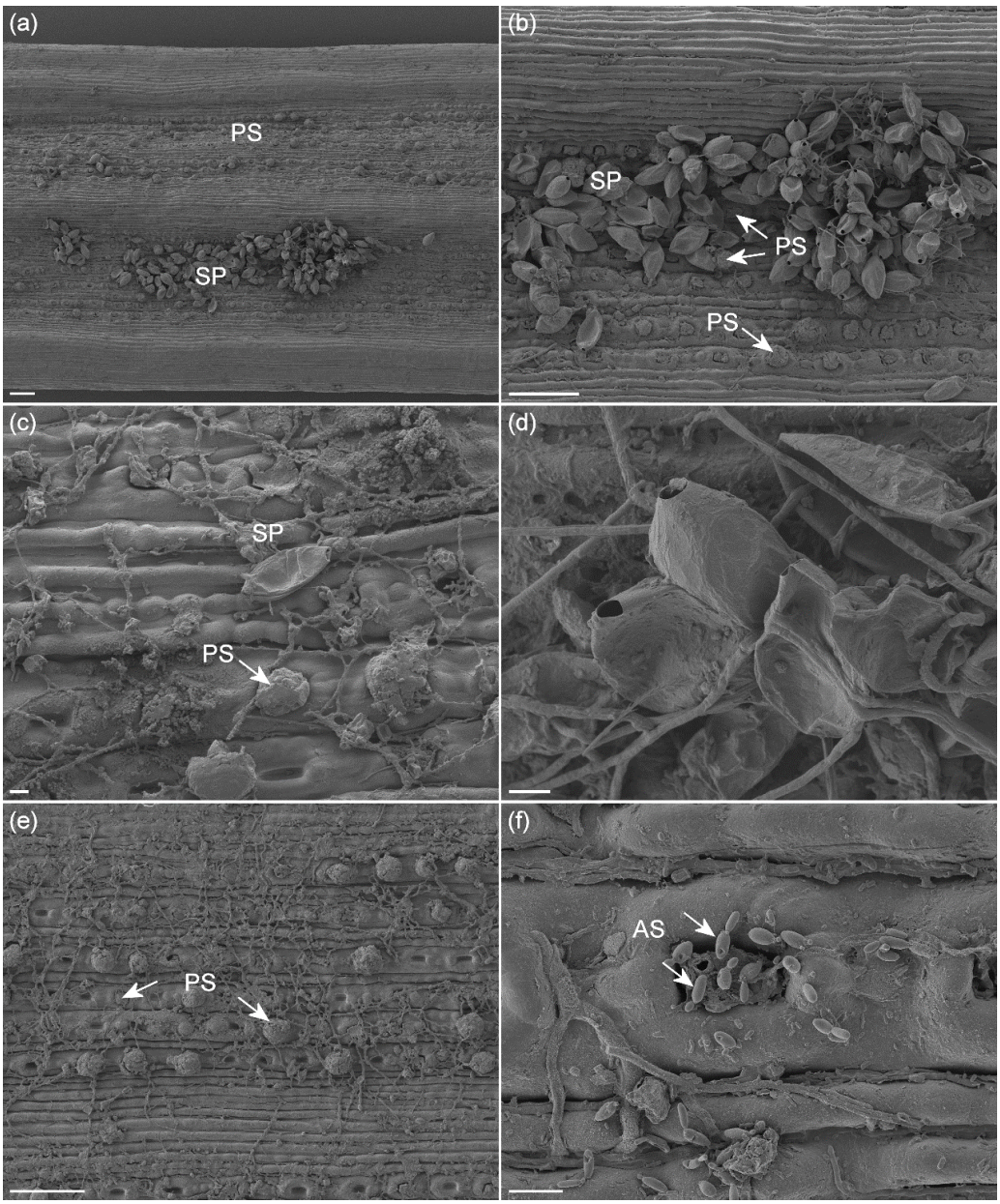

Figure 4.4. Scanning electron micrographs showing fruiting bodies of both *Phythophthora pluvialis* (a-d) and *Nothphaeocryptopus geaumannii* (a-c, e-f) on Douglas-fir needles sampled on the 31st of August 2017 in New Zealand. (a) Occupation of needle stomata by *N. gaeumannii* pseudothecia (PS) and clusters of *P. pluvialis* sporangia (SP). (b) Detail of neighbouring *P. pluvialis* sporangia and *N. gaeumannii* pseudothecia

at different stages of maturity. (c) Detail of an empty sporangia next to a mature pseudothecium. (d) Detail of discharged *P. pluvialis* sporangia. (e) *N. geaumannii* hyphae and pseudothecia at different stages of maturity. (f) *N. gaeumannii* ascospores (AS) being released from mature asci. Bars: a-b, e = 100 µm; c-d, f = 10 µm.

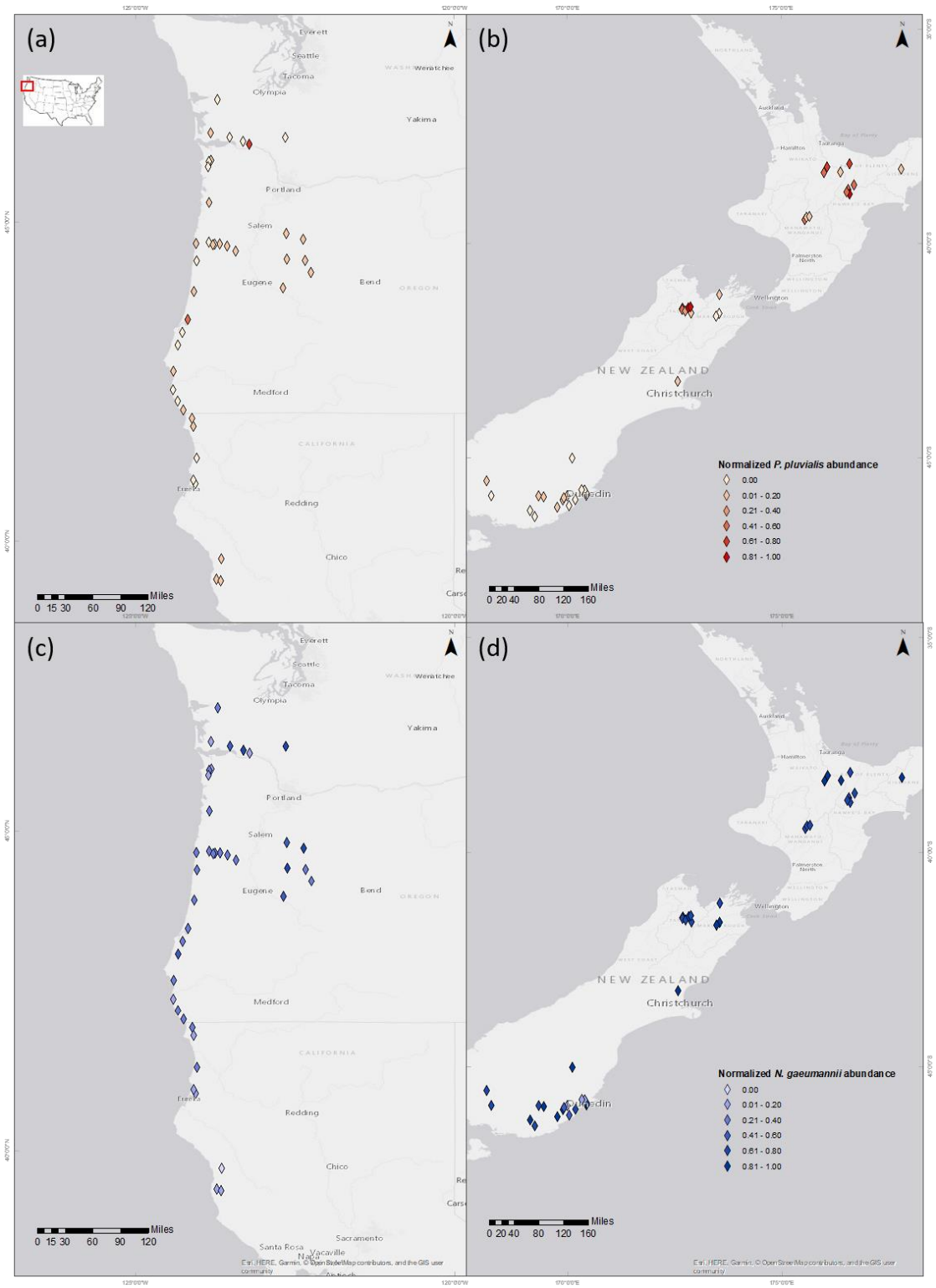

Figure 4.5. Pathogen-to-host DNA ratio for *Phytophthora pluvialis* (a, b) and *Nothophaeocryptopus gaeumannii* (c, d) per site in the regional sampling in the PNW (a, c) and New Zealand (b, d). Ratios are normalized in the 0-1 range to be comparable across countries and pathogens.

When analysing the proportion of infected trees at the regional level, the comparison between a GAM with a common smoother for the mean winter RH for both NZ and the PNW and a GAM with separate smoothers for both countries lent support to the latter suggesting a mean winter RH × country interaction (L = 4.34, df = 0.91, P = 0.03). In NZ, *P. pluvialis* abundance increased significantly with higher mean winter RH (Table 4.3, Fig 4.6b). The number of *P. pluvialis* infected trees increased significantly with increasing GDD (Table 4.3, p < 0.001), irrespective of the country.

Table 4.3. Results from the best-fitted generalized additive models for the pathogen-to-host DNA ratio and the proportion of positive qPCR per site for the regional sampling. Country, PNW (reference) vs. New Zealand; GDD, growing degree days with 5 ºC base temperature; WinterRH, mean winter relative humidity; WinterT, mean winter temperature. Ng: *Nothophaeocryptopus geaumannii* abundance*;* Pp: *Phytophthora pluvialis* abundance. edf: estimated degrees of freedom; s: smoother term.

	***P. pluvialis* abundance** Family: tweedie (1.55). Link: log R^2 adj: 0.45			**Proportion of *P. pluvialis* infected trees** Family: binomial. Link: logit R^2 adj: 0.57			***N. gaeumanni* abundance** Family: tweedie (1.28). Link: log R^2 adj: 0.69		
Parametric coefficients	**Estimate (SE)**	**t**	**P**	**Estimate (SE)**	**t**	**P**	**Estimate (SE)**	**t**	**P**
Intercept	0.52 (6.69)	0.08	0.94	-4.68 (1.11)	-4.21	<0.001	-0.38 (0.16)	-2.30	0.02
Country	-59.95 (10.7)	-5.59	<0.001	-7.24 (9.68)	-0.75	0.45	0.18 (0.26)	0.71	0.48
Ng	-2.80 (1.33)	-2.10	0.04						
Ng * Country	4.31 (2.04)	2.12	0.04						
WinterRH	-0.03 (0.08)	-0.41	0.69						
WinterRH * Country	0.66 (0.13)	5.19	<0.001						
GDD				0.22 (0.06)	3.79	<0.001			
WinterT							-0.14 (0.04)	-3.89	<0.001
WinterT * Country							0.16 (0.05)	3.02	0.003
Pp							-1.84 (0.82)	-2.24	0.03
Pp * Country							2.02 (0.84)	2.39	0.02
Smooth terms	**edf**	**F**	**P**	**edf**	**Chi.sq**	**P**	**edf**	**F**	**P**
s (Winter RH): OR				1.39	0.41	0.74			
s (Winter RH): NZ				2.92	43.76	<0.001			

Mean winter RH showed a linear positive correlation with *P. pluvialis* abundance in NZ, but not in the PNW (Table 4.3, Fig 4.6b). In turn, *N. gaeumannii* abundance only explained the variation in *P. pluvialis* abundance in the PNW, but not in NZ. Remarkably, higher *P. pluvialis* abundance was predicted with lower levels of *N. gaeumannii* in the PNW (Table 4.3, Fig 4.6a). In addition, when *N. gaeumannii* abundance was modelled at the regional level, lower *P. pluvialis* abundance resulted in higher levels of *N. gaeumannii*. Mean winter T explained a significant proportion of the

variation seen in *N. gaeumannii* abundance but only in the PNW, and surprisingly as an inverse correlation (Table 4.3, Fig 4.6b).

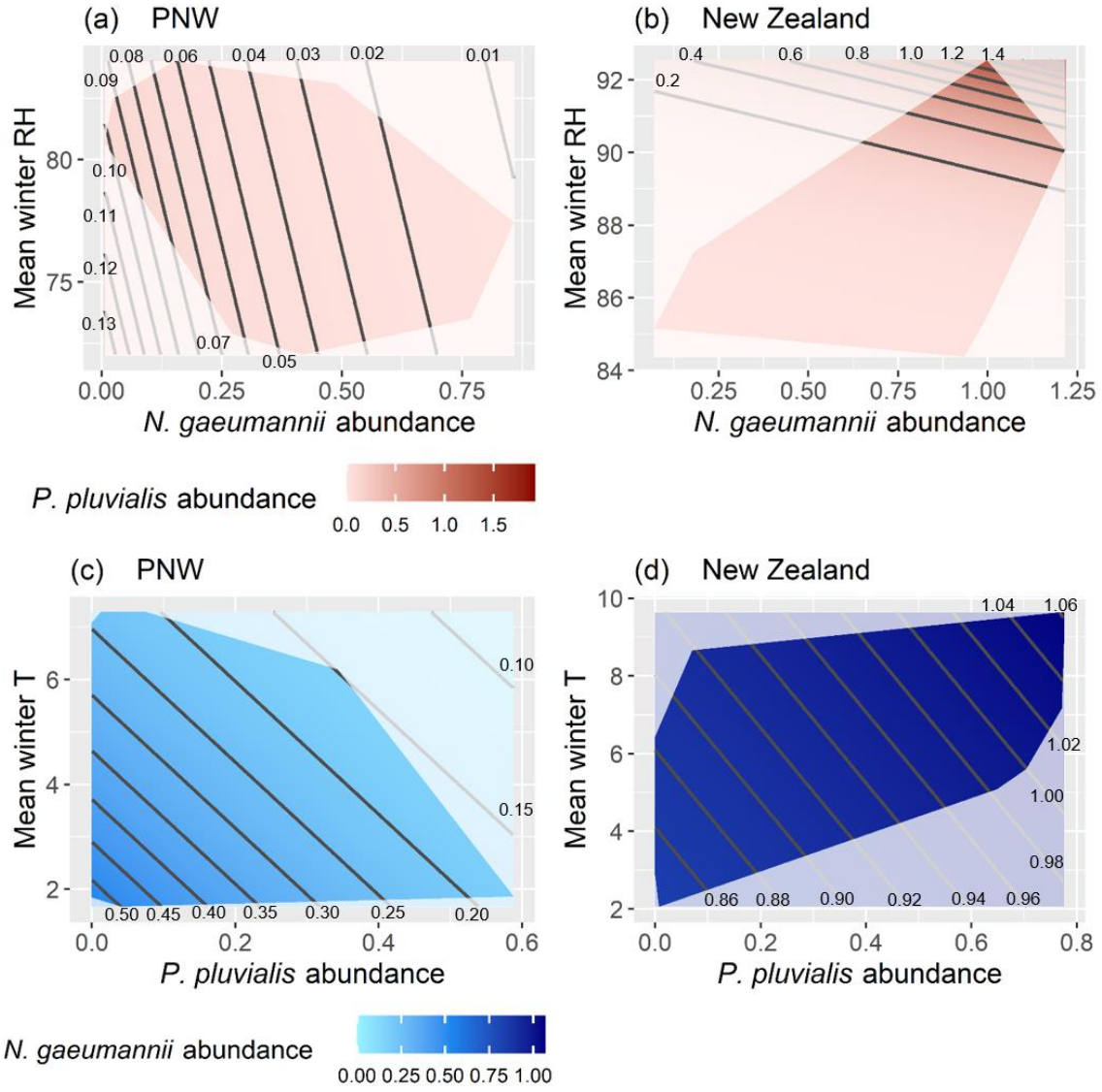

Figure 4.6. Predicted *Phytophthora pluvialis* (a, b) and *Nothophaeocryptopus gaeumannii* abundance (c, d) as a function of mean winter RH and T, respectively, and the abundance of the competing pathogen. Predictions were derived from generalized additive models applied to the regional sampling data. Highlighted polygons indicate the range of the original data, and predictions outside this range should not be considered. In panel (a) only the x-axis variable is statistically significant; in panel (b) and (c), both variables are significant; in panel (d), neither of them are statistically significant.

Discussion

With the recent emergence of *P. pluvialis* as a pathogen causing early defoliation of Douglas-fir, the aim of this study was to investigate (i) the extent of the epidemic in both countries (NZ and the PNW); and (ii) the interaction of *P. pluvialis* with *N. gaeumannii.* Our results suggest that the

coexistence of both *N. gaeumannii* and *P. pluvialis* across spatial scales from regions to needles. Furthermore, an inverse correlation was observed between the relative abundance of the two pathogens in the PNW, where they have likely coexisted for longer.

Phytophthora pluvialis epidemics and seasonality

Our regional and fortnightly sampling demonstrated that *P. pluvialis* infects the lower canopy of Douglas-fir throughout both countries (Fig 4.1). In NZ, *P. pluvialis* was more abundant in the NI and decreased gradually towards the south of the SI (Fig 4.5b). Mean winter RH (June-August previous to the sampling period) was the only significant climatic factor explaining the variation in the relative abundance of *P. pluvialis* across NZ. *P. pluvialis* has partially caducous sporangia, which are produced on the surface of infected needles (Reeser et al. 2013, Hansen et al. 2017), releasing zoospores in conditions of high RH which are disseminated by water splash (Dick et al. 2014). The positive correlation between winter RH and *P. pluvialis* abundance suggests that active inoculum build-up takes place during winter months and is favoured by high RH values in NZ. In contrast, this effect was not found in the PNW. A lower non-overlapping range in winter RH was recorded in the PNW, suggesting that low RH is a limitation to *P. pluvialis* inoculum production.

The most likely explanation for the limited presence of *P. pluvialis* in the south of the SI could be a later arrival of the pathogen, given that the previous two *P. pluvialis* population clusters were found in the NI and the north of the SI (Brar et al. 2018). Suboptimal conditions for disease development within tree canopies could have also slowed inoculum development, although our climatic variable analysis does not support this conclusion.

The great abundance of *P. pluvialis* in NZ samples could also be explained by the exposure of NZ sites to high levels of *P. pluvialis* inoculum. Surrounding radiata pine plantations with severely infected canopies likely provided large amounts of inoculum resulting in greater levels of infection in NZ compared to the PNW. Conversely, reduced *P. radiata* infection at the KER site in NZ, resulted in no *P. pluvialis* isolates and relatively small amounts of pathogen DNA. The surrounding geothermal conditions at the KER site, involving high sulphur levels, seem to provide an unconducive environment for *P. pluvialis* implying that this site may not be considered representative of NZ Douglas-fir plantations. The effect of sulphur on oomycetes has not been given sufficient attention in previous research. Contradictory reports show no effect on *Phytophthora palmivora* under the presence of elemental sulphur (Cooper and Williams 2004, Williams and Cooper 2004), and increased susceptibility to *Phytophthora brassicae* in sulphur-deficient plants (Dubuis et al. 2005). However, KER samples presented similarly high levels of *N. gaeumannii* compared to the other 5 sites. This supports the hypothesis that the amount of available inoculum plays an important role in the infection, regardless of the amount of *N. gaeumannii*, and that radiata pine, may be a key driver of the epidemiology of *P. pluvialis* on Douglas-fir in NZ.

The levels of *P. pluvialis* recorded during the fortnightly sampling suggest different dynamics of infection between countries. These differences are likely related to the temperature limits of the

pathogen. The sampling design was based on prior knowledge of *P. pluvialis* epidemiology on radiata pine in NZ. The infection cycle typically begins in autumn, with a peak in winter and early spring, leading to defoliation of the symptomatic portion of the canopy during the subsequent summer (Dick et al. 2014). Our fortnightly sampling was designed to cover the spring season to capture a window during which *P. pluvialis* was active, given that *N. gaeumannii* can be detected all year round (Stone, Capitano, et al. 2008).

The proportion of infected trees increased with increasing GDD (Table 4.2). Thus, in both countries, disease epidemics developed during spring. However, *P. pluvialis* abundance decreased with an increase in GDD in the PNW (Table 4.2, Fig 4.3a), while no effect was observed in NZ. This inverse correlation may be partially explained by the small amount of inoculum available in the PNW compared to NZ. In NZ, *P. pluvialis* infection progresses through winter allowing for a longer period of inoculum build-up, whereas in the PNW, winter appears to be a limiting period for *P. pluvialis* development. Recorded mean winter T previous to sampling (December 2016 - February 2017) ranged from 1.8 to 6.8 ºC in the PNW, compared to higher NZ temperatures (6 to 9.6 ºC, June - August 2017). The differences in pathogen abundance may be explained by the differences in climatic variables between the two countries as well as other factors, such as presence of alternative hosts (i.e. *P. radiata* in NZ). The relative contributions of climate variables and the features derived from an exotic environment cannot be disentangled from the analyses presented here, and should be investigated further.

Differences in the interaction between *P. pluvialis* and *N. gaeumannii* in the US Pacific Northwest and New Zealand

One of the most interesting findings of the current study is that the abundance of both pathogens are inversely correlated in the PNW (Table 4.3, Fig 4.6a, c). This correlation could be explained by a potential lack of alternative hosts (*Pinus radiata* in NZ) serving as an inoculum source in the PNW. Alternatively, it may be due to a longer period of competition between both pathogens in the PNW. It is not known how long *P. pluvialis* has been present in the PNW and the origin of the species is unknown (Brar et al. 2018). However, it has been suggested that the NZ population most probably originated from the US population (Brar et al. 2018). This indicates that, regardless of its origin, *P. pluvialis* and *N. gaeumannii* have coexisted for longer in the PNW than in NZ.

While SNC has been studied in the PNW for some time (Ritokova et al. 2016), the association of *P. pluvialis* with Douglas-fir is relatively recent (Reeser et al., 2013). It is however likely that defoliation associated with *P. pluvialis* has been overlooked for some time and attributed to SNC. The symptoms of *P. pluvialis* infection on Douglas-fir are more difficult to detect than those on radiata pine, as needles tend to cast when green or with a faint pale-olive discolouration. The polycyclic nature of *P. pluvialis* infection reduces the time window during which sporulating structures can be detected, unlike *N. gaeumannii* whose pseudothecia are visible throughout most of the year. Previous sampling methods for SNC severity have been based on mid-crown observations (Ritokova et al. 2016), which might have favoured *N. gaeumannii* detection over *P. pluvialis*. In fact, the latter has been primarily observed to impact the lower canopy meaning that

SNC assessment protocols may have unknowingly overlooked *P. pluvialis* in the past. The possibility of *P. pluvialis* establishing symptomless associations with Douglas-fir, prior to any report of early defoliation, remains to be explored. Indeed, numerous plant pathogens can hold a broad range of ecological interactions with their hosts, including the capacity of asymptomatic colonization before they become pathogenic (Hansen 2008, Porras-Alfaro and Bayman 2011, Malcolm et al. 2013, Stergiopoulos and Gordon 2014, Harris et al. 2018).

A longer competition process between *P. pluvialis* and *N. gaeumannii* abundance could have led to spatial niche specialization (Abdullah et al. 2017) at the site level in the PNW, with variable amounts of both pathogens, in contrast to homogeneous levels of *N. gaeumannii* in NZ. Our statistical analyses from the regional data indicate that one pathogen typically dominated within each site in the PNW (Fig 4.6a, c; compare individual sites in Fig 4.5a, c). This suggests some degree of within-site segregation between both pathogens but not mutual exclusion, as *N. gaeumannii* was present across all sites. Indeed, microscopy revealed the ability of both pathogens to co-infect and sporulate from the stomata of individual needles (Fig 4.2). Biotrophy, direct competition and survival of both pathogens within needles warrens further investigation.

Our sampling procedure prioritized detection of *P. pluvialis* by sampling lower branches within a maximum height of 2 m from the ground. We observed that branches closer to the ground across the sampled trees cast higher amounts of needles. These needles were frequently *P. pluvialis* positive in agreement with RNC disease development beginning in the lower crown. A previous study on the vertical distribution within the canopy by *N. gaeumannii* in the Oregon Coast Range found that the upper canopy showed the lowest values of foliage retention associated with SNC (Shaw et al. 2014). This pattern would appear contrary to the usual paradigm generally applied to foliar diseases, which typically favour lower canopy infection (Shaw et al. 2014). This raises the question of whether *P. pluvialis* is related to this unusual pattern and to a spatial niche differentiation within the tree (Abdullah et al. 2017). Differential distribution of pathogens within the tree has been also suggested in the interaction between *Phytophthora ramorum*, the causal agent of the Sudden Oak Death, and *Phytophthora nemorosa*, a close relative to *P. pluvialis* (Kozanitas et al. 2017). There are no comprehensive studies on the within-tree distribution of *N. gaeumannii* in NZ and hence clear vertical patterns have not been reported. However, in one NZ-based study (Hood and Sandberg 1979), lower levels of *N. gaeumannii* were found in the upper canopy suggesting a different vertical pattern spread than in the PNW. Understanding within canopy infection dynamics may further elucidate the role and interaction between both pathogens in needle cast episodes of Douglas-fir.

When only the fortnightly data was considered, *N. gaeumannii* had an overall positive impact on *P. pluvialis* abundance (Table 4.2, Fig 4.4). This positive correlation may be an artefact driven by the large amount of both pathogens present in the NZ samples, and the low levels of *P. pluvialis* in the PNW. The great abundance of *N. gaeumannii* may be explained by the sampling procedure, which forced the detachment of needles from the branches. Prematurely shed needles most likely hold higher pathogen loads than needles remaining on the tree. Furthermore, *P. pluvialis* infection may have enhanced *N. gaeumannii* growth rates. Co-infection is thought to trigger higher within-host growth rates as pathogens compete for limited resources (Alizon and van Baalen 2008, Laine

2011). *P. pluvialis* in NZ appears to be in its initial phase of colonization. Presumably, establishment will largely rely on niche specialization shaped by environmental conditions conducive to *P. pluvialis* infection and its interactions with symbionts, hosts, antagonists and competitors (Dickie et al. 2017). In the NZ context, this interaction is likely to be influenced by the association between *P. pluvialis* and radiata pine. Both interactions may foster further colonization of NZ by *P. pluvialis* given these two hosts represent the most widely planted species in NZ forestry.

In the PNW, our fortnightly data corroborated previous studies that associate SNC severity with mild winter temperatures and wet springs in the PNW (Rosso and Hansen 2003, Manter et al. 2005, Stone, Coop, et al. 2008, Zhao et al. 2011, Lee et al. 2013, 2016), as expected given that the six sampling sites were located within the same area of the cited studies. In our study, *N. gaeumannii* abundance increased with increasing spring RH values reaching a peak around 72% RH followed by a decline at higher RH. This effect was notable when winter T values exceeded 6 ºC. A similar effect was found in NZ by (Watt et al. 2010) who reported a decline in the *N. gaeumannii* infection index at very high spring rainfall. However, this effect was reversed in the regional sampling (i.e. including Northern Californian coast), supporting previous studies that suggest complex site-specific factors modulating SNC impact (Lee et al. 2013). Other site characteristics (elevation, aspect) will likely contribute to variability in *N. gaeumannii* and *P. pluvialis* abundance in Douglas-fir stands.

Our study confirms the recognition of *P. pluvialis* as a foliar pathogen of Douglas-fir in the PNW and NZ. Both *P. pluvialis* and *N. gaeumannii* appear to be fine-tuned to different ecological conditions, through spatial niche specialization in the PNW, while both pathogens are in large abundance suggesting competition over limited resources, through high growth rates, in NZ. Further research on *P. pluvialis* epidemiology, climate drivers, origin and ecological role should be conducted to fully elucidate the impacts of *P. pluvialis* and *N. gaeumannii* on Douglas-fir. Our findings open a new chapter in the research on aerial *Phytophthora* pathogens and their interaction with foliar fungal diseases in forest systems.

Supplementary material

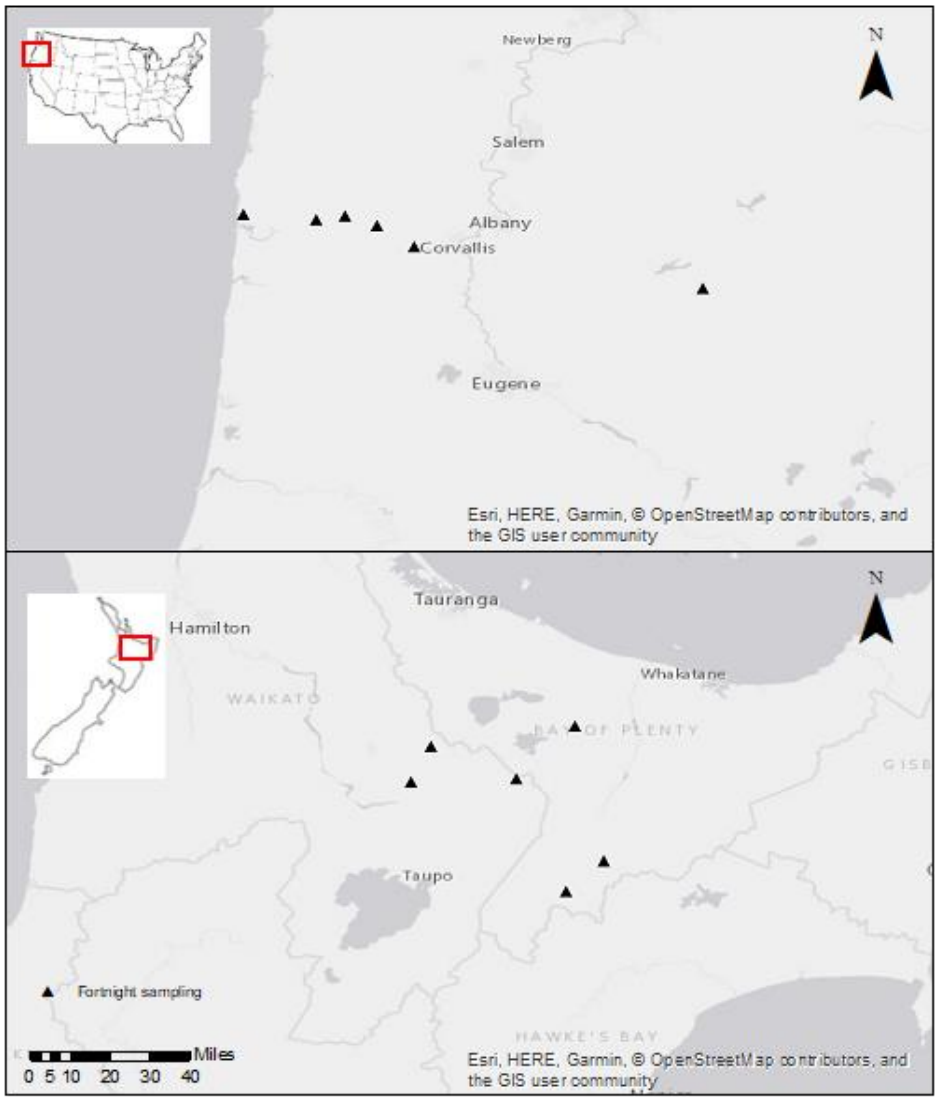

Figure S4.1. Location of the sites included in the fortnightly sampling in Oregon and New Zealand.

Table S4.1. Location of the sites for both the fortnight and regional sampling. OR, Oregon state; CA, California state; WA, Washington state; NI, North Island in New Zealand; SI, South Island in New Zealand.

SITE	COUNTRY	REGION	LATITUDE	LONGITUDE	SAMPLING DATE
N04	US	Central OR	44.66566	-124.04421	02/03-02/06/2017
N151	US	Central OR	44.66002	-123.67449	02/03-02/06/2017
N152	US	Central OR	44.62573	-123.55839	02/03-02/06/2017
N251	US	Central OR	44.54884	-123.42373	02/03-02/06/2017
CAS	US	Central OR	44.39933	-122.37292	07/04-02/06/2017
WOW	US	Central OR	44.64705	-123.78023	21/04-02/06/2017
N55	US	Central OR	44.65741	-123.75455	02/03/2017
SEE	US	Central OR	44.68678	-123.84403	03/05/2017
F02	US	Central OR	44.39540	-124.03533	26/04/2017
F04	US	Central OR	43.91451	-124.07800	26/04/2017
CB05	US	Coastal South OR	43.27175	-124.26165	26/04/2017
CB02	US	Coastal South OR	43.47398	-124.17537	26/04/2017
CB51	US	Coastal South OR	43.07405	-124.33093	26/04/2017
G01	US	Coastal South OR	42.36992	-124.40651	27/04/2017
G02	US	Coastal South OR	42.05574	-124.24577	27/04/2017
G03	US	Coastal South OR	42.66601	-124.40005	26/04/2017
G04	US	Coastal South OR	42.19033	-124.33551	27/04/2017
ROW	US	Coastal North CA	41.92475	-124.10868	27/04/2017
JED	US	Coastal North CA	41.79943	-124.08723	28/04/2017
BAL	US	Coastal North CA	41.30146	-124.03523	27/04/2017
MUR	US	Coastal North CA	40.95580	-124.08679	27/04/2017
FIC	US	Coastal North CA	40.89530	-124.05767	27/04/2017
ANG	US	Coastal North CA	39.71946	-123.65056	04/05/2017
HAR	US	Coastal North CA	39.39705	-123.72683	04/05/2017
NOY	US	Coastal North CA	39.37112	-123.65929	04/05/2017
ODF1	US	Cascade Mountains	44.73454	-122.36593	31/05/2017
ODF3	US	Cascade Mountains	44.82031	-122.63087	01/06/2017
QUA	US	Cascade Mountains	44.42194	-122.61955	19/05/2017
YUK	US	Cascade Mountains	44.40035	-122.33424	19/05/2017
AND	US	Cascade Mountains	44.21660	-122.24414	19/05/2017
FALL	US	Cascade Mountains	43.97183	-122.68083	19/05/2017
CAM	US	Cascade Mountains	44.51527	-122.73900	23/05/2017
HEB	US	Coastal North OR	45.31077	-123.84017	09/05/2017
GWR1	US	Coastal North OR	45.97331	-123.81069	23/04/2017
GWR3	US	Coastal North OR	45.97342	-123.80997	24/05/2017
GWR4	US	Coastal North OR	45.95564	-123.84575	24/05/2017
GWR5	US	South WA	45.87258	-123.85675	24/05/2017
WAD1	US	South WA	46.22242	-123.21182	17/05/2017
WAD2	US	South WA	46.40192	-123.81805	17/05/2017
WAD3	US	South WA	46.92948	-123.71059	17/05/2017
WAD4	US	South WA	47.10418	-123.01192	23/05/2017
SKA	US	South WA	46.33064	-123.51940	19/05/2017
ELO	US	South WA	46.26900	-123.30900	21/04/2017
TOU	US	South WA	46.32750	-122.64500	22/04/2017
TAR	NZ	Central NI	-38.13933	176.59114	31/08-21/11/2017
KER	NZ	Central NI	-38.33564	176.38888	23/08-21/11/2017
MAM	NZ	Central NI	-38.21667	176.07955	31/08-21/11/2017
KIN	NZ	Central NI	-38.33564	176.00222	23/08-21/11/2017
BOU	NZ	Central NI	-38.73420	176.56734	23/08-21/11/2017
MIN	NZ	Central NI	-38.62117	176.70416	23/08-21/11/2017
1553	NZ	Central NI	-38.82938	176.60303	08/10/2017
1531	NZ	Central NI	-38.78774	176.53165	08/10/2017
KAR1	NZ	Central NI	-39.44804	175.55012	17/10/2017
KAR2	NZ	Central NI	-39.39450	175.59176	17/10/2017
KAR5	NZ	Central NI	-39.37665	175.65720	17/10/2017
MAN	NZ	East NI	-38.28091	177.80823	25/10/2017

SITE	COUNTRY	REGION	LATITUDE	LONGITUDE	SAMPLING DATE
GD57	NZ	North SI	-41.51999	172.69786	28/09/2017
GD58	NZ	North SI	-41.53807	172.68359	28/09/2017
GD59	NZ	North SI	-41.55140	172.68930	28/09/2017
GD73	NZ	North SI	-41.59233	172.76258	30/09/2017
GD80	NZ	North SI	-41.63706	172.89679	01/10/2017
GD94	NZ	North SI	-41.51333	172.83492	03/10/2017
GD00	NZ	North SI	-41.48953	172.88632	12/10/2017
RAI	NZ	North SI	-41.19829	173.55828	16/10/2017
REN	NZ	North SI	-41.64658	173.55637	16/10/2017
NET	NZ	North SI	-41.70940	173.48594	16/10/2017
HAN	NZ	Central SI	-42.51128	172.84396	30/10/2017
ASH	NZ	Central SI	-43.22369	172.58270	26/10/2017
NAS	NZ	South SI	-45.01324	170.11615	10/10/2017
MOR	NZ	South SI	-46.38809	169.24526	10/10/2017
GOW	NZ	South SI	-45.55909	168.11407	10/10/2017
AVO	NZ	South SI	-45.90268	168.22590	10/10/2017
TAP	NZ	South SI	-45.90696	169.33235	10/10/2017
BEA	NZ	South SI	-45.93266	169.45228	10/10/2017
KAI	NZ	South SI	-46.24390	169.13533	12/10/2017
DOO	NZ	South SI	-45.99834	169.90057	12/10/2017
HILL	NZ	South SI	-46.16514	169.77588	12/10/2017
TAK	NZ	South SI	-45.98977	170.19181	24/10/2017
RES	NZ	South SI	-45.88983	170.45022	25/10/2017
FLA	NZ	South SI	-45.84272	170.45165	25/10/2017
MAU	NZ	South SI	-45.90696	170.00479	02/11/2017
BRO	NZ	South SI	-45.95265	169.92341	31/10/2017
ALL1	NZ	South SI	-45.77705	170.40739	01/11/2017
ALL5	NZ	South SI	-45.76562	170.33886	01/11/2017
AKA	NZ	South SI	-46.13396	170.04762	02/11/2017

Chapter 5. Physiological impact of aerial *Phytophthora pluvialis* on *Pinus radiata*

This chapter comprises a co-authored manuscript submitted to Tree Physiology.

Gómez-Gallego, M., Williams, N. M., Leuzinger, S., Scott, P. M., Bader, M. K.-F. A two-year defoliation experiment in *Pinus radiata* grafts: does the lower canopy matter?

Prelude

Phytophthora pluvialis is a foliar pathogen, which is associated with premature casting of needles. Hence, the main impact on the host is driven by the impairment of photosynthetic activity. The reduction of leaf area through defoliation presumably decreases carbon assimilation, and tree growth and carbon storage may be impacted. The infection by the RNC disease typically starts from the bottom canopy and progresses to the top under severe infection episodes. The affected foliage is commonly 1-year-old or older foliage in the lower canopy. During late winter and early summer the symptomatic needles are cast. New foliage matures after defoliation in early summer, with an apparent recovery, leading to green but thin canopies. Initial studies have shown that severe defoliation events associated with RNC can reduce tree growth by up to 38% in the year following infection (Beets P, McKinley R et al. 2013). However, no mechanistic studies on growth loss and changes in carbon storage within the tree under RNC-induced defoliation had been undertaken.

As an approach to understand the impact of defoliation on carbon allocation within the tree, I performed a two-year artificial defoliation experiment. The defoliation treatments followed the same pattern observed in the RNC disease in the field. I report the impact on the photosynthesis of the remaining needles, growth, biomass, and non-structural carbohydrates concentrations in stem, roots and needles. Although artificial defoliation does not allow to account for the carbon allocated to defense compounds, the manuscript presented in this chapter addresses how the defoliation pattern of RNC can impact carbon assimilation and allocation in radiata pine grafts.

Abstract

Biotic and abiotic stressors can lead to different defoliation patterns within trees. Foliar pathogens of conifers commonly prefer older needles and infection and ensuing defoliation frequently progresses from the bottom canopy to the top. During mild defoliation episodes, only old foliage in the lower canopy is affected, which represents a defoliation pattern that has received little attention in past research. A two-year artificial defoliation experiment was performed using 2-year-old *Pinus radiata* grafts to investigate the effects of lower-canopy defoliation on carbon (C) assimilation and allocation. Sixty-two grafts received one of the following treatments in consecutive years: Control-Control, Control-Defoliated, Defoliated-Control and Defoliated-Defoliated. Stomatal conductance, *A/Ci* curves, diameter, height, biomass and non-structural carbohydrate concentrations in needles, stems, and roots were measured before and after each treatment. No upregulation of photosynthesis either biochemically or through stomatal control was observed in response to defoliation. Reduced growth occurred in only one of the two genotypes (genotype B), with diameter growth rate reduced after one year (23% reduction) and decrease in height apparent two growing seasons after defoliation (36% reduction). Root:shoot ratio and leaf mass were not affected by any treatment, suggesting prioritization of canopy regrowth following defoliation. In genotype B, defoliation appeared to impose C shortage and caused reduced aboveground growth and sugar storage in roots, while in genotype A, neither growth nor storage was altered. Root C storage in genotype B decreased only transiently and recovered over the second growing season. Our results suggest genotype-specific defoliation tolerance in *P. radiata*. In genotype A, the contribution of the lower canopy to the whole-tree C uptake appears to be negligible presumably conferring resilience to foliar pathogens affecting the crown base. A general redundancy of lower-canopy foliage in terms of C assimilation is shown, raising a fundamental ecological question on the role of the lower canopy in the plant carbon budget.

Introduction

Forest productivity and resilience are increasingly influenced by global change-driven biotic and abiotic factors. Pathogens, insects, drought and any combination thereof have the potential to result in forest decline though different pathways (McDowell et al. 2011, Anderegg et al. 2015). The main consequences of those stressors are progressive growth reduction and defoliation, which have been both linked to forest decline and tree mortality, and used as predictors for tree death (Dobbertin and Brang 2001, Bréda et al. 2006, Carnicer et al. 2011, Cailleret et al. 2017). Due to its dramatic consequences for forest functioning and stability, drought-induced defoliation and tree mortality have been well studied over the last decade (Galiano et al. 2011, Allen et al. 2015, Adams et al. 2017). Defoliation events caused by insects have also been given considerable attention, e.g. bark beetle outbreaks, alone or in interaction with drought (Gaylord et al. 2013, Anderegg et al. 2015, Arango-Velez et al. 2016), and leaf-feeding insects (Krause and Raffa 1992, Quentin et al. 2010, Eyles, Smith, et al. 2011, Stone et al. 2013, Chen et al. 2017). However, there is a remarkable lack of studies on the impact of pathogen-induced defoliation on tree productivity and resilience through a mechanistic approach, even though disease alerts for invasive plant pathogens have been largely increasing since the beginning of the century (Anderson et al. 2004, Fisher et al. 2012). This gap of knowledge makes it challenging to establish process-based growth loss models and include those in a wider framework of tree decline and death, accounting for the interaction with other stressors (McDowell et al. 2011, Dietze and Matthes 2014).

Fungal and oomycete pathogens can attack different plant tissues with widely varying impacts. Root rot and stem cankers impair the vascular system and can be the primary cause of tree death. This is the case with *Phytophthora cinammomi* in several tree species (Shearer et al. 2004), as a root pathogen, and *Cryphonectria parasitica* causing the chestnut blight (Anagnostakis 1987). The contribution of defoliation caused by root rot pathogens and canker and shoot dieback pathogens, as a predisposing factor to forest decline has previously been analysed (Aguade et al. 2015, Oliva et al. 2016), but the physiological impact of those pathogens on the tree lays on different premises than foliar pathogenic infection. Foliar pathogens rarely cause tree death, but result in defoliation and reduced growth rates. Several characteristics of the foliar pathogenic infection make it difficult to extrapolate the results of insect- and drought-induced defoliation studies to the impacts of defoliation caused by foliar pathogens. In evergreen hosts, foliar pathogen infection and defoliation most frequently affects old leaves in the lower-canopy, although the infection can progress up to the whole canopy (Scharpf 1993, Goheen and Willhite 2006, Tattar 2012). Drought-induced defoliation typically starts at the upper crown, where leaves experience more negative water potentials (Scharpf 1993, Tattar 2012). Leaf-feeding insects may show both patterns, either preference towards current-year leaves or older leaves, and either the top or across the whole canopy (Krause and Raffa 1992, Pinkard, Eyles, et al. 2011, Barry and Pinkard 2013, Jetton and Robison 2014). Other differences include defence mechanisms and duration of the defoliation period, with periods of several weeks of foliar pathogenic infection

preceding defoliation, compared to the few minutes that leaf-feeding insects need to eat leaves (Krause and Raffa 1992).

Few studies have analysed the impact of pathogen-induced defoliation on C assimilation and C allocation. Important research has been conducted on the impacts of the defoliation caused by the Swiss needle cast disease on Douglas-fir productivity and resilience (Manter et al. 2003, Lee et al. 2013, Saffell et al. 2013, 2014). This disease has an unusual defoliating pattern, as Swiss needle cast infection is higher in the upper canopy (Shaw et al. 2014). Lower-canopy defoliation, affecting other than current-year leaves, has not been the aim of previous studies.

It is most typically reported that plant responses to defoliation seek to compensate for the reduction in leaf area. Defoliation decreases whole-canopy net C assimilation and alters the source:sink ratio in a tree. Most frequently, the source:sink ratio decreases following defoliation, leading to compensatory photosynthesis in remaining leaves (Wareing and Patrick 1975, Lavigne et al. 2001, Battaglia et al. 2011), although the increase of C uptake by the remaining leaves does not always take place (Cerasoli et al. 2004, Wiley et al. 2013). This photosynthetic upregulation may be only short-term (Eyles et al. 2009, Eyles, Robinson, et al. 2011). In addition, it does not appear to occur when defoliation does not impose C limitations on growth, for example, when drought stress is limiting tree growth instead (Pinkard et al. 2011, Quentin et al. 2012). Canopy formation in the following season can completely compensate for the foliage loss if defoliation is not severe. However, that does not come without a cost. Canopy regrowth, as a sink, can compete with carbon storage and stem growth, hence defoliation may result in transient changes in C allocation, to invest more C in canopy development (Barnes and Edwards 1980, Chen et al. 2017). The imposition of C (source) limitation by defoliation is controversial and has not been proved *per se*. Most canopies are actually saturated in terms of light and photosynthesis (Körner 2018). However, it has been suggested that, at least, under severe defoliation, C supply becomes indeed limiting to growth (Wiley and Helliker 2012, Wiley et al. 2013, Palacio et al. 2014). Further, fast recovery of non-structural carbohydrate (NSC) concentrations in defoliated trees to the levels of non-defoliated trees have been reported (Barnes and Edwards 1980, Palacio et al. 2012, Saffell et al. 2013, Wiley et al. 2013, 2017, Piper et al. 2015, Puri et al. 2015, Chen et al. 2017). This suggests either the prioritization of storage over growth, or the fact that C becomes non-limiting again, after rapid foliage recovery, and NSC subsequently increases passively. The dynamics of C allocated to growth and storage has direct implications for tree productivity and resilience to future stress episodes. Therefore, it is crucial to understand those changes and under which defoliation intensities and patterns they take place.

The aim of this study was to examine the impact of lower-canopy defoliation on C assimilation and C allocation to better understand pathogenic impacts on tree physiology. We used repeated artificial defoliation in *Pinus radiata* grafts to simulate the defoliation pattern by the Red needle cast disease (RNC), a new foliar disease caused by *Phytophthora pluvialis* (Dick et al. 2014). We removed 1-year-old or older needles from the bottom half canopy of the grafts. We hypothesized that (1) the removal of old foliage from the lower canopy will not cause pronounced upregulation of photosynthesis due to the lack of change in light conditions on the remaining leaves in the upper canopy. (2) The growth in diameter will be more reduced than height, and the reductions

will be larger in grafts that undergo two consecutive defoliation treatments. We also expected that (3) NSC pools will experience small reductions and will recover after a growing season following defoliation.

Material and methods

Plant material and defoliation treatments

A total of 72 two-year-old radiata pine grafts were grown in 45 L bags under sheltered conditions in the Scion nursery (Rotorua, New Zealand), where they were drip irrigated on a timer throughout the experiment. The grafts were ramets of two RNC-susceptible genotypes: 33 of them were ramets of genotype A, and 39, of genotype B. Ten grafts were harvested for biomass at the beginning of the experiment with each treatment harvested for biomass at the completion of their respective assessment periods (Fig 5.1). From the 62 treated grafts, 31 were artificially defoliated mimicking the impact of the RNC disease in winter 2016 (August 10-11), while another 31 grafts served as control. In early spring 2017 (September 18-19), 12 of the defoliated grafts underwent a second defoliation, and in addition, 12 of the original controls were defoliated to allow comparison between a single and two consecutive defoliation events. The first-year defoliation treatment consisted of the removal of 75% of 1-year-old and older needles in the lower half of the canopy, while in second-year defoliation treatment a 100% of 1-year-old and older needles in the lower half of the canopy were removed. The distribution of treatments, sample size, measurements and dates can be followed in Fig 5.1.

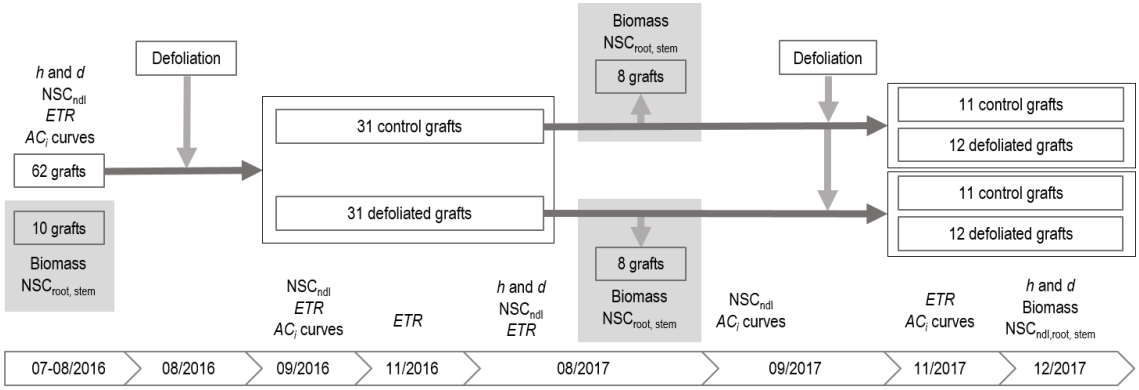

Figure 5.1. Flowchart with the experimental design, measurements and dates. Shaded areas represent destructive measurements. $NSC_{ndl,\ root,\ stem}$, non-structural carbohydrates sampled from needles, roots and stems, respectively; *ETR*, apparent electron transport rate measured by means of chlorophyll fluorescence; *h*, height; *d*, diameter; dates are expressed in mm/yyyy.

Biomass sampling and growth measurements

Height (*h*, m) and diameter (*d*, mm) at 3 cm up from the graft union were measured of each graft on three occasions: the 1st July 2016, before any treatment was performed; the 1st August 2017,

one year after the first defoliation treatments; and the 15th December 2017, three months after second year defoliation treatments. Data from the first-measurements were used to stratify treatments within each of the four height value quartiles, to minimize the effect of initial graft size.

After growth measurements were performed, subsamples of 10 and 16 grafts were processed to obtain biomass data for the first and second measurement dates, respectively (Fig 5.1). In addition, all grafts were harvested for biomass after the last measurement date at the end of the experiment. Aboveground plant material was partitioned into stem (including branches) and needles. Soil was carefully washed off roots to avoid breaking off fine roots. All plant material was oven-dried at 70 ºC for at least 72 h. Dry weight of each part was recorded. Root:shoot ratios were calculated for each graft. Leaf area (*LA*) was measured in all the needles of the 10 grafts (subsample before any treatment was performed) with a LI-3100C area meter (LI-COR Biosciences, Lincoln, Nebraska). A linear model was fitted for *LA* as response variable, including leaf dry mass (*LM*) and genotype as predictors, using the R software version 3.5.1 (R Core Team 2017). The best-fitted model (adjusted R^2 = 0.88) was used to calculate *LA* from *LM* data for the second and final harvest to assess canopy recovery from defoliation treatments.

Gas exchange and chlorophyll fluorescence measurements

All gas-exchange and chlorophyll fluorescence measurements were taken on mature current-year needles from a lateral shoot in the upper half of the canopy. Instant light-response curves were performed in a subsample of 10 grafts to assess saturating levels of the photosynthetic photon flux density ($PPFD_{sat}$) at maximum apparent electron transport rate (*ETR*), using an Imaging-PAM chlorophyll fluorometer (M-series, Walz, Effeltrich, Germany) (Rascher et al. 2000). The value of $PPFD_{sat}$ (i.e. 600 µmol m^{-2} s^{-1}) was used in all the gas exchange and chlorophyll fluorescence measurements. Hourly time series measurements of chlorophyll fluorescence and gas exchange were performed from 8 am to 2.30 pm (using 30 min at each time slot) in a subsample of 10 grafts using a coupled chlorophyll fluorescence and gas-exchange system (Imaging-PAM M-Series and GFS-3000, Walz, Effeltrich, Germany) at 400 ppm CO_2 concentration, 20 ºC cuvette temperature, 60% relative humidity and at $PPFD_{sat}$. We assessed differences between time slots for the parameters *ETR*, net photosynthetic rates (*A*) and stomatal conductance (*g*) by fitting a linear mixed model for each response variable with 'graft identity' as random factor, and 'time slot' as fixed factor (function lme, package nlme, R Core Team 2017). The last two hours (from 1 to 2.30 pm) were significantly different from the others, and forthcoming measurements were performed only from 8 am to 12.30 pm.

To assess compensatory photosynthesis in the remaining upper half of the canopy, we monitored the apparent *ETR* derived from chlorophyll fluorescence measurements at $PPDF_{sat}$ light level using an Imaging-PAM chlorophyll fluorometer at four dates: before treatments (8th-9th August 2016), three weeks (7th-8th August 2016), three months (15th-16th November 2016) and one year (14th-15th August 2017) after first-year defoliation treatments, and two months after second-year defoliation treatments (24th November 2017). *A/Ci* curves were recorded in a subsample of grafts (*n* = 20 to assess first-year treatments, and *n* = 40 for second-year treatments) using the

coupled fluorometer-gas-exchange system to assess leaf area of needles inside the cuvette by means of chlorophyll fluorescence. *A/Ci* curves were measured at four different dates: before any treatment, five weeks and one year after first year defoliation, and two months after the second year defoliation. Gas exchange rates were first recorded at a leaf chamber CO_2 concentration (C_a) of 400 ppm CO_2, before C_a was stepwise reduced to 200, 100, and 40 ppm, subsequently C_a was returned to 400 ppm (to check if the initial rate could be restored) and then increased to 600, 800, 1,000, 1,500, and 2,000 ppm. All *A/Ci* curves were performed at 20 ºC cuvette temperature, 60% relative humidity and at $PPFD_{sat}$. Individual response curves were completed within 30-40 min. *A/Ci* curves were fitted following an asymptotic function (Eq 5.1), analysing the following parameters: photosynthetic capacity (*Amax*), which is the upper asymptote of the curve; dark respiration (*Amin*), which is the lower asymptote; and the CO_2 compensation point (*gamma*), which is CO_2 concentration when net photosynthetic rate equals 0. Values for *g* obtained in the first measurement of the *A/Ci* curves (i.e. at 400 ppm) were used to assess possible compensatory photosynthesis due to stomatal control.

$$A = A_{max}\left(1 - \left(1 - \frac{A_{min}}{A_{max}}\right)^{1-\frac{C_i}{gamma}}\right) \quad (5.1)$$

Non-structural carbohydrates

Non-destructive NSC sampling of needles was performed on five different dates on all the grafts: before treatments (9th August 2016), one month after first-year defoliation (12th September 2016), 12 months after first-year defoliation (23rd August 2017), 13 months after the first-year defoliation (18th September 2017), and 3 months after the second-year defoliation (5th December 2017). Two fascicles from the upper half canopy were sampled, chopped in ca. 3 mm long pieces into 5 mL tubes and immediately frozen in liquid nitrogen. After being frozen, samples were stored in a portable cooler during the sampling and stored in a -80 ºC freezer once in the lab. Stem and root NSC sampling was performed on the same grafts and dates than biomass assessments. Fine and coarse roots were sampled (ca. 50% each), washed, rinsed in paper towels. Two stem 2 mm-thick sections were cut at 4 cm above the graft union with a pair of secateurs. Hardwood and bark was discarded (processing the vascular system). Stem and root samples were each chopped into 2 mL tubes and frozen and stored as previously explained. All NSC samples were overnight freeze-dried using a FreeZone Freeze Dry System (Model 7934037, Labconco, Kansas City, Missouri, US). The needle samples were added 4 mL grinding metal balls (SPEX) and then grinded to fine powder using GenoGrinder 2010 (SPEX SamplePrep, Stanmore, UK). Stem and root samples were grinded in impact-resistant 2 mL tube containing 2 mm glass beads and 2 mm yellow zirconium oxide beads (Lysing Matrix H, MP Biomedicals, Auckland, New Zealand) using a bead mill homogenizer (Omni bead ruptor 24, Omni International, Kennesay, Georgia, US).

We used the models presented by Ramirez et al. (2015) to predict the NSC concentrations in our samples from the spectra measured in a FT-NIR analyser (Bruker MPA Multi Purpose FT-NIR Analyzer). Reflectance spectra were taken from 1300 to 2650 nm, at a resolution of 16 cm^{-1} and averaged over 32 scans. We used the models presented by Ramirez et al. (2015) to estimate

sugar and starch contents (referred to as 'all tissues' models in their publication). The range of both sugar and starch concentrations we obtained for our samples contained negative and close-to-zero values consistent with previous reports on *P. radiata* (Cranswick et al 1987). To account for the yet unresolved issue of negative values in samples whose NSC content is close to or below the detection limit of chemical methods and to maintain the relative differences, we shifted the values to a positive range. The absolute value of the minimum NSC content was added to all observations.

Data analysis

All statistical computations and graphics were performed using software R version 3.5.1 (R Core Team 2017). Both light-response curves and *A/Ci* curves were fitted by generalised nonlinear least squares (gnls function, package nlme, Pinheiro et al. 2018). For light-response curves, we used the Eilers-Peeters equation (Eilers and Peeters 1988). Heteroscedasticity, suggested by the model diagnostic plots, was modelled by the combination (varComb function) of different coefficients of variance per plant (varIdent function, with plant identity as a group variable) and an exponential variance function using the light intensity as variance covariate (varExp function). We used inverse interpolation to derive $PPFD_{sat}$ value from the fitted values (light level at 90% of ETR_{max}). For *A/Ci* curves, heteroscedasticity was modelled using intercellular CO_2 concentration as a variance covariate. We determined the upper and lower asymptote (*Amax* and *Amin*), respectively. We used inverse interpolation to determine the CO_2 compensation point . Effects of defoliation treatment and genotype on *g*, *Amax*, *Amin* and CO_2 compensation point were analysed separately for each measuring point: five weeks and one year after the first defoliation treatment, and two months after the second defoliation treatment. In the first two dates, only two levels of treatment were considered ('control' and 'defoliated'). In the last date, the four levels of treatment were considered ('control-control', 'control-defoliated', 'defoliated-control', 'defoliated-defoliated'). Linear models were fitted, and optimal predictors were determined by backwards model selection comparing nested models using the Akaike Information Criterion (AIC) test. Effects of defoliation, genotype and its interaction on the *ETR* were assessed in the same way, but in four measuring dates: three weeks, 3 months and one year after the first defoliation, and two months after second defoliation. In the case of *g*, as a response variable, we used linear mixed-effect models to include 'time slot' as a random effect, because *g* was the more sensitive variable to the measuring time. Four categories were considered in 'time slot', namely, from 8 to 9 am, from 9 to 10.30 am, from 10.30 to 11.30 am, and from 11.30 am to 12.30 pm.

Effects of defoliation treatment and genotype on *h*, *d*, aboveground biomass, root:shoot ratio were likewise analysed by fitting linear models, separately at two measuring dates: one year after the first year defoliation and three months after the second-year defoliation. Stem and root soluble sugar and starch concentrations were analysed using linear mixed models (lme function) separately at the two sampling dates: one year after the first defoliation and three months after the second defoliation. In these models, 'tissue' (stem or root) was included as a random factor, and 'genotype' and 'treatment' and their interaction were considered as fixed factors. Needle sugar and starch concentrations were analysed at the same sampling dates. The effect of the

first-year defoliation was assessed by a linear mixed model with ‘graft identity’ as a random factor instead, and ‘defoliation’ and ‘genotype’ and its interaction, and ‘sampling date’ (one month, 12 months and 13 months after first-year defoliation) as fixed factors. To analyse the effect of the two-year defoliation treatments on the needle sugar and starch concentrations, a linear model was fitted, with the same fixed factors. All model selection was based on AIC. Post-hoc tests were carried out using the emmeans function (package emmeans, Lenth 2018) for pairwise comparisons of least squares means.

Results

Compensatory photosynthesis

No differences in the photosynthetic parameters measured in the remaining needles (*ETR*, *A/Ci* curves) were found between genotypes and defoliation treatments two months after the second-defoliation treatment (Table S5.1, Figs 5.2 and 5.3). Parameters derived from *A/Ci* curves (*Amax*, *Amin* and CO_2 compensation point) remained unaffected both by the first-year defoliation, five weeks and one year after the treatment, and by the second-year defoliation, three months after the treatment (Table S5.1, Fig 5.2). Genotype B showed higher photosynthetic capacity than genotype A, five weeks after the first defoliation, regardless of the treatment (Table 5.S1, Fig 5.1a-b). Similarly, at the same time point, stomatal conductance was higher in genotype B than A (Table 5.S1, Fig 5.3a-b). One year after the first defoliation, no physiological impacts were detected apart from a reduction in stomatal conductance in genotype A compared to the genotype B and control grafts (Table S5.1, Fig 5.3 c-f).

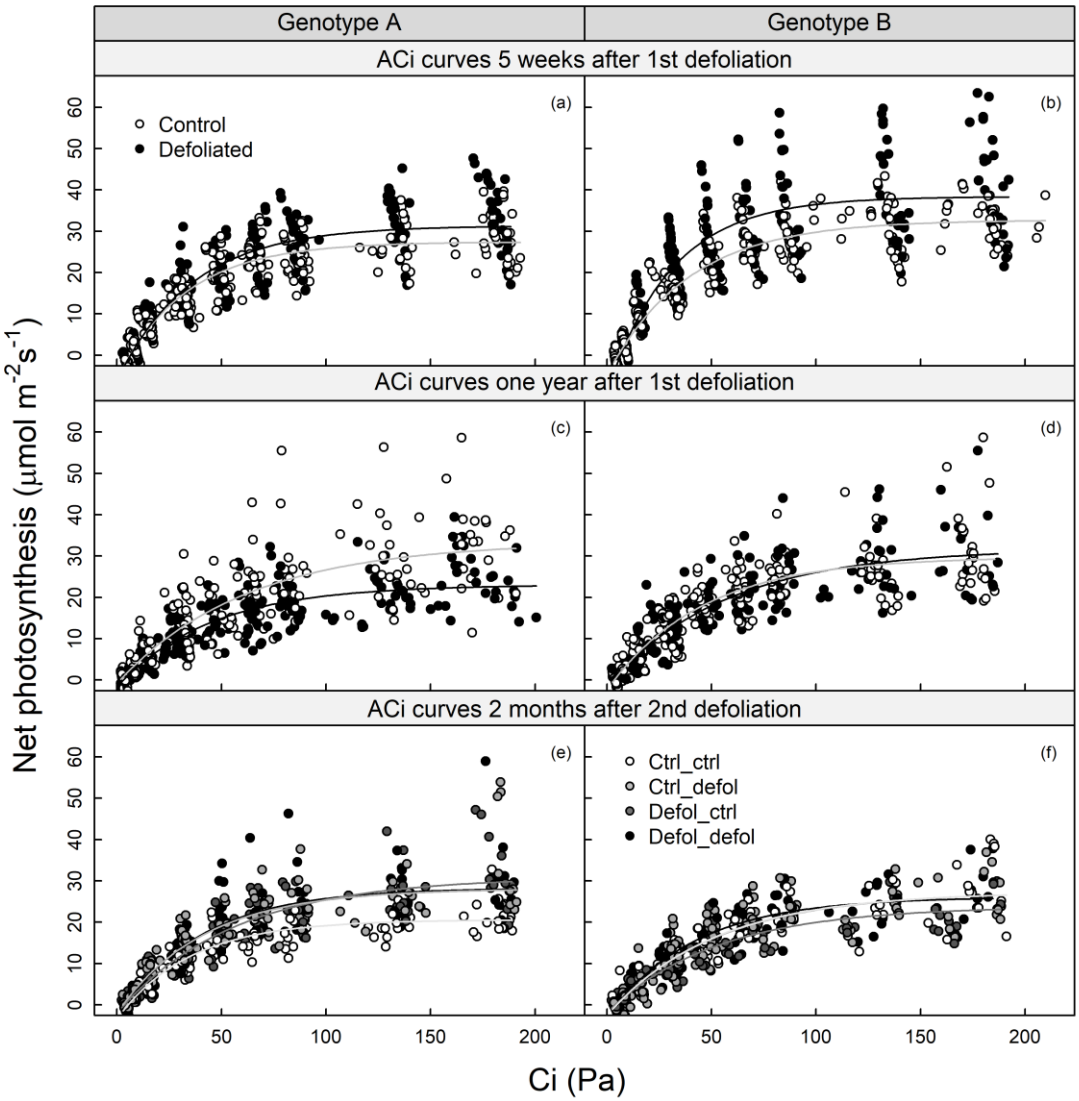

Figure 5.2. Response to defoliation of net photosynthesis as a function of intercellular CO_2 concentration (Ci) 5 weeks (a-b) and one year following first-year defoliation (c-d), and 2 months following second-year defoliation (e-f), for genotype A (a, c, e) and genotype B (b, d, f).

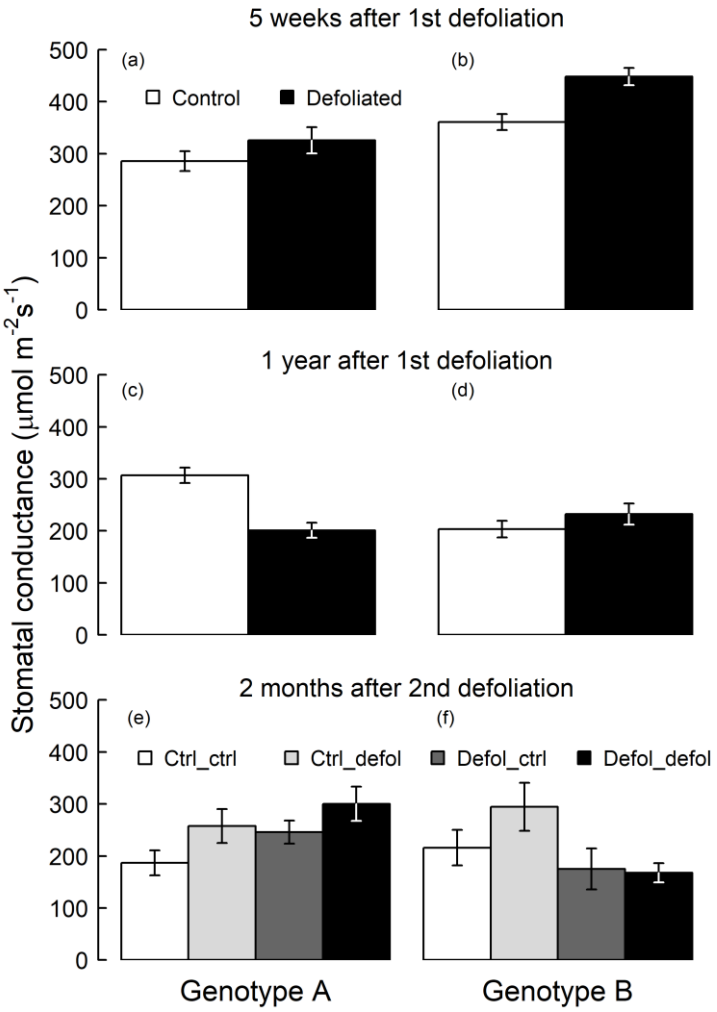

Figure 5.3. Response to defoliation stomatal conductance 5 weeks (a-b) and one year following first-year defoliation (c-d), and 2 months following second-year defoliation (e-f).

Growth and biomass

Genotype A growth and biomass were not affected by any defoliation treatment at any time (Table S5.2, Figs 5.4a, c and 5.5c), except for *LA* and *LM* which were reduced three months after a single defoliation treatment (second-year defoliation, Table 5.2, Fig 5.6a, c). This short-term effect was not detected one year after the first defoliation treatment. In genotype B, one year after the first defoliation, diameter was the only parameter impacted by defoliation (23% reduction, Table S5.2, Fig 5.4d). After the second-year defoliation, the decrease in diameter in first-year defoliated grafts was accentuated (32% lower than control grafts, Table S5.2, Fig 5.4d). In addition, height and total aboveground biomass were reduced in first-year defoliated grafts after the second growing season by 36% and 55% in genotype B (Figs 5.4b and 5.5d). Root:shoot ratio was unaffected by the treatments, but it showed higher values for genotype A.

The correlation between *LM* and *LA* was significant and varied among genotypes (significant *LM* × genotype interaction, P = 0.02). The best-fitted model (adjusted R^2 = 0.88) was used to estimate *LA* from *LM*. Genotype A presented higher overall *LA* values than genotype B (Fig 5.6a-b). Even though *LM* did not differ between genotypes one year after defoliation, genotype B presented lower *LA*, irrespective of the treatment (Table S5.2, Fig 5.6). After the second growing season (at the end of the experiment), genotype B grafts, which had undergone defoliation the first year, presented lower *LM* and *LA* compared to control trees. In contrast, genotype A defoliated grafts showed similar *LM* and *LA* values than control grafts, one year after defoliation (Table S5.2, Fig 6). Remarkably, while *LA* values for genotype A control grafts were higher than genotype B, *LM* values were lower (Table S5.2).

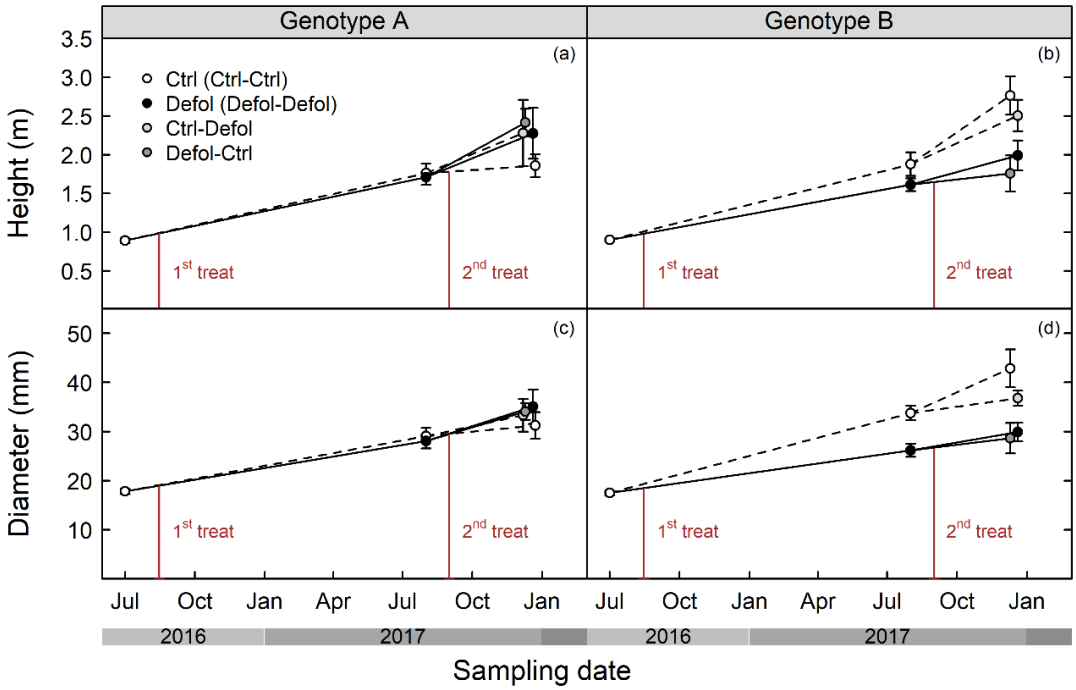

Figure 5.4. Response to defoliation of height (a-b) and diameter (c-d) for genotype A (a, c) and genotype B (b, d). Means ± SE.

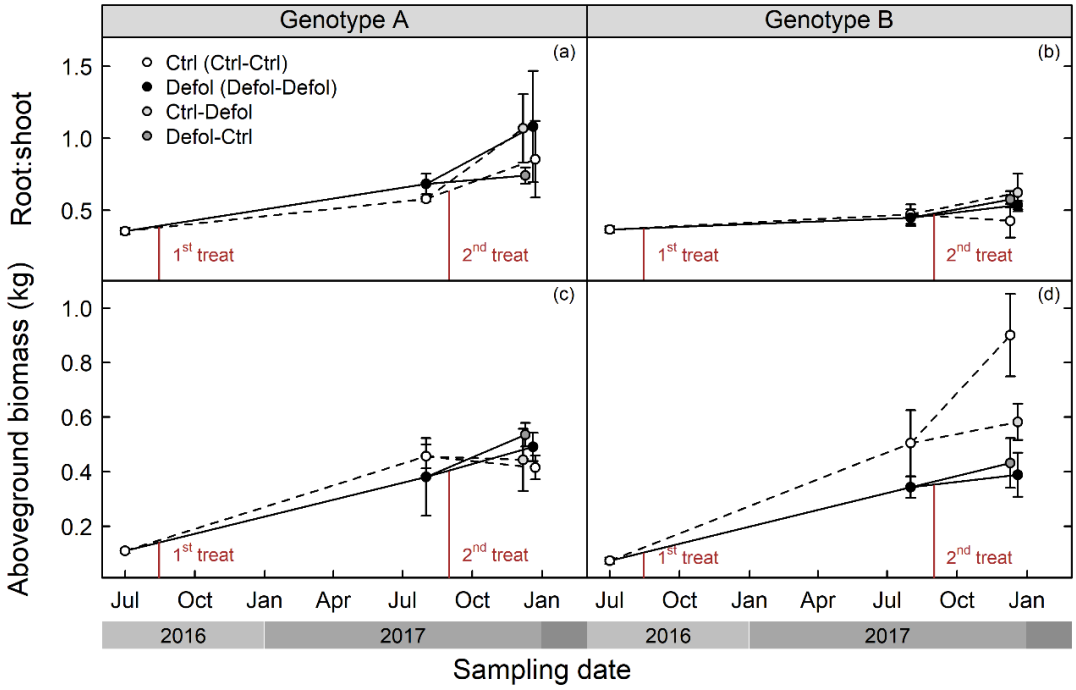

Figure 5.5. Response to defoliation of root:shoot ratio (a-b) and aboveground biomass including needle mass (c-d) for genotype A (a, c) and genotype B (b, d). Means ± SE.

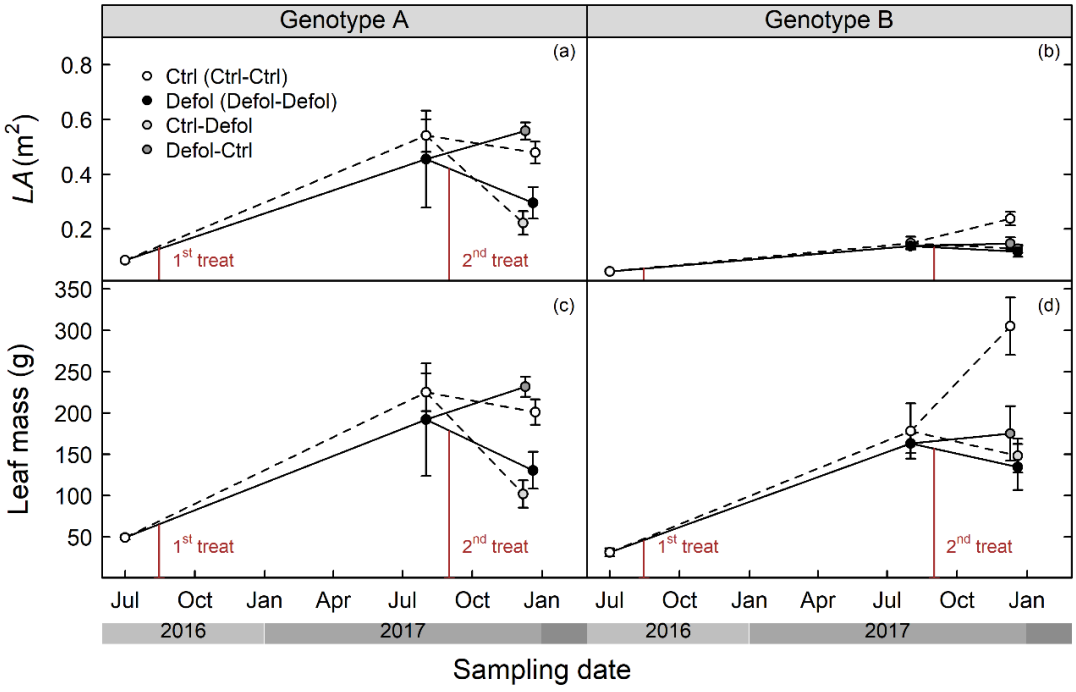

Figure 5.6. Response to defoliation of leaf area (*LA*) (a-b) and leaf mass (c-d) for genotype A (a, c) and genotype B (b, d). Leaf mass was directly measured. *LA* was directly measured only before treatments, and then predicted by leaf mass using regression equations. Means ± SE.

Non-structural carbohydrates

In genotype B, the first-year defoliation led to a decrease in sugar storage in roots after the first growing season, followed by a recovery of root sugar reserves over the second spring season (toward the end of the experiment; Table S5.3, Fig 5.7f). Genotype A grafts that experienced two defoliation treatments showed lower sugar concentrations in needles than those from genotype B (Table S5.3, Fig 5.7a-b). Similar levels of sugar concentration in stems were found across genotypes and treatments. Starch content in any of the analyzed tissues was similar among genotypes and remained unaffected by defoliation (Table S5.3).

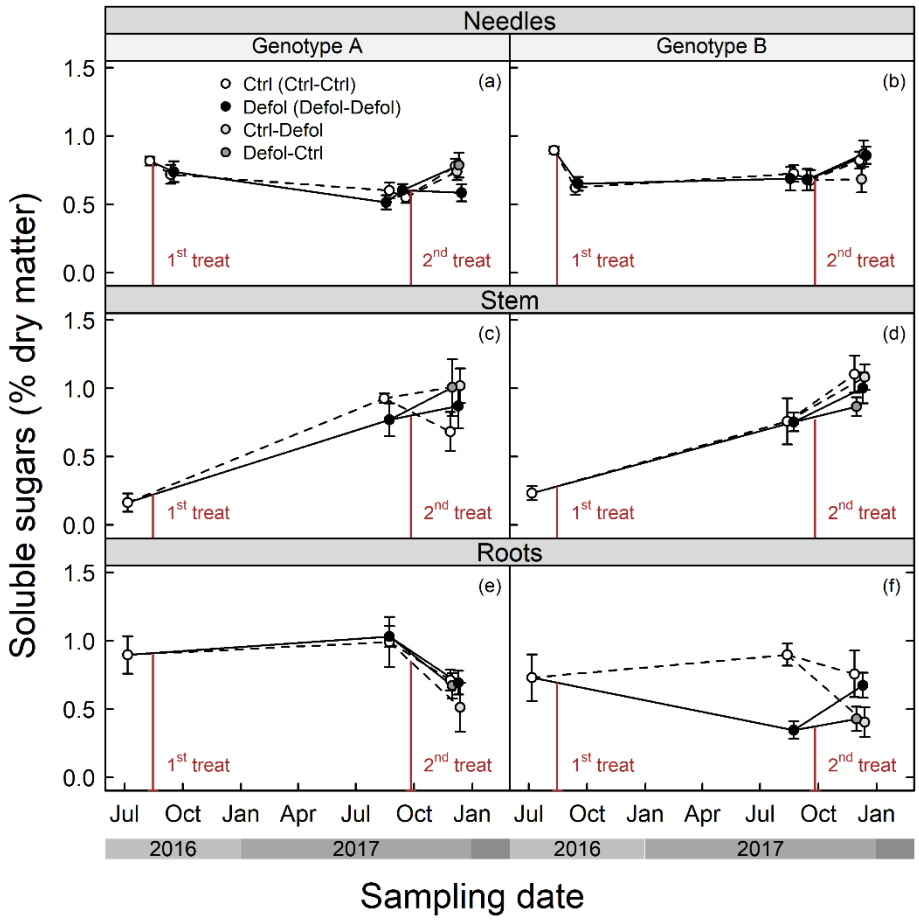

Figure 5.7. Response to defoliation of soluble sugar concentrations in needles (a-b), stem (c-d) and roots (e-f) for genotype A (a, c, e) and genotype B (b, d, f). Means ± SE.

Discussion

Carbon assimilation under lower-canopy defoliation

We hypothesized no or little photosynthetic upregulation in the remaining foliage following defoliation. We found no evidence of photosynthetic upregulation, neither biochemically nor through stomatal control, in the remaining needles in response to lower canopy defoliation. This outcome is contrary to earlier findings, which support compensatory photosynthesis in

angiosperms (Eyles et al. 2009, Quentin et al. 2010, 2012, Pinkard, Eyles, et al. 2011, Barry and Pinkard 2013, Borzak et al. 2017) and gymnosperms (Reich et al. 1993, Vanderklein and Reich 1999, Little et al. 2003), including *P. radiata* (Eyles, Smith, et al. 2011). However, each of these studies focused on either upper- or whole-crown defoliation, mainly to simulate impacts of insect herbivory. Unlike lower-canopy defoliation, removal of upper-crown foliage may substantially increase light penetration through to lower-canopy leaves, enhancing the photosynthetic activity of residual leaves through increased leaf conductance (Reich et al. 1993). If the defoliation is severe enough, the source:sink ratio decreases. This unbalance has been recognized as a mechanism leading to photosynthetic upregulation (Wareing and Patrick 1975, Lavigne et al. 2001, Battaglia et al. 2011). In our experiment, the intensity of our first defoliation treatment did not seem to be strong enough to change the source:sink ratio to cause any stimulatory effects on gas exchange in the remaining upper-crown needles. Further, the light conditions for upper-canopy foliage remained unchanged with the removal of lower-canopy leaves.

None of the genotypes showed compensatory photosynthesis. Genotype A did not appear to be affected by C shortage, since primary and secondary growth and NSC content across tissues was similar in defoliated and control grafts. Plant canopies can present high leaf area index values beyond saturation with no further contribution to C assimilation (Thomas and Sadras 2001, Weiner and Freckleton 2010, Körner 2018). Genotype A appeared to be saturated in terms of leaf area, even after defoliation. However, genotype B underwent reduced growth and biomass accumulation one year following the first defoliation treatment (see next section). Intriguingly, few studies have also reported no effect of defoliation on photosynthetic C uptake, but have reported an altered C allocation (Cerasoli et al. 2004) and prioritization of carbon storage at the expense of growth (Wiley et al. 2013). In genotype B, defoliation caused carbon shortage but presumably not a decrease in the source:sink ratio, as no upregulation was detected. This could be explained by a reduction of growth-related sink demands, due to the winter period, which coincided with the defoliation-induced decrease in C uptake. Alternatively, the source:sink ratio might have decreased as a result of foliage removal, but upper-canopy leaves may have been photosynthesizing already at maximum capacity, unable to respond to the increase in sink strength.

Carbon allocation under lower-canopy defoliation

Carbon shortage and changes in C allocation due to defoliation differed among genotypes. In genotype B, defoliation reduced both aboveground growth and sugar storage in roots, while no such effects were observed in genotype A. Impacts on secondary growth became apparent one year after the first defoliation in genotype B, whose defoliated grafts showed lower diameter increase than control grafts (Table S5.2, Fig 5.4d). The second defoliation in first-year control plants did not have an impact on diameter three months after the treatment (Table S2, Fig 5.4d). This indicates that a longer period may be needed to detect the impact on secondary growth, as after one year we found these effects, but we did not after three months. Primary growth reduction (reduced height increase) was noted only after the second growing season, at the end of the experiment, and it was caused by a single first defoliation treatment, regardless of the second-

year treatment (Table S5.2, Fig 5.4b). Such an impact of defoliation on radial growth is well documented, ranging from 0 to 37% reduction in 50% defoliation, and from 40 to 88% reduction in complete defoliation treatment (Little et al. 2003, Wills et al. 2004, Saffell et al. 2013, Jacquet et al. 2014, Piper et al. 2015, Puri et al. 2015, Wiley et al. 2017). Our results further support the idea of radial growth being more sensitive to defoliation than height growth (Rook and Whyte 1976, Quentin et al. 2010, Jetton and Robison 2014, Lombardero et al. 2016, Borzak et al. 2017). The extent to which diameter and height growth are reduced may vary depending on the intensity of defoliation -height growth was only altered in severe defoliation episodes (Rook and Whyte 1976)-, upregulation of photosynthesis in remaining leaves (Eyles, Robinson, et al. 2011, Quentin et al. 2012), competing sink strength of carbon pools (Palacio et al. 2012); time of the defoliation respect to leaf phenology (Chen et al. 2017), and portion of affected canopy (see final section).

The defoliation treatments in our experiment did not appear to impose C shortage in genotype A, but they did so in genotype B. Previous studies on defoliation impacts demonstrated that, below a given threshold, the impact on growth is negligible, and this threshold can be variable across experiments (Rapley et al. 2009, Jetton and Robison 2014), even within conifer species (Vanderklein and Reich 1999, Jacquet et al. 2014, Deslauriers et al. 2015, Lombardero et al. 2016). This threshold seems to be different in the genotypes analyzed here, which might be related to differences in leaf traits. Interestingly, genotype A presented higher *LA* at similar values of *LM*, i.e. higher specific leaf area (*SLA*), which has been associated with a more efficient use of resources (Hodgkinson 1974, Alderfer and Eagles 1976, Niinemets 1999, Warren and Adams 2000). Initial differences in *SLA* between genotypes might have contributed to the divergent defoliation impacts. Even though similar proportional number of needles were artificially removed in both genotypes, lower *SLA* saw greater *LM*, and hence C resources, removed from genotype B. This genotype was the most affected by C shortage after defoliation. It is widely accepted that leaves with lower *SLA* values have higher C content (Bresinsky et al. 2013), and remain photosynthetically active for a longer period of time to compensate for their high C cost and deliver sufficient assimilates to the plant (Reich et al. 1992, Bresinsky et al. 2013). Hence, defoliation in genotype B, which showed lower *SLA* values, meant a higher C loss and a decrease in photosynthetically active tissue, which is consistent with the resulting C shortage following defoliation in genotype B. In our study, *SLA* values were measured at the beginning of the experiment to derive allometric relationships used to estimate *LA* from measured *LM*. While it has been shown that *SLA* remains invariable by defoliation in *P. radiata* (Eyles, Robinson, et al. 2011), we cannot assure this is true for our experiment, since we did not monitor *SLA* after defoliation treatments. However, the impact of the initial differences in *SLA* on the output of the defoliation still applies.

In our experiment, new biomass production after defoliation was preferentially shifted towards foliage regeneration to restore *LA* and root:shoot ratios to control levels, one year after the first defoliation (Figs 5.5a-b and 5.6a-b). Similar biomass allocation patterns have been observed to maintain *LA* (Barry and Pinkard 2013) and root:shoot ratios after defoliation (Wareing and Patrick 1975, Krause and Raffa 1992, Reich et al. 1993). However, at the end of our experiment, genotype B grafts that were defoliated at least once presented lower *LM* than the control grafts

(Table S5.2, Fig 5.6d). This observed long-term decrease in C allocation to leaf regeneration, together with the sustained decrease in aboveground growth (Table S5.2, Figs 5.4b, d and 5.5d), occurred at the expense of reduced translocation of soluble sugars to roots in first-year defoliated grafts (Table S5.3, Fig 5.7f). Thus, in the short term, the first-year defoliation in genotype B led to canopy formation and restoration of the root:shoot ratio at the expense of sugar content in roots, while, in the long term, NSC storage in roots was prioritized over aboveground growth. Those results are in line with transient NSC decreases following defoliation previously reported (Palacio et al. 2008, 2012, Saffell et al. 2013), especially in root reserves (Vanderklein and Reich 1999, Quentin et al. 2011, Landhausser and Lieffers 2012), with NSC restoration more successful than growth re-establishment (Chen et al. 2017).

Starch concentrations across tissues and genotypes remained unaffected by any defoliation treatment. Defoliated grafts, even under carbon shortage as in genotype B, actively maintained similar levels of starch than control grafts. Starch pools were not mobilized in the recovery process either, probably to maintain a baseline level of NSC (Wiley and Helliker 2012). Indeed, starch concentrations appeared to be already relatively low in our grafts. This is consistent with previous reports for New Zealand-grown *P. radiata*, as a result of its year-round, continuous sink activity in New Zealand (Cranswick et al. 1987). A two-year artificial defoliation experiment in *Pinus resinosa* and *Larix leptolepis*, similar to the one presented here, also showed a preferential, butsmall, reduction in sugar reserves rather than starch upon defoliation (Vanderklein and Reich 1999). Starch concentrations have been shown to be well correlated with the ability of trees to survive defoliation events (Webb 1981) which explains why plants tend to maintain starch reserves unless facing severe stress.

The defoliation treatments performed here occurred during late winter, before the critical period of leaf formation in spring, and had little impact on NSC reserves. It has been proved that defoliation occurring before regeneration of foliage causes less growth retardation and lower impact on carbon reserves, than defoliation by the end of growing season (Rook and Whyte 1976, Barnes and Edwards 1980, Chen et al. 2017). Thus, seasonality of the RNC disease could mean a lower impact on tree growth than pathogens affecting canopy development during spring and summer.

The enigmatic role of the lower canopy

Our findings put forward a new factor to take into account in carbon dynamics within the defoliation framework: the portion of the canopy affected by defoliation. Defoliation treatments performed in our experiment aimed at mimicking the RNC disease, removing 1-year-old and older needles from the bottom half of the canopy. In the case of genotype A, the removal of this portion of the canopy did not impose any C shortage on the plant. The contribution of older, lower-canopy needles to whole-tree carbon assimilation is smaller than that of current-year needles in the upper canopy (Leuning et al. 1991, Bresinsky et al. 2013). Therefore, artificial removal of those leaves would lead to little impact on tree C balance. Why would a tree spend carbon and energy to maintain this ‘extra’ foliage? The importance of the lower-canopy foliage is certainly controversial. Moreira

et al. (2012) found that *P. radiata* needles had better developed chemical defenses, both resin and phenolic compounds, in the lower canopy of the plant, despite their apparent lower value measured by lower N concentrations. This output is contrary to the Optimal Defense Theory by which plants have higher levels of chemical defenses in the tissues that are contributing more to plant fitness (Zangerl and Bazzaz 1992). This well-defended lower-canopy foliage could thus be a buffer to stop pathogenic infection to go further up infecting high valuable leaves, i.e. upper-canopy and current-year foliage, which contribute most to whole-plant C assimilation. It has been suggested that excess foliage can serve as nutrient storage that can be translocated to younger foliage (Hirose 2012, Körner 2018). Those leaves are rich in C, as opposed to N, if compared to current-year and top canopy leaves (Leuning et al. 1991). Thus, it can also be speculated that those leaves accomplish a C reserve function for future stress episodes.

Old leaves also seem to play somehow an important role for the plant. A study by Little et al. (2003) showed that, across the whole canopy, the pattern of removal of 1-year-old and older foliage had a greater impact on growth than the removal of current-year foliage in balsam fir. Those findings were consistent with observations in the field according to which tree recovery is slower after defoliation by balsam fir sawfly (former defoliation pattern) than by spruce budworm (latter pattern) (Piene et al. 2001). Another intriguing artificial defoliation experiment compared the effect of different needle cohorts on the defoliation, across the whole canopy, in *P. radiata* (Rook and Whyte 1976). This study confirmed that the removal of only current-year needles had significantly less impact on diameter and height growth than the removal of 1- to 3-year-old needles. Further, even the removal of current- and 1-year-old needles had less impact on growth than defoliation of 1- to 3-year-old needles.

There are very few studies on the impact of foliar pathogen-induced defoliation on C assimilation and C allocation. The Swiss needle cast disease and its impact on Douglas-fir trees, caused by the ascomycete fungus *Nothophaeocryptopus gaeumannii*, has been thoroughly studied (Manter, Bond, et al. 2003, Saffell et al. 2013, 2014). In contrast to the majority of foliar pathogens, *N. gaeumannii* presents higher rates of infection in the upper- than the lower-crown. Typical foliar diseases in pine forest systems, such as RNC and *Dothistroma* needle blight, are dispersed by rain splash and fog and require high humidity in the needle environment (Bulman et al. 2013, Dick et al. 2014). Thus, those pathogens typically start infection from the bottom canopy, which may spread up to the top of the live canopy as long as conducive environmental conditions concur. Although growth losses have been documented in a few studies, very little is known about the mechanisms leading to reduced growth rates. A recent study on the infection of *Pinus nigra* by *Dothistroma septosporum* showed a correlation between infection and reduction in shoot length, which may compromise the development of photosynthetic capacity of the tree and contribute to reduced volume growth (Mullett and Brown 2018). Krause and Raffa (1992) also reported reduced shoot production following defoliation by the foliar pathogen *Mycosphaerella laricinia* on *Larix* sp., suggesting a long-term impact on growth and survival of larch through reduction of its optimum photosynthetic area and biomass productivity. In the same study, the comparison between pathogen- and insect-induced defoliation elucidated that, when it is complete, pathogen-induced defoliation causes more serious damage to the tree. Indeed, while insect attacks cause fast

defoliation (only minutes), pathogen-infected leaves may remain on shoots for longer (several weeks) (Krause and Raffa 1992), becoming carbon sinks until they are shed (Manter, Bond, et al. 2003). Therefore, in pathogenic infection and defoliation, the process of pathogen defence appears to be longer and C costly. Moreover, if the disease progresses to the upper-canopy and causes complete defoliation, its impact on tree productivity may be larger (Rook and Whyte 1976, Krause and Raffa 1992).

Conclusions

The physiological response of *P. radiata* to lower canopy defoliation is genotype-specific. Even though the two studied genotypes were similarly susceptible to the RNC disease, they showed different tolerance to defoliation. This has important implications for forest disease management. This finding highlights the importance of factors other than disease susceptibility, such as leaf functional traits, for the resilience and productivity of *P. radiata* stands and thus implies far-reaching implications for future forest disease management.

Our experiment was a first approach to understand the role and function of the lower canopy, as target foliage by pathogens, and raises the question of the ecological role of mild foliar pathogenic infections. Pathogen-induced defoliations have not been given sufficient attention because it is perceived as a biotic stress that does not lead to tree death. However, defoliations have been broadly recognized to be a predisposing event for the tree to enter a spiral of decline when other biotic or abiotic stress episodes concur (Manion 2003, Oliva et al. 2016). Further research is needed to approach remaining open questions. Are pathogenic outbreaks more damaging than insect attacks when the whole canopy is affected, so that it justifies higher investment in chemical compounds in the lower canopy as a buffer for an early stop of infection progress? What are the thresholds for pathogen-induced defoliation in terms of tree productivity and survival? Does the lower canopy have a function of buffering pathogenic infection to protect highly productive foliage, but providing a substrate for pathogen to help the tree control competing vegetation? While *Pythium* (Oomycete) diseases have been proved a major cause of seedling mortality driving diversity in forests through density-dependent mortality, this takes places for host-specific pathogens (Janzen 1970, Connell 1971, Packer and Clay 2000). Generalist pathogens may cause a different effect, even possibly helping control competing vegetation to favour recruitment success. It is yet unknown if *P. pluvialis* can infect other understory vegetation in Douglas-fir forests. A common framework bringing together different disciplines - plant pathologists, tree physiologists and chemists - is needed to fully address the fundamental ecological questions raised here.

Supplementary material

Table S5.1. Photosynthetic parameters for control (Ctrl) and defoliated (Defol) grafts of genotypes A and B, five weeks and one year after the first-year defoliation treatment, and three months after the second-year defoliation treatment. Number in parenthesis indicate standard errors. Different letters indicate statistically significant differences between groups at α = 0.05 on a multiple comparison procedure using Tukey contrasts.

	Genotype A				Genotype B			
Five weeks after	**Ctrl**		**Defol**		**Ctrl**		**Defol**	
Amax	27.49 (2.50) [a]		30.81 (2.50) [a]		33.93 (2.58) [b]		37.26 (2.67) [b]	
Amin	-9.03 (1.54) [a]		-6.81 (1.61) [a]		-6.80 (1.54) [a]		-11.25 (1.70) [a]	
CO_2 comp point	6.05 (0.78) [a]		6.25 (0.78) [a]		6.04 (0.81) [a]		6.24 (0.83) [a]	
g	273.83 (26.83) [a]		373.83 (27.73) [a]		330.90 (27.73) [b]		430.88 (28.68) [b]	
One year after	**Ctrl**		**Defol**		**Ctrl**		**Defol**	
Amax	35.59 (4.09) [a]		27.96 (4.25) [a]		35.59 (4.09) [a]		28.40 (4.25) [a]	
Amin	-1.57 (0.68) [a]		-1.65 (0.63) [a]		-3.03 (0.65) [a]		-3.10 (0.68) [a]	
CO_2 comp point	2.55 (0.70) [a]		2.78 (0.64) [a]		3.19 (0.67) [a]		3.42 (0.70) [a]	
g	301.33 (35.69) [a]		191.04 (38.15) [b]		212.16 (35.69) [a]		234.53 (35.69) [a]	
Two months after	**Ctrl-Ctrl**	**Ctrl-Defol**	**Defol-Ctrl**	**Defol-Defol**	**Ctrl-Ctrl**	**Ctrl-Defol**	**Defol-Ctrl**	**Defol-Defol**
Amax	24.68 (3.48) [a]	29.73 (3.48) [a]	29.91 (3.66) [a]	29.16 (3.48) [a]	22.12 (3.48) [a]	27.17 (3.48) [a]	27.35 (3.99) [a]	26.60 (3.48) [a]
Amin	-3.47 (0.62) [a]	-2.63 (0.62) [a]	-2.46 (0.66) [a]	-3.19 (0.62) [a]	3.73 (0.62) [a]	-2.90 (0.62) [a]	-2.73 (0.72) [a]	-3.46 (0.62) [a]
CO_2 comp point	4.66 (0.75) [a]	3.69 (0.75) [a]	3.43 (0.79) [a]	3.98 (0.75) [a]	5.54 (0.75) [a]	4.57 (0.75) [a]	4.31 (0.86) [a]	4.86 (0.74) [a]
g	207.73 (43.79) [a]	291.42 (43.79) [a]	237.35 (46.03) [a]	242.32 (43.79) [a]	176.61 (43.79) [a]	260..31 (43.78) [a]	206.24 (50.23) [a]	211.21 (43.79) [a]

Table S5.2. Height (*h*, m), diameter (*d*, mm), root:shoot ratio, woody aboveground biomass (abvgr biomass, kg), leaf area (*LA*, m^2), and leaf biomass (*LM*, g) for control (Ctrl) and defoliated (Defol) grafts of genotypes A and B, one year after the first-year defoliation treatment, and three months after the second-year defoliation treatment. Number in parenthesis indicate standard errors. Different letters indicate statistically significant differences between groups at α = 0.05 on a multiple comparison procedure using Tukey contrasts.

	Genotype A				Genotype B			
One year after	**Control**		**Defoliated**		**Control**		**Defoliated**	
h	1.82 (0.11) [a]		1.65 (0.11) [a]		1.83 (0.10) [a]		1.66 (0.10) [a]	
d	29.0 (1.5) [a]		28.5 (1.5) [a]		33.7 (1.4) [b]		26.1 (1.4) [a]	
Root:shoot	0.61 (0.05) [a]		0.63 (0.06) [a]		0.45 (0.05) [b]		0.47 (0.05) [b]	
Abvgr biomass	2.07 (0.50) [a]		2.08 (0.55) [a]		2.57 (0.50) [a]		2.59 (0.52) [a]	
LA	0.46 (0.06) [a]		0.55 (0.06) [a]		0.10 (0.06) [b]		0.19 (0.06) [b]	
LM	189.5 (25.6) [a]		230.6 (27.9) [a]		153.2 (25.3) [a]		194.3 (26.4) [a]	
Three months after	**Ctrl-Ctrl**	**Ctrl-Defol**	**Defol-Ctrl**	**Defol-Defol**	**Ctrl-Ctrl**	**Ctrl-Defol**	**Defol-Ctrl**	**Defol-Defol**
h	1.86 (0.26) [a]	2.28 (0.26) [a]	2.41 (0.26) [a]	2.27 (0.26) [a]	2.76 (0.26) [b]	2.51 (0.24) [ab]	1.76 (0.24) [a]	1.99 (0.24) [ab]
d	31.2 (2.9) [a]	33.3 (2.9) [a]	34.1 (2.9) [a]	35.1 (2.9) [a]	42.9 (2.9) [b]	36.8 (2.6) [ab]	28.7 (2.6) [a]	29.9 (2.6) [a]
Root:shoot	0.83 (0.13) [a]	1.04 (0.13) [a]	0.85 (0.13) [a]	0.98 (0.15) [a]	0.45 (0.13) [b]	0.65 (0.13) [b]	0.46 (0.13) [b]	0.60 (0.14) [b]
Abvgr biomass	1.99 (0.49) [a]	0.92 (0.49) [a]	1.20 (0.49) [a]	0.93 (0.56) [a]	3.14 (0.49) [b]	2.07 (0.49) [b]	2.35 (0.50) [b]	2.07 (0.51) [b]
LA	0.48 (0.03) [a]	0.22 (0.03) [b]	0.56 (0.03) [a]	0.30 (0.03) [b]	0.24 (0.03) [c]	0.13 (0.03) [bc]	0.15 (0.03) [c]	0.12 (0.03) [c]
LM	201.0 (24.1) [ab]	101.8 (24.1) [c]	231.6 (24.1) [b]	130.4 (24.1) [ac]	305.1 (24.1) [d]	148.1 (24.1) [c]	175.2 (24.1) [bc]	134.3 (24.1) [ac]

Table S5.3. Soluble sugar and starch concentrations (% dry matter) for control (Ctrl) and defoliated (Defol) grafts of genotypes A and B, one year after the first-year defoliation treatment, and three months after the second-year defoliation treatment, in roots and stem; and in needles during three sampling dates following first year defoliation and final sampling after second-year defoliation. Number in parenthesis indicate standard errors. Different letters indicate statistically significant differences between groups at α = 0.05 on a multiple comparison procedure using Tukey contrasts.

	Genotype A				**Genotype B**			
Tissue	**ROOT**		**STEM**		**ROOT**		**STEM**	
One year after	**Ctrl**	**Defol**	**Ctrl**	**Defol**	**Ctrl**	**Defol**	**Ctrl**	**Defol**
Sugar	0.99 (0.12) [a]	1.03 (0.13) [a]	0.93 (0.12) [a]	0.77 (0.12) [a]	0.90 (0.12) [a]	0.35 (0.16) [bc]	0.76 (0.12) [a]	0.75 (0.12) [ac]
Starch	1.35 (0.27) [a]	1.55 (0.30) [a]	1.29 (0.28) [a]	1.49 (0.27) [a]	1.49 (0.28) [a]	1.69 (0.32) [a]	1.43 (0.27) [a]	1.63 (0.28) [a]

	Ctrl		**Defol**		**Ctrl**		**Defol**		**Ctrl**		**Defol**		**Ctrl**		**Defol**	
3 months after	**Ctrl**	**Defol**	**Ctrl**	**Defol**	**Ctrl**	**Defol**	**Ctrl**	**Defol**	**Ctrl**	**Defol**	**Ctrl**	**Defol**	**Ctrl**	**Defol**	**Ctrl**	**Defol**
Sugar	0.66 (0.12)[a]	0.51 (0.12)[a]	0.71 (0.11)[a]	0.71 (0.11)[a]	0.72 (0.12)[ab]	1.00 (0.12)[b]	1.00 (0.11)[bc]	0.87 (0.11)[ab]	0.81 (0.12)[ac]	0.41 (0.11)[a]	0.39 (0.11)[b]	0.66 (0.11)[a]	1.07 (0.12)[c]	1.10 (0.10)[bc]	0.87 (0.11)[c]	1.00 (0.11)[bc]
Starch	1.39 (0.09) [a]	1.19 (0.09) [a]	1.29 (0.09) [a]	1.29 (0.09) [a]	3.68 (0.09) [b]	3.48 (0.09) [b]	3.59 (0.09) [b]	3.59 (0.09) [b]	1.41 (0.09) [a]	1.21 (0.09) [a]	1.31 (0.09) [a]	1.31 (0.09) [a]	3.70 (0.09) [b]	3.50 (0.09) [b]	3.61 (0.09) [b]	3.61 (0.09) [b]

	Genotype A						**Genotype B**					
NEEDLES	**1 month after**		**12 months after**		**13 months after**		**1 month after**		**12 months after**		**13 months after**	
1st treatment	**Ctrl**	**Defol**	**Ctrl**	**Defol**	**Ctrl**	**Defol**	**Ctrl**	**Defol**	**Ctrl**	**Defol**	**Ctrl**	**Defol**
Sugar	0.67 (0.08)[a]	0.65 (0.08)[a]	0.70 (0.10)[a]	0.68 (0.10)[a]	0.61 (0.09)[a]	0.59 (0.08)[a]	0.65 (0.07)[a]	0.62 (0.07)[a]	0.68 (0.10)[a]	0.65 (0.10)[a]	0.59 (0.08)[a]	0.56 (0.08)[a]
Starch	2.05 (0.11)[a]	2.10 (0.11)[a]	2.18 (0.14)[a]	2.23 (0.14)[a]	2.08 (0.12)[a]	2.14 (0.12)[a]	1.88 (0.10)[a]	1.93 (0.10)[a]	2.01 (0.14)[a]	2.06 (0.15)[a]	1.91 (0.10)[a]	1.97 (0.10)[a]

1st treatment	**Ctrl**		**Defol**		**Ctrl**		**Defol**	
2nd treatment	**Ctrl**	**Defol**	**Ctrl**	**Defol**	**Ctrl**	**Defol**	**Ctrl**	**Defol**
Sugar	0.78 (0.08) [a]	0.74 (0.08) [a]	0.79 (0.08) [a]	0.58 (0.08) [a]	0.82 (0.08) [ab]	0.68 (0.07) [ab]	0.87 (0.07) [ab]	0.86 (0.07) [b]
Starch	2.12 (0.16) [a]	2.03 (0.15) [a]	2.20 (0.15) [a]	2.06 (0.15) [a]	2.22 (0.16) [a]	2.12 (0.15) [a]	2.30 (0.15) [a]	2.15 (0.15) [a]

Chapter 6. Discussion and conclusions. Putting the red needle cast disease into perspective

Epidemiology of *P. pluvialis* in New Zealand and Oregon

Empirical data from the inoculation experiments and their fit into the epidemiological model provided and understanding of the *P. pluvialis* infection dynamics in *P. radiata* under controlled conditions. Important insights from those assays regarding infection dynamics are:

- In a single cycle of infection, *P. pluvialis* starts sporulating 4 days after the beginning of infection (primary infection).
- A polycyclic infection episode, at the plant level, presents a peak in 22 days, when it starts a decreasing phase (secondary infection).

Those parameters were derived under controlled conditions, simulating winter season. Therefore, no new needles were formed during the experiment, which may have slowed down the epidemic. In the field, I speculate that, if *P. pluvialis* maintains infection until spring, the addition of available healthy needles from the new flush would enhance sustained infection over the year. Empirical data from field experiments and monitoring plots to be fitted in the epidemiological model would elucidate which factors influence seasonality of the infection period. That would disentangle the relative contribution of environmental conditions and the phenology of the trees as providers of substrate for infection.

From the conclusions of the epidemiological model, I moved on to study the extension of *P. pluvialis* epidemic on Douglas-fir in the field, in New Zealand and Oregon. That study was motivated by understanding the association between *P. pluvialis* and *N. gaeumannii*. Detached-needle and -twig assays demonstrated that *N. gaeumannii* should be considered when studying *P. pluvialis* infection of Douglas-fir. This field survey allowed me to analyse the effect of a wide range of environmental variables on *P. pluvialis* development, and to compare the impact of the pathogens in the host's native and exotic environment of Oregon and New Zealand, respectively.

From the data analyses and the observations in the field, the high levels of *P. pluvialis* recorded in NZ compared to Oregon during spring time suggest different dynamics of infection between regions. These differences were likely related to colder winter temperatures and drier winter air relative humidity in Oregon compared to NZ (Oregon: 1.8-6.8 ºC and 74-84% RH; NZ: 6-9.6 ºC and 84-93% RH). These hardly overlapping winter temperature and relative humidity ranges strongly suggest that winter can be the limiting season in Oregon, while summer is observed to

be the limiting period in NZ. I combined the available information I gathered in a comprehensive conceptual epidemiological model (Fig 6.1) to compare *P. pluvialis* epidemiology in NZ and Oregon, which can be outlined as follows:

1. In NZ, *P. pluvialis* infection progresses from autumn peaking in late winter and spring, increasing the number of infected trees (positive correlation with GDD, Table 4.2). The infection reaches epidemic levels at the beginning of spring. The growth of the *P. pluvialis* on the needles increases exponentially through winter reaching a plateau in spring (no effect of GDD, Table 4.2). This plateau may correspond to a physical limitation to the amount of pathogenic infection needles can support, with *N. gaeumannii* already widely present.
2. *P. pluvialis* infection decreases in summer in NZ, driven by drier weather conditions.
3. In the PNW, winter conditions may suppress *P. pluvialis* development to minimum levels. Several infection cycles are assumed to take place until the inoculum levels reach the minimum threshold to allow sustained exponential growth through late spring to autumn. The number of infected trees may increase (positive correlation with GDD, Table 4.2), but they support only low levels of infection on the needles (inverse correlation with GDD, Table 2.2, Fig 2.5b).

A note of caution is in order here since the sampling covered only one spring period. This is the most likely explanation based on the data I present throughout my studies and additional observations in the field. However, any conclusive statement on *P. pluvialis* dynamics in the PNW should be supported by further exploration of the pathogen levels throughout the year.

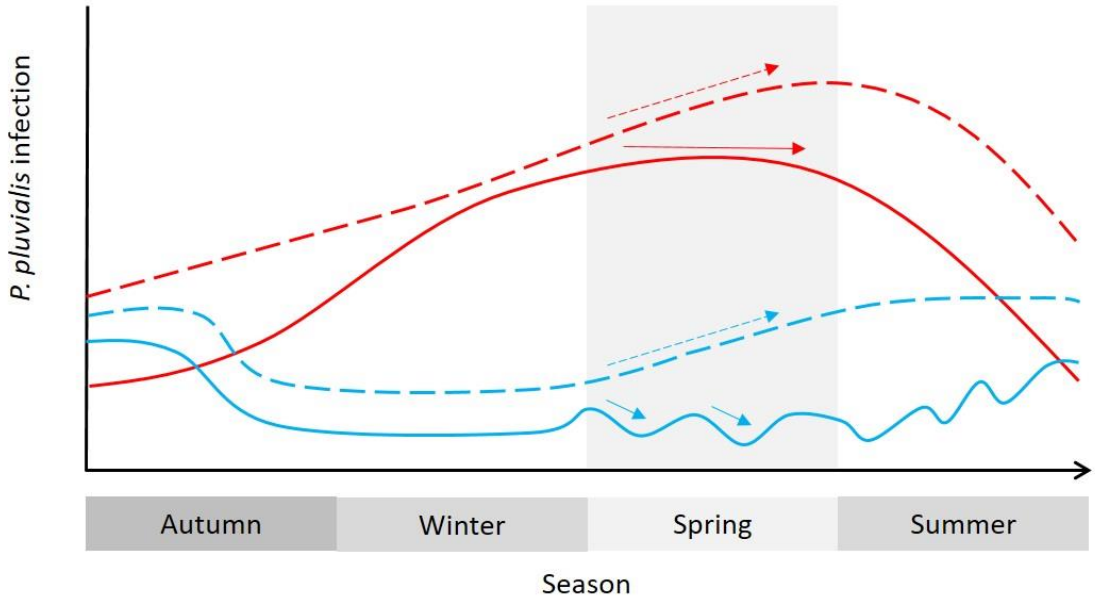

Figure 6.1. Conceptual diagram of *Phytophthora pluvialis* epidemiology in Oregon (blue) and New Zealand (red). Solid lines represent the abundance of the pathogen in the needles; dashed lines, the proportion of infected trees. The sampling period (from survey in chapter 4) is shadowed. Arrows indicate either positive (ascendant) or negative (descendent) correlation between growing degree days and *P. pluvialis* abundance (Table 4.2). Horizontal arrow indicate absence of correlation between growing degree days and *P. pluvialis* abundance (Table 4.2).

Implications for disease management

In NZ, long-term management strategies to fight the RNC disease consist of identification of susceptible and resistant genotypes. Short-term measures focus on chemical control. Phosphite and copper-based fungicides have been proved effective at reducing *P. pluvialis* infection of radiata pine needles (Ganley et al. 2014, Rolando et al. 2014, 2017). The potential for improving tolerance to RNC disease in *P. radiata* through breeding is good (Graham et al. 2018). Number of lesions and lesion length have been used to phenotype susceptible and tolerant clones (Dungey et al. 2014, Graham et al. 2018). The results from chapter 2 have made an important contribution to our understanding of the susceptibility and resistant to RNC.

Susceptibility and resistance

Using the epidemiological model, I have been able to identify the main differences and important similarities between susceptible and resistant *P. radiata* genotypes. Those differences are:

- The infection rates and the incubation times are similar for resistant and susceptible genotypes (Table 2.3).
- The pathogen death rate is 2.5 times higher for resistant than susceptible genotypes.
- Only 28% of the resistant ramets produced mycelium and sporangia, whereas 90% of the susceptible ramets did so (Table 2.3).

This shows that resistant genotypes can host the pathogen but mycelium growth and sporulation are reduced, impeding the progression of disease to epidemic levels. This difference is crucial. In other foliar Phytophthora diseases, such as *P. ramorum* infecting Japanese larch, sporulating hosts have a key role in the spread of the disease. In this sense, comparing with a similar approach primary and secondary infection rates for the alternative larch hosts *L. decidua*, *L.* x *marschlinsii* and *L.* x *eurolepis*. Further exploration with epidemiological models could be used at the stand level to tailor alternative plantation arrangements through spatial heterogeneities of susceptible and resistant plants to reduce disease impact. This aims to compensate for the loss of genetic diversity in monoculture plantations, which has been reported to show less resilience to pathogens (Dodd et al. 2012, Ennos 2015). Similar studies have been performed in agriculture (Mammeri et al. 2014) and can be an excellent tool to define optimal control measures based on cultural practices.

In chapter 5, I explored how the defoliation of the lower canopy impacts productivity and resilience of *P. radiata* grafts. I used two different genotypes that were susceptible to the RNC disease. However, each genotype presented different tolerance to defoliation in terms of both growth and resilience (which I measured through C storage). Based on my results, genotypes could be selected by traits related to tolerance to defoliation instead of or as a complement to susceptibility to the RNC disease. Both genotypes presented different initial *SLA*, which appeared to be related to the different behaviour regarding defoliation tolerance. Lower *SLA* values implied more C

resources removed from the plant under the same defoliation intensity. In that case, defoliation episodes would have greater impact on the plant C budget. Further research on the role of *SLA* in the RNC infection and subsequent defoliation would be useful, as *SLA* is an easy-to-measure trait. Moreover, as *SLA* is also nutrient-dependent, investigating the within-genotype variation in *SLA* in response to soil nutrients would inform an integral approach to forest and disease management.

The importance of good assessment methods

Across the experiments presented in this thesis, I used different methods to assess *P. pluvialis* infection: lesion length measurement, isolation in culture media (carrot- and corn- based) and qPCR. Lesions caused by *P. pluvialis* in *P. radiata* are characterized by pale-olive discolouration and black resinous bands. These lesions can be easily distinguished in laboratory assays, when *P. pluvialis* is inoculated in healthy needles. However, in the field, needles hardly ever present single pathogenic infection. Other pathogens' infection can confound the attribution of symptoms to RNC. This clearly poses a problem in Douglas-fir needle infection, as highlighted in the detached-needle assays presented in chapter 3. That study showed that diagnosis solely based on visual symptoms is not able to distinguish SNC from RNC. Moreover, the asymptomatic phase during the first days after inoculation, both in radiata pine and Douglas-fir (3 days in the detached-needle assays, and 4-6 days in on-plant inoculation) may mislead diagnostics and quantification. For those reasons, it is required to confirm *P. pluvialis* infection by isolation and/or molecular techniques.

In detached-needle assays, where the pathogen is inoculated and growing in optimal conditions, isolations were more successful in *P. radiata* (90%, 3 days after inoculation, Fig 2.4a-b) than in Douglas-fir (35%, 11 days after inoculation, Fig 3.1b), presumably due to the unnoticed presence of *N. gaeumannii*. The on-plant inoculation allowed comparison between isolations and qPCR detection in a setup more similar to forest conditions. As a whole, qPCR was able to detect *P. pluvialis* twice as much as isolations. Moreover, both methods yielded peaks of infection at different times after inoculation, resulting in misleading disease predictions depending on the used method. The peak reached by qPCR detection occurred earlier than by isolations. By the end of the experiment, qPCR was not as efficient as isolations, leading to a quicker decrease in the epidemic output. Detection by qPCR was presumably influenced by presence of secondary pathogens whose infection was observed by the end of the experiment. Detection and quantification methods were the single most important factor influencing parameter estimates in the on-plant inoculation. Therefore, the choice of good assessment methods is crucial. I argue that a combination of both techniques would result in optimal assessment of the RNC. However, qPCR detection would suffice in the early stages of the RNC disease.

The challenge of multiple-pathogenic infections

The results presented here raised the importance of taking into account the interaction of foliar pathogens and their contribution to defoliation events. The co-existence of *P. pluvialis* and *N. gaeuamannii* in Douglas-fir at different scales, from region to needles indicates that both pathogens can contribute to defoliation episodes in the field. My assessments took place during a single spring season. This presents some limitations. On the one hand, multiple-pathogenic infections are likely to vary seasonally. Each pathogen's individual interaction with weather conditions and their interaction among each other during one season would lead to variable levels of inoculum at the beginning of the next season, which would, in turn, interact again with weather conditions. On the other hand, the interactions of both pathogens with the host will have an impact on both next year's level of available substrate and the ability of a possible weakened host to fight disease.

I did not explore multiple-pathogenic infections on *P. radiata*, but the on-plant inoculation elucidated that other pathogens are likely to coexist and interact with each other in radiata pine plantations in NZ. Some important pathogens are: *Dothistroma pini* (Butin) DiCosmo and *Cyclaneusma minor* Hulbary (Bulman 1993). They have different ecological requirements, and hence their interaction with *P. pluvialis* will be different. For example, *Cyclaneusma* affects one-year-old needles, while *Dothistroma* affects current-year foliage. Further, *Cyclaneusma* severity in enhanced by mild wet winters, and the infection is common in 11- to 20-year-old plantations. By contrast, a wet summer increases *Dothistroma* severity, and trees older than 15 years are commonly resistant (Bulman 1993). The diversity of ecological niches and physiological impact make it counter-intuitive to infer any prediction of synergy/antagonism among pathogens. The defoliation experiment presented in chapter 5 introduces seasonality of the infection as a factor determining the physiological impact of a defoliation episode. Putting those three pathogens, their ecological requirements and their main impact on the host into a common modelling framework is important to understand foliar disease impacts on radiata pine plantations in NZ. This a challenging, but necessary step.

Physiological impact of *P. pluvialis*

The physiological response of *P. radiata* to lower canopy defoliation is genotype-specific. I studied the impact of artificial defoliation mimicking the RNC defoliation pattern on two RNC-susceptible genotypes. The main initial difference between both genotypes was the *SLA* values. Higher *SLA* would confer a wider tolerance to defoliation, since C resources removed from canopy are lower under the same defoliation intensity. Therefore, leaf traits appear to be important in *P. radiata* tolerance to defoliation. When defoliation imposed carbon limitation, as was the case of genotype B in my chapter 5 experiment, the impacts on growth and C reserves were as follows:

- Diameter was the only growth parameter affected by defoliation with 23% reduction, which was exacerbated following the second growing season (32% reduction).

- Height and total aboveground biomass reductions were only noted in the second growing season after defoliations (36% and 55%, respectively).
- Root:shoot ratios were unaffected by defoliation.
- Leaf mass recovered one year after defoliation.
- Defoliation reduced sugar storage in roots during canopy development, followed by a recovery in root sugar reserves after the second growing season.

From the results, I conclude growth is more impacted than reserves. While the impact of defoliation on growth is higher after the second growing season, the reduction in root sugar storage is reversed after the second growing season. Therefore, reserves appear to be maintained at a certain level, similar to control plants, and only varied transiently during canopy development to account for the foliage loss.

This artificial defoliation experiment gives a first insight on the impact of the RNC disease which affects the lower canopy. However, the cost of defence to infection is not accounted for in artificial defoliation, and hence those results cannot be extrapolated to infection and defoliation episodes taking place under field conditions. The next step would be to assess RNC-induced defoliation to account for the previous potential C investment in defence during the infection period prior to defoliation. Assessment of defoliation under field conditions together with growth measurements, levels of infection, and NSC concentrations, would be very informative to understand C dynamics under RNC infection.

Unresolved fundamental ecological questions

A general redundancy of lower-canopy foliage in terms of C assimilation was shown in the artificial defoliation experiment. However, the needles in the lower canopy of radiata pine have been proved to be well defended (Moreira et al. 2012). This apparent contradiction calls for an ecological explanation. I speculate that well defended foliage from the lower canopy can serve as a buffer against foliar pathogenic infection. Thus, foliage which is more efficiently photosynthesizing escapes infection. The extra foliage could also have the role of providing substrate for pathogenic infection, so that the pathogen population, although kept at relatively low levels, could help the tree control competing vegetation under its canopy, as long as the pathogen is a generalist. Given the fact that temperate coniferous forests generally provide little diversified understories (Glenn-Lewin 1977, Barbier et al. 2008), coevolved foliar pathogens could help those trees control competing vegetation, establishing a certain degree of mutualism. The ecological role of the mild infection of the lower crown of trees by foliar pathogens such as aerial Phytophthoras is unclear. Further research is needed to fully elucidate foliar Phytophthoras' behaviour to shed light on best management practices.

Implications for plantation forestry in New Zealand

The two most widely planted species, radiata pine and Douglas-fir, in NZ forestry are *P. pluvialis* hosts. As suggested by the survey presented in chapter 4, RNC proliferation in radiata pine

increases the inoculum source and may have contributed to the high levels of *P. pluvialis* found in Douglas-fir. This situation is not ideal for successful disease management, as the inoculum levels are inherently able to develop at the highest potential, with abundant substrate for infection. The application of the epidemiological model together with high pathogen loads in NZ compared to the host's native environment suggest that controlling the pathogen inoculum levels below a threshold can prevent disease from reaching epidemic levels. There are several management strategies to control inoculum levels, from chemical control to suitable silvicultural practices.

In the case of plantations, the first management decision is the selection of planting material. It is widely accepted that exotic species in a monoculture setup are more susceptible to be infected by newly introduced pathogens and potentially pathogenic native fungal and fungal-like organisms (Pautasso et al. 2005, 2015, Ramsfield et al. 2016). New, creative plantation forestry setups may include under consideration the following:

- A more varied species choice at the landscape level, if the species does not support mixed species plantations, creating a mosaic of plots dominated by different species. Although a multi-clonal set up is not as efficient as natural populations in terms of buffering pathogenic infection, they have been suggested to suffer less pathogen damage (Ennos 2015, and cites therein).
- An increased genetic diversity if monoculture is still the main choice. Alternate resistant and susceptible genotypes can be combined within the same plantation arrangement so that the level of inoculum is minimized (see section 'Susceptibility and resistance' above).
- Incorporation of native species in a plantation forestry setup, i.e. 'Indigenous Forestry'.

Silvicultural practices can be reviewed so that inoculum levels are minimized to have the least impact on tree productivity. Given that the lower crown has been proved redundant under the artificial defoliation experiment presented here, early pruning of lower canopy branches could be considered and incorporated in silvicultural and economic models. Thinning regimes could also be reviewed to manipulate the humidity conditions in the lower canopy environment.

RNC disease management strategies should also consider to minimize the risk of spillover onto native plants through assessment of the susceptibility of key native plants to *P. pluvialis*.

Under climate change, RNC disease should be tested for its interactions with new climatic scenarios. The review presented in chapter 6 attempts to analyse the impact of drought events, predicted in NZ under climate change, on the RNC development. It may have sounded counter-intuitive as *P. pluvialis* needs wet conditions to develop. But the interaction of both factors can be combined seasonally through their respective impact on the tree. While drought conditions may have a negative effect on inoculum levels, they may also have such a negative effect on host health condition of the host, which might become more vulnerable to infection.

I advocate for the use of epidemiological models integrated to physiological models and economic models to thoroughly examine smarter, future-proof plantation forestry setups and their impact on inoculum levels, disease epidemic, impact on productivity and resilience, and economical impact in forest industry. To face this challenge, interdisciplinary collaboration is required to bring together expertise in plant pathology, ecophysiology, chemistry and forest economy.

Appendix 1. Insights on the impact of drought on the RNC disease

This appendix comprises the following co-authored review paper published in Australasian Plant Pathology:

Wakelin, S.A., Gómez-Gallego, M., Jones, E., Smaill, S., Lear, G., Lambie, S. 2018. Climate change induced drought impacts on plant diseases in New Zealand. Australasian Plant Pathology 47(1): 101-114.

Prelude

Climate change can change disease distributions and impacts. The magnitude of climatic variables as well as the frequency of extreme events, such as drought, are predicted to change under climate change and, in turn, to impact disease expression. The contribution and direction of these impacts are disease-specific, and they need to be analysed for each particular disease and region.

The review included in the present chapter addresses the impact that climate change-induced drought events can be expected to have in the most important diseases present in New Zealand, based on our current knowledge. The review provides a comprehensive framework to understand the impact that drought can have in disease development. Further, it explores whether drought may have a positive, negative or neutral effect on the most important diseases in New Zealand. A case study on the interaction between drought and RNC is presented, taking into account the drought impact on both the host and the pathogen. It is highlighted that a drought event followed by periods of extended rainfall would be the worst scenario for the productivity and survival of *P. radiata*, as the trees would have debilitated conductive systems and decreased carbon reserves for defence, but *P. pluvialis* would have favourable conditions for infection.

Abstract

Climate change is expected to increase the frequency and duration of drought in many parts of New Zealand. This may affect the natural lifecycles of plant pathogens, influence host predisposition to infection or disease expression, shift the natural ranges of the pathogens, and alter the rate of genetic change in pathogen populations. Collectively, these influences are likely to affect a range of pathosystems of significant economic importance to New Zealand's productive sectors. We undertook analyses of potential drought impacts on several diseases of plants important to New Zealand's economy: pea root rot (caused by *Aphanomyces euteiches*), onion white rot (*Sclerotium cepivorum*), wheat take-all (*Gaeumannomyces graminis* var. *tritici*), wheat crown rot (*Fusarium* spp.), brassica black leg (*Leptosphaeria maculans*), grapevine black foot (*Ilyonectria/Dactylonectria* spp.), kiwifruit sclerotinia rot (*Sclerotinia sclerotiorum*), and radiata pine red needle cast (*Phytophthora pluvialis*). For most pathosystems, increased drought is expected to increase disease expression. However, drought may reduce the severity of some diseases, such as *Sclerotina* rot of kiwifruit and red needle cast of radiata pine. To exemplify how drought can affect different components of the host-pathogen-environment interaction, a case study on red needle cast of radiata pine is presented. We recommend that land-based productive sectors need to better prepare for the deleterious impacts or beneficial opportunities of increased drought for plant diseases in New Zealand.

Drought impacts on plant diseases in New Zealand

At least 100 years ago, plant pathologists recognised the importance of the three-way interaction between susceptible host, virulent pathogen, and favourable environment, needed for disease expression (Duggar, 1909 cited by Francl, 2001). While adapted and modified over time, this concept of the disease triangle (Fig A1) remains highly useful for understanding the aetiology of plant diseases in productively managed ecosystems.

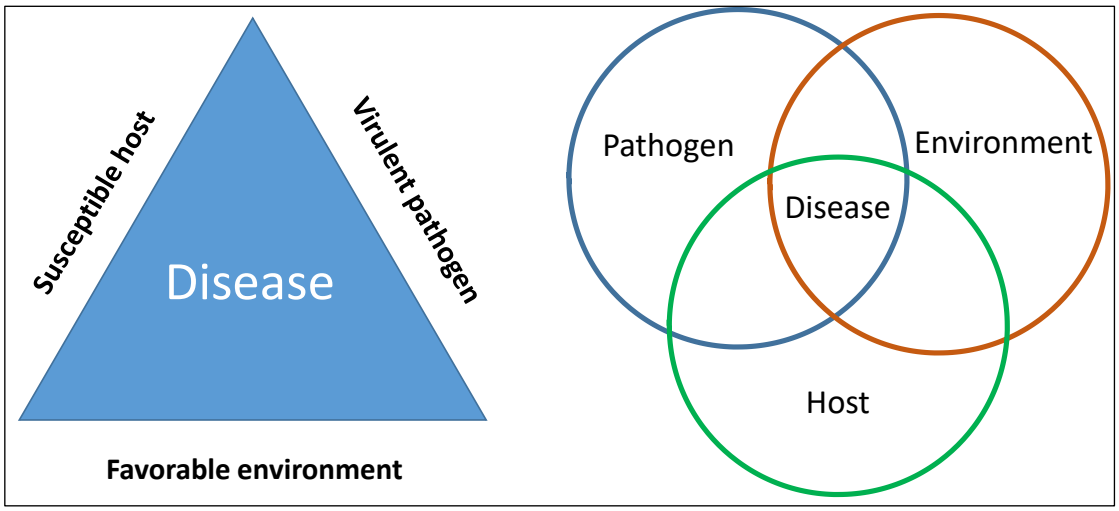

Figure A1. The disease 'triangle' has been a useful way of visualizing how the interaction between the presence of a virulent pathogen, a susceptible host plant, and conducive environmental conditions collectively express to result in plant disease. This concept is appropriate for understanding the projected impacts of drought on plant diseases, as these will occur not just through environmental influences, but also because drought impacts the ecophysiology and fitness of a pathogen and its host. Note that 'environment' is not just the abiotic environment, but can include the microbiome environment of the host or pathogen that affects their respective fitness.

The impacts of drought on diseases are likely to be expressed across all components of the disease triangle. The combined outcome of these effects need to be interpreted within each pathosystem. These vary extensively across New Zealand's productive sectors, spanning diverse agricultural, horticultural, and forestry systems operating within a broad range of climatic zones. As such, there is a vast diversity in pathoecosystems across New Zealand, and this diversity precludes our capacity for assessment of impacts of drought for all diseases. Furthermore, while several studies have been performed for crops of global significance (e.g. IPCC, 1996), these need to be interpreted within the context of New Zealand's agroecological regions and account for the prediction of impacts of expected climate change induced drought. Thus, to investigate the effects of drought on disease in New Zealand, we take an ecophysiological approach that assesses the impact of drought within each component of the disease triangle.

Impacts of drought on host plants

There has been considerable research on the effects of drought stress on plant physiology and resistance to disease (Desprez-Loustau et al. 2006). Impacts of drought on hosts can include

altering nutritional status, shifts in growth between above and belowground tissues, shift in allocation of resources to tissues, and a predisposition of hosts to infection through general weakening and/or suppressed disease resistance. Drought, as a general stress factor, may also activate systemic defence mechanisms resulting in increased resistance to infection. These effects are considered below.

Changes in plant tissues

Drought, in addition to reducing tissue moisture content, has wide-ranging effects on plant physiology (Hsiao 1973). These include changes in fundamental metabolic processes associated with formation of carbohydrates, proteins, lipids, amino-acids, phytohormone levels, in secondary-metabolism pathways, and formation of reactive oxygen species (Hsiao 1973, Cruz De Carvalho 2008, Xu et al. 2010, Niinemets 2015).

The best characterised effects occur though alteration of resources among plant tissues. These include plant access to nutrients in the soil, and the direct reallocation of existing resources among host tissues that are altered under drought conditions (Peuke and Rennenberg 2011, Poorter et al. 2012, Gargallo-Garriga et al. 2014, He and Dijkstra 2014). Changes in the nutrient state alter the 'resource quality' of plant tissues (Desprez-Loustau et al. 2006) – i.e. the quality of the substrate for the pathogen to colonise and proliferate. Along with drought-induced influences on tissue micronutrient content (B, Fe, Mn, S, Mg, and others), these changes can affect success of pathogen invasion, colonisation, and resources (principally energy) required for spread to new hosts or formation of survival structures (e.g. Walters and Bingham, 2007; Dordas, 2008). These effects, therefore, overlap into impacts on pathogen fitness and disease epidemiology.

Mild drought has been shown to stimulate shifts in plant biomass accumulation, particularly increases in the growth of root biomass relative to above ground tissues, and proliferation of fine-roots required for capturing soil moisture and nutrients. Above ground, chronic drought can cause reduced leaf area, reduced stomatal conductance, and lowering of photosynthetic rates. These effects are triggered by phytohormone signalling networks, such as formation of abscisic acid (ABA) in the root system when moisture deficit is sensed (Ton et al. 2009). However, it is apparent that the species, provenance and genotype of *P. radiata* plays a critical role in determining the extent of drought-driven changes in ABA production and accumulation, and the implications for other hormones involved in defences responses (e.g. Corcuera, Gil-Pelegrin and Notivol, 2012; De Diego et al., 2015; Arango-Velez et al., 2016). Collectively, these effects fundamentally change the opportunities for host infection both by root and foliar pathogens.

The activity of mycorrhizal fungi and plant growth promoting rhizobacteria (PGPR) can reduce the impact of drought on plants. The production of the enzyme 1-aminocyclopropane-1-carboxylic acid (ACC) deaminase by PGPR can increase tolerance to drought by attenuating the in planta 'stress ethylene' response (Grover et al. 2011, Zhou et al. 2013), while the release of hygroscopic extracellular polysaccharides (EPS) can increase soil water retention through increased aggregation (Sandhya et al. 2009). Arbuscular mycorrhizal fungi (AMF) and ectomycorrhizal fungi (EMF) can also substantially mitigate drought effects, as both enhance access to smaller soil pore

spaces (Lehto and Zwiazek 2011, Ruiz-Lozano et al. 2012) and produce various molecules that enable the plant host to better tolerate water stress (Sharma and Gobi 2016). However, these interactions are essentially delaying tactics that provide protection from low intensity or transitory droughts, and will only delay the onset of deleterious effects from prolonged drought conditions.

Change in secondary metabolism and plant defence/resistance systems

Across several plant species, stress has been shown to induce profound changes in plant gene expression thereby resulting in altered plant chemistry (De Vos et al. 2005, Zhang et al. 2014, Sampaio et al. 2016). As altered plant metabolic systems are numerous, effects are extensively expressed across the host's wider physiology. Given this, these have been the subject of extensive previous review (Hsiao 1973, Cruz De Carvalho 2008, Edreva et al. 2008, Pavarini et al. 2012). Of most relevance for drought, they include changes in allocation of carbon into C-rich compounds such as succinate, and production of many classes of secondary metabolites, including phenolic acids, flavonoids, anthocyanins, tannins, gamma amino butyric acid, and acid-alcohols (Ramakrishna and Ravishankar 2011, Pavarini et al. 2012). Many of these classes of compounds have broad spectra of biological activity and, in many cases, they suppress growth both of microbial and invertebrate pathogens (Bennett and Wallsgrove 1994). Generalised stress responses, triggered by abiotic stresses such as drought, may result in increased disease resistance, and the net impact of these is balanced against potential predisposition of hosts to infection in their otherwise weakened states. Exposure to low-levels of stress may incur hormesis-type effects within plants, resulting in wide-reaching beneficial outcomes (Terry et al. 2007, Hooper et al. 2010).

Plants also have specialised responses to infection by plant pathogens, such as systemic acquired resistance (SAR) (Durner et al. 1997). This is regulated by phytohormone signalling pathways, triggered at the sites of pathogen infection (or detection), then spreading systemically through the plant. Key to these are pathways based on salicylic acid (SA) (McDowell and Dangl 2000). Paradoxically, the SA pathway is negatively regulated by ABA (Xiong and Yang 2003, Yasuda et al. 2008). As the effects of drought stimulates ABA production in root tissues (Rowe et al. 2016), changes occur in leaf area and photosynthetic rate (Flors et al. 2009) to reduce plant moisture demand. However, as SA is required for SAR, the consequence of drought-induced down-regulation of SA is increased host susceptibility to infection.

Although the wider relationships between abiotic and biotic stress, hormones, and other secondary metabolites and plant metabolism are complex (Rowe et al. 2016), the key aspect is high interconnectivity among these pathways. As such, outcome effects are highly dependent on the plant species and its wider physiological state (e.g. nutrition, life-stage). As drought and disease may occur simultaneously, and plant responses can shift towards the most recent stress applied (Davila Olivas et al. 2016), the assessment of plant physiological responses to combined stressors must be considered (Ramegowda and Senthil-Kumar 2015). The plant physical responses to the effects of drought remain difficult to accurately predict.

Drought impacts on plant pathogens

The ecological niches for all organisms are bounded to ranges in temperature, nutrient requirements, pH, moisture availability, and other factors (Barton and Northup 2011). Water availability, as affected by drought, will therefore directly affect the environmental ranges of microbial and invertebrate taxa, particularly in soil ecosystems (Ogunseitan 2005). For phytopathogens, these boundaries may differ across the phases of pathogen life-cycles and during host infection: saprophytic growth and survival (where appropriate), survival during dormancy, windows of opportunity for dispersal (e.g. spores), conditions favouring host infection and disease formation and development (Agrios 2005). Some of these effects are discussed in the Environment section below.

Mismatch between individual pathogen moisture requirements and water availability will drastically impact the pathogen at many stages of its life cycle. These impacts may disrupt infection and/or otherwise reduce pathogenicity. For example, while downy-mildew (*Sclerophthora macrospora*) infection of wheat foliage requires the presence of free water, whereas water is not required on leaf surfaces for infection by powdery mildew (*Blumeria graminis* f. sp. *tritici*). Alteration of soil moisture content may affect the development of disease complexes, which often involve highly different taxa such as pathogenic fungi and nematodes (Back et al. 2002).

Each pathosystem will have a 'critical water deficit' whereby the balance between plant water stress and pathogen aggressiveness (as affected by moisture) intersect to be favourable or not for disease (Schoeneweiss, 1986 as cited in Desprez-Loustau et al., 2006). However, even for pathogens regarded as xerophytic, the relationship between drought and disease may be indirect (Marçais and Desprez-Loustau 2014). This, again, highlights the importance between understanding impacts of drought on disease by looking across effects among the host, pathogen, and environment interactions (Fig A1).

Pathogens may also be affected by drought at population level. For pathogens with a life phase involving sexual reproduction (genetic recombination), the beneficial or deleterious impacts of drought will impact population size and generation time (Chakraborty et al. 2000). When genetic diversity is present, it provides greater opportunities for development of more pathogenic strains, increases the potential for pathogens to overcome host resistance genes (gene-for-gene resistance relationship; Flor, 1971), and provides opportunities for pathogens to evolve drought tolerance traits (Garrett et al. 2006). The rate of acquisition of new genetic traits through gene transfer or gene mutation can be greatly enhanced under environmentally stressed conditions such drought and other impacts of climate change (Newton et al. 2011). Furthermore, increases in trade provide increased opportunity for mixing of new pathogenicity elements (e.g., virulence genes) into populations of actual or potential pathogens. This may provide new combinations of genes to increase the virulence or host range of existing pathogens, introductive virulence into currently avirulent but potentially pathogenic species, or accelerate genetic mutation and/or recombination of genes associated with host range and virulence. Overall, the outcome is emergence of enhanced or new diseases of plants that can reduce primary production.

Environment

As the frequency and magnitude of drought change in New Zealand, and intensity among regions and agroecological zones varies, the conditions suiting the establishment of new pests and diseases, or the change in range of ones already present, will manifest. Along with gradual change in wider environmental conditions favourable to the range of the pathogens, and/or the invertebrate vectors that transmit them, new plant disease pressures are expected to occur (Anderson et al. 2004), with potentially devastating impacts for New Zealand's productive sectors.

Environmental conditions affecting drought can be categorised: first, the biophysical environment, with changes in edaphic and environmental properties; secondly, the trade environment, involving the transfer and movement of goods and material on a global, national, or local scales.

Biophysical environment

Changes in the wider biophysical environment will strongly affect pathogen fitness, with potentially different impacts across the various parts of the life cycle and across of pathogens (i.e. from seed borne to soil inhabiting). Given the immediate impacts of drought on a wide range of edaphic properties, including soil moisture, the strongest influences are likely to be most pronounced on soil-borne pathogens.

The best characterised impact of drought is reduced soil moisture availability. As soils dry, pore spaces between soil aggregates increasingly shift from water-to-air-filled (decreased water potential), reducing hydraulic connectivity among aggregates. This can decrease movement of solutes and nutrients though the soils, including host-root compounds that may be necessary for energy or comprise host-specific compounds needed to trigger or fight pathogen infection (e.g. Brencic and Winans, 2005). The speed and extent to which this occurs are a combined result of the magnitude of drought, extent of water already stored in the soil, and the soil mineral and organic content which determine how strongly moisture is retained (i.e., distribution of pore size classes, Singleton, Mihail and Rush, 1992). These effects are well recognised for growth of plants, where critical thresholds of soil water that support growth are calculated (wilting points). However, effects of reduced water potential also profoundly impact soil microorganisms and their physiology (Schimel et al. 2007). Microbial groups differ in their capacity to withstand the effects of drying and the increased ionic-stress and osmotic pressure in soils as water is removed (Manzoni et al. 2012). Ecophysiological groupings for microorganisms based on their water potentials can be determined. These range from tolerant taxa, such as Actinobacteria, through to sensitive taxa such as Gram-negative bacteria and water moulds (oomycetes). Soil-borne plant pathogens extend across this range, e.g., from the *Streptomyces* spp. (Actinobacteria) that cause common scab of potato, through to *Aphanomyces* spp. (oomycete) that cause root disease of legumes and other crops (Singleton et al. 1992). In some instances, reduced water potential may have no effect on pathogen survival and populations in soil, as even drought sensitive organisms, such as oomycetes and many true fungi, can produce survival structures that are tolerant to variation in environmental conditions. For pathogens that don't have such survival strategies, particularly some Gram-negative bacteria, survival in soil may be affected by drought and their populations

subsequently reduced. Impacts of drought on disease may also be expressed during the growth of the pathogen in soil during the infection stage. For example, *Aphanomyces* spp. motile zoospores can travel short distances through soil moisture to host root tissue (Kerr 1964). The removal of water from soil can reduce the hydraulic connectivity between the pathogen propagule in the soil and the host root, reducing infection. The net effect of drought on disease will be the combined outcome of the impacts on the subcomponents affecting multiple parts of a pathogen's life cycle, from occurrence of resting (survival) stages, through to requirements for free-water to support infection and also growth to the host.

Future scenarios of climate change induced drought will occur in combination with e[CO_2]. The effect of e[CO_2] on pathogen-plant interactions may be affected by variation between host species adaptation strategies under e[CO_2]. Lake and Wade (2009) suggest that Arabidopsis thaliana leaf morphological adaptation to e[CO_2], such as increased stomatal index, may allow for greater establishment of *Erysiphe cichoracearum* in juvenile foliage. However, Mcelrone et al. (2005) found that *Phyllosticta minima* infection incidence and severity in Acer rubrum was minimised under e[CO_2], despite the positive effect of e[CO_2] on *P. minima* growth. It was possible that reduced infection of *P.minima* was a result of reduced stomatal conductance and nutritive quality in response to e[CO_2].

Trade environment

As many biogeographical constraints to pathogen dispersal are removed, pre- and post-border biosecurity measures have become critically important in reducing pathogen distribution. Regardless of this, new incursions of pests and diseases into New Zealand's productive ecosystems continue (Goldson et al. 2015). Increasing travel and movement of material within New Zealand is also providing greater opportunities for pests and diseases dispersal. Furthermore, as a result of increased extreme weather events (storms, floods, winds) (IPCC 2013), a positive feedback for movement and effects of phytopathogens may occur (Orwin et al. 2015).

Except for a few highly damaging diseases, the nature (pathogen species), extent, and economic costs of soil-borne diseases are unknown, but thought to be considerable (e.g. Dignam et al., 2016; Wakelin et al., 2016). Root diseases, for example, are widely recognised as a significant 'biological-brake' limiting the productive potential of the primary sector, and these increase susceptibility of plants to impacts of other abiotic or biotic stresses. There is little or no active monitoring of the frequency of incursion of soil-borne diseases into New Zealand.

Impacts for New Zealand's productive sector

There is limited information on the effects of drought on the diseases of importance to New Zealand's productive sector. In most cases, therefore, cases must be taken from overseas and extrapolated to local conditions. For example, dry soil conditions are recognised as favourable to *Sclerotium cepivorum* (which causes onion white rot), *Streptomyces scabies* (potato common

scab), and *Fusarium oxysporum* (*Fusarium* wilt of pea, Pandey et al., 2015). Although the impacts of climate change on these pathogens have not been assessed within New Zealand, these crops have considerable value to the economy: $50.8 million p.a. for onion, $232.4 million p.a. for potato, and $103.8 million p.a. for pea (NZIER 2015). Paradoxically, increased drought may increase disease caused by some oomycete pathogens that are normally associated with excess water. While wet conditions are often required for oomycete pathogen dispersal, dry or drought conditions can trigger manifestation of disease (Singleton et al. 1992). Examples of these include *Aphanomyces* root rot of pea and *Phytophthora* foliar disease of *Pinus radiata*. The value of forest plantations of *P. radiata* in New Zealand is $4.45 billion (Forest Owners Association New Zealand 2016), so any decline in productivity will have significant economic consequence for the country.

The direct and indirect impacts on drought are complex and may differentially affect the components of the disease triangle (Fig A1). Depending on the pathosystem, these influences are expressed to either increase or decrease disease. Except for a few key diseases, it would be impossible to empirically assess all effects for all pathosystems across New Zealand's productive sectors. Ecophysiological-based models must be used to predict disease outcomes. For most diseases, the impact of drought on each component of the model is unlikely to be assessed. Best-knowledge estimates, based on fundamental principles, must be employed.

We used this approach to predict the impacts of increased drought on some key diseases for New Zealand's agricultural, horticultural and forest sectors (Table A1). For approximately half the diseases assessed (pea root rot, onion white rot, wheat take all, brassica black leg, and radiata pine red needle cast), the impacts of drought varied depending on when the drought occurred. Drought occurring during pathogen germination, sporulation, and dispersal generally resulted in reduced potential for disease development (Table A1). However, drought occurring 'late season', i.e. after host infection, resulted in increased expression of disease through reduced host vigour. Given several of these crops are annual, where drought can be expected late in the season (summer to autumn), we predict an overall increase in disease and reduction in plant production for many pathosystems. The only disease for which drought was very likely to reduce disease was *Sclerotinia* rot of kiwifruit (Table A1).

Case study: forestry sector and *Phytophthora*

Globally, the synthesis of published information related to drought impacts on plant health indicates drought increases disease severity (Desprez-Loustau et al. 2006). Most above and belowground fungal diseases of trees (broadleaf and conifer) are favoured by drought, or disease expression is exacerbated by wider drought effects on tree health. In only a small number of cases, the incidence or severity of disease reduced. These impacts will be highly conditional to individual pathosystems, as highlighted by a meta-analysis of the impacts of drought on forest pests and diseases (Jactel et al. 2012). A consensus of 40 published studies found that impacts of primary pests and pathogens living in wood are reduced in severity by drought, while those living in foliage tissues will more severely damage water-stressed trees. However, a net increase in disease effects in forests, coinciding with drought impacts, are likely to strongly contribute to

the decline of forest health within very large biomes, such as the Canadian boreal forests (Peng et al. 2011).

Perhaps one of the most important diseases of forestry, both currently and potentially, are those caused by *Phytophthora* spp. During the last decade, foliar *Phytophthora* diseases affecting conifer trees have been reported (Durán et al. 2008, Brasier and Webber 2010). *Phytophthora pluvialis* is one of these, causing red needle cast (RNC) in Pinus radiata (radiata pine) and Douglas fir in Oregon and New Zealand (Dick et al. 2014, Hansen et al. 2015). In New Zealand, radiata pine represents 90% of the 1.7 million hectares of the exotic plantation estate, followed by Douglas fir, planted on approximately 110 thousand hectares (New Zealand Forest Owners Association 2014). *Phytophthora pluvialis* infects radiata pine and Douglas fir needles, producing olive-coloured lesions which will eventually result in the rapid senescence and cast of the needles (Dick et al. 2014). Defoliation and decrease in the growth rates are the main impacts of RNC on host plants. However, little is known about the potential interactions of drought on *Phytophthora* infection. Motivated by the complexity of the *Phytophthora* pathosystems, and the economic importance of RNC in New Zealand, the case study outlined here aims to review and identify the gaps of knowledge in the interaction of this disease and the prediction of increased severity and frequency of drought.

Table A1. Potential impacts of increased drought on eight different pathosystems important for productive land use in New Zealand. ↓ = reduced disease, ↑ = increased disease, - = no effect, ? = unknown or cannot be predicted.

Host	Pathogen	Disease	Pathogen survival out of host	Pathogen germination and growth	Pathogen sporulation and dispersion	Host infection	Disease progression/ expression	Host physiology & disease susceptibility	Potential for new or increased pathogenicity	Net impact on disease
Field pea	*Aphanomyces euteiches*	Root rot	-[1]	↓[2]	↓[2]	↓[2]	↑[3]	↑[3]	-[4]	- drought early season ↑ drought late season
Onion	*Sclerotium cepivorum*	White rot	↑[5]	↓[5]	-[6]	↓[6]	↑[7]	↑[6]	-[8]	↓ drought early season ↑ drought late season
Wheat	*Gaeumannomyces graminis* var *tritici*	Take all	-[9]	↓[10]	↓[10]	↓[10,11]	-[10]	↑[10]	-[12]	↓ drought early season - drought late season
Wheat	*Fusarium pseudograminearum/ graminearum*	*Fusarium* crown rot	↑[13]	↑[14]	↑[14]	↑[11]	↑[11, 15]	↑[15]	↑[16]	↑[17]
Brassica	*Leptosphaeria maculans*	Black leg	↑[18]	↓[19]	↓[19]	↓[18]	↑[18]	↑[20]	↑[21]	↓ drought early season ↑ drought late season
Grapevine	*Ilyonectria/Dactylonectria* spp.	Black foot	-[22]	↓[23]	↓[23, 24]	↓[24]	↑[25]	↑[24]	-[26]	↑
Kiwifruit	*Sclerotinia sclerotiorum*	*Sclerotinia* rot	-[27]	↓[28]	↓[28]	↓[29]	↓[30]	↓[31]	-[32]	↓[31]
Radiata pine	*Phytophthora pluvialis*	Red needle cast	-	↓[33]	↓[33]	↓[33]	↓[33]	?	?	↓ during drought -/↑ after drought under conducive conditions

[1]Pfender (1984); [2]Scharen (1960); [3]Kerr (1964); [4]Oyarzun, Gerlagh and Zadoks (1998); [5]Crowe and Hall (1980); [6]Crowe (2008); [7]Entwhistle (1990); [8]Couch and Kohn (2000); [9]Murray, Heenan and Taylor (1991); [10]Cook (2003); [11]Smiley, Collins and Rasmussen (1996); [12]Harvey, Langridge and Marshall (2001); [13]Lakhesar, Backhouse and Kristiansen (2010); [14]Singh, Backhouse and Kristiansen (2009); [15]Liu and Liu (2016); [16]Talas and McDonald (2015); [17]Cook (1980); [18]West et al. (2001); [19]Khangura et al. (2009); [20]Lopisso (2014); [21]Howlett et al. (2015); [22]Agustí-Brisach and Armengol (2013); [23]Agustí-Brisach and Armengol (2012); [24]Wilcox, Gubler and Uyemoto (2015); [25]Pouzoulet et al. (2014); [26]Pathrose et al. (2014); [27]Jones et al. (2016); [28]Clarkson et al. (2004); [29]Hoyte et al. (2011); [30](Goh and Lyons 1992); [31]Wang et al. (2011); [32]Lehner et al. (2016); [33]Dick et al. (2014).

Drought as a predisposing event

The impacts of drought on the host physiology can shape the interaction with the pathogen infection in two ways (Desprez-Loustau et al. 2006): (1) causing multiple stresses by the combination of both drought and pathogenic infection, at a particular time, and (2) modifying host susceptibility to infection and disease development. The first pathway is unlikely to take place in the RNC pathosystem, as *P. pluvialis* has seldom been recorded in the needles from field samples taken during summer (Dick et al. 2014). Summer drought would correspond to the survival phase of *P. pluvialis*, inoculum of which is speculated to occur in forest soils. Oospores survive in the soil during summer, then germinate as soon as wet favourable conditions occur. However, under experimental conditions, *P. pluvialis* is capable of infecting radiata pine roots causing fine root loss and reductions in the number of fine root tips (P. Scott, unpublished data). The possibility of this sub-lethal infection taking place in field conditions, either between or during seasonal foliar outbreaks, should be tested. In this case, a multiple stress scenario could take place.

The RNC pathosystem would follow the second interaction pathway, with drought more likely to occur in summer, and with the seasonal onset of RNC developing during late autumn and winter. Thus, drought would more likely act as a predisposing event in radiata pine trees, shifting the outcome toward resistance or susceptibility to pathogens (Bostock et al. 2014). Specific responses to drought are determined by the degree to which the tree water status is hydraulically regulated. This strategy, together with the drought intensity, will define the processes leading to greater susceptibility to disease or even to host death. Under drought conditions, radiata pine can experience reductions in carbon uptake associated to closure of stomata (De Diego et al. 2012, Mitchell et al. 2013). While carbon demand for dark respiration remains insensitive to the drought conditions (Atkin and Macherel 2009), except for extended drought events and preceding host death (Mitchell et al. 2013), radiata pine trees compensate for the reduced carbon supply with decreasing growth rates (Mitchell et al. 2013, 2014). Further, with intense and/or prolonged drought episodes the trees react with reduction of leaf area (Thabeet et al. 2009, Galiano et al. 2011). Therefore, after a drought episode, radiata pine trees would have less leaf area as substrate for *P. pluvialis* infection, and less carbon in their needles. As biotrophic foliar pathogens derive carbon from host cells, they are favoured by the development of new foliage and by carbon rich tissues (Oliva et al. 2014). The reduced carbohydrate concentration in the needles could make them less supportive of *P. pluvialis* during its biotrophic phase.

The impacts of drought on the carbohydrate utilization in plants is very dependent on the intensity and duration of particular drought events (Duan et al. 2015). Radiata pine plants have been shown to substantially deplete non-structural carbohydrates after prolonged and gradual water deficit (Mitchell et al. 2013). In contrast, drastic and rapid soil dehydration did not result in carbohydrate depletion even at seedling death, due to the lack of mobilization of stored carbohydrates between organs (Duan et al. 2015).

Therefore, the susceptibility of radiata pine needles for *P. pluvialis* infection after a drought episode will depend on the intensity and duration of the drought they have experienced. Gradual

drought may lead to carbon shortage in needles reducing the carbon available for defence but making needles less susceptible to *P. pluvialis* infection, while severe drought can result in carbohydrate presence in tissues, making them suitable for infection, but a weakened or impaired conductive system that can lead to a decline spiral (Manion 1991). Thus, there is a trade-off similar to that for the opposing hypotheses of Plant Vigour (Price 1991) and Plant Stress (White 1969), developed to describe the effects of drought stress on insect herbivores. The way drought can modulate the minimum carbon available for effective host defence, and the minimum carbon present in the needles to allow infection, is yet to be outlined for the RNC pathosystem.

Increased e[CO_2] is anticipated to enhance water use efficiency during photosynthesis (Kirschbaum 2004, Tubiello et al. 2007), which may enable carbohydrate production and concentrations to be maintained under increased moisture stress, but only if other resources do not become limiting. In forest tree species, in the absence of drought, the increase in photosynthetic rate derived from e[CO_2] has not resulted in growth stimulation (Bader et al. 2010, Fatichi and Leuzinger 2013), with foliar NSC concentrations being reported to either increase or remain unaffected by e[CO_2] (Bader et al. 2010, Mašková et al. 2017). In drought-stressed pine seedlings, starch concentrations have been shown not to react to e[CO_2] conditions. Moreover, the increase in soluble sugars under drought and e[CO_2] conditions has been found to be temporary, disappearing after a second consecutive drought episode (Bachofen et al. 2017). Thus, it remains unclear whether e[CO_2] conditions, under drought conditions, would contribute significantly to an increased fitness of *P. pluvialis* infection of carbon-richer needles, as exposed above.

Impacts of drought on P. pluvialis

As for most fungal and oomycete pathogens, *P. pluvialis* requires high humidity conditions for zoospore dispersal, sporangium and oospore germination, and host penetration/infection. If drought conditions begin in spring, a reduced amount of long-term survival structures could be produced on already-infected needles. Nevertheless, the amount of long-term survival structures already present in the soil will remain unaffected by drought and, given the adequate conditions, these will germinate to start new infection cycles in the forest canopy. Drought episodes would delay the resulting RNC outbreaks to later in the season (late winter), once the soil recover enough water to allow *P. pluvialis* to build inoculum for successful infection. Thus, a drought episode followed by periods of extended rainfall would be the worst scenario for radiata pine productivity and survival, as the trees would have debilitated conductive systems and decreased carbon reserves for defence, but *P. pluvialis* would have favourable conditions for infection.

Temporal effects on interactions between drought and P. pluvialis infection

Depending on the environmental conditions after drought and the resilience of host trees, drought-stressed trees could experience leaf regrowth (recovery), leaf necrosis, or leaf loss (decline), which will determine pathogen infection (Whyte et al. 2016). Trees will enter a decline recovery fluctuation, where the frequency, magnitude and order of the stressors will tip the balance towards

either recovery or decline (Whyte et al. 2016). For example, a severe *P. pluvialis* infection followed by a drought episode is more likely to make the host enter a decline than the drought occurring first. While single defoliation events rarely cause mortality, repeated defoliation episodes in stressed trees can trigger decline processes, where trees cannot restore their crowns, show drastically reduced growth and may ultimately die (Dietze and Matthes 2014, Oliva et al. 2016).

As the final desired product from forest trees is wood, it is important to quantify the decrease in radiata pine growth caused by the interactions of drought and *P. pluvialis*, and the threshold of the combination of both stressors at which tree survival is compromised. This has not been simple, as the combined impact of both stressors is not likely to be the sum of the parts (Mitchell et al. 2013). Therefore, there is urgent need to study the impacts of the combination of different levels of drought and different levels of RNC severity to understand the thresholds at which radiata pine plantations would still accomplish their economic and ecological roles.

Irrigation

One of the most obvious mechanisms to mitigate against the effects of drought is via irrigation. In New Zealand, the area under irrigation has expanded to 720,000 Ha (~6% of productive land; Irrigation New Zealand, 2015). The majority of this is used to support livestock grazing (e.g. dairy), with only 10% being used for production of vegetable, fruits, wine grapes etc. In summer dry regions, such as Canterbury, rapid expansion of irrigation now means that many agroecosystems do not experience significant or prolonged moisture stress. This significantly changes the ecology of plant pathosystems, particularly those associated with forage plants (pastures) and their diseases. Although complex mixtures of pathogen occur in pasture soils (Skipp and Watson 1996), until recently control of these was not economically viable. However, with increased value of production, the economic costs of lost-production due to soil-borne disease can exceed NZ$1500 ha^{-1} y^{-1} (Wakelin et al. 2016). While these maybe attributable to a range of pathogens, significant correlations between productive loss and oomycete pathogens have been determined (Wakelin et al. 2016). These include multi-host range taxa that benefit from high soil moisture content, such as *Pythium irregulare* (Singleton et al. 1992). For pastoral agriculture, it seems an inadvertent outcome of the expansion of irrigation is increased root disease and associated productive and economic costs.

Irrigation may, however, be a useful tool to reduce disease in some pathosystems. For example, the inoculum of the take-all fungus, Ggt, over-summers in infested plant material. The decomposition of these, by soil saprophytic activity, can lead to reduction in pathogen potential for the subsequent crop (Garrett 1938). The application of soil moisture during the summer-fallow phase may provide a useful mechanism to decrease disease potential. Similarly, disease caused by powdery mildews maybe reduced by overhead misting of water onto plant leaves (Yarwood 1978). The maintenance of a film of water on the leaf surface is disruptive to conidium germination and therefore reduces host infection.

Unlike the other productive plant-based sectors, plantation forestry in New Zealand is not (yet) irrigated. As such, the moisture impacts on the pathosystems present are directly dependent on

rainfall, properties of the soil related to moisture retention, evapotranspiration, and plant (weed) competition. Changes in rainfall patterns occurring climate disruption will translate effects on disease via moisture-related interactions. With increased disease pressure under climate change, other methods disease control must be sought to protect the forestry sector.

Conclusions

Increased drought in New Zealand is very likely to increase the severity of a wide range of diseases affecting the plant-based productive sectors. Given the importance of these to New Zealand's gross domestic product, empirical assessment of drought effects for major diseases should be undertaken. In addition to predicting potential economic losses, the key points where drought influences disease outcomes need to be assessed. These can be used as starting points for the development of strategies for disease prevention and control. We also note that drought does not occur as a single abiotic stress, but usually coincides with elevated temperatures and CO_2. As such, the wider effects of climate change may exacerbate the impacts of drought on the expression of many diseases, making the findings of the present investigation conservative.

References

Abdul Latif NS, Wake GC, Reglinski T, Elmer PAG (2014) Modelling induced resistance to plant diseases. Journal of Theoretical Biology 347:144–150.

Abdullah AS, Moffat CS, Lopez-Ruiz FJ, Gibberd MR, Hamblin J, Zerihun A (2017) Host–Multi-Pathogen Warfare: Pathogen Interactions in Co-infected Plants. Frontiers in Plant Science 8:1–12.

Adams HD, Zeppel MJB, Anderegg WRL, Hartmann H, Landhäusser SM, Tissue DT, Huxman TE, Hudson PJ, Franz TE, Allen CD, Anderegg LDL, Barron-Gafford GA, Beerling DJ, Breshears DD, Brodribb TJ, Bugmann H, Cobb RC, Collins AD, Dickman LT, Duan H, Ewers BE, Galiano L, Galvez DA, Garcia-Forner N, Gaylord ML, Germino MJ, Gessler A, Hacke UG, Hakamada R, Hector A, Jenkins MW, Kane JM, Kolb TE, Law DJ, Lewis JD, Limousin JM, Love DM, Macalady AK, Martínez-Vilalta J, Mencuccini M, Mitchell PJ, Muss JD, O'Brien MJ, O'Grady AP, Pangle RE, Pinkard EA, Piper FI, Plaut JA, Pockman WT, Quirk J, Reinhardt K, Ripullone F, Ryan MG, Sala A, Sevanto S, Sperry JS, Vargas R, Vennetier M, Way DA, Xu C, Yepez EA, McDowell NG (2017) A multi-species synthesis of physiological mechanisms in drought-induced tree mortality. Nature Ecology and Evolution 1:1285–1291.

Agrios GN (2005) Plant pathology, 5th Editio. Academic Press, New York.

Aguade D, Poyatos R, Gomez M, Oliva J, Martinez-Vilalta J (2015) The role of defoliation and root rot pathogen infection in driving the mode of drought-related physiological decline in Scots pine (*Pinus sylvestris* L.). Tree Physiology 35:229–42.

Agustí-Brisach C, Armengol J (2012) Effects of temperature, pH and water potential on mycelial growth, sporulation and chlamydospore production in culture of Cylindrocarpon spp. Associated with black foot of grapevines. Phytopathologia Mediterranea 51:37–50.

Agustí-Brisach C, Armengol J (2013) Black-foot disease of grapevine: An update on taxonomy, epidemiology and management strategies. Phytopathologia Mediterranea 52:245–261.

Al-Naimi FA, Garrett KA, Bockus WW (2005) Competition, facilitation, and niche differentiation in two foliar pathogens. Oecologia 143:449–457.

Alderfer RG, Eagles CF (1976) The effect of partial defoliation on the growth and photosynthetic efficiency of bean leaves. Botanical Gazette 137:351–355.

Alizon S, van Baalen M (2008) Multiple Infections, Immune Dynamics, and the Evolution of Virulence. The American Naturalist 172:150–168.

Alizon S, Hurford A, Mideo N, Van Baalen M (2009) Virulence evolution and the trade-off hypothesis: History, current state of affairs and the future. Journal of Evolutionary Biology 22:245–259.

Allen CD, Breshears DD, McDowell NG (2015) On underestimation of global vulnerability to tree mortality and forest die-off from hotter drought in the Anthropocene. Ecosphe 6:art129.

Allen RN, Newhook FJ (1973) Chemotaxis of zoospores of *Phytophthora cinnamomi* to ethanol in capillaries of soil pore dimensions. Transactions of the British Mycological Society 61:287-IN12.

Anagnostakis SL (1987) Chestnut blight: the classical problem of an introduced pathogen. Mycologia 79:23–37.

Anderegg WRL, Hicke JA, Fisher RA, Allen CD, Aukema J, Bentz B, Hood S, Lichstein JW, Macalady AK, McDowell N, Pan Y, Raffa K, Sala A, Shaw JD, Stephenson NL, Tague C, Zeppel M (2015) Tree mortality from drought, insects, and their interactions in a changing climate. New Phytologist 208:674–83.

Anderson PK, Cunningham AA, Patel NG, Morales FJ, Epstein PR, Daszak P (2004) Emerging infectious diseases of plants: pathogen pollution, climate change and agrotechnology drivers. Trends in ecology & evolution 19:535–44.

Arango-Velez A, El Kayal W, Copeland CCJ, Zaharia LI, Lusebrink I, Cooke JEK (2016) Differences in defence responses of *Pinus contorta* and *Pinus banksiana* to the mountain pine beetle fungal associate *Grosmannia clavigera* are affected by water deficit. Plant, Cell and Environment 39:726–744.

Atkin OK, Macherel D (2009) The crucial role of plant mitochondria in orchestrating drought tolerance. Annals of Botany 103:581–597.

Australian Bureau of Agricultural and Resource Economics and Sciences (2018) Australian Forest and Wood Products Statistics: September and December quarters 2017.

van Baalen M, Sabelis MW (1995) The Dynamics of Multiple Infection and the Evolution of Virulence. The American Naturalist 146:881–910.

Bachofen C, Moser B, Hoch G, Ghazoul J, Wohlgemuth T (2017) No carbon 'bet hedging' in pine seedlings under prolonged summer drought and elevated CO2. Journal of Ecology:1–16.

Back MA, Haydock PPJ, Jenkinson P (2002) Disease complexes involving plant parasitic nematodes and soilborne pathogens. Plant Pathology 51:683–697.

Bader MKF, Siegwolf R, Körner C (2010) Sustained enhancement of photosynthesis in mature deciduous forest trees after 8 years of free air CO_2 enrichment. Planta 232:1115–1125.

Barbier S, Gosselin F, Balandier P (2008) Influence of tree species on understory vegetation diversity and mechanisms involved-A critical review for temperate and boreal forests. Forest Ecology and Management

Barnes RL, Edwards NT (1980) Seasonal changes in energy allocation by white oak (*Quercus alba*). Canadian Journal of Forest Research 10:379–388.

Barry KM, Pinkard EA (2013) Growth and photosynthetic responses following defoliation and bud removal in eucalypts. Forest Ecology and Management 293:9–16.

Barton LL, Northup DE (2011) Microbial Ecology, John-Wiley. New Jersey, USA.

Battaglia M, Pinkard EA, Sands PJ, Bruce JL, Quentin A (2011) Modelling the impact of defoliation

and leaf damage on forest plantation function and production. Ecological Modelling 222:3193–3202.

Beets P, McKinley R, Oliver G, Pearce S, Bulman L (2013) Impact of Red Needle Cast defoliation of radiata pine stand on growth at Wharerata Forest.

Belda M, Holtanová E, Halenka T, Kalvová J (2014) Climate classification revisited: From Köppen to Trewartha. Climate Research 59:1–13.

Bennett RN, Wallsgrove RM (1994) Secondary metabolites in plant defence mechanisms. New Phytologist 127:617–633.

Borzak CL, Potts BM, Barry KM, Pinkard EA, O'Reilly-Wapstra JM (2017) Genetic stability of physiological responses to defoliation in a eucalypt and altered chemical defence in regrowth foliage. Tree Physiology 37:220–235.

Bostock RM, Pye MF, Roubtsova T V (2014) Predisposition in plant disease: exploiting the nexus in abiotic and biotic stress perception and response. Annual review of phytopathology 52:517–49.

Boyce JS (1940) A needle cast of Douglas-fir associated with *Adelopus gaeumannii*. Phytopathology 30:649–659.

Brar S, Tabima JF, McDougal RL, Dupont PY, Feau N, Hamelin RC, Panda P, LeBoldus JM, Grünwald NJ, Hansen EM, Bradshaw RE, Williams NM (2018) Genetic diversity of *Phytophthora pluvialis*, a pathogen of conifers, in New Zealand and the west coast of the United States of America. Plant Pathology 67:1131–1139.

Brasier CM, Beales PA, Kirk SA, Denman S, Rose J (2005) *Phytophthora kernoviae* sp. nov., an invasive pathogen causing bleeding stem lesions on forest trees and foliar necrosis of ornamentals in the UK. Mycological Research 109:853–859.

Brasier CM, Robredo F, Ferraz JFP (1993) Evidence for *Phytophthora cinnamomi* involvement in Iberian oak decline. Plant Pathology 42:140–145.

Brasier C, Webber J (2010) Plant pathology: Sudden larch death. Nature 466:824–825.

Bréda N, Huc R, Granier A, Dreyer E (2006) Temperate forest trees and stands under severe drought: a review of ecophysiological responses, adaptation processes and long-term consequences. Annals of Forest Science 63:625–644.

Brencic A, Winans SC (2005) Detection of and Response to Signals Involved in Host-Microbe Interactions by Plant-Associated Bacteria. Microbiology and Molecular Biology Reviews 69:155–194.

Bresinsky A, Körner C, Kadereit J, Neuhaus G, Sonnewald U (2013) Strasburger's Plant science. Springer-Verlag Berlin Heidelberg.

Bulman LS (1993) Cyclaneusma needle cast and Dothistroma needle blight in NZ pine plantations. New Zealand Forestry 38:21–24.

Bulman LS, Dick MA, Ganley RJ, McDougal RL, Schwelm A, Bradshaw RE (2013) Chapter 22:

Dothistroma needle blight. In: Infectious Forest Diseases.pp 436–457.

Bustin SA, Benes V, Garson JA, Hellemans J, Huggett J, Kubista M, Mueller R, Tania N, Pfaffl MW, Shipley GL, Vandesompele J, Wittwer CT (2009) The MIQE Guidelines: Minimum Information for Publication of Quantitative Real-Time PCR Experiments. Clinical Chemistry 55:1–12.

Cailleret M, Jansen S, Robert EMR, Desoto L, Aakala T, Antos JA, Beikircher B, Bigler C, Bugmann H, Caccianiga M, Čada V, Camarero JJ, Cherubini P, Cochard H, Coyea MR, Čufar K, Das AJ, Davi H, Delzon S, Dorman M, Gea-Izquierdo G, Gillner S, Haavik LJ, Hartmann H, Hereş AM, Hultine KR, Janda P, Kane JM, Kharuk VI, Kitzberger T, Klein T, Kramer K, Lens F, Levanic T, Linares Calderon JC, Lloret F, Lobo-Do-Vale R, Lombardi F, López Rodríguez R, Mäkinen H, Mayr S, Mészáros I, Metsaranta JM, Minunno F, Oberhuber W, Papadopoulos A, Peltoniemi M, Petritan AM, Rohner B, Sangüesa-Barreda G, Sarris D, Smith JM, Stan AB, Sterck F, Stojanović DB, Suarez ML, Svoboda M, Tognetti R, Torres-Ruiz JM, Trotsiuk V, Villalba R, Vodde F, Westwood AR, Wyckoff PH, Zafirov N, Martínez-Vilalta J (2017) A synthesis of radial growth patterns preceding tree mortality. Global Change Biology 23:1675–1690.

Cairns AJG (1990) Epidemics in heterogeneous populations: II. Nonexponential incubation periods and variable infectiousness. IMA Journal of Mathematics Applied in Medicine & Biology 1990:219–230.

Cara M, Yaseen T, Merkuri J (2018) First Report of Phytophthora Blight of Cucurbit Caused by *Phytophthora capsici* in Albania. Plant Disease 102:253.

Carnicer J, Coll M, Ninyerola M, Pons X, Sánchez G, Peñuelas J (2011) Widespread crown condition decline, food web disruption, and amplified tree mortality with increased climate change-type drought. Proceedings of the National Academy of Sciences of the United States of America 108:1474–8.

Castaño C, Colinas C, Gómez M, Oliva J (2014) Outbreak of Swiss needle cast caused by the fungus *Phaeocryptopus gaeumannii* on Douglas-fir in Spain. New Disease Reports 29:19.

Cerasoli S, Scartazza A, Brugnoli E, Chaves MM, Pereira JS (2004) Effects of partial defoliation on carbon and nitrogen partitioning and photosynthetic carbon uptake by two-year-old cork oak (*Quercus suber*) saplings. Tree physiology 24:83–90.

Chakraborty S, Tiedemann A V., Teng PS (2000) Climate change: potential impact on plant diseases. Environmental Pollution 108:317–326.

Chen Z, Wang L, Dai Y, Wan X, Liu S (2017) Phenology-dependent variation in the non-structural carbohydrates of broadleaf evergreen species plays an important role in determining tolerance to defoliation (or herbivory). Scientific Reports 7:1–11.

Chettri P, Calvo AM, Cary JW, Dhingra S, Guo Y, McDougal RL, Bradshaw RE (2012) The veA gene of the pine needle pathogen *Dothistroma septosporum* regulates sporulation and secondary metabolism. Fungal Genetics and Biology 49:141–151.

Clarkson JP, Phelps K, Whipps JM, Young CS, Smith JA, Watling M (2004) Forecasting *Sclerotinia* disease on lettuce: toward developing a prediction model for carpogenic germination of sclerotia. Phytopathology 94:268–279.

Cook RJ (1980) Fusarium root rot of wheat and its control in the Pacific Northwest. Plant Disease 64:1061–1066.

Cook RJ (2003) Take-all of wheat. Plant Pathology 62:73–86.

Cooper RM, Williams JS (2004) Elemental sulphur as an induced antifungal substance in plant defence. Journal of Experimental Botany 55:1947–1953.

Corcuera L, Gil-Pelegrin E, Notivol E (2012) Aridity promotes differences in proline and phytohormone levels in *Pinus pinaster* populations from contrasting environments. Trees - Structure and Function 26:799–808.

Couch BC, Kohn LM (2000) Clonal spread of *Sclerotium cepivorum* in onion production with evidence of past recombination events. Phytopathology 90:514–521.

Cranswick AM, Rook DA, Zabkiewicz JA (1987) Seasonal changes in carbohydrate concentration and composition of different tissue types of *Pinus radiata* trees. New Zealand Journal of Forestry Science 17:229–245.

Crowe FJ (2008) White Rot. In: Schwartz J.F. (ed) Compendium of Onion and Garlic Diseases and Pests. APS Press, St. Paul, MN.p pp 22-26.

Crowe FJ, Hall DH (1980) Soil temperature and moisture effects on sclerotium germination and infection of onion seedlings by *Sclerotium cepivorum*. Phytopathology 70:74–78.

Cruz De Carvalho MH (2008) Drought stress and reactive oxygen species: Production, scavenging and signaling. Plant Signaling and Behavior 3:156–165.

Cunniffe NJ, Stutt ROJH, van den Bosch F, Gilligan CA (2012) Time-Dependent Infectivity and Flexible Latent and Infectious Periods in Compartmental Models of Plant Disease. Phytopathology 102:365–380.

Davila Olivas NH, Coolen S, Huang P, Severing E, van Verk MC, Hickman R, Wittenberg AHJ, de Vos M, Prins M, van Loon JJA, Aarts MGM, van Wees SCM, Pieterse CMJ, Dicke M (2016) Effect of prior drought and pathogen stress on *Arabidopsis* transcriptome changes to caterpillar herbivory. New Phytologist 210:1344–1356.

Day WR (1938) Root-rot of Sweet chestnut and beech caused by species of *Phytophthora*: I. Cause and symptoms of disease: its relation to soil conditions. Forestry 12:101–116.

Deslauriers A, Caron L, Rossi S (2015) Carbon allocation during defoliation: testing a defense-growth trade-off in balsam fir. Frontiers in Plant Science 6:1–13.

Desprez-Loustau M-L, Marçais B, Nageleixen L-M, Piou D, Vannini A (2006) Interactive effects of drought and pathogens in forest trees. Annuals of Forest Sciences 63:597–612.

Desprez-Loustau ML, Massot M, Toïgo M, Fort T, Aday Kaya AG, Boberg J, Braun U, Capdevielle X, Cech T, Chandelier A, Christova P, Corcobado T, Dogmus T, Dutech C, Fabreguettes O,

Faivre d'Arcier J, Gross A, Horta Jung M, Iturritxa E, Jung T, Junker C, Kiss L, Kostov K, Lehtijarvi A, Lyubenova A, Marçais B, Oliva J, Oskay F, Pastirčák M, Pastirčáková K, Piou D, Saint-Jean G, Sallafranque A, Slavov S, Stenlid J, Talgø V, Takamatsu S, Tack AJ (2018) From leaf to continent: The multi-scale distribution of an invasive cryptic pathogen complex on oak. Fungal Ecology 36:39–50.

Dick MA, Williams NM, Bader MK-F, Gardner JF, Bulman LS (2014) Pathogenicity of *Phytophthora pluvialis* to *Pinus radiata* and its relation with red needle cast disease in New Zealand. New Zealand Journal of Forestry Science 44:6.

Dickie IA, Bufford JL, Cobb RC, Desprez-Loustau ML, Grelet G, Hulme PE, Klironomos J, Makiola A, Nuñez MA, Pringle A, Thrall PH, Tourtellot SG, Waller L, Williams NM (2017) The emerging science of linked plant-fungal invasions. New Phytologist 215:1314–1332.

De Diego N, Pérez-Alfocea F, Cantero E, Lacuesta M, Moncaleán P (2012) Physiological response to drought in radiata pine: Phytohormone implication at leaf level. Tree Physiology 32:435–449.

De Diego N, Saiz-Fernandez I, Rodriguez JL, Perez-Alfocea P, Sampedro MC, Barrio RJ, Lacuesta M, Moncalean P (2015) Metabolites and hormones are involved in the intraspecific variability of drought hardening in radiata pine. Journal of Plant Physiology 188:64–71.

Dietze MC, Matthes JH (2014) A general ecophysiological framework for modelling the impact of pests and pathogens on forest ecosystems. Ecology Letters 17:1418–1426.

Dignam BEA, O'Callaghan M, Condron LM, Raaijmakers JM, Kowalchuk GA, Wakelin SA (2016) Challenges and opportunities in harnessing soil disease suppressiveness for sustainable pasture production. Soil Biology and Biochemistry 95:100–111.

Dobbertin M, Brang P (2001) Crown defoliation improves tree mortality models. Forest Ecology and Management 141:271–284.

Dodd RS, Hüberli D, Douhovnikoff V, Harnik TY, Afzal- Z, Garbelotto M, Afral-rafii Z, Harnikl Y, Dodd S, Hiiberli D (2012) Is variation in susceptibility to *Phytophthora ramorum* correlated with population genetic structure in coast live oak (*Quercus agrifolia*)? New Phytologist 165:203–214.

Dordas C (2008) Role of nutrients in controlling plant diseases in sustainable agriculture. A review. Agron Sustain 28:33–46.

Duan H, O'Grady AP, Duursma RA, Choat B, Huang G, Smith RA, Jiang Y, Tissue DT (2015) Drought responses of two gymnosperm species with contrasting stomatal regulation strategies under elevated [CO_2] and temperature. Tree Physiology 35:756–770.

Dubuis PH, Marazzi C, Städler E, Mauch F (2005) Sulphur deficiency causes a reduction in antimicrobial potential and leads to increased disease susceptibility of oilseed rape. Journal of Phytopathology 153:27–36.

Duggar BM (1909) Fungous diseases of plants. Ginn and Co., New York.

Dungey HS, Williams NM, Low CB, Stovold GT (2014) First evidence of genetic-based tolerance

to red needle cast caused by *Phytophthora pluvialis* in radiata pine. New Zealand Journal of Forestry Science 44:31.

Durán A, Gryzenhout M, Slippers B, Ahumada R, Rotella A, Flores F, Wingfield BD, Wingfield MJ (2008) *Phytophthora pinifolia* sp. nov. associated with a serious needle disease of *Pinus radiata* in Chile. Plant Pathology 57:715–727.

Durner J, Shah J, Klessig DF (1997) Salicylic acid and disease resistance in plants. Trends in Plant Science 2:266–274.

Edreva A, Velikova V, Tsonev T, Dagnon S, Gürel A, Aktaş L, Gesheva E (2008) Stress-protective role of secondary metabolites: diversity of functions and mechanisms. General and Applied Plant Physiology 34:67–78.

Eilers PHC, Peeters JCH (1988) A model for the relationship between light intensity and the rate of photosynthesis in phytoplankton. Ecological Modelling 42:199–215.

Ennos RA (2015) Resilience of forests to pathogens: An evolutionary ecology perspective. Forestry 88:41–52.

Entwhistle AR (1990) Allium white rot and its control. Soil use and management 6:201–209.

Erwin DC, Ribeiro OK (1996) *Phytophthora* diseases worldwide. American Phytopathological Society (APS Press), St. Paul, Minnesota (US).

Eyles A, Pinkard EA, O'Grady AP, Worledge D, Warren CR (2009) Role of corticular photosynthesis following defoliation in Eucalyptus globulus. Plant, Cell and Environment 32:1004–1014.

Eyles A, Robinson AP, Smith D, Carnegie A, Smith I, Stone C, Mohammed C (2011) Quantifying stem growth loss at the tree-level in a *Pinus radiata* plantation to repeated attack by the aphid, *Essigella californica*. Forest Ecology and Management 261:120–127.

Eyles A, Smith D, Pinkard EA, Smith I, Corkrey R, Elms S, Beadle C, Mohammed C (2011) Photosynthetic responses of field-grown *Pinus radiata* trees to artificial and aphid-induced defoliation. Tree Physiology 31:592–603.

FAO (2015) Global forest resources assessment 2015: How are the world's forests changing? Rome.

Fatichi S, Leuzinger S (2013) Reconciling observations with modeling: The fate of water and carbon allocation in a mature deciduous forest exposed to elevated CO_2. Agricultural and Forest Meteorology 174–175:144–157.

Fawke S, Doumane M, Schornack S (2015) Oomycete Interactions with Plants: Infection Strategies and Resistance Principles. Microbiology and Molecular Biology Reviews 79:263–280.

Fisher MC, Henk D a., Briggs CJ, Brownstein JS, Madoff LC, McCraw SL, Gurr SJ (2012) Emerging fungal threats to animal, plant and ecosystem health. Nature 484:186–194.

Fitt BDL, Huang Y-J, van den Bosch F, West JS (2006) Coexistence of related pathogen species

on arable crops in space and time. Annual Review of Phytopathology 44:63–82.

Flor HH (1971) Current status of the gene-for-gene concept. Annual Review of Phytopathology 9:275–296.

Flors V, Ton J, Mauch-Mani B (2009) Role of Abscisic Acid in Disease Resistance. In: Signal cross talk in plant stress responses. Wiley-Blackwell, Oxford, UK

Foreman-Mackey D, Hogg DW, Lang D, Goodman J (2013) emcee: the MCMC hammer. Publications of the Astronomical Society of the Pacific 125:306.

Forest Owners Association New Zealand (2016) Facts and Figures 2016/17. Wellington, New Zealand.

Francl LJ (2001) The Disease Triangle: A plant pathological paradigm revisited. The Plant Health Instructor:doi: 10.1094/PHI-T-2001-0517-01.

Galiano L, Martínez-Vilalta J, Lloret F (2011) Carbon reserves and canopy defoliation determine the recovery of Scots pine 4yr after a drought episode. New Phytologist 190:750–759.

Ganley RJ, Williams NM, Rolando CA, Hood IA, Dungey HS, Beets PN, Bulman LS (2014) Management of red needle cast, caused by *Phytophthora pluvialis*, a new disease of radiata pine in New Zealand. New Zealand Plant Protection 67:48–53.

Gargallo-Garriga A, Sardans J, Pérez-Trujillo M, Rivas-Ubach A, Oravec M, Vecerova K, Urban O, Jentsch A, Kreyling J, Beierkuhnlein C, Parella T, Peñuelas J (2014) Opposite metabolic responses of shoots and roots to drought. Scientific Reports 4:1–7.

Garrett SD (1938) Soil conditions and the take-all disease of wheat. III Decomposition of the resting mycelium of *Ophiobolus graminis* in infected wheat stubble buried in soil. Annals of Applied Biology 25:742–767.

Garrett KA, Dendy SP, Frank EE, Rouse MN, Travers SE (2006) Climate Change Effects on Plant Disease: Genomes to Ecosystems. Annual Review of Phytopathology 44:489–509.

Gaylord ML, Kolb TE, Pockman WT, Plaut JA, Yepez EA, Macalady AK, Pangle RE, Mcdowell NG (2013) Drought predisposes piñon-juniper woodlands to insect attacks and mortality. New Phytologist 198:567–578.

Gerland P, Raftery AE, Ševcíková H, Li H, Gu D, Spoorenberg T, Alkema L, Fosdick BK, Chunn J, Lalic N, Bay G, Buettner T, Heilig GK, Wilmoth J (2014) World Population Stabilization Unlikely This Century. Science 346:234–237.

Gilligan CA, Kleczkowski A (1997) Population dynamics of botanical epidemics involving primary and secondary infection. Philosophical Transactions of the Royal Society B: Biological Sciences 352:591–608.

Glenn-Lewin DC (1977) Species diversity in North American temperate forests. Vegetatio 33:153–162.

Goh HH, Lyons SN (1992) Sclerotinia infection in two kiwifruit orchards in the Bay of Plenty. In: Proceedings of the 45th New Zealand Plant Protection Conference.p pp 180-183.

Goheen EM, Willhite EA (2006) Field guide to the common diseases and insect pests of Oregon and Washington conifers. USDA Forest Service, Pacific Northwest Region, Portland, US.

Goldson SL, Bourdôt GW, Brockerhoff EG, Byrom AE, Clout MN, McGlone MS, Nelson WA, Popay AJ, Suckling DM, Templeton MD (2015) New Zealand pest management: current and future challenges. Journal of the Royal Society of New Zealand 45:31–58.

Gomez-Gallego M, Bader MK-F, Scott PM, Leuzinger S, Williams NM (2017) *Phytophthora pluvialis* Studies on Douglas-fir Require Swiss Needle Cast Suppression. Plant Disease 101:1259–1262.

Goodman J, Weare J (2010) Ensemble samplers with affine invariance. Communications in applied mathematics and computational science 5:65–80.

Graham NJ, Suontama M, Pleasants T, Li Y, Bader MKF, Klápště J, Dungey HS, Williams NM (2018) Assessing the genetic variation of tolerance to red needle cast in a Pinus radiata breeding population. Tree Genetics and Genomes 14:55.

Grover M, Ali SZ, Sandhya V, Rasul A, Venkateswarlu B (2011) Role of microorganisms in adaptation of agriculture crops to abiotic stresses. World Journal of Microbiology & Biotechnology 27:1231–1240.

Haas SE, Hooten MB, Rizzo DM, Meentemeyer RK (2011) Forest species diversity reduces disease risk in a generalist plant pathogen invasion. Ecology Letters 14:1108–1116.

Häder D-P (1999) Gravitaxis in unicellular microorganisms. Advances in Space Research 24:843–850.

Hansen EM (2008) Alien forest pathogens: *Phytophthora* species are changing world forests. Boreal Env Res 13:33–41.

Hansen EM (2015) *Phytophthora* Species Emerging as Pathogens of Forest Trees. Curr Forestry Rep 1:16–24.

Hansen EM, Reeser PW, Davidson JM, Garbelotto M, Ivors K, Douhan L, Rizzo DM (2003) *Phytophthora nemorosa*, a new species causing cankers and leaf blight of forest trees in California and Oregon, USA. Mycotaxon 88:129–138.

Hansen EM, Reeser PW, Sutton W (2017) Ecology and pathology of *Phytophthora* ITS clade 3 species in forests in western Oregon, USA. Mycologia 109:100–114.

Hansen E, Reeser P, Sutton W, Gardner J, Williams N (2015) First report of *Phytophthora pluvialis* causing needle loss and shoot dieback on Douglas-fir in Oregon USA and New Zealand. Plant Disease 99:727.

Hansen EM, Stone JK, Capitano BR, Rosso P, Sutton W, Winton L, Kanaskie A, McWilliams MG (2000) Incidence and Impact of Swiss Needle Cast in Forest Plantations of Douglas-fir in Coastal Oregon. Plant Disease 84:773–778.

Harris AR, Mullett MS, Webber JF (2018) Changes in the population structure and sporulation behaviour of *Phytophthora ramorum* associated with the epidemic on *Larix* (larch) in Britain.

Biological Invasions 20:2313–2328.

Harris AR, Webber JF (2016) Sporulation potential, symptom expression and detection of *Phytophthora ramorum* on larch needles and other foliar hosts. Plant Pathology 65:1441–1451.

Harvey PR, Langridge P, Marshall DR (2001) Genetic drift and host-mediated selection cause genetic differentiation among *Gaeumannomyces graminis* populations infecting cereals in southern Australia. Mycological research 105:927–935.

Hayden KJ, Hardy GESJ, Garbelotto M (2013) Oomycete Diseases. In: Gonthier P, Nicolotti G (eds) Infectious Forest Diseases, 1st Editio.pp 519–546.

He M, Dijkstra FA (2014) Drought effect on plant nitrogen and phosphorus: A meta-analysis. New Phytologist 204:924–931.

Hirose T (2012) Leaf-level nitrogen use efficiency: Definition and importance. Oecologia 169:591–597.

Hodgkinson KC (1974) Influence of partial defoliation on photosynthesis, photorespiration and transpiration by lucerne leaves of different ages. Functional Plant Biology 1:561–578.

Hood IA (1982) *Phaeocryptopus gaeumannii* on *Pseudotsuga menziesii* in southern British Columbia. New Zealand Journal of Forestry Science 12:415–424.

Hood IA (1999) Swiss needle cast of Douglas-fir. A review from a New Zealand perspective. New Zealand Forest Research Institute, Rotorua, New Zealand.

Hood IA, Kershaw DJ (1975) Distribution and infection period of *Phaeocryptopus gaeumannii* in New Zealand. New Zealand Journal of Forestry Science 5:201–208.

Hood IA, Sandberg CJ (1979) Changes within tree crowns following thinning of young Douglas-fir infected by *Phaeocryptopus gaeumannii*. New Zealand Journal of Forestry Science 9:177–184.

Hood IA, Sandberg CJ, Barr CW, Holloway WA, Bradbury PM (1990) Changes in needle retention associated with the spread and establishment of *Phaeocryptopus gaeumannii* in planted Douglas fir. European Journal of Forest Pathology 20:418–429.

Hooper PL, Hooper PL, Tytell M, Vígh L (2010) Xenohormesis: Health benefits from an eon of plant stress response evolution. Cell Stress and Chaperones 15:761–770.

Howlett BJ, Lowe RGT, Marcroft SJ, van de Wouw AP (2015) Evolution of virulence in fungal plant pathogens: exploiting fungal genomics to control plant disease. Mycologia 107:441–451.

Hoyte SN, Beresford RM, Long PG (2011) Effects of temperature and relative humidity on the colonisation of kiwifruit (*Actinidia deliciosa*) petals by *Sclerotinia sclerotiorum* ascospores. In: XIth International Sclerotinia Workshop, York, England.

Hsiao TC (1973) Plant response to water stress. Annual Review of Plant Physiology 24:519–570.

Hughes KJD, Tomlinson JA, Griffin RL, Bonnham N, Inman AJ, Lane CR (2006) Development of

a one-step real-time polymerase chain reaction assay for diagnosis of *Phytophthora ramorum*. Phytopathology 96:975-981.

Hurley BP, Slippers B, Sathyapala S, Wingfield MJ (2017) Challenges to planted forest health in developing economies. Biological Invasions 19:3273–3285.

IPCC (1996) Agriculture. In: Watson RT., Zinyowera M.C., Moss, R.H. (eds) Climate Change 1995: Impacts, Adaptation and Mitigation of Climate Change: Contributions of Working Group II to the Second Assessment Report of the Intergovernmental Panel on Climate Change.

IPCC (2013) Climate Change 2013: The Physical Science Basis. Contribution of Working Group I to the Fifth Assessment Report of the Intergovernmental Panel on Climate Change. Cambridge University Press, Cambridge and New York.

Irrigation New Zealand (2015) New Zealand irrigation industry snapshot.

Jacquet JS, Bosc A, O'Grady A, Jactel H (2014) Combined effects of defoliation and water stress on pine growth and non-structural carbohydrates. Tree Physiology 34:367–376.

Jactel H, Petit J, Desprez-Loustau ML, Delzon S, Piou D, Battisti A, Koricheva J (2012) Drought effects on damage by forest insects and pathogens: A meta-analysis. Global Change Biology 18:267–276.

Jandl R, Schüler S, Schindlbacher A, Tomiczek C (2013) Forests, Carbon Pool, and Timber production. In: Lal R., Lorenz K., Hüttl R., Schneider B., von Braun J. Ecosystem Services and Carbon Sequestration in the Biosphere.pp 101–130.

Janzen DH (1970) Herbivores and the Number of Tree Species in Tropical Forests. The American Naturalist 104:501–528.

Jeffers SN, Martin SB (1986) Comparison of two media selective for *Phytophthora* and *Pythium* species. Plant Disease 70:1038–1043.

Jetton RM, Robison DJ (2014) Effects of Artificial Defoliation on Growth and Biomass Accumulation in Short-Rotation Sweetgum (*Liquidambar styraciflua*) in North Carolina. Journal of Insect Science 14:1–14.

Jones EE, Bienkowski D, Stewart A (2016) Effect of water potential on growth, germination and parasitism of *Sclerotinia sclerotiorum* by *Trichoderma* species. Annals of Applied Biology 168:41–51.

Jonkers W, Estrada AER, Lee K, Breakspear A, May G, Kistler HC (2012) Metabolome and transcriptome of the interaction between *Ustilago maydis* and *Fusarium verticillioides* in vitro. Applied and Environmental Microbiology 78:3656–3667.

Jung HW, Tschaplinski TJ, Wang, Lin, Glazebrook J, T G (2009) Priming in Systemic Plant Immunity Priming in Systemic Plant Immunity. Science 324:89–91.

Kasuga T, Bui M, Bernhardt E, Swiecki T, Aram K, Cano LM, Webber J, Brasier C, Press C, Grünwald NJ, Rizzo DM, Garbelotto M (2016) Host-induced aneuploidy and phenotypic

diversification in the Sudden Oak Death pathogen *Phytophthora ramorum*. BMC Genomics 17:1–17.

Kerr A (1964) Influence of soil moisture on infection of peas by *Pythium ultimum*. Australian Journal of Biological Science 17:676–685.

Khangura R, Speijers J, Barbetti MJ, Salam MU, Diggle AJ (2009) Epidemiology of blackleg (*Leptosphaeria maculans*) of canola (*Brassica napus*) in relation to maturation of pseudothecia and discharge of ascospores in Western Australia. Phytopathology 97:1011–1021.

Kimberley MO, Hood I a, Knowles RL (2011) Impact of Swiss needle-cast on growth of Douglas-fir. Phytopathology 101:583–93.

Kirschbaum MUF (2004) Direct and Indirect Climate Change Effects on Photosynthesis and Transpiration. Plant Biology 6:242–253.

Körner C (2018) Concepts in empirical plant ecology. Plant Ecology & Diversity 00:1–24.

Kozanitas M, Osmundson TW, Linzer R, Garbelotto M (2017) Interspecific interactions between the Sudden Oak Death pathogen *Phytophthora ramorum* and two sympatric *Phytophthora* species in varying ecological conditions. Fungal Ecology 28:86–96.

Krause SC, Raffa KF (1992) Comparison of insect, fungal, and mechanically induced defoliation of larch: effects on plant productivity and subsequent host susceptibility. Oecologia 90:411–416.

Laine AL (2011) Context-dependent effects of induced resistance under co-infection in a plant-pathogen interaction. Evolutionary Applications 4:696–707.

Lake JA, Wade RN (2009) Plant-pathogen interactions and elevated CO_2: Morphological changes in favour of pathogens. Journal of Experimental Botany 60:3123–3131.

Lakhesar DPS, Backhouse D, Kristiansen P (2010) Accounting for periods of wetness in displacement of *Fusarium pseudograminearum* from cereal straw. Annals of Applied Biology 157:91–98.

Landhausser SM, Lieffers VJ (2012) Defoliation increases risk of carbon starvation in root systems of mature aspen. Trees Structure and Function 26:653–661.

Lanier L (1966) Les maladies cryptogamiques du Douglas en France. Rev For Fr 18:247–265.

Lavigne MB, Little CHA, Major JE (2001) Increasing the sink:source balance enhances photosynthetic rate of 1-year-old balsam fir foliage by increasing allocation of mineral nutrients. Tree Physiology 21:417–426.

Leclerc M, Doré T, Gilligan CA, Lucas P, Filipe JAN (2014) Estimating the delay between host infection and disease (incubation period) and assessing its significance to the epidemiology of plant diseases. PLoS ONE 9:e86568.

Lee EH, Beedlow PA, Waschmann RS, Burdick CA, Shaw DC (2013) Tree-ring analysis of the fungal disease Swiss needle cast in western Oregon coastal forests. Canadian Journal of

Forest Research 43:677–690.

Lee EH, Beedlow PA, Waschmann RS, Tingey DT, Wickham C, Cline S, Bollman M, Carlile C (2016) Douglas-fir displays a range of growth responses to temperature, water, and Swiss needle cast in western Oregon, USA. Agricultural and Forest Meteorology 221:176–188.

Lehner MS, Lima RC, Carneiro JES, Paula TJ, Vieira RF, Mizubuti ESG (2016) Similar aggressiveness of phenotypically and genotypically distinct isolates of Sclerotinia sclerotiorum. Plant Disease 100:360–366.

Lehto T, Zwiazek JJ (2011) Ectomycorrhizas and water relations of trees: A review. Mycorrhiza 21:71–90.

Lenth R (2018) emmeans: Estimated Marginal Means, aka Least-Squares Means. R package version 122:https://CRAN.R-project.org/package=emmeans.

Leuning R, Cromer RN, Rance S (1991) Spatial distributions of foliar nitrogen and phosphorus in crowns of *Eucalyptus grandis*. Oecologia 88:504–510.

Little CHA, Lavigne MB, Ostaff DP (2003) Impact of old foliage removal, simulating defoliation by the balsam fir sawfly, on balsam fir tree growth and photosynthesis of current-year shoots. Forest Ecology and Management 186:261–269.

Liu XL, Liu CL (2016) Effect of drought stress on Fusarium crown rot development in barley. PLoS ONE 11:e0167304.

Lombardero MJ, Ayres MP, Bonello P, Cipollini D, Herms DA (2016) Effects of defoliation and site quality on growth and defenses of *Pinus pinaster* and *P. radiata*. Forest Ecology and Management 382:39–50.

Lopisso DT (2014) Studies on resistance of oilseed rape (Brassica napus) to Verticillium longisporum – Interaction with drought stress, role of xylem sap modulations and phenotyping under controlled and field conditions. PhD thesis, Georg-August-University Göttingen, Germa

Maguire D a., Kanaskie A, Voelker W, Johnson R, Johnson G (2002) Growth of Young Douglas-Fir Plantations Across a Gradient in Swiss Needle Cast Severity. Western Journal of Applied Forestry 17:86–95.

Malcolm GM, Kuldau GA, Gugino BK, Jiménez-Gasco M del M (2013) Hidden Host Plant Associations of Soilborne Fungal Pathogens: An Ecological Perspective. Phytopathology 103:538–544.

Mammeri Y, Burie JB, Langlais M, Calonnec A (2014) How changes in the dynamic of crop susceptibility and cultural practices can be used to better control the spread of a fungal pathogen at the plot scale? Ecological Modelling 290:178–191.

Manion PD (1991) Tree Disease Concepts. Second ed. Prentice-Hall, New Jersey, USA.

Manion PD (2003) Evolution of concepts in forest pathology. Phytopathology 93:1052–1055.

Manter DK, Bond BJ, Kavanagh KL, Rosso PH, Filip GM (2000) Pseudothecia of Swiss needle

cast fungus, *Phaeocryptopus gaeumannii*, physically block stomata of Douglas fir, reducing CO_2 assimilation. New Phytologist 148:481–491.

Manter DK, Bond BJ, Kavanagh KL, Stone JK, Filip GM (2003) Modelling the impacts of the foliar pathogen, *Phaeocryptopus gaeumannii*, on Douglas-fir physiology: net canopy carbon assimilation, needle abscission and growth. Ecological Modelling 164:211–226.

Manter DK, Kelsey RG, Stone JK (2001) Quantification of *Phaeocryptopus gaeumannii* colonization in Douglas-fir needles by ergosterol analysis. Forest Pathology 31:229–240.

Manter DK, Reeser PW, Stone JK (2005) A Climate-Based Model for Predicting Geographic Variation in Swiss Needle Cast Severity in the Oregon Coast Range. Phytopathology 95:1256–1265.

Manter DK, Winton LM, Filip GM, Stone JK (2003) Assessment of swiss needle cast disease: Temporal and spatial investigations of fungal colonization and symptom severity. Journal of Phytopathology 151:344–351.

Manzoni S, Schimel JP, Porporato A (2012) Responses of soil microbial communities to water stress: results from a meta-analysis. Ecology 93:930–938.

Marçais B, Desprez-Loustau M-L (2014) European oak powdery mildew: impact on trees, effects of environmental factors, and potential effects of climate change. Annals of Forest Science:633–642.

Mašková P, Radochová B, Lhotáková Z, Michálek J, Lipavská H (2017) Nonstructural carbohydrate-balance response to long-term elevated CO_2 exposure in european beech and Norway spruce mixed cultures: Biochemical and ultrastructural responses. Canadian Journal of Forest Research

Matthiesen RL, Abeysekara NS, Ruiz-Rojas JJ, Biyashev RM, Maroof MAS, Robertson AE (2016) A method for combining isolates of *Phytophthora sojae* to screen for novel sources of resistance to Phytophthora stem and root rot in soybean. Plant Disease 100:1424–1428.

McDowell NG, Beerling DJ, Breshears DD, Fisher R a., Raffa KF, Stitt M (2011) The interdependence of mechanisms underlying climate-driven vegetation mortality. Trends in Ecology and Evolution 26:523–532.

McDowell JM, Dangl JL (2000) Signal transduction in the plant immune response. Trends in biochemical sciences 25:79–82.

Mcelrone AJ, Reid CD, Hoye KA, Hart E, Jackson RB (2005) Elevated CO_2 reduces disease incidence and severity of a red maple fungal pathogen via changes in host physiology and leaf chemistry. Global Change Biology 11:1828–1836.

Mcgowan J, Fitzpatrick DA (2017) Genomic, netwok, and phylogenetic analysis of the oomycet effector arsenal. mSphere 2:1–22.

Merrill W, Longenecker J (1973) Swiss needle cast of Douglas-fir in Pennsylvania. Plant Disease Reporter 57:984.

Mideo N (2009) Parasite adaptations to within-host competition. Trends in Parasitology 25:261–268.

Mitchell PJ, O'Grady AP, Tissue DT, White DA, Ottenschlaeger ML, Pinkard EA (2013) Drought response strategies define the relative contributions of hydraulic dysfunction and carbohydrate depletion during tree mortality. New Phytologist 197:862–872.

Mitchell PJ, O'Grady AP, Tissue DT, Worledge D, Pinkard EA (2014) Co-ordination of growth, gas exchange and hydraulics define the carbon safety margin in tree species with contrasting drought strategies. Tree Physiology 34:443–458.

Moreira X, Zas R, Sampedro L (2012) Differential allocation of constitutive and induced chemical defenses in pine tree juveniles: A test of the optimal defense theory. PLoS ONE 7:1–8.

Morton HL, Patton RF (1970) Swiss Needle Cast of Douglas-fir in the Lake States. Plant Disease Reporter 54:612–616.

Mullett MS, Brown A V. (2018) Effect of Dothistroma needle blight on needle and shoot lengths. Forest Pathology 48:1–7.

Murray GM, Heenan DP, Taylor AC (1991) The effect of rainfall and crop management on take-all and eyespot of wheat in the field. Australian Journal of Experimental Agriculture

New Zealand Forest Owners Association (2014) New Zealand Plantation Forest Industry. Facts and figures. Wellington, New Zealand: Ministry for Primary Industries

Newhook F, Podger F (1972) The role of *Phytophthora cinnamomi* in Australian and New Zealand forests. Annual Review of Phytopathology 10:299–326.

Newton AC, Johnson SN, Gregory PJ (2011) Implications of climate change for diseases, crop yields and food security. Euphytica 179:3–18.

Niinemets U (1999) Components of leaf dry mass per area —thickness and density— alter leaf photosynthetic capacity in reverse directions. New Phytologist 144:35–47.

Niinemets Ü (2015) Uncovering the hidden facets of drought stress: Secondary metabolites make the difference. Tree Physiology 36:129–132.

Nowak MA, May RM (1994) Superinfection and the evolution of parasite virulence. Proceedings of the Royal Society: Biological Sciences 255:81–89.

NZIER (2015) How valuable is that plant species? Application of a method for enumerating the contribution of selected plant species to New Zealand's GDP. Report to the Ministry for Primary Industries.

O'Hanlon R, Choiseul J, Grogan H, Brennan JM (2016) In-vitro characterisation of the four lineages of Phytophthora ramorum. European Journal of Plant Pathology 2:1–9.

O'Hanlon R, Grogan H, McCracken A, de la Mata Saez L, Doohan F, Jia J, Harrington T, Brennan J, Choiseul J (2015) Understanding *Phytophthora ramorum* in Irish larch forests. :1–4.

O'Neill R, Mcdougal R, Fraser S, Banham C, Cook M, Claasen A, Simpson S, Williams N (2018) Validating outsourced high throughput automated qPCR for increased research outputs

from forest pathology trials. New Zealand Plant Protection 71:30843.

Ogunseitan O (2005) Microbial Diversity. Oxford, UK: Blackwell Science Ltd.

Oliva J, Stenlid J, Grönkvist-Wichmann L, Wahlström K, Jonsson M, Drobyshev I, Stenström E (2016) Pathogen-induced defoliation of *Pinus sylvestris* leads to tree decline and death from secondary biotic factors. Forest Ecology and Management 379:273–280.

Oliva J, Stenlid J, Martinez-Vilalta J (2014) The effect of fungal pathogens on the water and carbon economy of trees: implications for drought-induced mortality. The New phytologist 203:1028–1035.

Orwin KH, Stevenson BA, Smaill SJ, Kirschbaum MUF, Dickie IA, Clothier BE, Garrett LG, Van Der Weerden TJ, Beare MH, Curtin D (2015) Effects of climate change on the delivery of soil-mediated ecosystem services within the primary sector in temperate ecosystems: a review and New Zealand case study. Global change biology 21:2844–2860.

Osorio O. M (2007) Detección del hongo defoliador *Phaeocryptopus gaeumannii* en plantaciones de *Pseudotsuga menziesii* de Valdivia, Chile. Bosque 28:69–74.

Otten W, Filipe JAN, Bailey DJ, Gilligan CA (2003) Quantification and analysis of transmission rates for soilborne epidemics. Ecology 84:3232–3239.

Oyarzun PJ, Gerlagh M, Zadoks JC (1998) Factors associated with soil receptivity to some fungal root rot pathogens of peas. Applied Soil Ecology 10:151–169.

Palacio S, Hernández R, Maestro-Martínez M, Camarero JJ (2012) Fast replenishment of initial carbon stores after defoliation by the pine processionary moth and its relationship to the re-growth ability of trees. Trees - Structure and Function 26:1627–1640.

Palacio S, Hester AJ, Maestro M, Millard P (2008) Browsed *Betula pubescens* trees are not carbon-limited. Functional Ecology 22:808–815.

Palacio S, Hoch G, Sala A, Körner C, Millard P (2014) Does carbon storage limit tree growth? New Phytologist 201:1096–1100.

Pandey P, Sinha R, Mysore KS, Senthil-Kumar M (2015) Impact of concurrent drought stress and pathogen infection on plants. In: Combined Stresses in Plants. Springer, pp 203–222.

Pathrose B, Jones EE, Jaspers M V., Ridgway HJ (2014) High genotypic and virulence diversity in *Ilyonectria liriodendri* isolates associated with black foot disease in New Zealand vineyards. Plant Pathology 63:613–624.

Pautasso M, Holdenrieder O, Stenlid J (2005) Susceptibility to Fungal Pathogens of Forests Differing in Tree Diversity. In: Scherer-Lorenzen M., Körner C., Schulze ED. (eds) Forest Diversity and Function. Ecological Studies (Analysis and Synthesis), vol 176. Springer, Berlin, Heidelberg.

Pautasso M, Schlegel M, Holdenrieder O (2015) Forest Health in a Changing World. Microbial Ecology 69:826–842.

Pavarini DP, Pavarini SP, Niehues M, Lopes NP (2012) Exogenous influences on plant secondary

metabolite levels. Animal Feed Science and Technology 176:5–16.

Peng C, Ma Z, Lei X, Zhu Q, Chen H, Wang W, Liu S, Li W, Fang X, Zhou X (2011) A drought-induced pervasive increase in tree mortality across Canada's boreal forests. Nature climate change 1:467.

Peuke AD, Rennenberg H (2011) Impacts of drought on mineral macro-and microelements in provenances of beech (Fagus sylvatica L.) seedlings. Tree Physiology 31:196–207.

Pfender WF (1984) Aphanomyces root rot. In: Hagedorn D.J. (ed) Compendium of Pea Diseases. St Paul, American Phytopathological Society.

Piene H, Ostaff DP, Eveleigh ES (2001) Growth loss and recovery following defoliation by the balsam firsawflyin young, spaced balsam fir stands. Can Entomol 133:675–686.

Pinheiro J, Bates D, DebRoy S, Sarkar D, Team RC (2018) nlme: Linear and nonlinear mixed effects models. R package version 31-137:URL: https://CRAN.R-project.org/package=nlme.

Pinkard EA, Battaglia M, Roxburgh S, O'Grady AP (2011) Estimating forest net primary production under changing climate: Adding pests into the equation. Tree Physiology 31:686–699.

Pinkard EA, Eyles A, O'Grady AP (2011) Are gas exchange responses to resource limitation and defoliation linked to source:sink relationships? Plant, Cell and Environment 34:1652–1665.

Piper FI, Gundale MJ, Fajardo A (2015) Extreme defoliation reduces tree growth but not C and N storage in a winter-deciduous species. Annals of Botany:1093–1103.

Poorter H, Niklas KJ, Reich PB, Oleksyn J, Poot P, Mommer L (2012) Biomass allocation to leaves, stems and roots: meta-analyses of interspecific variation and environmental control. New Phytologist 193:30–50.

Porras-Alfaro A, Bayman P (2011) Hidden Fungi, Emergent Properties: Endophytes and Microbiomes. Annual Review of Phytopathology 49:291–315.

Pouzoulet J, Pivovaroff AL, Santiago LS, Rolshausen PE (2014) Can vessel dimension explain tolerance toward fungal vascular wilt diseases in woody plants? Lessons from Dutch elm disease and esca disease in grapevine. Frontiers in Plant Science 5:1–11.

Price PW (1991) The Plant Vigor Hypothesis and Herbivore Attack. Oikos 62:244–251.

Puri E, Hoch G, Körner C (2015) Defoliation reduces growth but not carbon reserves in Mediterranean Pinus pinaster trees. Trees 29:1187–1196.

Quentin AG, Beadle CL, O'Grady AP, Pinkard EA (2011) Effects of partial defoliation on closed canopy *Eucalyptus globulus* Labilladière: Growth, biomass allocation and carbohydrates. Forest Ecology and Management 261:695–702.

Quentin AG, O'Grady AP, Beadle CL, Mohammed C, Pinkard EA (2012) Interactive effects of water supply and defoliation on photosynthesis, plant water status and growth of Eucalyptus globulus Labill. Tree Physiology 32:958–967.

Quentin AG, Pinkard EA, Beadle CL, Wardlaw TJ, O'Grady AP, Paterson S, Mohammed C (2010) Do Artificial and Natural Defoliation Have Similar Effects on Physiology of *Eucalyptus*

globulus Labill. Seedlings? Annals of Forest Science 203:1–9.

Ramakrishna A, Ravishankar GA (2011) Influence of abiotic stress signals on secondary metabolites in plants. Plant Signaling and Behavior 6:1720–1731.

Ramegowda V, Senthil-Kumar M (2015) The interactive effects of simultaneous biotic and abiotic stresses on plants: Mechanistic understanding from drought and pathogen combination. Journal of Plant Physiology 176:47–54.

Ramirez JA, Posada JM, Handa IT, Hoch G, Vohland M, Messier C, Reu B (2015) Near-infrared spectroscopy (NIRS) predicts non-structural carbohydrate concentrations in different tissue types of a broad range of tree species. Methods in Ecology and Evolution 6:1018–1025.

Ramsfield TD, Bentz BJ, Faccoli M, Jactel H, Brockerhoff EG (2016) Forest health in a changing world: Effects of globalization and climate change on forest insect and pathogen impacts. Forestry 89:245–252.

Rankin DJ, Bargum K, Kokko H (2007) The tragedy of the commons in evolutionary biology. Trends in Ecology and Evolution 22:643–651.

Rapley LP, Potts BM, Battaglia M, Patel VS, Allen GR (2009) Long-term realised and projected growth impacts caused by autumn gum moth defoliation of 2-year-old *Eucalyptus nitens* plantation trees in Tasmania, Australia. Forest Ecology and Management 258:1896–1903.

Rascher U, Liebig M, Lüttge U (2000) Evaluation of instant light-response curves of chlorophyll fluorescence parameters obtained with a portable chlorophyll fluorometer on site in the field. Plant, Cell and Environment 23:1397–1405.

Reeser P, Sutton W, Hansen E (2013) *Phytophthora pluvialis*, a new species from mixed tanoak-Douglas-fir forests of western Oregon, U.S.A. North American Fungi 8:1–8.

Reich PB, Walter MB, Ellsworth DS (1992) Leaf life-span in relation to leaf, plant, and stand characteristics among diverse ecosystems. Ecol Monogr 62:365–392.

Reich PB, Walters MB, Krause SC, Vanderklein DW, Raffs KF, Tabone T (1993) Growth, nutrition and gas exchange of *Pinus resinosa* following artificial defoliation. Trees 7:67–77.

Ritokova G, Shaw DC, Filip G, Kanaskie A, Browning J, Norlander D (2016) Swiss needle cast in western oregon douglas-fir plantations: 20-Year monitoring results. Forests 7:1–11.

Rolando CA, Dick MA, Gardner J, Bader MK-F, Williams NM (2017) Chemical control of two Phytophthora species infecting the canopy of Monterey pine (*Pinus radiata*). Forest Pathology:1–10.

Rolando C, Gaskin R, Horgan D, Williams N, Bader M (2014) The use of adjuvants to improve uptake of phosphorous acid applied to *Pinus radiata* needles for control of foliar Phytophthora diseases. New Zealand Journal of Forestry Science 44:8.

Rook DA, Whyte AGD (1976) Partial defoliation and growth of 5-year-old radiata pine. New Zealand Journal of Forestry Science 6:40–56.

Rosso PH, Hansen EM (2003) Predicting swiss needle cast disease distribution and severity in

young douglas-fir plantations in coastal Oregon. Phytopathology 93:790–798.

Rowe JH, Topping JF, Liu J, Lindsey K (2016) Abscisic acid regulates root growth under osmotic stress conditions via an interacting hormonal network with cytokinin, ethylene and auxin. New Phytologist 211:225–239.

Roy BA, Alexander HM, Davidson J, Campbell, Burdon JJ, Sniezko R, Brasier C (2014) Increasing forest loss worldwide from invasive pests requires new trade regulations. Frontiers in Ecology and the Environment 12:457–465.

Ruiz-Lozano JM, Porcel R, Bárzana G, Azcón R, Aroca R (2012) Contribution of arbuscular mycorrhizal symbiosis to plant drought tolerance: State of the art. In: Aroca R. (ed) Plant Responses to Drought Stress: From Morphological to Molecular Features. Springer-Verlag, Berlin, Germany.pp 335–362.

Ryals JA, Neuenschwander UH, Willits MG, Molina A, Steiner H, Hunt MD (1996) Systemic acquired resistance. The Plant Cell 8:1809–1819.

Saffell BJ, Meinzer FC, Voelker SL, Shaw DC, Brooks JR, Lachenbruch B, Mckay J (2014) Tree-ring stable isotopes record the impact of a foliar fungal pathogen on CO_2 assimilation and growth in Douglas-fir. Plant, Cell and Environment 37:1536–1547.

Saffell B, Meinzer F, Woodruff D, Shaw D, Voelker S, Lachenbruch B, Falk K (2013) Seasonal carbohydrate dynamics and growth in Douglas-fir trees experiencing chronic, fungal-mediated reduction in functional leaf area. Tree Physiology 34:218–228.

Salas C, Donoso PJ, Vargas R, Arriagada CA, Pedraza R, Soto DP (2016) The Forest Sector in Chile: An Overview and Current Challenges. Journal of Forestry 114:562–571.

Sampaio BL, Edrada-Ebel R, Da Costa FB (2016) Effect of the environment on the secondary metabolic profile of Tithonia diversifolia: a model for environmental metabolomics of plants. Scientific reports 6:29265.

Sandhya V, Z. AS, Grover M, Reddy G, Venkateswarlu B (2009) Alleviation of drought stress effects in sunflower seedlings by the exopolysaccharides producing *Pseudomonas putida* strain GAP-p45. Biology and Fertility of Soils 46:17–26.

Santini A, Ghelardini L, De Pace C, Desprez-Loustau ML, Capretti P, Chandelier A, Cech T, Chira D, Diamandis S, Gaitniekis T, Hantula J, Holdenrieder O, Jankovsky L, Jung T, Jurc D, Kirisits T, Kunca A, Lygis V, Malecka M, Marcais B, Schmitz S, Schumacher J, Solheim H, Solla A, Szabò I, Tsopelas P, Vannini A, Vettraino AM, Webber J, Woodward S, Stenlid J (2013) Biogeographical patterns and determinants of invasion by forest pathogens in Europe. The New phytologist 197:238–50.

Scharen AL (1960) Germination of oospores of *Aphanomyces euteiches* embedded in plant debris. Phytopathology 50:274–277.

Scharpf RF (1993) Diseases of Pacific Coast Conifers. USDA, Forest Service, Agriculture Handbook 521. Pacific Southwest Research Station, Albany, CA.

Schena L, Hughes KJD, Cooke DEL (2006) Detection and quantification of *Phytophthora*

ramorum, *P. kernoviae*, *P. citricola* and *P. quercina* in symptomatic leaves by multiplex real-time PCR. Molecular Plant Pathology 7(5):365-379.

Schimel J, Balser TC, Wallenstein M (2007) Microbial stress-response physiology and its implications for ecosystem function. Ecology 88:1386–1394.

Schmid M, Pautasso M, Holdenrieder O (2014) Ecological consequences of Douglas fir (*Pseudotsuga menziesii*) cultivation in Europe. European Journal of Forest Research 133:13–29.

Schoeneweiss DF (1986) Water stress predisposition to disease, and overview. In: Ayres P.G., Boddy L. (eds.) Water, fungi and plants. Cambridge University Press.pp 157–174.

Sharma SB, Gobi TA (2016) Impact of drought on soil and microbial diversity in different agroecosystems of the semiarid zones. In: Hakeen K.R., Akhtar M.S., Abdullah S.N.A. (eds.) Plant, soil and microbes. Volume 1; Implications in crop science. Springer International Publishing, Switzerland.pp 149–162.

Shaw D, Woolley T, Kanaskie A (2014) Vertical Foliage Retention in Douglas-Fir Across Environmental Gradients of the Western Oregon Coast Range Influenced by Swiss Needle Cast. Northwest Science 88:23–32.

Shearer BL, Crane CE, Cochrane A (2004) Quantification of the susceptibility of the native flora of the South-West Botanical Province, Western Australia, to *Phytophthora cinnamomi*. Australian Journal of Botany 52:435–443.

Simpson DR, Thomsett MA, Nicholson P (2004) Competitive interactions between *Microdochium nivale* var. *majus*, *M. nivale* var. *nivale* and *Fusarium culmorum* in planta and in vitro. Environmental Microbiology 6:79–87.

Singh DP, Backhouse D, Kristiansen P (2009) Interactions of temperature and water potential in displacement of *Fusarium pseudograminearum* from cereal residues by fungal antagonists. Biological Control 48:188–195.

Singleton LL, Mihail JD, Rush CM (1992) Methods for Research on Soilborne Phytopathogenic Fungi Second Printing Edition. American Phytopathological Society, St Paul MN.

Skipp RA, Watson RN (1996) Disease complexes in New Zealand pastures. Pasture and forage crop pathology:429–451.

Smiley RW, Collins HP, Rasmussen PE (1996) Diseases of wheat in long-term agronomic experiments at Pendleton, Oregon. Plant Disease 80:813–820.

Stergiopoulos I, Gordon TR (2014) Cryptic fungal infections: the hidden agenda of plant pathogens. Frontiers in Plant Science 5:10–13.

Stone JK, Capitano BR, Kerrigan JL (2008) The histopathology of *Phaeocryptopus gaeumannii* on Douglas-fir needles. Mycologia 100:431–444.

Stone JK, Coop LB, Manter DK (2008) Predicting effects of climate change on Swiss needle cast disease severity in Pacific Northwest forest. Canadian journal of plant pathology 30:169–

176.

Stone C, Melville G, Carnegie A, Smith D, Eyles A, Nagel M (2013) Crown damage by the aphid *Essigella californica* in a *Pinus radiata* plantation in southern New South Wales: causality and related management issues. Australian Forestry 76:16–24.

Talas F, McDonald BA (2015) Genome-wide analysis of *Fusarium graminearum* field populations reveals hotspots of recombination. BMC genomics 16:996.

Tattar TA (2012) Diseases of Shade Trees, Revised Edition. Academic Press, San Diego, California.

Telfer E, Graham N, Stanbra L, Manley T, Wilcox P (2013) Extraction of Pine Genomic DNA for use in a High-Throughput Genotyping Platform. New Zealand Journal of Forestry Science 43:1–8.

Temel F, Johnson GR, Stone JK (2004) The relationship between Swiss needle cast symptom severity and level of *Phaeocryptopus gaeumannii* colonization in coastal Douglas-fir (*Pseudotsuga menziesii* var. *menziesii*). Forest Pathology 34:383–394.

Temel F, Stone JK, Johnson GR (2003) First report of Swiss needle cast caused by *Phaeocryptopus gaeumannii* on Douglas-fir in Turkey. Disease Notes 87:1536.

Terry LA, Chope GA, Bordonaba JG (2007) Effect of water deficit irrigation and inoculation with *Botrytis cinerea* on strawberry (*Fragaria* x *ananassa*) fruit quality. Journal of Agricultural and Food Chemistry 55:10812–10819.

Thabeet A, Vennetier M, Gadbin-Henry C, Denelle N, Roux M, Caraglio Y, Vila B (2009) Response of *Pinus sylvestris* L. to recent climatic events in the French Mediterranean region. Trees 23:843–853.

Thomas H, Sadras VO (2001) The capture and gratuitous disposal of resources by plants. Functional Ecology 15:3–12.

Ton J, Flors V, Mauch-Mani B (2009) The multifaceted role of ABA in disease resistance. Trends in Plant Science 14:310–317.

Tubiello FN, Soussana J-F, Howden SM (2007) Crop and pasture response to climate change. Proceedings of the National Academy of Sciences 104:19686–19690.

UNDESA (2015) World population prospects: the 2015 revision, key findings and advance tables.

Vanderklein DW, Reich PB (1999) The effect of defoliation intensity and history on photosynthesis, growth and carbon reserves of two conifers with contrasting leaf lifespans and growth habits. New Phytologist 144:121–132.

VanderPlas J (2014) Frequentism and bayesianism: a python-driven primer. arXiv preprint arXiv:14115018

Vergu E, Busson H, Ezanno P (2010) Impact of the infection period distribution on the epidemic spread in a metapopulation model. PLoS ONE 5:e9371.

Vettraino AM, Brasier CM, Brown A V., Vannini A (2011) *Phytophthora himalsilva* sp. nov. an

unusually phenotypically variable species from a remote forest in Nepal. Fungal Biology 115:275–287.

Vettraino AM, Morel O, Perlerou C, Robin C, Diamandis S, Vannini A (2005) Occurrence and distribution of *Phytophthora* species in European chestnut stands, and their association with Ink Disease and crown decline. European Journal of Plant Pathology 111:169–180.

Vettraino AM, Sukno S, Vannini A, Garbelotto M (2010) Diagnostic sensitivity and specificity of different methods used by two laboratories for the detection of *Phytophthora ramorum* on multiple natural hosts. Plant Pathology 59:289-300.

De Vos M, Van Oosten VR, Van Poecke RMP, Van Pelt JA, Pozo MJ, Mueller MJ, Buchala AJ, Métraux J-P, Van Loon LC, Dicke M, Pieterse CMJ (2005) Signal Signature and Transcriptome Changes of *Arabidopsis* During Pathogen and Insect Attack. Molecular Plant-Microbe Interactions 18:923–937.

Wake G, Williams N, Pleasants T (2018) A dynamical systems model for poly-cyclic foliar forest pathogens. ANZIAM Journal 59:1–14.

Wakelin SA, Eslami Y, Dake K, Dignam BEA, O'Callaghan M (2016) Cost of root disease on white clover growth in New Zealand dairy pastures. Australasian Plant Pathology 45:289–296.

Walters DR, Bingham IJ (2007) Influence of nutrition on disease development caused by fungal pathogens: Implications for plant disease control. Annals of Applied Biology 151:307–324.

Wang Y, Ma F, Li M, Liang D, Zou J (2011) Physiological responses of kiwifruit plants to exogenous ABA under drought conditions. Plant growth regulation 64:63–74.

Wareing PF, Patrick J (1975) Source - sink relations and the partition of assimilates in the plant. In: Cooper JP, ed. Photosynthesis and productivity in different environments. Cambridge University Press.pp 481–499.

Warren CR, Adams MA (2000) Trade-offs between the persistence of foliage and productivity in two Pinus species. Oecologia 124:487–494.

Watt MS, Stone JK, Hood IA, Palmer DJ (2010) Predicting the severity of Swiss needle cast on Douglas-fir under current and future climate in New Zealand. Forest Ecology and Management 260:2232–2240.

Webb WL (1981) Relation of Starch Content to Conifer Mortality and Growth Loss after Defoliation by the Douglas-fir Tussock Moth. Forest Science 27:224–232.

Weiner J, Freckleton RP (2010) Constant Final Yield. Annual Review of Ecology, Evolution, and Systematics 41:173–192.

West JS, Kharbanda PD, Barbetti MJ, Fitt BDL (2001) Epidemiology and management of *Leptosphaeria maculans* (phoma stem canker) on oilseed rape in Australia, Canada and Europe. Plant Pathology 50:10–27.

White TCR (1969) An Index to Measure Weather-Induced Stress of Trees Associated With Outbreaks of Psyllids in Australia. Ecology 50:905–909.

Whyte G, Howard K, Hardy GESJ, Burgess TI (2016) The Tree Decline Recovery Seesaw; a conceptual model of the decline and recovery of drought stressed plantation trees. Forest Ecology and Management 370:102–113.

Wilcox WF, Gubler WD, Uyemoto JK (2015) Compendium of grape diseases, disorders, and pests. Am Phytopath Society.

Wiley E, Casper BB, Helliker BR (2017) Recovery following defoliation involves shifts in allocation that favour storage and reproduction over radial growth in black oak. Journal of Ecology 105:412–424.

Wiley E, Helliker B (2012) A re-evaluation of carbon storage in trees lends greater support for carbon limitation to growth. New Phytologist 195:285–289.

Wiley E, Huepenbecker S, Casper BB, Helliker BR (2013) The effects of defoliation on carbon allocation: can carbon limitation reduce growth in favour of storage? Tree Physiology 33:1216–1228.

Williams JS, Cooper RM (2004) The oldest fungicide and newest phytoalexin - a reappraisal of the fungitoxicity of elemental sulphur. Plant Pathology 53:263–279.

Wills AJ, Burbidge TE, Abbott I (2004) Impact of repeated defoliation on jarrah (*Eucalyptus marginata*) saplings. Australian Forestry 67:194–198.

Wingfield MJ (2003) Increasing threat of diseases to exotic plantation forests in the Southern Hemisphere: Lessons from *Cryphonectria* canker. In: Australasian Plant Pathology.pp 133–139.

Wingfield MJ, Brockerhoff EG, Wingfield BD, Slippers B (2015) Planted forest health: The need for a global strategy. Science 349:832–836.

Winton LM, Manter DK, Stone JK, Hansen EM (2003) Comparison of Biochemical, Molecular, and Visual Methods to Quantify *Phaeocryptopus gaeumannii* in Douglas-Fir Foliage. Phytopathology 93:121–126.

Winton LM, Stone JK, Watrud LS, Hansen EM (2002) Simultaneous one-tube quantification of host and pathogen DNA with real-time polymerase chain reaction. Phytopathology 92:112–116.

Wood S, Scheipl F (2017) gamm4: Generalized Additive Mixed Models using ‘mgcv’ and ‘lme4’. R package version 02-5 https://CRANR-project.org/package=gamm4

Xiong L, Yang Y (2003) Disease resistance and abiotic stress tolerance in rice are inversely modulated by an abscisic acid–inducible mitogen-activated protein kinase. The Plant Cell 15:745–759.

Xu Z, Zhou G, Shimizu H (2010) Plant responses to drought and rewatering. Plant Signaling and Behavior 5:649–654.

Yarwood CE (1978) Water and the infection process. Water Deficits and Plant Growth, Water and Plant Disease 5:141–173.

Yasuda M, Ishikawa A, Jikumaru Y, Seki M, Umezawa T, Asami T, Maruyama-Nakashita A, Kudo T, Shinozaki K, Yoshida S, Nakashita H (2008) Antagonistic Interaction between Systemic Acquired Resistance and the Abscisic Acid-Mediated Abiotic Stress Response in Arabidopsis. The Plant cell 20:1678–1692.

Young GK, Cooke LR, Watson S, Kirk WW, Perez FM, Deahl KL (2018) The role of aggressiveness and competition in the selection of *Phytophthora infestans* populations. Plant Pathology 67:1539–1551.

Zangerl AR, Bazzaz FA (1979) Theory and Pattern in Plant Defense Allocation. In: Fritz R, Simms E, eds. Plant resistance to herbivores and pathogens, ecology, evolution and genetics. Chicago: University of Chicago Press.pp 363–391.

Zangerl AR, Bazzaz FA (1992) Theory and pattern in plant defense allocation. In: In: Fritz R, Simms E, eds. Plant resistance to herbivores and pathogens, ecology, evolution and genetics. Chicago: University of Chicago Press.p pp 363–391.

Zhang JY, Cruz De Carvalho MH, Torres-Jerez I, Kang Y, Allen SN, Huhman D V., Tang Y, Murray J, Sumner LW, Udvardi MK (2014) Global reprogramming of transcription and metabolism in *Medicago truncatula* during progressive drought and after rewatering. Plant, Cell and Environment 37:2553–2576.

Zhao J, Mainwaring DB, Maguire DA, Kanaskie A (2011) Regional and annual trends in Douglas-fir foliage retention: Correlations with climatic variables. Forest Ecology and Management 262:1872–1886.

Zhou X, Smaill SJ, Clinton PW (2013) Methane oxidation needs less stressed plants. Trends in Plant Science